Supply chain decisions for an adaptive, decentralized renewable energy system

Fokkema, Jan Eise

DOI:
[10.33612/diss.195396548](https://doi.org/10.33612/diss.195396548)

IMPORTANT NOTE: You are advised to consult the publisher's version (publisher's PDF) if you wish to cite from it. Please check the document version below.

Document Version
Publisher's PDF, also known as Version of record

Publication date:
2021

[Link to publication in University of Groningen/UMCG research database](#)

Supply chain decisions for an adaptive, decentralized renewable energy system

Jan Eise Fokkema

Supply chain decisions for an adaptive, decentralized renewable energy system

PhD thesis

to obtain the degree of PhD at the
University of Groningen
on the authority of the
Rector Magnificus Prof. C. Wijmenga
and in accordance with
the decision by the College of Deans.

This thesis will be defended in public on

Monday 13 December 2021 at 11.00 hours

by

Jan Eise Fokkema

born on 10 March 1988
in Colombo, Sri Lanka

Contents

Chapter 1

Introduction

Supply chain and operations management decisions are important in the transition from fossil-based energy sources to renewable energy. They form the basis for infrastructural designs that need to be able to efficiently handle the increased complexity associated with intermittent and decentralized renewable energy production. These infrastructural designs encompass the challenging interplay between production, storage, and distribution to avoid excess installed capacity, losses related to curtailment and conversion, inefficient transportation of energy, and grid congestion.

This thesis addresses decision-making problems related to balancing and organizing the storage and distribution of biogas, solar energy, and wind energy for energy producers. The decisions aim at balancing and operating storage, production, and transportation in rural areas to avoid excess production or storage capacity, electricity grid congestion, and curtailment. They further aim at the efficient distribution of energy, to determine the shares of different renewable sources in the energy mix, and to provide a stable supply of renewable energy to rural communities. This thesis also addresses the use of LNG in the transportation sector, by showing under which conditions LNG-fueled ships are more economically viable than conventional ships. We employ a wide variety of methods that include Mixed-Integer and Linear Programming, simulation, and Markov-Decision Processes.

In introducing this thesis, we first provide an overview of the logistics challenges related to renewable energy supply in general, followed by discussions of solution

directions. The solutions that are studied in this thesis combine a decentralized approach with the application of energy storage to adapt to the energy transition. Finally, we specify the three domains of the energy transition to which this thesis will contribute, including the research questions that will be addressed in each chapter. These domains include transportation logistics, seasonal matching of supply and demand, and the operation of storage facilities.

1.1   Logistics challenges of renewable energy supply

The need for a more sustainable energy system and the shift to renewable energy and less-polluting fuels causes logistics problems related to the renewable energy supply. In particular, the transition towards more renewables creates problems related to supply-driven energy generation, location differences between energy production and energy demand, and the mismatch in production and demand profiles over time.

Major logistics challenges arise from the supply-driven production of renewable energy, the location of production, and different profiles of supply and demand. Renewable energy is supply-driven because the production levels cannot be flexibly adjusted. Solar and wind energy are dependent on weather. Biogas is dependent on organic processes related to digestion.

Renewable energy is also generated at different locations than demand. For example, large solar fields are placed in rural areas in which land is more abundant and less expensive than in urban regions. Wind energy production tends to be located in rural areas and large offshore wind parks at sea. Biogas production facilities are also commonly located in rural areas near farms that have the availability of manure which can be fed to a digester.

The production of renewable energy follows a different pattern than energy demand. For example, the electricity demand of households fluctuates during the day, whereas biogas production is relatively constant as a result of biochemical processes and solar energy typically peaks during noon. Wind energy is more volatile as a result of weather changes.

The production profiles of solar and wind energy potentially create electricity grid congestion as a result of peak levels sent to the grid. At these times, the generated power becomes confined to the direct environment in which it is

produced. Grid congestion is a result of network constraints that threaten grid balance and cause outages (Vargas et al., 2014; Kumar et al., 2005). Electricity grids in terms of distribution networks that comprise the low to medium voltage grids, ranging between 0.4 to 2.3 kiloVolt (kV), are highly affected by increasing shares of renewables. Designing effective logistics systems which consider both storage and distribution of electricity is key in addressing the increasing need for congestion management.

1.2 Solution directions

The solutions to adapt to the new logistic challenges that are explored in this thesis combine a decentralized approach with the application of energy storage.

1.2.1 Decentralized approach

From both a logistics and societal standpoint, the production-related logistics problems should be addressed based on a decentralized approach, in which energy that is produced locally is consumed locally as much as possible. We refer to a decentralized approach as an approach in which energy production is relatively geographically dispersed and in which the supply is used as much as possible to satisfy energy demand that is close to production. While connecting energy systems on a large scale enables spatial smoothing of differences in supply and demand (Lund et al., 2015), it is also generally considered that unnecessary energy transportation over long distances should be avoided, if possible. This avoids both transmission losses, curtailment, conversion, and high requirements, and peak utilization of the scarce distribution infrastructure. This helps to avoid increasing congestion issues related to connecting renewable energy to energy grids.

From a societal perspective, a decentralized approach also addresses the desires of local communities that reside close to renewable energy production facilities. Increasingly, residents of local communities resist the establishment of renewable energy sources in nearby areas. Residents want to have a stable supply of green energy with a transparent origin but are reluctant to have windmills, digesters, and solar fields nearby when that energy is mostly consumed elsewhere.

1.2.2   Transportation systems

Even though production and consumption can both occur locally, a decentralized approach still requires efficient transportation systems to connect the supply to the demand elsewhere. This is because local small-scale and (partly) self-sufficient energy systems with fewer participants create fewer opportunities to smooth out renewable power generation and consumption over a wider area compared to large spatially-integrated energy systems. Fewer participants which supply and consume energy also lead to reduced opportunities for flexibility, because fewer actors are available to provide flexibility services. Therefore, the organization of logistics in these systems becomes increasingly important. Solar and wind energy need sufficient electricity distribution infrastructure in terms of the electricity grid, while transportation of gases such as hydrogen or biogas can be done employing either pipeline grids or ships and trucks with tube trailers.

Particularly in the transition period, transportation by truck or ship may be expected. To avoid diesel trucks or ships nullifying the gains of the renewable energy sources, also the transport sector itself should adapt, by making use of the multitude of cleaner fuels that become available, which include electricity, hydrogen, and LNG. While electric propulsion becomes increasingly more prevalent for road vehicles, the transition to future fuels for ships is less evident. For example, bio-LNG is the biofuel counterpart of Liquefied Natural Gas (LNG), which is held at extremely low temperatures. LNG is a promising fuel in both truck transportation (Post et al., 2018) and ships (Wang and Notteboom, 2014). However, the application of biogas as LNG and the adoption of LNG, in general, creates decision problems for the users of such fuels related to the investment in both infrastructure and ships (Wang and Notteboom, 2014).

Shipowners need to adapt to more tightening International Maritime Organization (IMO) regulations that prevent the usage of polluting fuels. These regulations dictate that ships cannot pass through Emission Controlled Areas (ECA) using high-pollution fuels (IMO, 2019). This creates challenges related to the economic viability of choosing future fuels to comply with regulations in the transportation sector that aim to migrate to cleaner fuels. Accordingly, ship owners need to decide whether or not to migrate to cleaner fuels such as (bio-) LNG or hydrogen. Unfortunately, these fuels are associated with higher investment costs. Shipowners decide to either use the more expensive and cleaner, but still polluting

oil blends such as Marine Gasoil (MGO) with conventional engines, or invest in newly-built ships that employ LNG-compliant engines.

When gas transport in a transition period is done by trucks or ships rather than pipelines, the non-continuous flow will require temporary storage of gasses. Traditionally, storage has also played a role in the grid-based gas supply chain to balance gas supply and demand. But this role extends due to the supply-driven character of a large part of the biogas production, which reduces the opportunities to adapt supply to demand. Storage has generally played a smaller role in electricity supply, where supply adjustments and market mechanisms resolved fluctuations in demand.

1.2.3   Short-term and long-term storage

Storage enables the adaptation to the intermittent and different production profiles of different sources and demands. The variable production levels can be stored, while the output of the storage facility can reflect the variable profile of demand levels. To reduce storage required, supply from multiple energy sources such as biogas, solar, and wind energy can be combined, which takes advantage of the different production profiles in matching supply and demand and uses the storage capacity more effectively. Also, biogas can be converted to electricity using a Combined Heat and Power (CHP) engine and can complement the electricity generated from solar and wind energy.

Storage may play an increasingly important role when adapting to the logistic challenges of the energy transition. It is a flexibility option that enables control over the time at which energy is provided to a consumer or a transportation system. Particularly when storing electricity, we have to distinguish between short-term storage and long-term storage.

Short-term storage of electricity can be realized with batteries to mitigate intra-day fluctuations in electricity production and consumption. They have limited conversion losses (Telaretti et al., 2016), but they are relatively heavy and expensive in large capacities, in which benefits related to economies of scale are limited. Moreover, batteries are associated with losses when energy is stored for longer periods.

Long-term storage can be realized using, for example, cleaned biogas in case of biogas or hydrogen in case of electricity supply. Storing biogas for longer periods

requires cleaning, compressing, and storing the biogas in cylinders. The biogas must first be cleaned by removing hydrogen sulfide and must then be compressed (SUSCON, 2005). Accordingly, long-term storage of biogas in cylinders is relatively expensive. Hydrogen is suitable for long-term storage of electricity in a gaseous form, due to limited time-related losses, a relatively high energy density, and economies of scale related to production and storage. Therefore, hydrogen can be used to bridge seasonal mismatches in production and demand. Electricity is then used in electrolysis to split water into hydrogen and oxygen, while fuel cells can reconvert hydrogen into electricity. This makes hydrogen suitable as a storage medium of electricity and it can play an important role in the congestion management, balancing, and load leveling of electricity grids (Lund et al., 2015). Hydrogen is associated with relatively high round-trip conversion losses when reconverting hydrogen back to electricity. Still, conversion to electricity might be sensible during periods of high electricity prices or to provide flexibility services to the electricity grid (Lund et al., 2015).

Hydrogen can be stored inside underground salt caverns which enable large-scale storage(HyUnder, 2014). This may enable supplying industrial consumers in the future with large amounts of hydrogen when needed. It is important to note that the reduced quality of hydrogen stored in salt caverns makes it less suitable for conversion to electricity using fuel cells since fuel cells require hydrogen with high purity (Andersson and Grönkvist, 2019). Hydrogen can also be stored inside cylinders with a maximum capacity of 16.5 MWh (Bünger et al., 2016)) and inside underground pipelines. Hydrogen facilities which include an electrolyzer, compressors, and cylindrical storage are still relatively expensive. According to The International Renewable Energy Agency (IRENA, 2019), the costs of electrolyzers at the time of writing range are 840 USD per installed kW and can be reduced to 200 USD per kW in the future, assuming that electrolyzers are at least utilized half of the time. Under these conditions, hydrogen production can be "competitive with average to high natural gas prices" for industry consumers (IRENA, 2019). However, this still excludes the costs of renewable energy production capacity. When including, for example, solar production capacity, hydrogen is still relatively expensive (IRENA, 2019).

Storage may fulfill different functions in the transition to renewable energy supply. The discussed challenges require energy systems that can adapt to

supply-driven production, intermittency in production, the mismatch in supply and demand, the location differences between production and demand, and grid congestion. Storage solutions enable storing the supply-driven production of biogas, wind, and solar energy for later use to avoid curtailment. Storage provides an approach to bridge intermittent supply of energy while providing the needed level of output to demand. It enables matching the different profiles of supply and demand more effectively by gaining more control over the supply of energy. Finally, storage enables more control over the distribution of energy to avoid peak use of grid infrastructure. Some further considerations also play a role in each of these functions of storage.

While renewable energy is supply-driven, which means that production can be less flexibly adjusted, storage can help in adapting to the increasing supply-driven energy production levels. This enables avoiding curtailment. During times of excess supply, energy can be stored and used at later times to supply peaks in demand. This enables avoiding both curtailments as a result of excess supply and avoids shortages during times of excess demand. In designing effective energy systems, balancing production capacity and storage capacity is important, because excess production capacity reduces the need for storage, but leads to excess supply. Avoiding all potential curtailment may lead to excess and overly expensive storage requirements.

Storage enables the adaptation to the intermittent and different production profiles of different sources and demands. The variable production levels can be stored, while the output of the storage facility can reflect the variable profile of demand levels. To reduce storage required, supply from multiple energy sources such as biogas, solar, and wind energy can be combined, which takes advantage of the different production profiles in matching supply and demand and uses the storage capacity more effectively. Also, biogas can be converted to electricity using a Combined Heat and Power (CHP) engine and can complement the electricity generated from solar and wind energy.

Storage enables adapting to the increasing seasonality associated with supply and demand and increasing levels of renewable sources. For example, the peaks of solar energy generated in the summer coincide with reduced levels of electricity consumption by households in the summer, whereas solar production levels are much lower in winter. Storage (e.g. in the form of hydrogen) enables the adaptation of energy systems to seasonality differences by bridging supply and demand across

seasons. It is important to note that the increased adoption of heating based on electricity (e.g. heat pumps) in the energy transition is likely to increase seasonal differences between supply and demand due to increased electricity consumption in the winter.

Finally, storage helps to adapt to increasing needs for flexibility services to the electricity grids. Connecting storage facilities to the electricity grid and local electricity demand enables more control over the times at which electricity is obtained or fed to the grid. The peak availability of electricity at solar parks may cause peaks in the supply to the electricity grid connection. Congestion can also occur elsewhere in the electricity grid, which can be solved by providing or obtaining energy to or from the grid at the right times. Storage can facilitate the mitigation of peak supply to the grid, as well as enable the adaptation of energy systems to congestion problems elsewhere in the electricity grid.

1.3 Problem statement

1.3.1 Aim of this thesis

This thesis is based on the project entitled "ADAPNER" (Adaptive logistics in a circular economy) which is financed by the Netherlands Organization for Scientific Research (NWO). The main objective of ADAPNER is "Determining optimized adaptable and sustainable configurations for different distribution alternatives regarding biomass and biogas in a circular economy".

The objective of this thesis is to determine these configurations for different decentralized renewable energy production, storage, and distribution alternatives. The scope of the alternatives considered in this thesis encompasses different renewable energy sources, storage types, and the connection to the electricity grid infrastructure. In particular, we focus on electricity generated by wind and solar photovoltaic (PV) energy. Biogas is both seen as a source to fulfill natural gas demand and also as a source for fulfilling electricity demand employing a CHP engine. We also include LNG as a potentially important fuel in the transportation sector. Furthermore, this thesis includes hydrogen storage as a way to bridge seasonal mismatches between renewable energy production and electricity demand, in which the hydrogen can be converted to electricity. Finally, we include the

electricity grid connection as a way to connect to the rest of the grid and to benefit from flexibility and availability of electricity that is consumed and generated elsewhere.

From the objective and scope above we formulate the **main research question** of this thesis as follows:

How should the decentralized storage and distribution of biogas, solar energy, and wind energy be organized and adapted to enable effective embedding in existing grid infrastructure?

To position the energy sources, forms, and storage possibilities related to the main research question, we use the reference diagram from the ENTSO-E (2021) model of the European transmission system in Figure 1.1. This diagram gives a holistic overview of generators, grids, storage, demand (sectors), and the links between them. Designing efficient logistics systems based on this complex diagram with all its interacting links (sector couplings) requires solving numerous 'pieces of the energy transition puzzle'. Our chosen scope of the main research question is denoted by the dotted rectangular box. Note that we leave out the hydroelectricity source since it has specific intermittency aspects and does not play a role in the Netherlands.
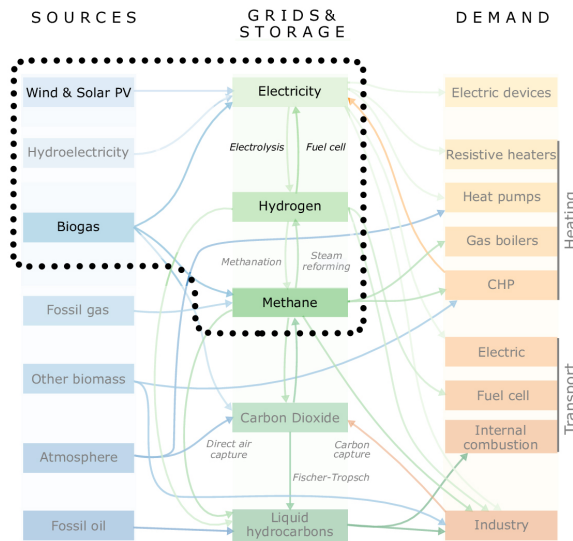
Figure 1.1: Scope of this thesis, depicted on the reference diagram of ENTSO-E (2021))

Furthermore, we identified three main research domains in the scope of our thesis to which our study aims to contribute. These research domains are:

- Transportation logistics

- Seasonal matching of supply and demand

- Operation of storage facilities

The depiction of the research domains in the scope of this thesis is shown in Figure 1.2.

1.3.2   Overview and structure of the thesis

The main body of this thesis, Chapters 2 – 6 addresses five studies executed, which successively cover different aspects of the three research domains. Finally, to conclude, Chapter 7 reflects upon the findings of these studies and their contribution to the main research question. An overview of the structure of the main body of the thesis together with the research domains we distinguish is depicted in Figure 1.2 below.
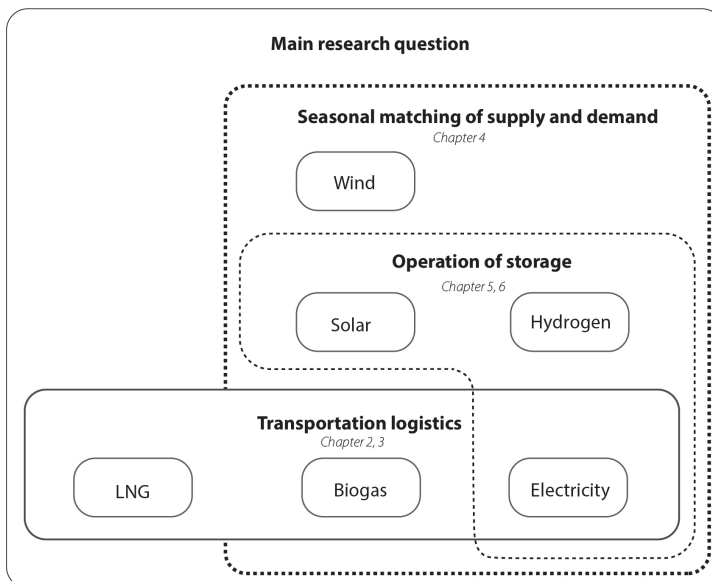
Figure 1.2: Overview of research domains and structure of the thesis

Firstly, Chapter 2 and Chapter 3, focus on the domain "Transportation logistics". This domain includes both logistics decisions related to transportation, and then the transition to cleaner fuels in the transportation sector. We first address the storage and transportation of biogas in a decentralized setting. To enable efficient transportation of biogas to gas injection and upgrading facilities, we determine the scheduling and routing of trucks that transport cylinders with biogas. This is important to enable the embedding of biogas into existing pipeline gas grids. We then focus on the transition to cleaner fuels in the transportation sector in which biogas can be applied in the form of LNG as a fuel in ships. To facilitate the transition to cleaner fuels in the transportation sector, it is important to determine the conditions under which investments in the usage of cleaner fuels are economically viable.

We address the following individual research questions as part of the domain of transportation logistics.

1. How should biogas be distributed using trucks with tube trailers from digesters to centralized upgrading facilities? (Chapter 2).

2. Under which conditions is the application of LNG economically viable for LNG-fueled ships? (Chapter 3).

Secondly, we focus on the domain "Seasonal matching of supply and demand". Chapter 4 studies combining electricity from biogas with other renewable energy sources such as wind and solar energy in a decentralized setting across seasons. We study different configurations of storage and production capacity levels and examine the shares of each source in the total production levels to effectively match the supply and electricity demand of a group of connected households.

1. How should biogas, wind, and solar energy be combined across seasons and how is this affected by the level of total production capacity and storage capacity? (Chapter 4).

Thirdly, we focus on the domain "Operation of storage". We investigate how solar parks with hydrogen should be operated when connected to existing electricity grids and a community of households that aim to be self-sufficient. Hydrogen storage enables the bridging of seasonality differences in supply and demand and contributes to avoiding grid congestion. However, the operational decisions of

solar parks with hydrogen storage to reach these goals are important to enable the effective embedding of solar parks in existing electricity grid infrastructure. The related sub-questions are summarized below.

1. Under which conditions should the owner of solar fields with hydrogen buy and sell from and to the grid to maximize profits? (Chapter 5).

2. How should solar fields with hydrogen storage be operated to alleviate congestion? (Chapter 6).

To conclude, Chapter 7 reflects upon the findings of the five studies and their contribution to the main research question.

In the next section, we give a short background of the studies which are covered in more detail in the subsequent chapters.

1.4 Background of the studies in this thesis

This section provides a short background for each of the studies in this thesis. The studies are described in detail in the subsequent Chapters 2 – 6, and are based on the following journal publications.

- Chapter 2:
  Fokkema, J. E., Land, M. J., Coelho, L. C., Wortmann, H., Huitema, G. B. (2020). A continuous-time supply-driven inventory-constrained routing problem. *Omega*, **92**, 102151.

- Chapter 3:
  Fokkema, J. E., Buijs, P., Vis, I. F. (2017). An investment appraisal method to compare LNG-fueled and conventional vessels. *Transportation Research Part D: Transport and Environment*, **56**, 229-240.

- Chapter 4:
  Fokkema, J. E., Land, M. J., Wortmann, H., Huitema, G. B. (2021). Combining biogas, wind and solar energy to match local demand: The production–storage trade-off. *Under Review*.

- Chapter 5:
  Fokkema, J. E., Uit het Broek, A.J., Schrotenboer, A.H., Land, M.J., Foreest, N.D.

(2021). Strategic seasonal hydrogen storage for renewable energy producers. *Under Review*.

1.4.1   Organizing biogas storage and transportation (Chapter 2)

Biogas can be produced from manure and other feedstock in digester facilities and is a result of biochemical processes in which microbes feed off biomass. Several aspects are important to effectively organize logistics.

Biogas production is relatively constant, due to the biochemical processes in which microbes feed off the biomass. Since it takes typically 20 days to initiate biogas processes in a digester, the production is highly inflexible and supply-driven. There are limited local storage options, in which uncompressed additional storage roofs are expensive and have a very low capacity. These reinforced plastic roofs are commonly used and enable limited storage of raw biogas with a capacity of up to one day of biogas production. Due to the limited capacity, biogas must either be curtailed, used for heating, or converted with conversion losses into electricity using a Combined Heat and Power (CHP) engine when excess production cannot be stored or distributed.

Instead of converting biogas to electricity, it can be injected into existing gas grids using upgrading facilities that purify the gas to meet the requirements of gas in the gas grid. However, these facilities require high investments and are generally not economically feasible when located at single farms. Therefore, these need to be used by multiple farms to achieve economies of scale.

Biogas can be produced by mono-digestion, which refers to solely feeding manure into a digester. Since mono-digestion does not rely on feedstock such as maize that needs to be procured expensively on the external market, it has relatively low variable costs. The stability of the input required also enables lower variable costs. However, it also creates a relatively low biogas output rate. While this may be a solution to the high abundance of manure, the high manure requirements relative to the biogas output create the need for external manure procurement to make mono-digesters economically feasible. Transportation of feedstock is considered inefficient, because of the relatively low energy density of manure relative to the energy consumption of truck transportation (Pierie et al., 2015).

Biogas produced by co-digestion is a result of combining manure with other feedstock. From an environmental perspective, co-digestion at the farm level

interferes with agricultural practices, since it leads to increased nitrogen emissions (Hoang et al., 2019). Even though it enhances biogas output, the feedstock must be externally procured. Consistency of quality of the feedstock is also important, which creates a high dependency on a single supplier and causes prices to be relatively high. This affects the economic viability of digesters. Since feedstock has a relatively low energy density, transportation by gasoline-consuming trucks from the source to the farm becomes soon unsustainable. It is associated with considerable inefficiency when fuel consumption exceeds the energy contents of transported feedstock.

The above-mentioned issues suggest that, from a transportation perspective, it is more efficient to decentralize digester locations close to biomass sources and to transport the gas to centralized gas upgrading and injection facilities rather than to centralize digesters. The supply-driven and inflexible production characteristics require biogas distribution to be orchestrated around supply rather than only demand. Distribution of biogas can be done using trucks with tube trailers. However, this creates specific routing and inventory problems in which the cylinders act as both a stationary and mobile storage unit and the trucks exchange empty cylinders for full ones.

Since the amount of transport related to biogas should be minimal, we aim to achieve this in Chapter 2 by examining how to minimize biogas transportation using smart planning of routes. We address the research question: *How should biogas be distributed using trucks with tube trailers from digesters to centralized upgrading facilities?* Minimizing biogas transportation is important since this contributes to the economic viability of biogas production for relatively small farms, which is limited in general (Lauer et al., 2018) and also depends on subsidies in, for example, the Netherlands. In Chapter 2, we develop a model that addresses the inventory and routing decisions of biogas transportation using trucks with tube trailers to distribute the gas to upgrading and pipeline injection facilities. In this setting, a decision must be made on choosing a set of routes in which the truck visits a set of farms to minimize the transportation time. The decision entails choosing the set of multiple routes within a planning horizon, the time at which a truck arrives at a farm, and the number of cylinders that the operator exchanges in which cylinders can be partly filled. The cylinders are movable storage units. To ensure consistency in the schedules, the routing and inventory replenishment decisions need to be repetitive within a predetermined planning horizon. We propose a mathematical formulation

that addresses this decision in continuous time and we indicate how to enhance the performance and practical applicability of the model.

1.4.2   LNG as a viable fuel in transportation (Chapter 3)

The adoption of methane in key sectors such as the transportation sector depends strongly on the economic viability of the investments that are necessary to enable its usage. For example, biogas can be upgraded to 'green' gas in which the quality is similar to methane in the gas pipeline grids. The methane can be liquefied at extremely low temperatures to create Liquefied Natural Gas (LNG). In the case of upgraded biogas, we refer to bio-LNG. For brevity, we shall from now on refer to LNG which can be either LNG or bio-LNG.

In the transportation sector, LNG is considered as a promising transition fuel in transitioning to a zero-emission transportation system (Post et al., 2018). For example, ships can be fitted with LNG engines which enable zero particle emissions and low greenhouse gas emissions. Moreover, International Maritime Organization (IMO) regulations in 2020 stipulate that cargo ships are no longer allowed to utilize high-polluting fuel-oils inside Emission Controlled Areas (ECA). Since LNG has been a much cheaper alternative to oil-based fuels based on past LNG prices, this has led to increased attractiveness of cleaner fuels such as LNG. However, the additional investment costs associated with installing LNG engines are still one of the key obstacles to adoption (Wang and Notteboom, 2014).

In Chapter 3, we address the research question: *Under which conditions is the application of LNG economically viable for LNG-fueled ships?* We show that and under which conditions, a cleaner fuel such as LNG can be more attractive than conventional fuels for newly-built ships. This enables ship owners to make better-informed decisions on the purchase of newly-built ships which are fitted with LNG-fueled engines. We develop a simulation model that enables comparing the total costs of newly-built LNG-fueled ships with conventional ships. LNG-fueled ships can have dual-fuel engines that enable utilizing and switching between different fuels while at sea. Since prices of the different fuels fluctuate, a decision must be made on how much of the different fuels to bunker for each trip. Our model takes into account the optimal bunker planning decisions of ship operators in choosing how much of which fuel to bunker. We identify under which conditions LNG-fueled ships are more cost-effective than conventional-fueled ships to facilitate

the increasing adoption of fuels such as LNG.

1.4.3   Combining biogas with solar and wind energy (Chapter 4)

Biogas can also be converted to electricity using a CHP engine. Accordingly, solar, wind, and biogas can all supply demand for electricity. Combining the constant and supply-driven profile of biogas with other energy sources such as wind and solar energy presents opportunities to achieve a better match between supply and demand. Wind, solar, and biogas have an important role in rural areas where land is relatively cheap, abundant and in which the local energy produced can be consumed in local communities and villages.

Since the profiles of biogas, wind and solar energy cannot be directly matched with the electricity consumption profiles of households in villages and communities, storage is needed to bridge the different profiles and the seasonality gap between supply and demand. However, both the share of each energy source in the total supply and the total installed production capacity affect the storage capacity that is needed to overcome short-term and seasonal differences in supply and demand. Accordingly, a trade-off arises in which a high production capacity leads to high curtailment and low storage requirements, and a lower production capacity requires higher levels of storage capacity.

In Chapter 4, we address the research question: *How should biogas, wind, and solar energy be combined across seasons and how is this affected by the level of total production capacity and storage capacity?* We provide insights on the choice of an appropriate mix of energy production and storage to reduce or avoid curtailment while supplying a local community of households with electricity. This enables decision-makers to understand how much storage and production capacity should be installed, and what is an appropriate mix of biogas, solar, and wind energy to most effectively match the resulting supply with demand. We develop a model that highlights the relationship between production and storage capacity requirements and the resulting energy mix while avoiding the inclusion of actual costs. Instead, we use weights to determine the relative importance of production capacity versus storage capacity. The model determines the hourly decisions on how much energy to supply to storage versus how much to provide directly to the electricity demand. We show how the mix of biogas, wind, and solar energy is affected by the different combinations of total installed production capacity and storage capacity

and highlight the implications for the curtailment of energy.

1.4.4   Strategic hydrogen storage for solar parks (Chapter 5)

The widespread adoption of solar parks in rural areas is causing increased electricity grid congestion at the distribution connection in the summer during peak production moments. Hydrogen storage is a promising alternative to grid capacity extension by storing the excess-produced electricity in the form of hydrogen and supply the energy later to a connected community of households. This could potentially help alleviate congestion problems, but also leads to new questions since the behavior of the storage owner is influenced by electricity prices. At low prices, it is interesting to store energy while selling becomes relevant at high prices. However, operating the storage facility is challenging, since the facility owner must provide a reliable supply of energy to the households while maximizing the revenues by interacting with the electricity grid and avoid curtailment. To make hydrogen storage economically viable to storage facility owners as market participants, operational decisions of when to buy and when to sell electricity from or to the grid are important in enhancing the economic viability of hydrogen storage.

In Chapter 5, we address the research question: *Under which conditions should the owner of solar fields with hydrogen buy and sell from and to the grid to maximize profits?* We show how the operator of the solar park and storage facility should operate the facility by interacting with the grid while maintaining a stable supply to the demand and maximize revenues. We consider the seasonality aspects of supply and demand and also show how this behavior affects the peak utilization of the cable connection. This enables grid operators to assess the consequences of the profit-maximizing behavior of the facility owners. We develop a Markov Decision Process model to determine the daily decisions of the owner of the solar field with hydrogen storage on how much to buy and sell to and from the grid. The objective of the facility owner is to maximize profits while directly providing sufficient electricity to the connected households. We explicitly consider the seasonality differences in supply and demand and the uncertain character of prices, electricity demand, and solar production. We examine the consequences of these profit-maximizing decisions on congestion levels at the grid distribution connection. In sensitivity analyses, we investigate the consequences of different capacity levels of the system components to the behavior of the owner and operator of the facility and the utilization of the

grid connection.

1.4.5   The operation of solar parks with hydrogen storage to enable evenly distributed grid feed-in (Chapter 6)

While storage may aid in alleviating congestion problems, the profit-maximizing objective of the facility owner may inhibit this due to opportunistic buying and selling. Moreover, electricity prices increasingly respond to solar energy availability due to the increasing adoption of solar energy. This raises the question of whether storage operation can be based on price-driven operational decisions such as those examined in Chapter 5. Moreover, this also raises the question of how storage should be operated to alleviate potential congestion.

In Chapter 6, we address the research question: *How should solar fields with hydrogen storage be operated to alleviate congestion?* We show how the operation of storage affects the peak utilization of the cable connection and the potential to create congestion problems due to volatility of the grid feed-in. We compare storage decisions that aim to maximize profits with decisions that are price-independent and provide insights into how expanding the cable capacity affects possible congestion problems. We develop a simulation model to compare the profit-oriented buying and selling policies of the facility owner with policies that do not respond to price signals. We develop two heuristics. The first aims to maximize profits and the second prioritizes the use of storage by always storing overages and obtaining shortages from storage. For both heuristics, we consider again seasonality and uncertainty in production, prices, and demand. We examine the consequences of potential congestion problems elsewhere in the grid. In a set of sensitivity analyses, we analyze the consequences of expanding the distribution capacity and different levels of price elasticity. We also examine the influences of grid expansion on the potential congestion and revenues for the facility owner. We provide recommendations to policy-makers and grid operators on the conditions in which it is advisable to expand the distribution capacity and on the operation of storage facilities.

Chapter 2

A continuous-time supply-driven inventory-constrained routing problem

Abstract. *We address an inventory routing problem (IRP) in which routing and inventory decisions are dictated by supply rather than demand. Moreover, inventory is held in containers that act as both a storage container and a movable transport unit. This problem emanates from logistics related to biogas transportation in which biogas is transported in containers from many suppliers to a single facility. We present a novel and compact formulation for the supply-driven IRP which addresses the routing decisions in continuous-time in which inventory levels within the containers are continuous. Valid inequalities are included and realistic instances are solved to optimality. For all experiments, we found that the total transportation time is minimized when the storage capacity at each supplier is larger than or equal to the vehicle capacity. These routes are characterized by tours in which mostly single suppliers are visited. In 95% of the instances, the average content level of the exchanged containers exceeded 99.6%.*

2.1   Introduction

This paper addresses a Supply-Driven Cyclic Inventory-Constrained Routing Problem (SDCICRP) in which the routing, scheduling and inventory decisions are dictated by supply rather than demand. We are the first to address the routing and inventory collection decisions in continuous time in which the inventory contents are continuous in discrete containers. These containers are movable transport units, but also represent the storage capacity at a supplier. We show by solving it in an extensive design, how this problem leads to very specific routing and inventory patterns within each cycle. The problem is also known as a reverse inventory routing problem (Mes, 2014) and emerges when biogas is transported from biogas-producing farmers to a centralized green-gas upgrading facility. Biogas is produced from biomass such as manure at livestock farms. Producers are unable to adjust biogas production to demand due to the underlying processes. The produced biogas must be collected before the available storage capacity in containers is exceeded. Therefore, logistics decisions need to be orchestrated around biogas producers that act as suppliers, creating the supply-driven characteristic. Another important aspect here is that biogas is compressed and stored in containers. These act as both local storage containers and movable transport units. A vehicle collects full or partly filled containers from biogas producers and exchanges these for empty ones. Given that production of biogas is stable, the problem is to find a repetitive schedule including a set of multiple tours that minimizes total transportation time and transports all produced gas and containers to the central facility. From a practical perspective, it is desirable that the schedule is cyclic in the sense that it is repeated after a fixed time period. From our experience in the Netherlands, realistic instances for this problem are typically small (up to 10 suppliers), since limited capacity of the centralized facility only enables a small set of suppliers to provide biogas. While instance size is generally expressed in the number of nodes, the number of vehicles or the number of time periods (for finite, multi-period planning horizons), our problem includes multiple tours for a set of nodes which increases difficulty and instance size.

Inventory routing problems (IRPs) have been studied in several papers and are a class of distribution problems that deal with both inventory replenishment and vehicle routing decisions simultaneously (Coelho et al., 2014). The main goal is to minimize the total inventory and transportation costs over the planning horizon

(Coelho et al., 2014; Ekici et al., 2015). While costs minimization is the most common objective function in the basic IRP literature, other functions can also be used. For example, the logistic ratio studied by Alvarez et al. (2018), Archetti et al. (2017) and Archetti et al. (2019), service level and green house gas footprint by Rahimi et al. (2017). We also refer to Rahimi et al. (2017) for a review of different objective functions in the literature. IRPs are also related to Vendor-Managed Inventory (VMI) problems in which the supplier decides on inventory policies for a set of customers and that enable cost savings by more effectively coordinating shipments and combining customer routes (Vansteenwegen and Mateo, 2014; Coelho et al., 2014). A separate class of IRPs are Cyclic IRPs (CIRP) that deal with finding repetitive routing schedules for long-term decision-making. In CIRPs, the time between replenishments is equal for each customer or the schedule for a fixed planning horizon repeats itself infinitely (Chitsaz et al., 2016; Raa and Aghezzaf, 2008).

Whereas most literature relies on either discretization of time and continuous cycle times between visits, the main difference with other studies is that our formulation addresses both the optimal continuous-time and continuous-inventory solution. We identify the exact point in time at which a supplier is visited and the exact amount of inventory collected in a discrete number containers. In contrast to traditional IRP literature that focuses on the trade-off between inventory and routing costs, we do not consider any cost components. Since we focus on minimizing transportation time in which the routing and inventory decisions are constrained by the container and vehicle storage capacities, the problem can be referred to as an inventory-constrained routing problem. Therefore, we will refer to our problem as a Supply-Driven Cyclic Inventory-Constrained Routing Problem (SDCICRP).

This paper proposes a novel and compact formulation with valid inequalities for the SDCICRP that enables solving realistic instances to optimality. In a design with thousands of experiments we reveal the characteristic routing and inventory patterns provided by these solutions. This study differs from existing approaches by combining the following characteristics. Firstly, we address both continuous time and continuous inventory contents in each container enabling containers to be exchanged while partly filled. Secondly, we address the problem in which a container acts as both a storage container and a movable transport unit. Thirdly, we combine these aspects with multiple tours in cyclic schedules that can be

repeated infinitely. Finally, we address an IRP that is supply-driven, rather than demand-driven in which the relationship between suppliers and a single customer is many-to-one, next to structures in existing literature that also include many-to-one (Hein and Almeder, 2016; Chitsaz et al., 2019) and many-to-many(e.g., Guimarães et al., 2019).

This paper is organized as follows. A literature review is presented in Section 2. Section 3 delineates the proposed MIP formulation and provides valid inequalities to strengthen the continuous relaxation of the model. Section 4 provides detailed computational results of the model and experimental insights on storage capacities at each supplier and routing and inventory collection decisions. Section 5 provides concluding remarks.

2.2   Literature review

In this section, we position our problem in the literature on IRPs for each of the different characteristics related to our problem (see Table 2.1). IRPs are well-studied and we refer to Coelho et al. (2014) for a detailed review. However, the IRP as developed in this paper has not yet been addressed in existing literature. This entails the combination of continuous time and continuous inventory contents, compartments which act as both storage capacity and movable transport units, cyclic schedules and supply-driven routing decisions.

Most IRPs are demand-driven, such that routes are designed in which one or many suppliers service customers that have a certain demand. Early research includes work by Bell et al. (1983), Federgruen and Zipkin (1984) and Golden et al. (1984). These basic versions of IRPs consist of determining routes by minimizing inventory costs while meeting customer demands by shipping products from a single supplier to a number of customers (Anily and Federgruen, 1990; Chien et al., 1989; Bertazzi et al., 2002). Most work on the IRP includes extensions of the basic (demand-oriented) IRP to include multiple items (Speranza and Ukovich, 1994; Viswanathan and Mathur, 1997; Sindhuchao et al., 2005) and heterogeneous fleet composition (Persson and Göthe-Lundgren, 2005; Christiansen, 1999). Other classifications include models with continuous time (Aghezzaf et al., 2006; Anily and Federgruen, 1990; Li et al., 2014; Al-Khayyal and Hwang, 2007; Stanzani et al., 2018; Agra et al., 2017; Christiansen, 1999), discrete time (e.g., Solyalı and Süral, 2008;

Table 2.1: Related themes in IRP literature

Authors	Supply-driven	Continuous time	Cyclic IRP	Transport in discrete containers
Aghezzaf et al. (2006)		✓	✓	
Aghezzaf et al. (2012)		✓	✓	
Agra et al. (2017)		✓		✓
Al-Khayyal and Hwang (2007)	✓	✓		✓
Alvarez et al. (2018)	✓			
Archetti et al. (2007)				
Archetti et al. (2017)				
Archetti et al. (2019)				
Anily and Federgruen (1990)		✓	✓	
Amponsah and Salhi (2004)	✓			
Avella et al. (2004)		✓		✓
Bard et al. (1998)				
Bell et al. (1983)				
Bertazzi et al. (2002)				
Boudia and Prins (2009)				
Campbell and Savelsbergh (2004)				
Chien et al. (1989)				
Chitsaz et al. (2016)		✓	✓	
Chitsaz et al. (2019)				
Christiansen (1999)	✓	✓		
Diz et al. (2017)				✓
Easwaran and Üster (2009)	✓			
Ekici et al. (2015)		✓	✓	
Federgruen and Zipkin (1984)				
Gallego and Simchi-Levi (1990)		✓	✓	
Golden et al. (1984)				
Guimarães et al. (2019)				✓
Hein and Almeder (2016)				
Iassinovskaia et al. (2017)	✓			
Johansson (2006)	✓			
Lahyani et al. (2015)	✓			✓
Larrain et al. (2017)				✓
Liu and Chung (2009)	✓			
Li et al. (2013b)				
Li et al. (2014)		✓		✓
Liu et al. (2015)			✓	
Mes (2014)	✓			
Persson and Göthe-Lundgren (2005)				
Savelsbergh and Song (2008)				✓
Shyshou et al. (2012)			✓	✓
Sindhuchao et al. (2005)		✓		
Solyalı and Süral (2008)				
Solyalı and Süral (2011)				
Soysal (2016)	✓			
Speranza and Ukovich (1994)			✓	
Srivastava (2008)				
Stanzani et al. (2018)	✓	✓		✓
Raa and Aghezzaf (2008)		✓	✓	
Raa and Aghezzaf (2009)		✓	✓	
Raa and Dullaert (2017)			✓	
Raa (2015)			✓	
Vansteenwegen and Mateo (2014)		✓	✓	
Vidović et al. (2014)				✓
Viswanathan and Mathur (1997)			✓	
Yamashita et al. (2019)	✓	✓		✓
Zhao et al. (2008)		✓		

[1]Adapted from Coelho et al. (2014)

Bertazzi et al., 2002; Diz et al., 2017) and both finite (Archetti et al., 2007; Savelsbergh and Song, 2008; Boudia and Prins, 2009) and infinite planning horizons (Raa and Aghezzaf, 2008; Zhao et al., 2008). Work that is supply-driven is still relatively limited.

In IRPs with discretized time periods, the precise time of a visit within a period does not affect the inventory level, as the demand is assumed to happen instantaneously at the begin or end of a period. These do not determine the exact point within a time period in which a node is visited and the exact amount of continuous inventory that is collected or replenished in discrete containers. Time is generally modeled in discrete time periods, which can either be fixed throughout the planning horizon (e.g., Archetti et al., 2007; Amponsah and Salhi, 2004; Lahyani et al., 2015; Larrain et al., 2017) or dynamic (Aghezzaf et al., 2006, 2012; Raa and Aghezzaf, 2008, 2009; Raa, 2015) in which the continuous cycle time between visits is calculated (see Table 2.1). This leads to decisions that are made for a specific time interval. Such schedules may be less accurate, because cyclic schedules in supply-driven problems depend strongly on the precise timing of arrivals in preventing the inventory levels to exceed storage limits. Discretization of time may have severe consequences (Boland et al., 2019). We address this gap by optimally obtaining both the points in time in which a supplier is visited and the exact amounts of inventory collected in each container without affecting calculation times.

To the best of our knowledge, there is limited work available which addresses movable inventory containers that also act as local storage at a supplier and that can be picked up while partly filled. Larrain et al. (2017) address an IRP in which ATMs are replenished using casettes in which the old casette is replaced by a new one with all of its contents. However, time is discretized in their model. Lahyani et al. (2015) address a multi-compartment IRP in which vehicles collect olive oil that need to be loaded inside separate compartments. These compartments do not act as local storage containers at the producer and are fixed at the vehicle. In most other literature, the individual containers are not picked up for transport and are only fully emptied at the supplier site. This assumption is also made in papers related to fuel transportation, in ch fuel is stored and transported in tanks (Avella et al., 2004; Vidović et al., 2014; Li et al., 2014; Savelsbergh and Song, 2008). Papers in which inventory levels are treated as continuous include Savelsbergh and Song (2008); Stanzani et al. (2018) in maritime contexts and Yamashita et al. (2019) in the

liquefied gas industry.

IRPs with a more supply-driven nature relate to waste collection (Mes, 2014; Johansson, 2006; Avella et al., 2004), olive oil collection (Lahyani et al., 2015) and shipping (Christiansen, 1999; Agra et al., 2017; Al-Khayyal and Hwang, 2007; Stanzani et al., 2018; Yamashita et al., 2019). A number of reverse inventory routing problems can be considered both demand-driven and supply-driven. These exist in the context of returnable items in which the returned items that influence the routing decisions and inventory policies (Li et al., 2013b; Liu et al., 2015; Soysal, 2016). Many-to-one structures have also been explored in production and/or assembly contexts, for example, Hein and Almeder (2016); Chitsaz et al. (2019). Guimarães et al. (2019) address a many-to-many IRP with multiple echelons and depots. However, demand has remained the primary mechanism dictating the routing decisions in most of the existing IPR-related literature.

Cyclic scheduling aspects are also an important characteristic of our problem in which multi-tour schedules can be repeated infinitely. In existing literature, cycle time is usually addressed as the time between visits to a location (Aghezzaf et al., 2006, 2012; Raa and Aghezzaf, 2008, 2009; Raa, 2015; Shyshou et al., 2012). In contrast, we replace cycle time by a planning horizon and obtain (multiple) exact times at which each supplier is visited within this planning horizon. The resulting schedule is repeated directly after this planning horizon. According to Vansteenwegen and Mateo (2014), rudimentary contributions on CIRPs stem from Anily and Federgruen (1990) and Gallego and Simchi-Levi (1990). Furthermore, Speranza and Ukovich (1994) and Viswanathan and Mathur (1997) considered repetitive transportation plans for multiple products. Aghezzaf et al. (2006) consider multiple tours and vehicles for the CIRP. In their work, vehicles are assigned to specific regions and service a subset of customers in a repetitive manner where the cycle times (i.e., time between replenishments for each customer) are equal for a given solution. Vansteenwegen and Mateo (2014) and Chitsaz et al. (2016) address a similar problem and treat cycle time as a key decision variable. Ekici et al. (2015) deal with cyclic schedules by setting beginning inventory levels equal to ending inventory levels for a predefined planning horizon, a condition that we adopt in this paper. Even though cycle times in the literature are modeled in continuous time, existing models have not addressed the routing and inventory collection decisions in continuous-time with continuous inventory contents in discrete containers.

2.3   Problem description

In this section, we describe in detail the SDCICRP and introduce a mathematical formulation. We consider a logistics system in which biogas from decentralized suppliers is transported to a single depot or customer. We summarize the definitions of sets, parameters and variables in Table 2.

2.3.1   The SDCICRP

The SDCICRP defined in this paper is represented on an undirected graph $\mathcal{G} = \{\mathcal{V}, \mathcal{E}\}$ in which $\mathcal{V} = \{0, \ldots, N+1\}$ represents the set of suppliers $\mathcal{V}^{'} = \{1, \ldots, N\}$ and includes the departure depot $\{0\}$ and arrival depot $\{N+1\}$. $\mathcal{V}^o = \{0, \ldots, N\}$ is defined as the set of suppliers which includes the origin depot and $\mathcal{V}^d = \{1, \ldots, N+1\}$ as the set of suppliers that includes the destination depot. Both the origin and destination depot are assumed to be at the same location. $\mathcal{E} = \{(i,j) : i, j \in \mathcal{V}, i \neq j\}$ denotes the set of edges. Each edge is associated with a transportation time T_{ij}. Each supplier $i \in \mathcal{V}^{'}$ produces at a constant rate W_i per unit of time. Furthermore, there exists an unordered set of available inventory containers $\mathcal{H} = \{1, \ldots, E\}$ at each supplier in which full containers are given the lowest numbers. The container capacity at each supplier in which gas inventory can be stored is represented by U. For each tour k in a set of tours $\mathcal{K} = \{0, \ldots, P\}$, a single vehicle with capacity Q (in number of containers) exchanges empty container(s) for (partly) filled one(s) at a subset of suppliers. The model assumes that each tour k cannot visit the same node twice, but two different tours can visit the same node. These tours occur during a predefined planning horizon D. Figure 2.1 illustrates one feasible solution for a single example tour k in one arbitrary instance of 3 suppliers in which containers at each supplier have different content levels.

The route is represented by a set of binary variables x_{ijk} that specify whether edge $(i,j) \in \mathcal{E}$ is included in tour $k \in \mathcal{K}$. s_{ik} represents the time at which the vehicle arrives at node $i \in \mathcal{V}$ in tour $k \in \mathcal{K}$ and is calculated as the sum of transportation times for edges traversed earlier in tour $k \in \mathcal{K}$. z_{ik} denotes the remaining travel time after the visit at supplier i before reaching the depot in tour $k \in \mathcal{K}$. g_{ik} represents the inventory after gas has been picked up, whereas a_{ik} denotes the amount of gas picked up at supplier $i \in \mathcal{V}^{'}$ for tour $k \in \mathcal{K}$. Moreover, b_k represents the vehicle waiting time at the depot before embarking on tour $k \in \mathcal{K}$. l_{ihk} indicates whether

container $h \in \mathcal{H}$ is exchanged at supplier $i \in \mathcal{V}'$ for tour $k \in \mathcal{K}$. Finally, variable y_i denotes the starting inventory levels for each supplier $i \in \mathcal{V}'$ at the beginning of the planning horizon. The main objective is to minimize total transportation time, which consists of the sum of transportation times related to the traversed edges.

Table 2.2: Sets, parameters and decision variables

Sets	
$\mathcal{V}$	Set of all nodes which includes the origin and destination depot and suppliers $\mathcal{V} = \{0, \ldots, N+1\}$
$\mathcal{V}'$	Set of all suppliers excluding the depots $\mathcal{V}' = \{1, \ldots, N\}$
$\mathcal{V}^o$	Set of suppliers and the origin depot $\mathcal{V}^o = \{0, \ldots, N\}$
$\mathcal{V}^d$	Set of suppliers and the destination depot $\mathcal{V}^d = \{1, \ldots, N+1\}$
$\mathcal{K}$	Set of tours $\mathcal{K} = \{0, \ldots, P\}$
$\mathcal{H}$	Set of containers at each supplier $\mathcal{H} = \{1, \ldots, E\}$
i, j	Indices on the set of nodes $i, j \in \mathcal{V}, i \neq j$
k	Index on the set of tours $k \in \mathcal{K}$
h	Index on the set of containers $h \in \mathcal{H}$
Parameters	
Q	Vehicle capacity in number of containers
T_{ij}	Transportation time associated with edge $(i,j) \in \mathcal{E}$
U	Container capacity
W_i	Production rate of supplier $i \in \mathcal{V}'$
D	Length of planning horizon
Variables	
x_{ijk}	Binary variable indicating whether or not edge $(i,j) \in \mathcal{E}, i \neq j$ is included in tour $k \in \mathcal{K}$
l_{ihk}	Binary variable indicating whether or not container $h \in \mathcal{H}$ has been exchanged at supplier $i \in \mathcal{V}'$ for tour $k \in \mathcal{K}$
s_{ik}	Arrival time of the vehicle at node $i \in \mathcal{V}$ of tour $k \in \mathcal{K}$
g_{ik}	Inventory at supplier $i \in \mathcal{V}'$ for tour $k \in \mathcal{K}$ after pickup
z_{ik}	Remaining travel time when arriving at node $i \in \mathcal{V}$ for tour $k \in \mathcal{K}$
b_k	Waiting time of the vehicle at the depot before embarking on tour $k \in \mathcal{K}$
a_{ik}	Amount of cargo picked up at supplier $i \in \mathcal{V}'$ for tour $k \in \mathcal{K}$
y_i	Starting inventory level at supplier $i \in \mathcal{V}'$

The mathematical formulation is as follows.

$$\min \quad \sum_{i \in \mathcal{V}} \sum_{j \in \mathcal{V}} \sum_{k \in \mathcal{K}} x_{ijk} T_{ij} \tag{2.1}$$

$$\text{s.t.} \sum_{j \in \mathcal{V}} x_{ijk} \leq 1 \qquad \forall\, i \in \mathcal{V},\ k \in \mathcal{K} \tag{2.2}$$

$$\sum_{i \in \mathcal{V}} x_{ijk} \leq 1 \qquad \forall\, j \in \mathcal{V},\ k \in \mathcal{K} \tag{2.3}$$

$$\sum_{i \in \mathcal{V}} x_{i,N+1,k} = 1 \qquad \forall\, k \in \mathcal{K} \tag{2.4}$$

$$\sum_{j \in \mathcal{V}} x_{0jk} = 1 \qquad \forall\, k \in \mathcal{K} \tag{2.5}$$

$$x_{iik} = 0 \qquad \forall\, i \in \mathcal{V},\ k \in \mathcal{K} \tag{2.6}$$
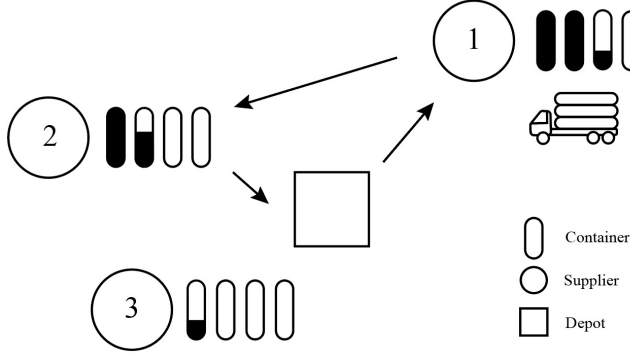
Figure 2.1: General graphical representation of the SDCICRP for a single example tour k with different container inventory levels ($Q = 3$ and $E = 4$)

$$\sum_{i \in \mathcal{V}^o} x_{ijk} - \sum_{i \in \mathcal{V}^d} x_{jik} = 0 \qquad\qquad \forall\, j \in \mathcal{V}^{'},\, k \in \mathcal{K} \qquad (2.7)$$

$$s_{jk} - s_{ik} \le T_{ij} + M(1 - x_{ijk}) \qquad\qquad \forall\, i \in \mathcal{V}^o,\, j \in \mathcal{V}^d,\, k \in \mathcal{K} \qquad (2.8)$$

$$s_{jk} - s_{ik} \ge T_{ij} - M(1 - x_{ijk}) \qquad\qquad \forall\, i \in \mathcal{V}^o,\, j \in \mathcal{V}^d,\, k \in \mathcal{K} \qquad (2.9)$$

$$s_{0k} = 0 \qquad\qquad \forall\, k \in \mathcal{K} \qquad (2.10)$$

$$z_{ik} = \sum_{m \in \mathcal{V}} \sum_{j \in \mathcal{V}} x_{mjk} T_{mj} - s_{ik} \qquad\qquad \forall\, i \in \mathcal{V},\, k \in \mathcal{K} \qquad (2.11)$$

$$g_{ik} = g_{ik-1} + W_i(z_{ik-1} + s_{ik} + b_k) - a_{ik} \qquad\qquad \forall\, i \in \mathcal{V}^{'},\, k \in \mathcal{K} \backslash \{0\} \qquad (2.12)$$

$$g_{i0} = y_i + W_i(s_{i0} + b_0) - a_{i0} \qquad\qquad \forall\, i \in \mathcal{V}^{'} \qquad (2.13)$$

$$g_{ik} + a_{ik} \le UE \qquad\qquad \forall\, i \in \mathcal{V}^{'},\, k \in \mathcal{K} \qquad (2.14)$$

$$g_{ik} \le UE - \sum_{h \in \mathcal{H}} Ul_{ihk} \qquad\qquad \forall\, i \in \mathcal{V}^{'},\, k \in \mathcal{K} \qquad (2.15)$$

$$g_{lk} = 0 \qquad\qquad \forall\, l \in \{0, N+1\},\, k \in \mathcal{K} \qquad (2.16)$$

$$a_{ik} \le \sum_{h \in \mathcal{H}} Ul_{ihk} \qquad\qquad \forall\, i \in \mathcal{V}^{'},\, k \in \mathcal{K} \qquad (2.17)$$

$$a_{ik} \ge U(-1 + \sum_{h \in \mathcal{H}} l_{ihk}) + \epsilon \qquad\qquad \forall\, i \in \mathcal{V}^{'},\, k \in \mathcal{K} \qquad (2.18)$$

$$\sum_{i \in \mathcal{V}} \sum_{j \in \mathcal{V}} \sum_{k \in \mathcal{K}} x_{ijk} T_{ij} + \sum_{k \in \mathcal{K}} b_k = D \qquad\qquad (2.19)$$

$$\sum_{i \in \mathcal{V}'} \sum_{h \in \mathcal{H}} l_{ihk} \le Q \qquad\qquad \forall\, k \in \mathcal{K} \qquad (2.20)$$

$$\sum_{h \in \mathcal{H}} l_{ihk} \leq E \sum_{j \in \mathcal{V}} x_{ijk} \qquad \forall\, i \in \mathcal{V}', k \in \mathcal{K} \quad (2.21)$$

$$y_i = g_{iP} + W_i z_{iP} \qquad \forall\, i \in \mathcal{V}' \quad (2.22)$$

$$\sum_{h \in \mathcal{H}} l_{ihk} \geq \sum_{j \in \mathcal{V}} x_{ijk} \qquad \forall\, i \in \mathcal{V}',\ k \in \mathcal{K} \quad (2.23)$$

$$\sum_{j \in \mathcal{V}} x_{jik} \geq l_{ihk} \qquad \forall\, i \in \mathcal{V}', h \in \mathcal{H}, k \in \mathcal{K}. \quad (2.24)$$

$$x_{ijk} \in \{0,1\} \qquad \forall\, i, j \in \mathcal{V}, k \in \mathcal{K} \quad (2.25)$$

$$l_{ihk} \in \{0,1\} \qquad \forall\, i \in \mathcal{V}, h \in \mathcal{H}, k \in \mathcal{K} \quad (2.26)$$

$$s_{ik} \geq 0 \qquad \forall\, i \in \mathcal{V}, k \in \mathcal{K} \quad (2.27)$$

$$g_{ik} \geq 0 \qquad \forall\, i \in \mathcal{V}, k \in \mathcal{K} \quad (2.28)$$

$$a_{ik} \geq 0 \qquad \forall\, i \in \mathcal{V}, k \in \mathcal{K} \quad (2.29)$$

$$y_i \geq 0 \qquad \forall\, i \in \mathcal{V} \quad (2.30)$$

$$z_i \geq 0 \qquad \forall\, i \in \mathcal{V} \quad (2.31)$$

$$b_i \geq 0 \qquad \forall\, i \in \mathcal{V}. \quad (2.32)$$

Constraints (2.2) ensure that the vehicle can only visit one destination node from origin i, whereas constraints (2.3) ensure that the vehicle can only come from one origin i to destination j for each tour. Constraints (2.4) and (2.5) ensure the vehicle starts at the origin depot 0 and ends at the destination depot $N+1$. Constraints (2.6) ensure that destination node is not the same node as the origin node i. Constraints (2.7) ensure that two edges are incident to every node that is visited by connecting nodes in a tour.

Constraints (2.8) and (2.9) ensure that the difference between the time of arrival at node i and node j for each tour k is equal to the transportation time between i and j when $x_{ijk} = 1$. The big M represents a VRP solution cost in which the transportation time of a single tour is maximized, which is calculated heuristically using a furthest neighbor approach. Constraints (2.10) ensure that the arrival time at the origin depot is 0 for each tour k. Constraints (2.11) determine the remaining transportation time for each visited node i before reaching the depot in tour k.

Constraints (2.12) determine the inventory levels after inventory has been picked up when visiting supplier i for each tour k. Constraints (2.13) calculate the inventory levels for each supplier i once that supplier is visited for tour $k = 0$. Constraints

(2.14) ensure that the inventory level before being picked up does not exceed the total capacity of the available containers at each supplier i. Constraints (2.15) ensure that the gas inventory after a pickup does not exceed the available capacity of the non-exchanged containers at supplier i for each tour k. Constraints (2.16) ensure that the gas inventory is equal to zero at the origin and departure depot for each tour k.

Constraints (2.17) ensure the amount that is picked up at supplier i does not exceed the available storage capacity in containers at that supplier for each tour k. Constraints (2.18) ensure that no additional empty containers are collected. For cases in which the vehicle capacity exceeds the total amount of gas collected during a tour (measured in containers), these constraints prevent exchanging additional empty containers which do not affect the objective value. The value of ϵ was set at a small number, 10^{-4}. Constraint (2.19) ensures that the sum of transportation times and waiting times are equal to the planning horizon. Constraints (2.20) ensure that the number of containers that can be exchanged in tour k does not exceed the vehicle capacity. Constraints (2.21) ensure that the number of containers exchanged at supplier i are less or equal to the available containers when visiting that supplier in tour k. Constraints (2.22) ensure that the starting inventory level at each supplier i is equal to the final inventory level at that supplier measured at the end of the last tour. Constraints (2.23) ensure that at least a container has to be exchanged at supplier i if that supplier is visited by tour k. Constraints (2.24) ensure that if a container exchange is performed at a supplier, that supplier must be included in a tour.

Constraints (2.25) and (2.26) define the route x_{ijk} and exchanged containers l_{ihk} to be binary. Finally, constraints (2.27) to (2.32) represent the non-negativity constraints of the decision variables.

2.3.2   Time windows

In practice, it may not be desirable for vehicles to arrive at a supplier at certain times outside working hours (e.g., at night). Therefore, our model can be extended to consider time windows in which a supplier can and cannot be visited. We define a set of time windows $f \in \mathcal{F}$, where $\mathcal{F} = \{0, \ldots, F\}$. Let t_{ik} denote the actual (cumulative) time at which supplier i is visited in tour k.

$$t_{in} = \sum_{k=1}^{n} s_{ik} + b_k + z_{ik-1} \qquad\qquad \forall\, n \in \mathcal{K}, i \in \mathcal{V}' \qquad (2.33)$$

$$t_{i0} = s_{ik} \qquad\qquad \forall\, i \in \mathcal{V}' \qquad (2.34)$$

We define u_f^- and u_f^+ as the beginning and end of time window f respectively. Moreover, we introduce an auxiliary binary variable r_{fk} which specifies whether t_{ik} occurs before u_f^- or after u_f^+. The following constraints ensure that these windows are avoided in the solution. The big M value was set as $M = D$.

$$t_{ik} \le u_f^- + M(1 - r_{fk}) \qquad\qquad \forall\, i \in \mathcal{V}', k \in \mathcal{K}, f \in \mathcal{F} \qquad (2.35)$$

$$t_{ik} \ge u_f^+ - M r_{fk} \qquad\qquad \forall\, i \in \mathcal{V}', k \in \mathcal{K}, f \in \mathcal{F}. \qquad (2.36)$$

2.3.3 Valid inequalities

Since multiple optimal solutions exist for a single instance, we provide valid inequalities (VIs) in order to strengthen the continuous relaxation of the model and reduce the number of optimal solutions without loss of generality. The valid inequalities are based on the relationship between exchanged containers, supplier visits and flows which leave the depot. These extend the model as described in Section 3.1.

A tour cannot be made after arriving at the destination depot and before departing at the origin depot.

$$\sum_{j \in \mathcal{V}} x_{N+1,jk} = 0 \qquad\qquad \forall\, k \in \mathcal{K} \qquad (2.37)$$

$$\sum_{i \in \mathcal{V}} x_{i0k} = 0 \qquad\qquad \forall\, k \in \mathcal{K}. \qquad (2.38)$$

The vehicle must either move from i to j or from j to i.

$$x_{ijk} + x_{jik} \le 1 \qquad\qquad \forall\, i, j \in \mathcal{V}', \ k \in \mathcal{K}. \qquad (2.39)$$

A container exchange also implies that a vehicle must have left the depot to a supplier. Hence, we can express this as follows.

$$\sum_{i \in \mathcal{V}'} x_{0ik} \geq l_{jhk} \qquad\qquad \forall\, j \in \mathcal{V}', h \in \mathcal{H}, k \in \mathcal{K}. \qquad (2.40)$$

The following inequalities are related to leaving the depot and visiting other nodes. If a tour is performed to serve a supplier, then that tour must have left the depot to another supplier.

$$\sum_{i \in \mathcal{V}'} x_{0ik} \geq x_{mjk} \qquad\qquad \forall\, m, j \in \mathcal{V}', k \in \mathcal{K}. \qquad (2.41)$$

In order to ensure that the final inventory levels do not exceed the initial inventory levels, a minimum number of container exchanges during the planning horizon are those for which full containers are exchanged. Therefore, the total number of container exchanges for each supplier is larger than or equal to the minimum amount of exchanges.

$$\sum_{h \in \mathcal{H}} \sum_{k \in \mathcal{K}} l_{ihk} \geq \left\lceil \frac{DW_i}{U} \right\rceil \qquad\qquad \forall\, i \in \mathcal{V}'. \qquad (2.42)$$

For each supplier, the number of visits in which a tour from the any supplier to the depot is performed should be larger than or equal to the minimum number of visits $\gamma = \left\lceil \dfrac{\sum_{i \in \mathcal{V}'} DW_i / U}{Q} \right\rceil$. The minimum number of visits is represented by single tours in which a single supplier is visited and Q containers are picked up while completely filled.

$$\sum_{i \in \mathcal{V}'} \sum_{k \in \mathcal{K}} x_{i,N+1,k} \geq \gamma. \qquad (2.43)$$

Since each supplier must be visited at least once in the planning horizon, we can select a specific supplier v, being the one that has the lowest production rate, to be

included in the last tour to reduce the number of optimal solutions.

$$\sum_{i \in \mathcal{V}} x_{ivP} = 1. \tag{2.44}$$

No containers can be exchanged at each supplier when tour k is empty and no suppliers are visited.

$$l_{ihk} + x_{0,N+1,k} \leq 1 \qquad \qquad \forall\, i \in \mathcal{V}', h \in \mathcal{H}, k \in \mathcal{K}. \tag{2.45}$$

Empty tours in which no suppliers are visited can be scheduled successively at the start of the planning horizon to reduce the number of optimal solutions without loss of generality.

$$x_{0,N+1,k+1} \leq x_{0,N+1,k} \qquad \qquad \forall\, k \in \{0, \ldots, P-1\}. \tag{2.46}$$

Since empty tours occur at the beginning of the planning horizon, the last tour must include one visit from the depot to a supplier and back and this tour cannot be empty.

$$\sum_{i \in \mathcal{V}'} x_{i,N+1,P} = 1 \tag{2.47}$$

$$x_{0,N+1,P} = 0. \tag{2.48}$$

Exchanged containers can be arranged such that container h must be exchanged before container $h+1$.

$$l_{ihk} \geq l_{i,h+1,k} \qquad \qquad \forall\, i \in \mathcal{V}', h \in \{1, \ldots, E-1\}, k \in \mathcal{K}. \tag{2.49}$$

Since container h must be exchanged before container $h+1$ and a container can only be exchanged when supplier i is visited, we can enforce l_{i1k} to always be one when supplier i is visited.

$$l_{i1k} - \sum_{j \in \mathcal{V}} x_{ijk} = 0 \qquad\qquad \forall\, i \in \mathcal{V}', k \in \mathcal{K}. \qquad\qquad (2.50)$$

The number of visits to supplier i during the planning horizon must be larger than or equal to the minimum number of visits required in order to pick up all inventory at that supplier.

$$\sum_{j \in \mathcal{V}^d} \sum_{k \in \mathcal{K}} x_{ijk} \geq \left\lceil \frac{DW_i}{UQ} \right\rceil \qquad\qquad \forall\, i \in \mathcal{V}'. \qquad\qquad (2.51)$$

In any given tour, the number of visited suppliers cannot exceed the vehicle capacity in containers.

$$\sum_{i \in \mathcal{V}'} \sum_{j \in \mathcal{V}^d} x_{ijk} \leq Q \qquad\qquad \forall\, k \in \mathcal{K}. \qquad\qquad (2.52)$$

Since waiting times before empty tours in which no suppliers are visited can have any value, we can set the waiting time b_k to zero for any empty tour to reduce the number of optimal solutions. We can define the big M as the maximum waiting time, which is denoted by the time to completely fill the minimum of the available storage capacity E or truck capacity Q minus the transport time from the depot to the fastest producer f and back, $M = (\min\{E, Q\}U)/W_f - 2T_{0f}$.

$$b_k \leq M(1 - x_{0,N+1,k}) \qquad\qquad \forall\, k \in \mathcal{K}. \qquad\qquad (2.53)$$

The difference between the total quantity produced and the total quantity of gas collected during the planning horizon must be zero.

$$W_i D - \sum_{k \in \mathcal{K}} a_{ik} = 0 \qquad\qquad \forall\, i \in \mathcal{V}'. \qquad\qquad (2.54)$$

Time windows

For the time windows extension of Section 2.3.2, we introduce the following valid inequalities in order to enhance the performance of the model.

An arrival in tour k that occurs before the beginning of time window u_f^- always occurs before the begining of time window u_{f+1}^-.

$$r_{f+1,k} \geq r_{fk} \qquad\qquad \forall\, f \in \{0, \ldots, F-1\}, k \in \mathcal{K}. \qquad (2.55)$$

Since empty tours are scheduled in the beginning of the planning horizon for which the cumulative arrival time at each supplier in that tour t_{ik} is zero, empty tours should always occur before an arrival to any time window.

$$x_{0,N+1,k} \leq r_{fk} \qquad\qquad \forall\, f \in \mathcal{F}, k \in \mathcal{K}. \qquad (2.56)$$

2.4   Computational results

In this section, we analyze the solution quality and computational efficiency of the model, and obtain experimental insights. In Section 2.4.1, we define the instance sets. In Section 2.4.2, we assess the solution quality and computational efficiency of the model and evaluate the impact of the valid inequalities (2.37) to (2.54). Section 4.3 evaluates the impact of the number of suppliers on computation times. Section 4.4 provides the general experimental insights. Finally, Section 4.5 provides a detailed illustrative example of the resulting routing and inventory decisions.

2.4.1   Sets of instances

The instance sets for the SDCICRP (see Table 2.3) are based on a real-life example. The instances are grouped in 5 sets. Sets 1 and 2 are used to asses the solution quality and computational efficiency. Set 1 is the benchmark set and set 2 is used to test the impact of larger numbers of suppliers. Set 3, 4 and 5 are included to gain experimental insights and determine parameter sensitivity. All instances in the sets have a cyclic planning horizon of one week. We consider production

rates that represent an integer number of container equivalents produced during the planning horizon. The production rates reflect rates that are common in practice. The transportation times between nodes are symmetric. The total number of tours P in the set of tours $\mathcal{K}$ was set to the minimal number of tours needed y, increased by 4. Based on computational tests, 5 additional tours did not lead to a change in objective values for the instances in set 1. Therefore, we assume that 4 additional tours is a sufficient number.

The first instance set comprises small-scale instances with 4 suppliers with randomly generated locations. The coordinates of both the suppliers and depot are randomly chosen within a range of 0 and 60 minutes travel time to calculate the transportation time matrix. The container size is set at 1500 which reflects the size in m^3 of compressed gas in movable containers for tube trailers in practice. The storage capacity at each supplier ranges between 2 to 4 containers and the vehicle capacity ranges between 3 to 5 containers, which represent existing configurations for trucks. Each combination of storage and vehicle capacities is in turn combined with 5 levels of randomly obtained production rates sampled from the range between 6 and 11 containers per week at each supplier reflecting rates of existing biogas producers.

The instances in the second set comprise an increased number of suppliers ranging between 5 and 9. The supplier coordinates of 9 suppliers have been fixed and the instances with less suppliers form a subset of these. The production speeds have been fixed for all instances in this set, in order to examine the effect of the amount of suppliers on calculation times. Both the storage capacity at each supplier and vehicle capacity range between 3 to 5 containers.

Based on the computational tests, 5 suppliers were used in the third set of instances. In this set, we generate 3200 instances as follows. We apply 4 levels for the storage capacity, vehicle capacity, and production rates. For each combination of these 3 variables, we solve 50 pregenerated instances with random depot and supplier coordinates within a range of 0 and 60 minutes on the x and y axis. The storage capacities and vehicle capacities both range between 2 to 5 containers. The 4 levels for production rates for the 5 suppliers consist of a combination with low mean and low variance (9, 5, 7, 8, 6), low mean, high variance (5, 6, 11, 12, 4), high mean, low variance (9, 11, 10, 13, 12) and high mean, high variance (5, 9, 12, 14, 13). The high production rates are on average 31% higher than the low production rates.

In set 4, the 3200 instances of set 3 were solved with time windows activated in

the model. In the planning horizon of one week, 7 time windows were implemented in which the vehicle can only visit a supplier between 06:00 and 18:00 during the day. It is assumed that the planning horizon starts on the first day at 06:00.

Set 5 consists of 3 instances that are solved in order to give a detailed illustration of routing and inventory decisions for existing locations of biogas producers. With fixed supplier coordinates and a vehicle capacity of 4 containers, we vary storage capacities between 2 and 4 containers.

Table 2.3: Summary of the experiments

Set	Number of instances	Number of suppliers	Storage capacity	Vehicle capacity	Time windows	Supplier and depot coordinates	Production rates
1	45	4	2-4	3-5	No	Random	Random
2	45	5-9	3-5	3-5	No	Fixed	Fixed
3	3200	5	2-5	2-5	No	50 random combinations [1]	4 combinations
4	3200	5	2-5	2-5	Yes	The same as set 3	The same as set 3
5	3	4	2-4	4	No	Fixed	Fixed

[1]50 instances of randomly generated locations for which the combinations of storage capacity, vehicle capacity and production rates are varied

2.4.2   Computational results and valid inequalities

We present the computational results of the model for the instances of set 1 by using the valid inequalities presented in Section 2.3.3. These were solved using Gurobi 7.0.2 within a computation time limit of 12000 seconds and a memory limit of 4Gb. The instances without valid inequalities required a memory limit of 8Gb.

Impact of all valid inequalities

Table 2.4 provides the results to generate multi-tour cyclic schedules for 4 suppliers. Columns 1 and 2 show the storage capacity at each supplier and the vehicle capacity in the number of containers. Column 3 (Solution) reports the objective value of the obtained solution, which is either the optimal solution (bold) or the upper bound in case the instance could not be solved to optimality. Columns 4 and 5 report the calculation times for the instances of set 1 with and without the proposed valid inequalities (cuts). Columns 6 and 7 report the optimality gap which is calculated as (Upper Bound − Lower Bound)/Lower Bound. The last column illustrates the percentage reduction in calculation time as a result of the valid inequalities. If an instance could not be solved, the last column indicates that a time reduction is not available. If only the instances with cuts could be solved in the time limit, the last column indicates the percentage time reduction relative to the time limit.

The results in Table 2.4 show that the valid inequalities highly affect the calculation times with an average time reduction of 93%. The valid inequalities also highly affect the ability to solve the instances to optimality within the specified time limit. Only 5 out of 45 instances could be solved without valid inequalities compared to 44 out of 45 instances with the valid inequalities within the time limit. For the instances with valid inequalities enabled, 34 out of the 45 instances could be solved in less than 10 minutes.

Impact of individual sets of valid inequalities

In order to assess the impact of each individual set of valid inequalities, we have performed additional experiments for each instance in set 1 (see Table 2.3). Firstly, Table 2.5 shows the percentage time increase for each set of VIs when it was omitted relative to the computation time in which all VIs were activated. In these experiments, a time limit of 12000 seconds was set in which all instances except instance 32 and 34 could be solved to optimality. Secondly, Table 2.6 shows the gap improvement in % points of the lower bound for the instances in set 1 in which the continuous relaxation was solved. This enables identifying the extent to which a set of VIs contributes to an improved lower bound in the root node.

The experiments in Table 2.5 indicate that omitting any of the sets of VIs leads to a positive increase in computation times on average, even though the effects vary across instances. In particular, Table 2.5 shows that omitting each of the VIs (37), (43), (44), (46), (49) and (54) lead to the strongest performance effect in which the average computation time increases range between 48% to 1298% relative to having all VIs activated. VIs (46) break symmetry in which empty tours are scheduled sequentially and in the beginning of the planning horizon. These are most effective with a 1298% time increase when omitted. VIs (44) which schedule the slowest producer in the last tour are also very effective (121%). VIs (49) sequentially arrange the order of container exchanges (79%). VIs (43) provide lower bounds on the number of tours (77%). VIs (37) ensure that tours departing from the destination depot cannot be made in each tour (50%). Omitting VIs (54) which enforce all gas to be collected leads to a 48% computation time increase.

The experiments in Table 2.6 show that the optimality gap improvement in % points of the lower bound in the root node as a result of each VI is strongest for VI (40), (43) and (45) and ranges between 23% and 25%. In contrast to the results in Table

Table 2.4: Valid inequalities improvements with 4 suppliers

E	Q	Solution	Time (seconds)		Gap (%)		Time reduction (%)	Production rates[2]			
			Cuts	No cuts	Cuts	No cuts		1	2	3	4
2	3	**885.3**	407.4	12000.4	0.0	9.7	96.6	10	8	8	7
2	3	**782.1**	745.6	12000.4	0.0	12.1	93.8	6	7	9	8
2	3	**924.1**	1174.2	12000.4	0.0	3.2	90.2	7	9	9	8
2	3	**880.4**	924.1	12000.2	0.0	1.4	92.3	9	9	10	6
2	3	**412.6**	21.9	6741.8	0.0	0.0	99.7	6	10	8	6
2	4	**915**	1133.9	12000.1	0.0	10.0	90.6	10	8	8	7
2	4	**877.2**	147.6	12000.3	0.0	10.5	98.8	6	7	9	8
2	4	**431.2**	110.1	12000.2	0.0	5.5	99.1	7	9	9	8
2	4	**754.3**	2566.4	12000.1	0.0	18.6	78.6	9	9	10	6
2	4	**933.1**	1019.8	12000.1	0.0	22.1	91.5	6	10	8	6
2	5	**741.3**	45.1	12000.2	0.0	1.6	99.6	10	8	8	7
2	5	**660.4**	2387.3	4748.3	0.0	0.0	49.7	6	7	9	8
2	5	**773.8**	458.1	12000.1	0.0	7.8	96.2	7	9	9	8
2	5	**452**	651.0	12000.1	0.0	11.3	94.6	9	9	10	6
2	5	**713.9**	42.6	12000.2	0.0	3.1	99.6	6	10	8	6
3	3	**949**	1092.4	12000.6	0.0	7.9	90.9	10	8	8	7
3	3	**906.3**	507.6	12000.1	0.0	6.2	95.8	6	7	9	8
3	3	**530.4**	3.3	12000.2	0.0	0.3	100.0	7	9	9	8
3	3	**926.2**	2.2	12000.2	0.0	6.4	100.0	9	9	10	6
3	3	**731.1**	10.7	12000.2	0.0	7.8	99.9	6	10	8	6
3	4	**528.7**	100.5	12000.1	0.0	3.2	99.2	10	8	8	7
3	4	**515.9**	33.2	12000.3	0.0	0.3	99.7	6	7	9	8
3	4	**520.5**	206.0	12000.2	0.0	2.6	98.3	7	9	9	8
3	4	**822.1**	25.3	12000.4	0.0	18.2	99.8	9	9	10	6
3	4	**605.2**	34.5	12000.2	0.0	0.9	99.7	6	10	8	6
3	5	**434**	24.3	12000.2	0.0	4.0	99.8	10	8	8	7
3	5	**496.7**	197.3	12000.3	0.0	4.6	98.4	6	7	9	8
3	5	**715.1**	239.1	12000.1	0.0	9.3	98.0	7	9	9	8
3	5	**284.6**	6.5	546.1	0.0	0.0	98.8	9	9	10	6
3	5	**427.8**	3.9	1370.1	0.0	0.0	99.7	6	10	8	6
4	3	**801.2**	26.4	12000.3	0.0	5.8	99.8	10	8	8	7
4	3	651.8	12000.5	12000.4	6.1	11.0	n.a.	6	7	9	8
4	3	**534.2**	30.9	12000.2	0.0	2.6	99.7	7	9	9	8
4	3	**463.9**	6887.1	12000.2	0.0	13.7	42.6	9	9	10	6
4	3	**918.4**	74.8	12000.2	0.0	15.6	99.4	6	10	8	6
4	4	**638**	2.4	12000.1	0.0	5.4	100.0	10	8	8	7
4	4	**684.7**	18.6	12000.5	0.0	8.5	99.8	6	7	9	8
4	4	**731.7**	1.5	12000.5	0.0	9.6	100.0	7	9	9	8
4	4	**333.4**	86.0	12000.5	0.0	14.1	99.3	9	9	10	6
4	4	**676.8**	46.2	12000.3	0.0	17.0	99.6	6	10	8	6
4	5	**518**	9.9	12000.5	0.0	0.1	99.9	10	8	8	7
4	5	**668.9**	334.4	12000.2	0.0	15.7	97.2	6	7	9	8
4	5	**676.7**	12.3	12000.9	0.0	10.7	99.9	7	9	9	8
4	5	**535.4**	28.4	12001.0	0.0	0.2	99.8	9	9	10	6
4	5	**365.1**	14.0	4328.3	0.0	0.0	99.7	6	10	8	6
Average		660.6	753.2	11061.0	0.1	7.1	93.0				

[2]Number of containers per week

2.5, the remaining VIs lead to either no improvement of a very small improvement up to 4.1% even though these VIs contribute much more strongly to a reduction in computation times when the model was solved to optimality (see Table 2.5). This suggests that the remaining VIs are more effective at lower branches in the branch-and-bound tree.

In sum, VIs (37), (43), (44), (46), (49) and (54) related to depot departures and arrivals, scheduling of empty tours, setting which of the containers are exchanged and setting the difference between production and gas collected are most effective in solving the model.

2.4.3   Computational results and number of suppliers

We present the computational results of the instances in set 2 that varies the number of suppliers. For all instances in set 2, the valid inequalities are applied. The experiments were again performed with a time limit of 12000 seconds and 4Gb memory limit.

Table 2.7 shows that the number of suppliers highly affect calculation times, as expected. Moreover, the model with the valid inequalities can solve instances containing 7 suppliers within the time limit of 12000 seconds. All instances with 5 suppliers could be solved to optimality within the time limit. Three out of 9 instances with 6 suppliers could be solved to optimality and one instance with 7 suppliers could be solved. This confirms the increasing difficulty of the problem for instances with more suppliers. Overall, 6 out of 45 instances could be solved optimally in less than 10 minutes, all with 5 suppliers. Overall, the remaining instances could not be solved within the time limit. The optimality gaps remain below 17.6% for these instances. It should be emphasized that instance size is not fully reflected by the number of suppliers as multiple tours are required for each supplier within the planning horizon as the experimental insights will show.

2.4.4   Experimental insights

The experiments of set 3 are executed to examine the effect of storage capacity, vehicle capacity and production rates at each supplier on the total transportation time and other indicators which reflect inventory collection patterns. These include the number of suppliers visited per tour, the number of exchanged containers per

Table 2.5: Percentage time increase due to omitting valid inequalities relative to all valid inequalities activated

Instance	Time (s) All cuts	Percentage time increase due to omitting VI relative to all VIs activated																	
		37	38	39	40	41	42	43	44	45	46	47	48	49	50	51	52	53	54
1	429.0	-7.9	10.9	59.2	22.9	-5.3	443.6	68.8	69.1	-14.7	-18.4	126.3	48.3	20.0	-6.4	57.9	184.2	67.9	235.6
2	761.3	-13.5	-33.7	9.7	-16.2	29.6	84.6	57.6	99.7	-4.5	1476.3	-43.6	49.5	50.1	-26.2	-36.7	19.1	-16.1	13.4
3	1208.9	9.0	225.4	136.2	6.6	103.4	73.0	144.2	1.5	54.7	892.7	127.6	-69.5	38.4	-31.2	8.1	22.8	73.2	71.1
4	979.9	17.8	-36.2	8.2	17.8	0.0	26.9	69.9	243.6	-14.5	51.9	20.6	-30.4	-27.8	-53.6	-25.3	-68.1	-33.2	2.9
5	20.7	-45.2	-0.8	-47.8	-48.8	-53.0	-60.0	-43.8	-39.9	-50.4	-50.9	-56.1	-49.3	-35.4	-46.5	-58.6	-23.7	8.4	-62.3
6	1117.0	26.5	20.8	65.6	65.4	147.8	115.7	-57.4	11.5	36.9	974.3	72.9	159.8	47.4	-30.0	29.5	36.0	22.7	70.3
7	157.5	133.2	-13.4	39.4	103.2	-35.6	73.5	80.3	184.9	123.4	5932.7	150.9	6.8	6.7	79.4	185.2	75.4	70.9	100.6
8	113.9	60.3	-13.7	-41.0	-5.0	17.8	17.8	-25.3	296.1	13.6	770.7	-55.0	-53.3	-23.0	-11.0	-31.7	-32.4	-41.0	25.0
9	2646.3	58.1	74.6	155.8	39.5	108.6	17.4	-27.1	353.5	173.8	353.5	116.8	7.3	4.7	125.3	288.4	226.6	105.8	-14.5
10	1008.5	-10.1	-52.8	34.2	-52.1	-42.8	-44.3	-51.7	213.9	-3.5	1089.9	-52.5	-55.7	-45.5	-30.4	-32.7	-23.6	-60.8	-45.2
11	47.5	12.4	64.9	4.5	1.7	7.2	26.2	-14.8	282.0	-24.9	1821.8	51.6	30.8	119.9	-7.4	28.0	-22.0	-16.3	2.2
12	2234.0	58.9	3.1	41.3	-35.8	17.6	-56.4	-45.3	-49.5	-29.0	29.5	-36.5	-46.9	27.8	26.0	-54.0	14.3	-42.4	54.1
13	453.5	29.2	50.7	-7.9	35.3	249.5	7.0	50.3	89.5	-30.3	2546.2	-24.6	-3.3	47.7	76.7	-0.7	30.0	-2.2	5.6
14	648.8	209.9	-8.6	111.6	0.3	23.7	240.6	407.2	314.2	90.4	1749.8	393.3	443.0	219.5	30.1	8.6	212.6	60.8	434.3
15	45.5	11.3	-1.5	19.1	74.7	16.0	36.4	19.3	154.4	47.8	920.8	61.0	65.6	26.2	9.9	6.1	-1.6	57.2	-6.7
16	1160.8	-1.6	-59.7	-58.5	-19.4	1.5	26.5	-38.2	37.2	24.5	688.4	-56.9	-45.5	183.5	35.3	-21.1	27.1	-48.3	16.2
17	511.4	96.8	27.2	22.6	21.0	19.0	78.5	-15.1	108.9	57.7	2108.5	12.1	38.8	188.2	144.2	-2.9		-27.7	15.7
18	3.7	150.0	-5.2	238.7	370.1	460.1	316.1	290.4	32.3	53.9	343.0	-18.0	459.5	331.2	254.6	17.2	18.7	34.2	192.9
19	2.1	51.1	-10.3	-8.2	-64.4	-49.4	17.3	784.1	117.1	-24.9	30.4	67.1	52.8	37.6	164.1	115.2	146.2	-8.1	27.6
20	10.8	25.6	16.0	184.5	32.8	4.6	-14.0	35.8	-0.2	-12.6	37.1	149.6	11.1	240.4	-27.4	-8.9	3.4	5.0	13.0
21	100.9	-0.9	-8.5	-26.9	-38.4	-12.5	39.4	5.9	107.4	-25.8	329.7	-24.9	-23.2	23.0	-27.4	-31.7	36.3	-26.6	113.7
22	32.8	3.2	-23.8	-39.5	-8.3	-22.5	-4.1	-1.0	85.3	-19.8	1472.2	-34.5	-20.8	-35.9	-21.1	-23.3	-21.2	-6.4	-17.4
23	202.4	203.1	109.3	99.2	2.4	76.6	187.2	95.2	410.7	80.2	5829.3	130.7	225.6	597.1	37.4	189.7	59.3	48.8	139.3
24	26.6	19.6	35.7	2.4	130.0	-3.5	26.9	23.0	94.1	110.0	65.0	21.9	4.6	28.3	39.3	20.7	15.1	26.7	2.5
25	32.9	87.9	20.9	130.0	-3.9	35.6	-57.4	-43.6	-49.1	-65.5	632.2	-55.7	-52.9	-48.1	-39.4	-51.8	-62.7	-42.8	-22.1
26	25.3	-28.8	-2.5	-47.0	-36.0	-61.9	-70.9	-40.9	612.1	-46.9	633.4	-52.4	-70.3	-43.8	-38.4	-65.0	-54.4	-44.0	38.9
27	200.8	58.2	-5.5	22.0	28.3	-31.0	-48.6	-54.5	213.6	-25.7	2466.2	29.0	11.4	-53.5	49.0	-38.8	-42.1	-8.4	7.3
28	238.7	46.8	23.5	-40.9	-59.7	-54.9	-26.0	161.3	-42.6	-10.1	-43.2	-52.4	-9.2	-31.5	17.5	-56.4	41.6	-50.4	409.1
29	6.1	-37.0	24.6	-64.0	0.0	-44.5	65.1	-8.2	101.7	-28.9	232.0	-3.3	23.6	38.8	40.2	33.8	35.3	33.0	25.9
30	4.4	6.0	20.9	41.2	-0.7	97.1	16.4	344.4	76.2	24.2	62.7	-19.0	17.5	-22.9	11.7	71.3	322.2	26.3	27.3
31	27.2	94.4	-4.8	57.3	0.0	239.2	0.0	0.0	0.0	0.0	0.0	0.0	0.0	0.0	0.0	0.0	0.0	-0.0	0.0
32	12000.7	-26.6	-58.9	-29.7	-8.1	-43.4	-25.3	10.3	-26.4	-38.0	35.9	-33.7	-47.0	0.0	5.9	-1.3	-23.7	8.1	-3.6
33	32.1	68.0	-70.4	68.0	-88.6	68.0	68.0	-88.5	68.0	68.0	-46.7	68.0	68.0	68.0	68.0	68.0	-63.2	68.0	68.0
34	7144.3	6.4	176.3	167.1	201.9	43.9	35.4	164.6	409.4	9.8	434.7	136.7	263.0	769.4	151.2	-26.8	55.1	166.2	163.8
35	86.4	83.1	98.0	87.0	219.3	380.7	47.0	26.7	282.3	-26.7	-33.4	45.9	33.0	11.1	22.8	76.7	32.4		
36	3.2	56.6	83.1	98.0	87.0	98.0	219.3	380.7	47.0	26.7	282.3	-26.7	-33.4	45.9	33.0	11.1	22.8	76.7	32.4
37	19.1	16.3	11.3	70.4	19.7	-5.7	-9.6	50.7	20.1	-0.5	851.1	43.8	8.5	28.4	-16.8	104.9	-6.1	8.7	-18.2
38	1.8	59.1	39.4	53.1	7.3	60.6	5.0	547.8	108.7	59.5	420.4	61.2	-20.0	408.8	101.1	201.4	13.2	-2.8	102.8
39	85.5	79.7	143.9	9.3	-54.0	2.0	-7.8	-7.5	267.0	2.9	673.4	-81.2	65.4	-41.9	-13.5	-10.5	-27.3	-12.3	43.7
40	45.5	-10.4	-29.5	-24.0	-56.4	-21.3	-17.4	-42.3	118.9	-3.5	682.3	-41.1	-21.2	-22.6	-57.6	-19.3	27.3	0.3	-27.7
41	14.8	-39.5	-39.6	-23.6	-47.9	-45.4	-11.9	70.2	-24.1	-49.7	71.2	-43.4	-37.7	-11.2	-37.6	-40.9	-40.2	-31.2	-40.8
42	329.8	88.4	-48.3	-34.1	-18.5	-42.4	18.3	0.4	0.4	-66.7	3539.2	-46.4	-21.1	-21.1	-22.5	-31.9	-39.1	-15.5	-26.2
43	12.8	153.9	16.1	105.4	18.3	63.5	45.6	98.4	94.4	32.1	789.5	74.4	69.2	49.8	64.2	71.5	34.7	27.8	51.8
44	29.3	452.1	39.9	31.9	113.6	74.6	1.8	-22.4	216.9	234.4	17103.4	13.7	-0.6	118.6	89.0	-16.1	25.3	75.6	12.0
45	14.2	-2.9	-22.7	-20.0	-18.3	-42.3	-30.8	-3.4	23.9	46.5	158.4	-20.2	-30.5	-16.2	-34.1	-24.0	-37.0	-8.2	-27.3
Average	761.7	49.5	15.3	34.9	12.2	33.6	37.4	77.4	121.3	15.4	1297.9	22.6	29.4	78.6	22.5	21.9	24.4	11.2	47.7

Table 2.6: Gap improvement relative to optimal solution in % points for including each set of valid inequalities, while solving the continuous relaxation

Instance	Solution	No cuts	37	38	39	40	41	42	43	44	45	46	47	48	49	50	51	52	53	54
									Gap improvement in % points of the lower bound										
1	885.3	330.0	0.0	0.7	0.7	13.7	13.7	0.0	0.0	0.0	0.0	10.2	0.0	0.0	0.8	0.0	0.0	0.0	0.0	0.0
2	782.1	291.4	0.5	0.8	7.6	42.8	10.5	2.9	33.4	2.2	32.6	0.8	3.2	4.3	3.8	5.8	0.5	13.7	3.4	
3	924.1	501.4	-1.9	0.2	10.3	26.1	-5.5	-0.8	13.4	1.3	24.0	0.3	1.1	-1.2	-0.7	-2.0	-1.8	-0.5	-1.8	
4	880.4	506.6	-3.9	-1.8	6.0	13.2	2.5	-1.5	12.7	1.6	12.7	-1.6	0.2	0.2	-3.9	7.4	-3.9	-3.6	0.4	
5	412.6	352.2	-0.2	0.3	0.5	11.6	5.7	0.1	8.3	-0.3	11.5	0.3	0.0	1.5	-3.9	-0.6	-1.8	-0.5	3.1	-0.5
6	915.0	575.8	0.0	1.4	16.1	4.7	0.2	16.1	-0.3	17.3	0.0	1.0	0.0	0.2	1.5	0.7	-0.4	4.3	0.0	
7	877.2	557.0	-2.0	0.6	1.9	23.3	5.4	5.4	22.0	2.1	20.1	0.0	2.3	2.3	3.0	0.7	8.5	4.3	0.0	
8	431.2	288.9	2.6	-2.1	3.0	16.1	-9.3	-2.4	5.3	1.8	17.3	-5.0	1.0	1.0	-2.4	2.6	1.4	3.1	-1.2	
9	754.3	400.1	0.4	1.0	3.6	19.8	2.6	2.7	19.6	1.3	17.4	2.0	0.6	0.6	-3.9	2.0	3.8	0.3	2.6	
10	933.1	358.3	-0.4	0.0	1.9	28.6	6.5	-0.9	25.3	-0.9	28.9	-1.1	1.9	1.9	2.0	2.0	7.1	0.0	0.3	
11	741.3	580.6	1.0	3.1	3.9	11.9	4.2	1.3	9.4	3.2	11.5	0.4	1.2	0.7	-0.9	3.1	0.0	4.1	-0.4	
12	660.4	446.6	-0.0	-0.0	2.9	0.9	-0.1	1.6	-0.3	-0.0	0.9	0.0	0.1	0.1	-0.5	0.1	3.1	0.3	-0.7	
13	773.8	538.5	0.0	0.0	1.0	11.8	2.7	4.6	11.2	2.6	11.8	0.0	1.8	1.0	0.0	-0.0	0.0	2.6	0.0	
14	452.0	227.9	0.0	0.0	0.0	4.6	4.6	11.2	4.6	12.5	-1.7	-2.7	1.0	-2.4	4.7	0.0				
15	713.9	572.8	0.0	0.3	8.7	4.6	0.3	8.8	0.2	5.8	-0.3	-0.7	-1.7	1.0	-1.6	6.5	0.0			
16	949.0	420.7	0.6	0.4	4.6	42.8	18.5	1.4	35.8	3.3	41.9	-0.5	3.5	2.3	-2.9	0.8	4.6	8.4	0.7	
17	906.3	348.6	1.1	-0.2	5.4	46.3	14.2	-3.6	39.5	8.2	42.1	1.1	2.5	3.4	-0.3	1.8	-1.2	-3.1	-6.4	
18	530.4	330.3	-1.5	-0.2	5.5	31.5	14.5	-3.3	30.9	1.4	31.5	0.9	2.9	2.9	-11.2	-3.7	-13.6	-2.1		
19	926.2	299.1	5.1	6.8	6.8	61.3	26.8	3.3	67.0	5.9	61.3	4.8	13.8	12.8	4.6	9.5	8.0	7.1		
20	731.1	339.0	1.1	4.3	44.8	20.0	-0.2	43.2	2.3	45.7	-0.7	4.8	5.4	-2.7	4.1	4.1	1.7			
21	528.7	387.0	-1.8	1.4	4.2	-3.4	-7.2	10.3	-0.9	10.2	-1.1	2.1	2.8	3.4	0.2	-0.6	7.3	-0.1		
22	519.9	267.4	0.0	-4.5	0.2	17.4	23.8	13.2	-0.3	-7.3	-7.3	-7.2	-7.2	-7.0	-0.1					
23	520.5	308.3	-3.5	0.4	3.2	1.6	-11.5	0.2	15.1	3.6	13.2	-2.5	0.0	2.4	-3.9	0.1	0.0	-2.7	-1.3	
24	822.1	311.4	0.0	0.0	2.9	32.0	0.2	0.1	31.8	2.4	28.7	0.0	0.3	0.0	0.2	1.8	0.0	2.4	0.0	
25	605.2	204.0	0.1	0.0	8.2	21.0	2.4	0.1	10.7	1.0	22.5	0.0	0.0	0.0	0.2	0.2	0.0	0.4	0.0	
26	434.0	307.5	-0.0	0.2	21.0	-12.6	10.8	2.2	67.0	-0.7	-4.1	-3.3	0.2	-10.5	0.1	-1.0	-0.3			
27	496.7	305.5	0.0	0.0	8.4	22.6	1.8	9.1	22.1	-1.0	0.0	0.2	0.2	0.1	0.0	1.1	0.0			
28	715.1	348.0	-3.9	0.2	12.4	-12.6	0.2	4.3	1.1	-3.7	-0.1	-2.1	3.8	-1.8	-0.7	-3.9				
29	284.6	227.7	0.0	0.3	1.3	-8.9	0.0	1.3	-3.0	-1.2	0.6	0.0	-2.1	0.1	-1.8	3.0				
30	427.8	273.9	0.0	13.6	22.7	-15.6	0.0	9.3	9.1	-6.4	-5.2	1.2	0.6	-7.9	0.0	0.0				
31	349.9	311.4	7.8	9.8	4.6	0.3	-0.2	18.4	21.2	0.0	4.5	1.2	10.7	13.7	9.4					
32	651.8	157.8	2.7	7.0	11.9	0.2	0.7	1.8	22.8	1.3	0.1	-0.3	9.9	1.3	0.0	-0.1				
33	534.2	213.9	12.0	10.1	35.9	5.2	4.1	18.5	11.3	0.1	0.3	13.4	-0.0	9.9	2.0					
34	463.9	173.1	-0.4	2.2	34.8	-1.0	2.7	23.3	31.5	2.4	0.0	0.2	0.1	-0.1	6.8	0.4				
35	918.4	283.3	4.2	4.9	50.0	10.4	0.4	52.0	33.6	3.5	2.2	4.1	0.0	2.5	3.7	0.4				
36	638.0	341.5	-19.8	1.5	31.7	8.6	-8.5	36.6	31.7	-1.3	-2.0	3.0	0.0	-6.1	0.7					
37	684.7	291.1	-15.0	7.2	22.2	0.8	-14.2	32.9	22.2	5.2	-4.2	2.5	2.0	-9.9	0.1					
38	731.7	175.0	15.1	20.8	66.5	34.1	-8.5	73.3	65.5	31.7	-15.0	24.6	22.1	3.8	0.1					
39	333.4	119.8	0.0	22.8	46.9	8.6	10.2	20.4	48.5	3.4	19.6	7.2	4.2	2.5	1.6					
40	676.8	166.4	0.2	0.1	57.4	16.7	0.8	60.6	48.5	22.2	-15.0	24.6	6.1	-0.3	-8.4	-7.0				
41	518.0	235.4	-5.7	0.1	34.8	3.8	1.5	54.7	7.0	6.2	-4.6	7.2	24.6	16.5	7.4					
42	668.9	171.2	-0.0	0.1	26.9	-0.0	-6.3	37.7	54.7	7.8	2.2	7.8	6.1	0.5	4.1	8.7				
43	676.7	176.3	2.2	7.2	52.9	11.0	7.2	27.0	34.7	2.3	-9.9	-2.7	7.4	1.3	8.7	-2.7				
44	535.4	224.1	-1.2	-1.0	16.1	-3.1	2.4	61.0	52.9	2.8	0.1	-0.0	-0.0	-0.1	4.5	0.0				
45	365.1	170.1	10.4	2.9	28.1	-3.6	2.1	28.5	16.1	2.1	-0.7	-1.0	6.4	3.0	-6.1	-1.2				
Average	660.6	321.2	0.2	1.4	4.1	25.1	3.8	0.1	24.8	2.5	24.3	-0.4	1.7	2.1	1.4	-0.1	0.3	-0.2	3.3	0.8

Table 2.7: Increasing the amount of suppliers

Suppliers	E	Q	Solution	Time (s)	Gap (%)
5	3	3	**621**	593.0	0.0
5	3	4	**539.7**	6030.5	0.0
5	3	5	**470.5**	2544.5	0.0
5	4	3	**621**	314.4	0.0
5	4	4	**461**	81.9	0.0
5	4	5	**418.7**	527.2	0.0
5	5	3	**621**	336.0	0.0
5	5	4	**461**	59.6	0.0
5	5	5	**389.8**	782.8	0.0
6	3	3	**849.5**	8301.1	0.0
6	3	4	739.7	12000.7	3.3
6	3	5	637.1	12000.4	2.9
6	4	3	**849.5**	4402.2	0.0
6	4	4	671	12000.4	3.7
6	4	5	585.6	12000.3	0.2
6	5	3	**849.5**	5101.0	0.0
6	5	4	671	12001.1	3.9
6	5	5	538.5	12000.4	2.8
7	3	3	**991.7**	10809.9	0.0
7	3	4	822.7	12000.8	7.8
7	3	5	703.5	12000.7	10.2
7	4	3	991.7	12000.7	2.1
7	4	4	763.2	12000.5	4.7
7	4	5	660.9	12000.4	8.1
7	5	3	991.7	12000.6	2.3
7	5	4	763.2	12000.7	4.8
7	5	5	612.3	12000.4	8.1
8	3	3	1271	12000.9	2.9
8	3	4	1050.6	12000.7	12.6
8	3	5	895.9	12000.9	17.2
8	4	3	1270.9	12000.9	2.9
8	4	4	985.9	12001.7	9.4
8	4	5	835.2	12001.7	14.4
8	5	3	1270.9	12002.1	2.1
8	5	4	978.7	12001.7	8.9
8	5	5	798.4	12000.9	13.1
9	3	3	1548.7	12001.1	5.3
9	3	4	1295.4	12000.9	13.3
9	3	5	1108.4	12000.8	17.6
9	4	3	1521.1	12001.7	3.7
9	4	4	1159	12001.0	8.3
9	4	5	1012.8	12000.8	16.9
9	5	3	1521.1	12001.2	3.4
9	5	4	1159	12001.0	8.3
9	5	5	940.1	12000.8	12.3

supplier, the average content levels of the collected containers and the number of performed tours.

Out of the 3200 instances with 5 suppliers, 2174 instances could be solved to optimality within a 12000 second time limit.

Overall, the results show that both the transportation time and the number of suppliers per tour are reduced for increasing storage capacities until the storage capacity equals the vehicle capacity. In contrast, the number of collected containers increases with increasing storage capacity levels. In 95% of the instances, the average content level of the exchanged containers exceeded 99.6%. Results indicate that the average transportation time is reduced for increasing vehicle capacities. Detailed results are described next.
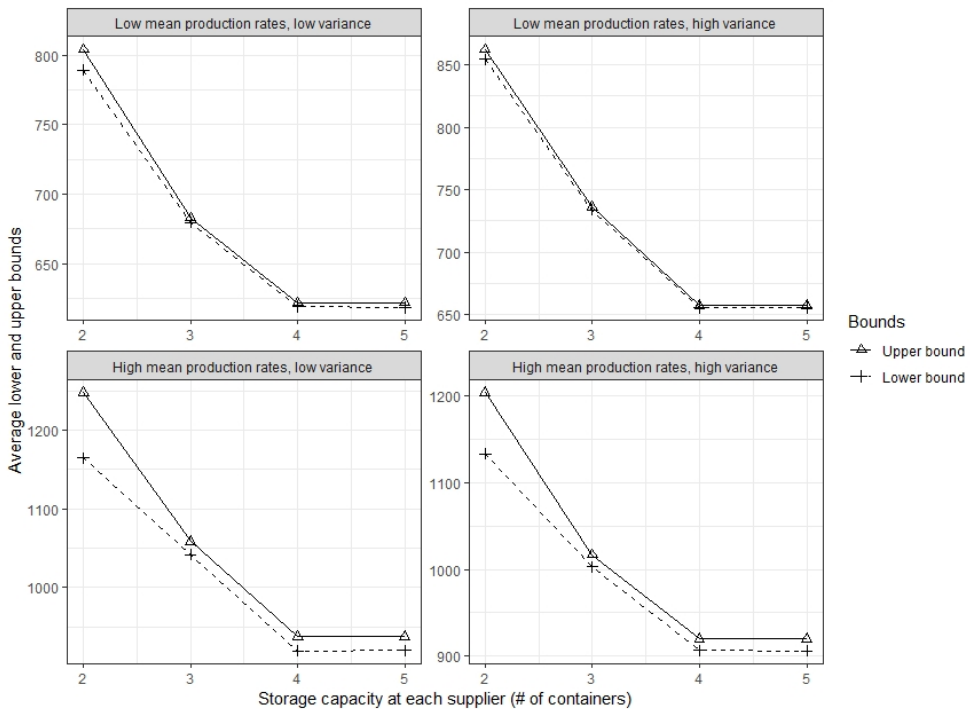

Figure 2.2: Storage capacity at each supplier and average lower and upper bounds ($Q = 4$)

Storage and vehicle capacity.

Figure 4.2 shows lower and upper bounds for the transportation time, when the vehicle capacity Q is 4 containers. The average lower and upper bounds decrease for higher storage capacities, as expected. In particular, the total average transportation times stop decreasing when the storage capacity becomes larger or equal to the vehicle capacity. This was found for all vehicle capacities and across all production rate combinations.

The behavior of the transportation time as a result of storage capacity appears to be similar for low and high production rates and low and high variance of the production rates. Moreover, higher production rates require more tours to be performed which increases the average transportation time during the planning horizon.

Figure 4.2 reveals a larger gap between the lower and upper bounds to the solution for storage capacities which are below the vehicle capacity for high production rates, indicating that such instances appear to be more difficult to solve within the time limit of 12000 seconds. For example, the average gaps for storage capacities of 2 and 3 containers are 2.2% and 0.7% respectively for high production rates. This can be explained by the larger number of tours required for lower storage capacities at each supplier.

Time windows

Figure 2.3 shows the lower and upper bounds for the transportation time when time windows are activated and for a vehicle capacity of 4 containers. Out of the 3200 instances with time windows activated, 1642 could be solved to optimality within the time limit. Moreover, the average optimality gap with time windows of 2.4% in experiment set 4 is 1.3% points higher than the experiments without time windows in set 3. This illustrates the increasing complexity associated with introducing time windows in the formulation.

Figure 2.3 indicates that the upper bounds are slightly higher when time windows are activated compared to the experiments in set 3. For a storage capacity of 2, a vehicle capacity of 4 containers and low mean production rates, the average percentage increases in upper bounds are 3.6% and 6.7% for the low and high variance cases of production rates respectively. For high mean

production rates, these average percentage increases were 5% and 2.5%. The average increase in transportation time is reduced for higher storage capacity levels up to 5 containers. This shows that introducing time windows leads to only slightly higher transportation times when storage capacity is limited relative to vehicle capacity. This effect may be overcome by installing sufficient storage capacity levels.
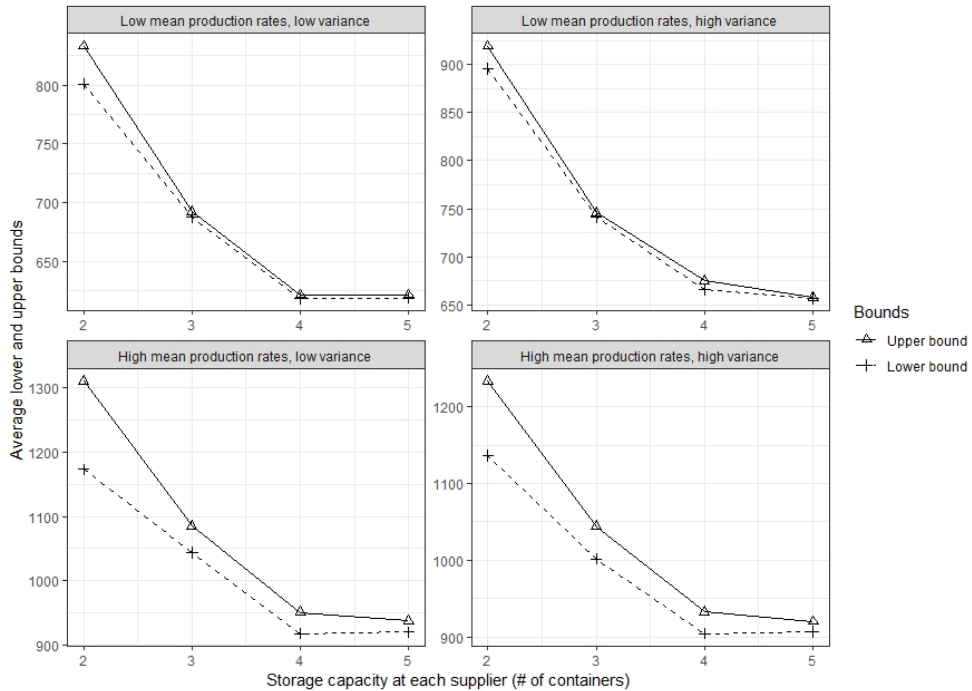

Figure 2.3: Time windows, storage capacity at each supplier and average lower and upper bounds ($Q = 4$)

Number of suppliers visited per tour.

Figure 2.4 indicates that the average number of suppliers visited per tour decreases for higher storage capacity levels at each supplier until the storage capacity is larger than or equal to the vehicle capacity. This effect was observed for all vehicle capacity levels and production rate combinations. The average number of suppliers visited per tour remains constant when vehicle capacity is larger than or equal to the storage capacity at each supplier. In that case, tours in which a single supplier is visited are

most efficient. The vehicle capacity can then be fully used to collect all inventory at a single supplier and this limits the required number of visits to a supplier and the total transportation time during the planning horizon.
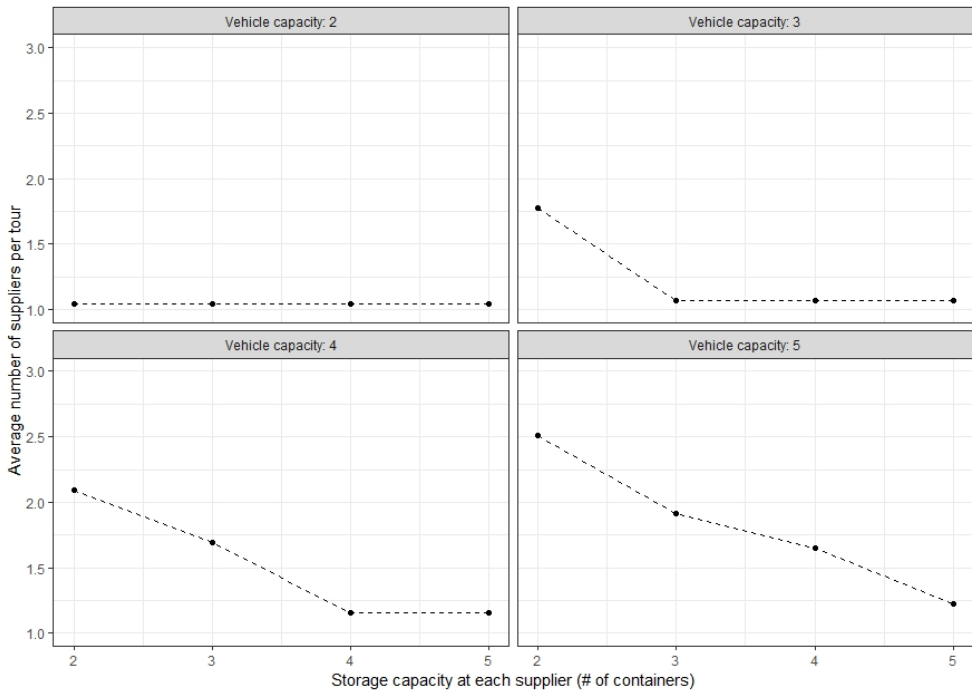

Figure 2.4: Average number of suppliers visited per tour for different vehicle capacities

Number of exchanged containers per supplier.

Figures 2.5 illustrates again that it is most efficient to collect multiple containers at a single supplier if the vehicle capacity and storage capacity enable doing so. The average number of containers exchanged per supplier per tour increases for higher storage capacity levels until it approaches the vehicle capacity. The number of exchanged containers does not fully reach the vehicle capacity for any combination of vehicle capacity and storage capacity. This is due to the fact that some tours are necessary in which multiple suppliers are visited, since the number of containers to be collected at a supplier during the planning horizon is not always a multiple of vehicle capacity.
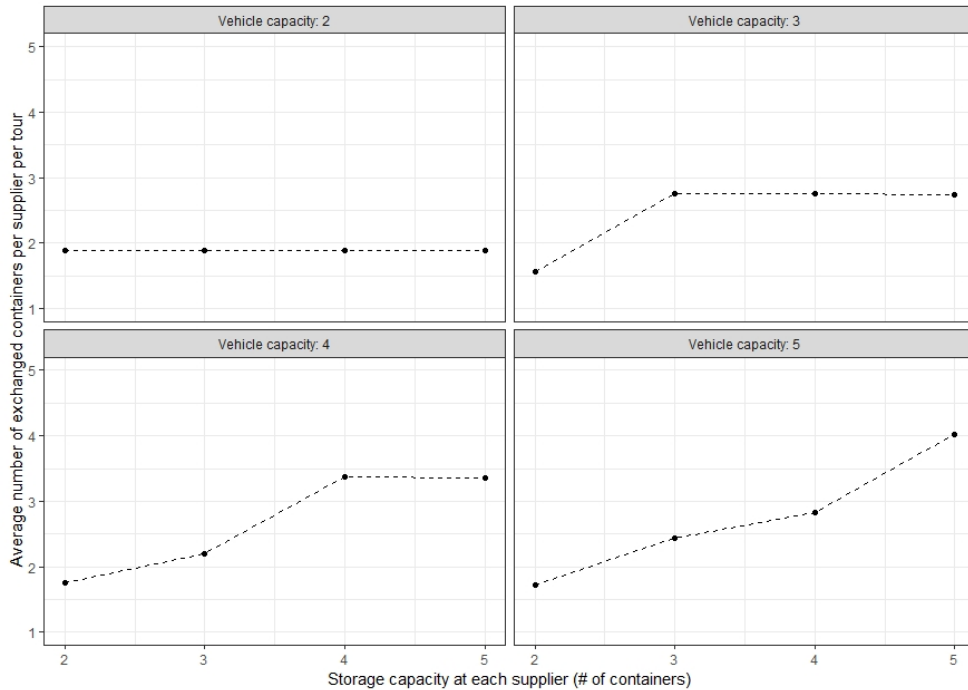
Figure 2.5: Average number of containers exchanged per supplier per tour for different vehicle capacities

Content level of collected containers.

In none of the instances, the average content level of exchanged containers was below 86.7%. In 95% of the instances, the average content level exceeded 99.6%. In 50% of the instances, the average content level even exceeded 99.5%. In instances with the lowest average content levels, partially filled containers were collected at suppliers that did not require a significant detour on a tour visiting other suppliers.

Number of tours required.

Figure 2.6 shows that the average number of tours scheduled during the planning horizon decreases for larger storage capacities for all vehicle capacities. We observe that the number of tours required is mostly affected when storage capacity is smaller than the vehicle capacity. Notice that the scales on the vertical axis had to be adapted for each vehicle capacity. For a storage capacity of 5, a vehicle capacity of 5 does

reduce the average number of tours by 56.5% compared to a capacity of 2 containers. But as more of the tours visit a single supplier (Figure 2.4), the increased storage capacity still reduces transportation time. In this case, more storage capacity does not lead to less tours but better tours.
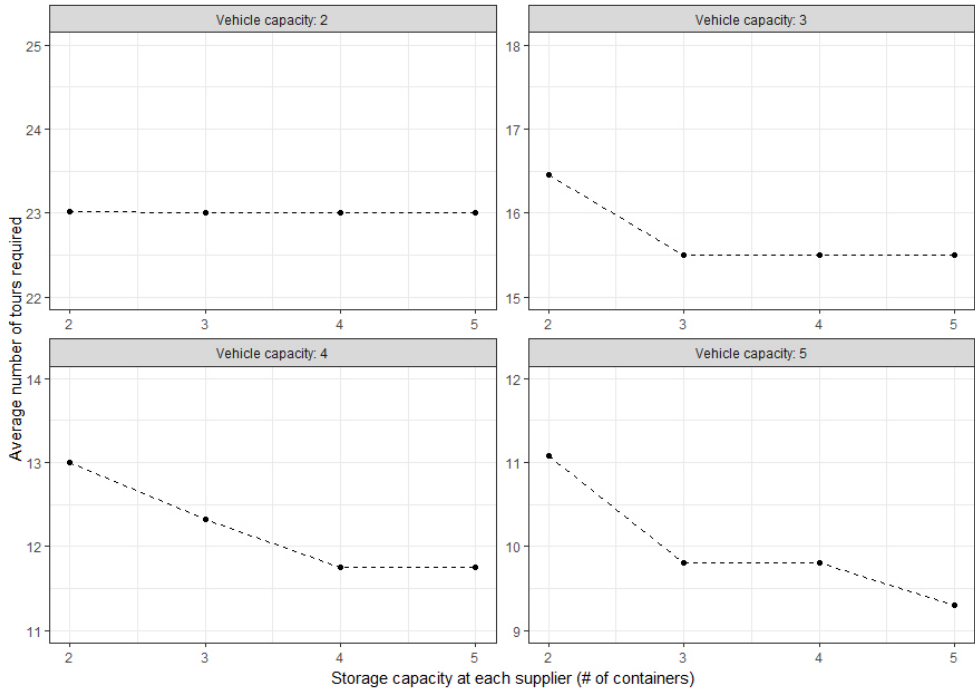
Figure 2.6: Average number of tours performed for different vehicle capacities

2.4.5   Illustrative example

In order to illustrate the relationships between storage capacities, vehicle capacities and the total transportation time, we consider a single example based on four locations of biogas producers in the Netherlands. In all experiments, we consider a planning horizon of one week and a vehicle capacity of 4 containers which is the most common in practice when using tube trailers. The container size is again set at 1500 m^3 of gas in uncompressed equivalents. The production rates are 12, 13, 10, and 11 container equivalents produced during the planning horizon for producers 1, 2, 3, and 4 respectively. Moreover, we test the storage capacities at each supplier

between 2 and 4 containers.

Routes.

Figure 2.7 illustrates the supplier visits. The numbers in the graph represent the order of visit in each tour for storage capacities of 2 to 4 containers, i.e. the last tour in the left-most graph, number 12, which first visits supplier 3 and next supplier 4. The following aspects can be seen in more detail for this example.

Consistent with the overall experimental results, the number of suppliers visited per tour decreases for increased storage capacities. For example, up to 4 suppliers are visited per tour for a storage capacity of 2 containers and at most 2 suppliers are visited per tour for a storage capacity of 4 containers.

For a storage capacity of 2, 2 producers are often combined in a single tour, collecting 2 containers from both. When the storage capacity increases to 3, it appears to be more efficient to regularly collect all 3 containers of a single producer and not make a detour to collect a fourth at another producer.

As a consequence, more tours are executed for a storage capacity of 3 containers than for a storage capacity of 2 containers, that is, 14 and 12 tours respectively. The experimental results in 4.4 have shown that, overall, multiple tours are not performed more often for higher storage capacities.

Figure 2.7: Suppliers visited per tour and the order of visit for different storage capacities

Inventory levels.

Figure 2.8, 2.9 and 2.10 show the inventory levels for each of the suppliers. The numbers in the graph specify the tour in which the inventory is depleted. The timing is such that all suppliers nearly reach their full storage capacity again at the next tour. For these tours, the supplier with the highest production rate dictates the departure time of the vehicle. Since the storage capacity limit of that supplier is reached first in consecutive tours, the containers of that supplier are collected full, whereas the containers of the next visited supplier are collected while partly filled. All suppliers were combined in the fourth tour to create a match between produced and collected gas within the planning horizon.

Notice that thus the optimal solution has 6 and 7 visits to supplier 1 and 3 respectively, while the storage capacity of 2 containers would enable 5 and 6 visits to collect their weekly productions of 10 and 12 containers respectively.

For a storage capacity of 3 containers, we recognize mostly single supplier visits in which all 3 available containers are collected. The vehicle capacity is not completely filled for these tours, and carries 3 out of 4 containers. For tours in which multiple suppliers are visited, the suppliers with the most similar production rates are visited in pairs (see tour 2, 10, 12 and 14). Because a storage capacity of 3 containers now enables the collection of 3 containers at the same supplier, we observe collected gas combinations of 1 and 3 containers (in tour 2 and 14) and 2 times 2 containers in tour 10 and 12.

For a storage capacity of 4 containers, Figure 2.10 illustrates that all 4 containers are collected in almost all tours in which single suppliers are visited per tour and then in tour 11, only 3 containers are collected at supplier 3. In tour 12, supplier 3 and 4 are combined for 2 containers each to ultimately realize a match between weekly production and collection of gas. This is required to set inventory levels at the end of the planning horizon equal to starting inventory levels. Notice that supplier 4 is always visited just before reaching its storage capacity limit as 3 times 4 containers are collected, while supplier 4 produces 11 full containers each week. Supplier 1 is producing 12 containers each week and is visited 3 times when exactly reaching its storage capacity limit.
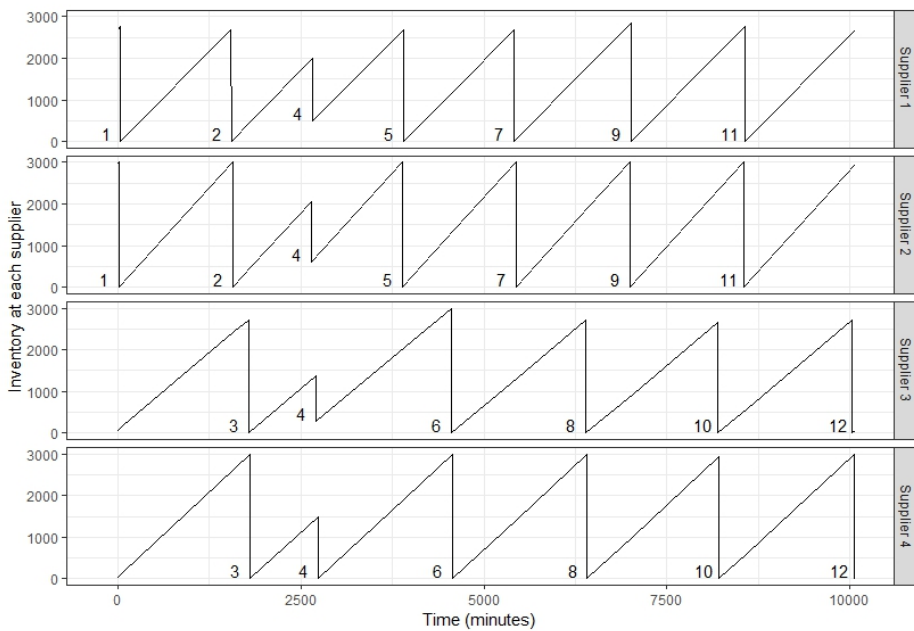
Figure 2.8: Inventory levels and the related tours for a storage capacity of 2 containers
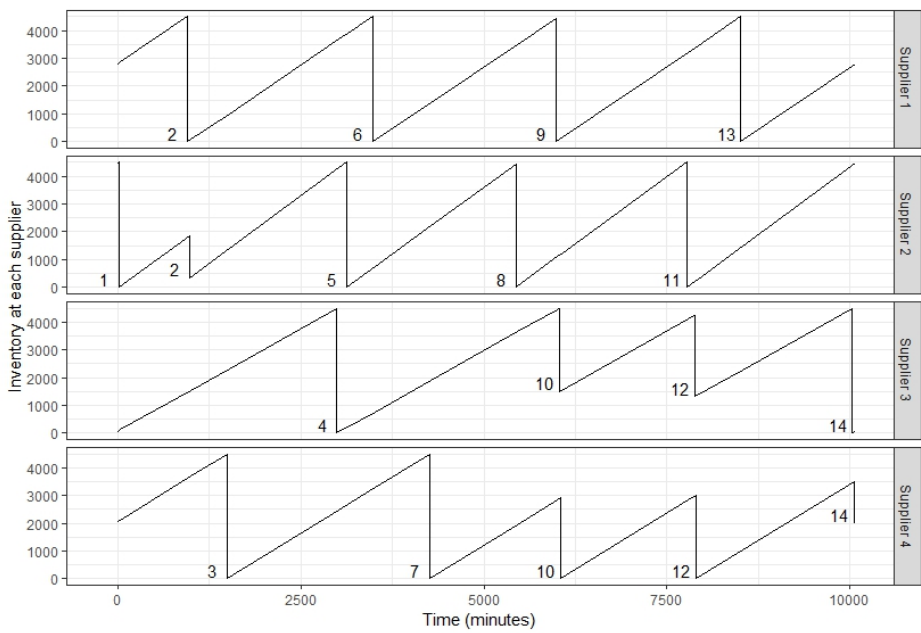
Figure 2.9: Inventory levels and the related tours for a storage capacity of 3 containers
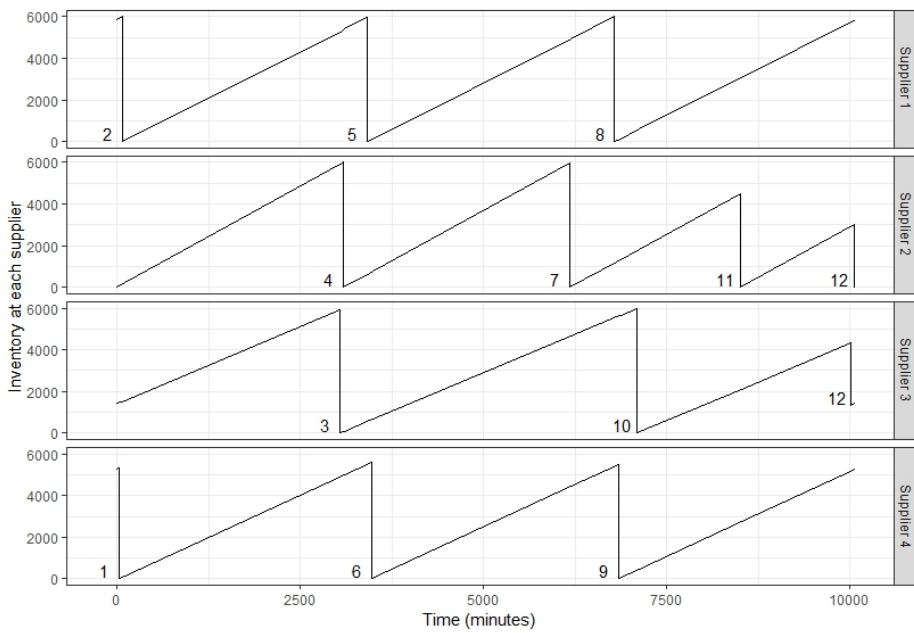
Figure 2.10: Inventory levels and the related tours for a storage capacity of 4 containers

2.5   Conclusion

In this paper, we have addressed the formulation of a continuous-time supply-driven inventory routing problem in which the routing and inventory collection decisions are dictated by supply rather than demand. To the best of our knowledge, this study is the first to optimally solve the combination of routing schedules in continuous time with continuous inventory contents in discrete containers. The inventory is stored in containers that act as both movable transport units and the available storage capacity at each supplier. This problem occurs when biogas needs to be transported from a set of decentralized suppliers to a single processing facility during a cyclic schedule. We have proposed a novel and compact formulation that enables solving realistic instances to optimality. We have developed valid inequalities that have a large impact on running times and have provided experimental insights by examining the routing and inventory collection decisions for different storage and vehicle capacities at each supplier.

The computational results illustrate the complexity of the problem. The valid inequalities are a necessity in solving instances of a realistic size and reduced running times with 93% on average. The analyses of the optimal solutions indicate that these approach the lowest level of transportation time when the storage capacity equals at least the vehicle capacity. This enables the more efficient solution to visit fewer suppliers per tour. Both the average transportation time and the average number of suppliers visited per tour generally decrease for larger storage capacities at each supplier until the storage capacity is larger than or equal to the vehicle capacity. For fixed storage capacity levels, a larger vehicle capacity reduces the average number of tours and the transportation time required. In 95% of the instances, the average content level exceeded 99.6%. An in-depth analysis of the routes and inventory patterns generated for a small set of instances reveals some remarkable characteristics of optimal schedules that would not have been expected by transport planners. These particularly relate to the requirements of weekly repeating schedules, while weekly production quantities do not allow for full truckloads.

Overall, the solution method is shown to be able to generate optimal solutions for real-life instances and points out where inefficiencies occur due to insufficient storage capacity at each supplier and the need to create cyclic schedules.

Inefficiencies may relate to 1) routes having to combine multiple suppliers, 2) vehicles that drive while not fully loaded and 3) storage capacities which are not fully used.

Avenues for future research may include extending the approach with multiple vehicles and the problem case where the fleet is heterogeneous. For the case with time windows, future research may formulate a different model which is solved with a branch-and-price algorithm.

Acknowledgements

Chapter 3

An investment appraisal method to compare LNG-fueled and conventional ships

Abstract. *Ever stricter emission regulations stimulate vessel owners to consider the adoption of alternative marine fuels, such as Liquefied Natural Gas (LNG). In deciding whether to invest in LNG-fueled vessels, initial investment and operating costs are decisive factors that have not yet been fully studied in the literature. In this paper, we present a new investment appraisal method to compare the costs of LNG-fueled vessels with conventional vessels. We analyze the fuel costs and overall exploitation costs by simulating bunker planning decisions under stochastic fuel prices, presence in emission controlled areas, and route lengths. Our analyses reveal that the fuel costs of LNG-fueled vessels are often lower than those of conventional vessels, even under unfavorable LNG prices. Due to the higher initial investment costs in LNG-fueled vessels, these fuel cost reductions do not always translate into lower overall exploitation costs. By conducting numerical experiments, we identified conditions under which the exploitation costs of LNG-fueled vessels are lower than conventional vessels.*

3.1 Introduction

With more stringent vessel emission regulations executed by the International Maritime Organization (IMO), such as the Emission Control Areas (ECA) in the Baltic Sea and along the North American coast, vessel owners increasingly seek for cost-effective solutions to comply with those regulations (Wang and Notteboom, 2014). Conventional-fueled vessels can comply with ECA regulations by using expensive low sulfur fuels such as Marine Gas Oil (MGO) and/or by installing scrubbers. An interesting ECA-compliant alternative is using Liquefied Natural Gas (LNG) as a marine fuel. Many factors could hamper the adoption of LNG as a marine fuel, such as the lack of a clear regulatory frameworks for bunkering operations, the extra space needed for an LNG fuel tank, potential methane slip, and a limited LNG bunkering infrastructure (Wang and Notteboom, 2014). Nevertheless, the impact on the financial bottom line of the ship owner is often the deciding factor.

While, compared to conventional-fueled vessels, LNG-fueled vessels have a considerably higher initial investment cost due to more expensive equipment and extra engineering costs in the design phase, they also have the potential to considerably reduce fuel costs during the exploitation period (Wang and Notteboom, 2014). In this paper, we present a new investment appraisal method to study the relation between the higher initial investment costs and potentially lower fuel costs associated with LNG-fueled vessels. Our method uses an optimal bunker planning policy, takes fluctuating fuel prices into account and considers variable travel times in ECA. Below, we discuss each of these aspects in more detail.

Thus far, the literature on economic analyses of ECA-compliant alternative fuels has generally assumed that vessels utilize only one type of fuel, that is, either oil-fueled for conventional vessels or LNG for LNG-fueled vessels (Adachi et al., 2014; Burel et al., 2013; Cullinane and Bergqvist, 2014; Jiang et al., 2014). In practice, LNG-fueled vessels are usually powered by dual-fuel engines, where the crew can switch between any of the available fuel types during a trip. Since prior literature has not considered the option of using different fuels, bunker planning policies have not yet been incorporated in existing investment appraisal methods. Doing so is imperative, as the overall fuel costs are strongly depending on the bunker choices made.

Furthermore, prior studies have assumed fixed ECA presence in their economic

analyses of different ECA-compliant alternatives. ECA presence is defined here as
the operational time spent in ECA regions during a trip (Cullinane and Bergqvist,
2014). In practice, cargo vessels sail different routes in which their operational time
in ECA is different for each trip. ECA presence levels affect the available fuel type
options that can be employed. Heavy Fuel Oil (HFO), for instance, can only be used
outside ECA regions. Consequently, ECA presence strongly affects fuel costs and
evaluating the economic viability of different ECA-compliant alternatives requires
incorporating variable ECA presence.

Lastly, extant literature has generally assumed deterministic fuel prices. Burel
et al. (2013) and Adachi et al. (2014), for example, have used deterministic fuel prices
in their economic analysis of LNG-fueled vessels. Jiang et al. (2014) consider changes
in fuel prices over time, but assume deterministic price trends in evaluating different
options to comply with ECA regulations. However, fuel prices not only change
according to a known price trend, but also fluctuate from day to day. LNG fuel
prices are particularly volatile compared to other fuels, because LNG does not have
a stable international market yet (Acciaro, 2014a; Burel et al., 2013). Since fuel prices
significantly affect fuel and operational costs in shipping (Holmgren et al., 2014), it
is essential to include price volatility in investment appraisal methods for vessels.

The main contributions of this paper are threefold. Firstly, our proposed
investment appraisal method extends deterministic fuel price scenarios from the
literature with daily fuel price fluctuations to better estimate fuel costs. Secondly,
we include bunker planning decisions in our investment appraisal method by
simulating bunker planning decisions for many days over the full exploitation
period of a vessel. The corresponding bunker planning model is used with different
stochastic fuel price scenarios and various trip profiles. Thirdly, we integrate our
analyses of fuel costs into an appraisal of the overall exploitation costs to determine
the economic viability of LNG-fueled vessels. By running an extensive set of
experiments, this study compares the exploitation costs of an LNG-fueled vessel
with its conventional-fueled counterpart for a real-world case and derives generic
insights about the conditions under which the exploitation costs of LNG-fueled
vessels are lower than conventional-fueled vessels.

The remainder of this paper is structured as follows. Section 2 describes the
problem setting in more detail. It also presents the formal definitions of decision
variables and parameters, and explains the modelling assumptions that were made.

Section 3 describes the investment appraisal method. Section 4 introduces the Dutch shipping company that provided data for the case experiments. This section also describes the numerical experiments and explains the stochastic fuel price scenarios considered in our study. An overview and discussion of the experimental results is included in Section 5. The paper is concluded in Section 6.

3.2   Problem description

The problem addressed in this paper concerns the decision to invest in a new build vessel either propelled by an LNG dual-fuel engine or a conventional fuel engine. We address this decision from an economic perspective, assessing differences in the overall exploitation cost for each type of propulsion, which consist of the cost of capital, overhead costs and fuel costs. We consider the discounted investment per month as cost of capital, with a higher cost for LNG dual-fuel propulsion. Monthly overhead costs, which consist of labor and maintenance costs, are considered equal for both propulsion types. The final component of the monthly exploitation costs concerns fuel costs, which can strongly differ between LNG dual-fuel and conventional fuel engines.

Estimating the additional investment required for LNG dual-fuel propulsion can be done rather precisely and is easily translated into a stable monthly cost of capital. Given the equal overhead costs for both propulsion types, the additional investment for an LNG engine can only be recovered by a lower fuel cost component. Actual fuel costs differ per trip, and depend on the length of the trip, fuel efficiency, the sailing time in emission controlled areas, which fuel—or fuels—the vessel sails on, and the prices of those fuels. Taking these factors as input, vessel operators aim to minimize the fuel costs of a trip by deciding how much of each fuel to bunker before departure.

Since bunker planning decisions strongly affect fuel costs, our appraisal method considers the underlying bunker planning problem. For any trip k, departing at day i, the objective of the problem is to minimize the total fuel costs by determining the amount of sailing time S_f on fuel type f. A vessel can bunker multiple fuel types before departure. Vessels with an LNG dual-fuel engine can bunker LNG ($f = 1$), MGO ($f = 2$) or HFO ($f = 3$); conventional-fueled vessels can only bunker MGO and HFO. Each trip is specified by a total travel time and a time in emission controlled

areas. Each fuel type is associated with a different fuel consumption rate due to differences in calorific contents of the fuels. The maximum travel time on fuel type is restricted due to fuel tank capacities. The underlying bunker planning problem can be modelled as follows:

$$\min \quad \sum_{f \in \mathcal{F}} S_f U_f P_f \tag{3.1}$$

$$\text{s.t.} \quad \sum_{f \in \{1,2\}} S_f \geq T^{ECA} \tag{3.2}$$

$$S_f \leq T_f^{max} \qquad\qquad \forall \, f \in \mathcal{F} \tag{3.3}$$

$$\sum_{f \in \mathcal{F}} S_f \geq T^{ECA} \tag{3.4}$$

$$\sum_{f \in \mathcal{F}} S_f = T^{total} \tag{3.5}$$

The objective function (3.1) minimizes the total fuel cost per trip. Constraints (3.2) imposes that only LNG and MGO can be utilized within emission controlled areas. Constraints (3.3) enforces that sailing times on a fuel type cannot exceed the maximum travel time. Constraints (3.4) makes sure that the sum of fuel specific sailing times equals the total travel time of a trip.

Above, we formulated the bunker planning decisions as a deterministic problem. However, both fuel consumption levels and fuel price differences may strongly differ throughout the lifetime of a vessel. Our investment appraisal method is designed specifically to address these uncertainties, for which we introduce a few additional parameters. For each fuel type f, we consider a linear price trend, resulting in a base price P_{fi}^{base} on a given day i. To express the stochastic behavior of fuel prices, we draw a daily price deviation D_{fi} from a probability distribution R_f^D to compute the fuel price P_{fi}. Since we assess monthly exploitation costs, we compute monthly fuel costs. The characteristics of a trip, in terms of its total length and ECA presence, will likely differ from trip to trip. Therefore, we obtain the length of a trip T_k^{total} from a probability distribution R^T and the proportion of travel time within emission controlled areas E_k from a probability distribution R^E. An overview of all variables and parameters is given in Table 3.1.

We make the following assumptions:

Table 3.1: An overview of the variables and parameters addressed in our problem.

Sets	
U_f	Fuel consumption (in metric ton per hour) using fuel type $f \in \mathcal{F}$
T_f^{max}	Maximum travel time (in hours) of fuel type $f \in \mathcal{F}$
T_k^{total}	Total travel time (in hours) of trip $k \in \mathcal{K}$
T_k^{ECA}	Travel time in ECA (in hours) of trip $k \in \mathcal{K}$, where $T^{ECA} = E_k T_k^{total}$
P_{fi}	Fuel price (in dollars per metric ton) of fuel type $f \in \mathcal{F}$ on departure day $i \in \mathcal{I}$, where $P_{fi} = P_{fi}^{base} + D_{fi}$
E_k	ECA presence (in percentage) of trip
P_{fi}^{base}	Fuel base price (in dollars per metric ton) of fuel type $f \in \mathcal{F}$ on day $i \in \mathcal{I}$
D_{fi}	Fuel price deviation (in dollars per metric ton) of fuel type $f \in \mathcal{F}$ on day $i \in \mathcal{I}$
R_f^D	Probability distribution for price deviation D_{fi} for fuel type $f \in \mathcal{F}$ on day $i \in \mathcal{I}$
R^T	Probability distribution for total travel time T_k^{total} for trip k
R^E	Probability distribution for ECA presence E_k for trip k
Variables	
S_{fki}	

- It is assumed that vessel operators always attempt to minimize total fuel costs by making bunker planning decisions before the departure of a specific trip.

- For each fuel type , the different fuel consumption rates are considered known and constant. We perform a numerical validation to study the fuel cost behavior as a result of different consumption rates for the same fuel.

- Fuel bunker quantities are assumed to precisely cover fuel consumption needed for a trip. Hence, we do not consider leftover fuel from previous trips.

- We assume all fuel bunkers are bought at spot prices, which are not subjected to local price differences. Bunkering at spot prices is a common practice in the maritime transportation sector (Ghosh et al., 2015; Plum et al., 2014).

Our investment appraisal method assesses differences in the overall exploitation cost for new build vessels with either LNG dual-fuel or conventional fuel propulsion. The method works with a fixed monthly cost of capital, which is higher for LNG dual-fuel than for conventional fuel propulsion, and a fixed monthly overhead cost, which is equal for both propulsion types. Determining the expected average fuel costs per month for both propulsion types is the main element of our method and computed by means of a simulation model.

The simulation model is implemented in Visual Basic for Applications (VBA) for Excel, according to the logic flow diagram presented in Fig. 3.1, using Xpress optimization software to find optimal bunker planning decisions for specific trips. To address the stochastic behavior of fuel prices and trip characteristics, the model

iteratively calculates an optimal bunker planning for a large number of trips and
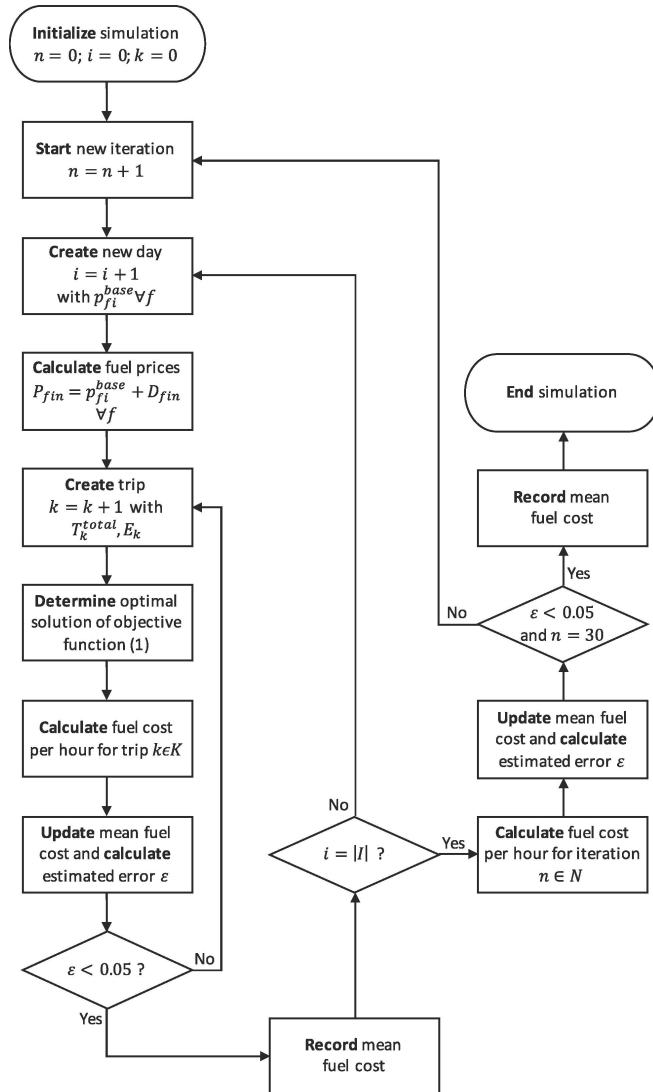days.

Figure 3.1: Logic flow diagram for the simulation model.

The simulation model is initiated with parameter values $n = 0$, $i = 0$ and $k = 0$.
In each new iteration ($n = n + 1$), a new day ($i = i + 1$) is created with base prices
P_{fi}^{base} for each fuel type. The "actual" fuel prices P_{fin} for that day are calculated by

drawing a price deviation D_{fin} from probability distribution R_f^D and adding that deviation up to the base price. This represents the fuel prices, in dollars per metric ton, to be paid at the day of departure. Subsequently, a new trip ($k = k + 1$) is created by drawing a total travel time T_k^{total} from probability distribution R^E and a percentage of ECA presence from probability distribution . For that specific trip, an optimal bunker planning is found according to objective function 3.1, which enables calculating the fuel costs per hour for that trip.

For each day in the simulation, the mean fuel costs per hour are computed by considering multiple trips with different travel times and ECA presence. Since the input values are independent and randomly distributed, the mean fuel costs will converge. Using the confidence interval method (Law, 2014), a new trip is created as long as the estimated error from the real mean (ϵ) is larger than, or equal to 5% with a 95% confidence interval. For each day i, the simulation keeps creating new trips, computing optimal bunker planning decisions and updating the mean fuel costs per hour until the estimated error $\epsilon < 0.05$. Then, the mean fuel costs per hour are recorded for that day.

The simulation model repeats creating new days for the full length of the exploitation period, i.e., as long as $i < |\mathcal{I}|$. When the end of the exploitation period is reached, the mean fuel costs per hour are calculated for iteration . New iterations are started as long as the estimated error from the real mean is larger than, or equal to 5% and n is smaller than 30 iterations. Finally, the mean fuel costs per hour are obtained for all performed iterations for both LNG dual-fuel and conventional fuel propulsion. These values serve as the final hourly fuel costs, which are used as a component of the overall investment appraisal.

3.3 Experiment definitions

This section provides an overview of the experiments we conducted in our study. Firstly, we present the case experiments in which we apply our investment appraisal method to a practical setting. Secondly, we execute experiments aimed at numerically validating our method and deriving generic insights on the behavior of fuel and overall exploitation costs under conditions that are different from the case setting.

3.3.1 Case experiments

For the case experiments, we obtained data from a Dutch shipping company that is active in the short-sea shipping sector. It primarily operates in the North Sea, Baltic Sea, Bay of Biscay and the Mediterranean Sea. At the start of our study, this shipping company had plans for the development of a new dry cargo vessel of roughly 13.000 dead weight ton and considered equipping it with either LNG dual-fuel or conventional fuel propulsion. The main engine should deliver around 3000 kW output, 1800 kW in service condition and the vessel should have a maximum speed of 13 knots. Vessel specifications were drawn up for both configurations, which indicated a 30% higher initial investment required for LNG dual-fuel propulsion. The shipping company expected similar overhead costs for both configurations. Table 3.2 shows the expected monthly exploitation costs (without fuel costs) for the LNG dual-fuel and conventional fuel configuration.

Table 3.2: Monthly exploitation costs without fuel costs.

	LNG dual-fuel	Conventional fuel
Monthly annuity on investment (3% interest)	€140.000	€110.000
Monthly overhead costs	€110.000	€110.000
Overall exploitation costs (without fuel)	€250.000	€220.000

We also obtained data about the total travel times and time in ECA for over 200 trips of 13 vessels, mainly operating in the North sea, Baltic region and Mediterranean. These trips had a profile similar to that of the planned new build vessel, with a mean total travel time of 202.32 h and a standard deviation of 109.1. The trip data were fitted to probability distributions to enable the creation of many trips in the simulation model. Since Gamma distributions are commonly used in simulation studies for task completion times (Robinson, 2014), and because this distribution showed a good fit with the original total travel time data, R^T is given by a Gamma distribution with parameters $\alpha = 3.2839$, $\beta = 62.166$). Data on ECA presence E_k could not be fitted to a common probability distribution function due to a large occurrence of the values zero and one, i.e., trips that were either executed totally outside or totally within ECA. Therefore, we assigned probabilities to the occurrence of zero ($p = 0.266$) and one (p=0.297) to express R^E, while all values in between (with $p = 0.437$) fitted a normal distribution ($\mu = 0.247$, $\sigma = 0.373$).

Fuel consumption and maximum travel time for the different fuels were computed according to several reports (U.S. Department of Energy (2005); Confidential Lab report of Dutch shipping company; Wild Ingenieurbüro (2005)) and discussions with the employees of the Dutch shipping company. Fuel consumption for HFO provided the basis for determining the MGO and LNG consumption, which were derived using differences in calorific energy contents of the three fuel types. Maximum travel times are based on fuel tank capacities common for short-sea dry cargo shipping. An overview of the data used for our fuel consumption and maximum travel time calculations is shown in Table 3.3.

Table 3.3: Values used for fuel consumption and maximum travel time calculations.

	HFO	MGO	LNG
Fuel consumption (metric ton per hour)	0.333	0.326	0.284
Maximum travel time (in hours)	1515	525.3	1229.4
Calorific energy contents (MBTU per metric ton)	39.49	40.44	46.41
Fuel tank capacity (in m3)	500	190	750
Density (in kg per m3)	1010	900	465

In order to demonstrate the applicability of our investment appraisal method, we conduct experiments with five different price scenarios. The first price scenario is the most realistic one, and is based on an industry report (Deloitte, 2015) and fuel price projections by Acciaro (2014b). The remaining four scenarios represent different "What if" scenarios, which enable exploring several other future fuel price developments based on questions raised by practitioners during discussions of initial versions of our method. Each scenario is defined by linear price developments for the three fuel types over the full exploitation period of the new build vessel, i.e., defining P_{fi}^{base} for any given day in the simulation. The five scenarios (see Fig. 3.6 in the Appendix) are:

- "Realistic" scenario: Fuel prices for HFO and MGO increase considerably while the price increase for LNG prices remains relatively limited (see Fig. 3.6a). This scenario reflects the common belief that oil prices will increase due to shrinking oil reserves while LNG prices remain stable due to ample natural gas reserves.

- Scenario "What if 1": A low HFO price. Fuel prices for LNG and MGO are the same as in the "Realistic" scenario, while the price for HFO increases

proportional to the price for LNG (see Fig.   3.6b).   Compared to the
"Realistic" scenario, this scenario reflects the expectation that more stringent
ECA regulations will reduce the demand for—and hence the price of—HFO.

- Scenario "What if 2": Proportional fuel price increases. All fuel prices increase
  proportional to that of LNG. Hence, the fuel price for LNG is the same as in
  previous scenarios, while both HFO and MGO increase proportionally (see Fig.
  3.6c). This scenario reflects the expectation that the price of all marine fuels
  (including LNG) will be linked to crude oil prices in the future.

- Scenario "What if 3" High LNG price. Fuel prices for HFO and MGO are the
  same as in "Realistic" scenario, while the price for LNG increases sharply (see
  Fig. 3.6d). This reflects the expectation that LNG prices will increase rapidly
  due to an increasing demand and adoption of LNG.

- Scenario "What if 4" High fuel prices. Fuel prices for HFO and MGO increase
  sharply (and proportionally), while the price for LNG also increases (at a
  similar level as HFO). MGO remains the most expensive fuel (see Fig. 3.6e).
  This scenario reflects the expectation that all marine fuel types will increase
  relatively sharply due to societal pressure and corresponding (fiscal) actions
  from regulators.

Our investment appraisal method takes daily fuel price volatility into account. To
this end, we analyzed historical fuel price data to determine daily deviations from
(linear) price trends for each fuel. First, linear price trends were determined using
ordinary least squares (OLS) regression modeling. We have chosen OLS because
simple regression models have shown to be able to outperform complex volatility
forecasting models in estimating price volatility (Brailsford and Faff, 1996). For HFO
and MGO, fuel price trends were based on historical spot market prices in the Port of
Rotterdam (Bunker Index, 2015) in the period January 2009 to September 2012. For
LNG, we used US-Henry Hub spot market prices (IEA, 2015) in the period December
2005 to May 2015.

Next, daily deviations from the regression lines were analyzed to determine
probability distribution functions for . These daily deviations were obtained and
filtered by removing time intervals larger than one day because equally spaced
intervals and removal of discontinuities facilitate time series analysis (Brockwell

et al., 1991; Eckner, 2012). The historical data of daily price deviations for HFO could not be fitted to any theoretical probability function. Therefore, an empirical distribution was developed, in which input data was generated by selecting randomly from a pool of historical price deviations (Law et al., 2000). The MGO and LNG price deviations showed a good fit with a Beta distribution ($\alpha = 12.5$, $\beta = 3.9$, with a range between -420.1 and 129.8) and Dagum distribution ($p = 0.7$, $\alpha = 5.7$, $\beta = 4.5$ and $\gamma = -4.1$, where γ corrects for negative values in the original data), respectively. A statistically significant fit was confirmed using the Kolmogorov-Smirnoff test, with $p = 0.64$ for the Beta and $p = 0.23$ for the Dagum distribution. These empirical and theoretical distribution functions are used to create values for D_{fin} during the experiments.

3.3.2   Numerical experiments

In addition to the case experiments, we performed experiments to numerically validate the proposed investment appraisal method and derive generic insights on the behavior of fuel and overall exploitation costs. Specifically, we examine the effects of daily price volatility, total travel times, fuel consumption levels and ECA presence on the expected monthly exploitation costs. Below, we introduce the experimental setup for studying each of these factors. An overview of all experiments is given in Table 3.4.

To study the effects of daily fuel price volatility, we ran experiments with a similar setup as the case experiments, but now with deterministic instead of stochastic fuel prices, hence where $P_{fin} = P_{fi}^{base}$ for each fuel type f and each day i. By conducting these experiments, we can assess the extent to which fuel price volatility is affecting the investment decision.

To study the effect of total travel time of trips, we ran experiments with a probability distribution R^T for total travel times. Specifically, the mean of the Gamma distribution used in the case experiments was multiplied by two. Trips longer than 340 hours were removed to prevent violation of fuel tank capacities for high fuel consumption levels and conventional vessels that sail fully in ECA and cannot use HFO.

To study the effect of fuel consumption levels, we ran experiments with different combinations of MGO and HFO fuel consumption levels relative to LNG fuel consumption. The fuel consumption levels considered in the case experiments are

based on discussions with experts from the shipping company. As these figures are
uncertain due to a variety of factors, we numerically test the outcomes with different
consumption levels. Specifically, we ran 25 experiments in which we let the values
for U_f range from 0.1 to 0.5 with steps of 0.1 for both LNG and conventional fuels,
where fuel consumption levels of MGO and HFO are coupled. These experiments
are repeated for each price scenario. Running these experiments enables finding the
maximum LNG fuel consumption level for which the monthly exploitation costs of
the LNG dual-fuel configuration remain below the conventional-fuel configuration.

To study the effect of ECA presence, we ran experiments where we change the
percentage of travel time of a trip in ECA. To this end, we use deterministic total
travel times, while step-wise increasing the values for ECA presence from 0 to 100%
in steps of 20 percentage points. We do this for both shorter ($T_k^{total} = 250$) and
longer trips ($T_k^{total} = 500$). In these experiments, the total travel time T_k^{total} is kept
smaller than the MGO fuel capacity limit to ensure that this limit is not exceeded
for conventional vessels that sail fully in ECA. These experiments aim to reveal if a
certain ECA presence is required to render LNG dual-fuel propulsion economically
viable.

The experiments for each of these factors are conducted for all five price
scenarios. Including the case experiments, we ran 190 experiments on desktop PCs
with Windows 7 and an Intel Core i5 processor. Computation times per experiment
were 24 hours for each experiment for the "Case experiments", "Total travel time"
and "Fuel consumption levels" (see Table 3.4). The remaining experiments needed 1
to 2 hours per experiment.

3.4   Results and discussion

In this section, we present and discuss the results of the experiments. These results
indicate how the exploitation costs for both types of vessels behave in response
to the experimental factors and feed into a discussion about the conditions under
which the exploitation costs of the LNG dual-fuel configuration are lower than the
conventional configuration.

Table 3.4: An overview of the experimental setup.

	Number of experiments	Price deviations D_{fi}	Total travel time (T_k^{total})	Fuel consumption per hour (U_f)	ECA (E_k)
Case experiments	5	$R_1^D = D(5.7, 4.5, 0.7)$ $R_2^D = Be(12.5, 3.9)$ R_3^D: Bootstrap	$R^T = \Gamma(3.28, 62.17)$ capped at 340	$U_1 = 0.284$ $U_2 = 0.326$ $U_3 = 0.333$	Stochastic
Daily fuel price volatility	5	Deterministic fuel prices	$R^T = \Gamma(3.28, 62.17)$ capped at 340	$U_1 = 0.284$ $U_2 = 0.326$ $U_3 = 0.333$	Stochastic
Total travel time	5	$R_1^D = D(5.7, 4.5, 0.7)$ $R_2^D = Be(12.5, 3.9)$ R_3^D: Bootstrap	$R^T = \Gamma(6.56, 62.17)$ capped at 340	$U_1 = 0.284$ $U_2 = 0.326$ $U_3 = 0.333$	Stochastic
Fuel consumption levels	125	$R_1^D = D(5.7, 4.5, 0.7)$ $R_2^D = Be(12.5, 3.9)$ R_3^D: Bootstrap	$R^T = \Gamma(3.28, 62.17)$ capped at 340	U_1 from 0.1 to 0.5. $U_2 = U_3$ from 0.1 to 0.5 (steps of 0.1)	Stochastic
ECA presence	50	$R_1^D = D(5.7, 4.5, 0.7)$ $R_2^D = Be(12.5, 3.9)$ R_3^D: Bootstrap	$T_k^{total} = 250$ $T_k^{total} = 500$ $T_k^{total} < T_2^{max}$	$U_1 = 0.284$ $U_2 = 0.326$ $U_3 = 0.333$	Deterministic ranging from 0 to 100% with steps of 20 percentage point

3.4.1   Case results

For the case experiments, we consider a specific trip profile to study the behavior of exploitation costs for both types of configurations. This enables examining whether the higher initial investment costs of the LNG dual-fuel configuration can be recovered by the potentially lower fuel costs.

The case results show that the fuel costs for the LNG dual-fuel configuration are lower than the conventional configuration for all price scenarios considered (See Fig. 3.2). Even when LNG prices end up considerably above than MGO and HFO (i.e., "What if 3"), fuel costs for the LNG dual-fuel configuration are 4% lower than conventional vessels. This somewhat counter-intuitive outcome can be attributed to the fact that vessels with the LNG dual-fuel configuration simply have an additional fuel to choose from. Due to the stochastic nature of the fuel prices, the LNG dual-fuel configuration can save fuel cost every time the LNG fuel price drops below that of MGO or HFO. For the other price scenarios, fuel cost reductions are much higher, ranging from 24% up to 47%.
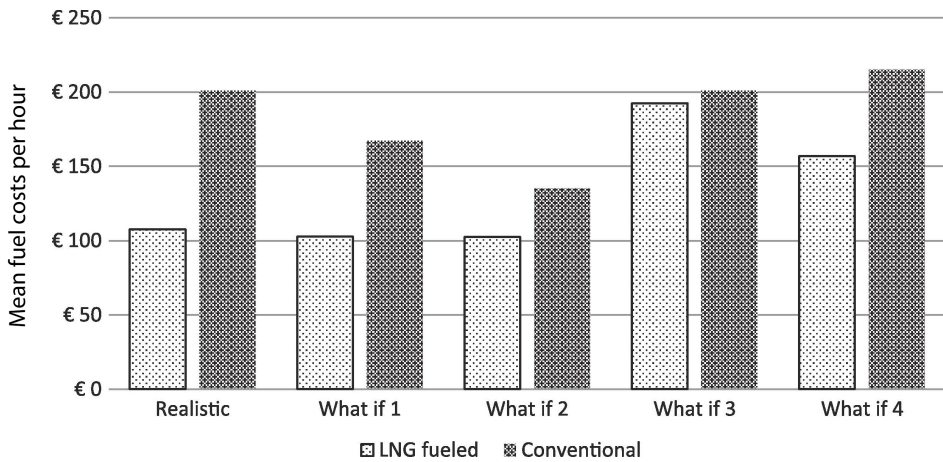

Figure 3.2: Mean fuel costs per hour.

For the LNG dual-fuel configuration to be economically viable, the fuel cost reductions should outweigh the additional initial investment costs. This is reflected in our analyses of the overall exploitation costs (see Fig. 3.3). These reveal that LNG-fueled vessels are more cost-effective than conventional vessels for price scenarios where LNG prices are similar to, or remain below, HFO prices, as long

as MGO prices remain the highest. These price developments are reflected in price scenarios "Realistic", "What if 1" and "What if 4". This implies that the additional initial investment costs of LNG-fueled vessels can even be recovered when the price for LNG rises above that of HFO, as long as the price for MGO remains—considerably—above that of LNG (e.g. price scenarios "What if 1" and "What if 4"). This can be attributed to the ECA regulations, which render conventional vessels more expensive because they have to sail on MGO within ECA.
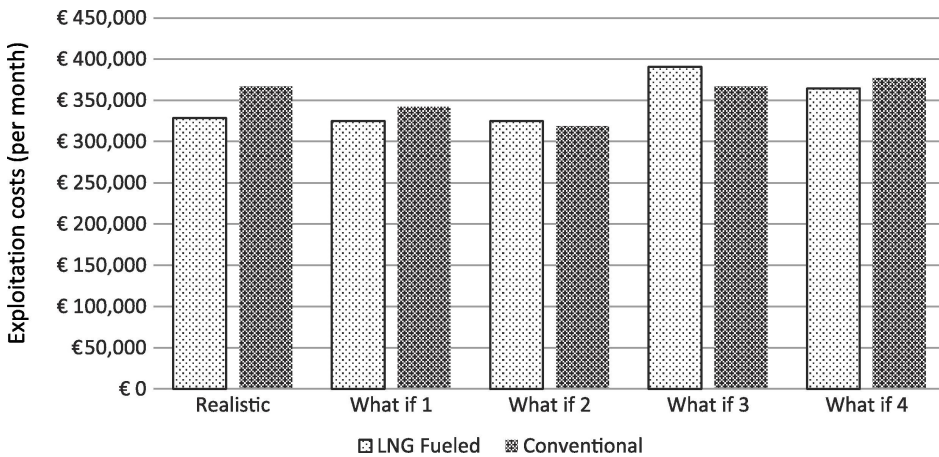

Figure 3.3: Average monthly exploitation costs.

For the other two what-if scenarios, the fuel cost reductions do not fully recover the additional investment required for the LNG dual-fuel configuration. These scenarios reflect the case where the current prices for MGO, LNG and HFO would keep increasing proportionally, with a price for LNG in between the price for MGO and HFO (i.e., "What if 2"), or where the LNG price rises sharply above the price for MGO and HFO (i.e., "What if 3").

3.4.2   Numerical results

In this section, we discuss the behavior of exploitation costs for both fuel configurations and study the wider applicability of our investment appraisal method. To this end, we consider settings that are different from the case experiments by changing the values (or probability distributions) of the fuel prices, route profiles, fuel consumption levels and ECA presence.

Table 3.5: Mean fuel costs per hour for stochastic and deterministic fuel prices.

	LNG			Conventional		
	Stochastic prices	Deterministic prices	% Change	Stochastic prices	Deterministic prices	% Change
Realistic	107.54	107.54	0%	201.09	201.09	0%
What if 1	102.72	104.51	1.75%	167.18	167.09	−0.06%
What if 2	102.51	104.51	1.96%	135.14	134.35	−0.58%
What if 3	192.50	193.95	0.76%	201.09	200.70	−0.20%
What if 4	156.92	156.92	0%	215.07	215.07	0%

Table 3.6: Mean fuel costs per hour for different Gamma distribution parameters for R^T.

	LNG			Conventional		
	$\alpha = 3.2839$ $\beta = 62.166$ $\mu = 0.053$	$\alpha = 6.5678$ $\beta = 62.166$ $\mu = 0.106$	% Change	$\alpha = 3.2839$ $\beta = 62.166$ $\mu = 0.053$	$\alpha = 6.5678$ $\beta = 62.166$ $\mu = 0.106$	% Change
Realistic	107.54	107.54	0%	201.09	201.09	0%
What if 1	102.72	102.72	0%	167.18	167.18	0%
What if 2	102.51	102.51	0%	135.14	135.14	0%
What if 3	192.50	192.50	0%	201.09	201.09	0%
What if 4	156.92	156.92	0%	215.07	215.07	0%

Daily fuel price volatility

Our experiments show that considering deterministic prices only slightly affects fuel and exploitation costs compared to stochastic prices (as can be seen in Table 3.5). It is noteworthy that fuel costs for the LNG dual-fuel configuration appear to be somewhat higher for deterministic prices when there is a relatively large price spread between LNG and MGO, while HFO is the cheapest fuel (i.e., scenario "What if 1" and "What if 2"). Overall, we conclude that using either stochastic or deterministic fuel prices yield very similar results. This implies that, in the long run, price volatility has little impact on the decision to invest in LNG-fueled vessels.

Total travel time

Our numerical results for experiments with a different route profile suggest that a different mean for the distribution R^T, which determines the length of trips, has little impact on the investment appraisal of LNG-fueled vessels. This change did not affect the mean fuel costs per hour for either of the two configurations (see Table 3.6).

Fuel consumption levels

Our analyses of different fuel consumption levels show the maximum allowed LNG consumption level, compared to a certain level of HFO and MGO consumption, before the LNG dual-fuel configuration becomes more expensive than a conventional configuration.

For fixed levels of HFO and MGO consumption, it was found that the overall exploitation costs increase and become constant when LNG consumption levels increase (see Fig. 3.4). This behavior can be explained by the fact that the optimal bunker planning chooses for HFO or MGO when LNG consumption levels are relatively high. In those cases, potentially higher HFO and MGO prices are offset by a large LNG fuel consumption. When LNG consumption becomes large ($U_2 \to 0.5$), the difference in exploitation costs between LNG-fueled and conventional vessels approaches the difference in monthly exploitation costs without fuel cost (i.e., €30,000) as can be seen in Fig. 3.4 for MGO and HFO consumption levels of 0.1 and 0.2. A similar pattern is found for the other price scenarios.
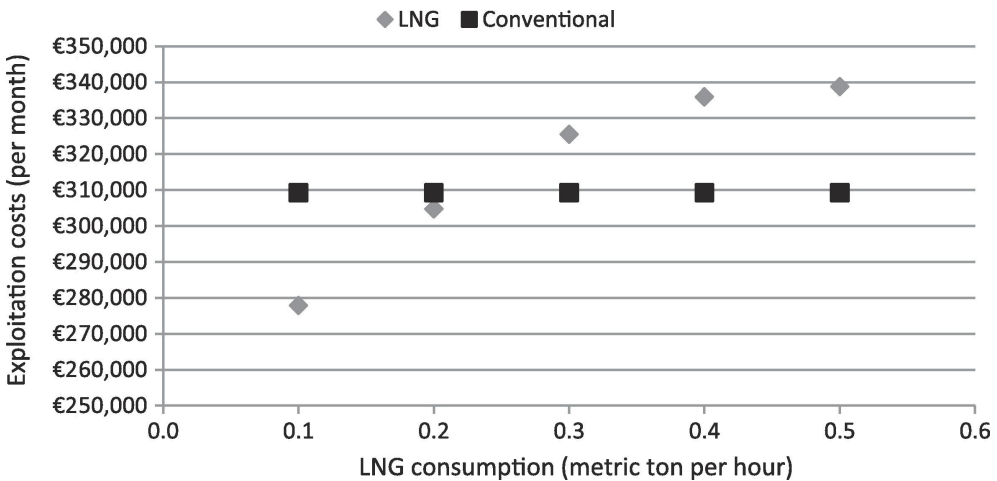

Figure 3.4: Monthly exploitation costs in "Realistic" scenario for different levels of LNG consumption relative to a fixed HFO and MGO consumption ($U_3 = U_2 = 0.2$).

Our results indicate that the maximum allowed LNG consumption level increases for higher levels HFO and MGO consumption levels in all experiments (see Table 3.7). This suggests that LNG vessels are more economically viable than conventional vessels at higher fuel consumption levels of all fuel types. For example,

LNG consumption can only be 10% above HFO and MGO consumption levels for
low HFO and MGO consumption levels ($U_2 = U_3 = 0.2$) for scenario "Realistic".
However, LNG fuel consumption can be 45% above MGO and HFO consumption
for high MGO and HFO consumption levels (see Table 3.7, $U_2 = U_3 = 0.4$). This was
pattern was observed in all experiments.

Table 3.7: Approximated maximum LNG consumption for a given level of HFO and
MGO consumption (in metric ton per hour).

HFO and MGO consumption (U_2 and U_3)	Realistic	What if 1	What if 2	What if 3	What if 4
0.2	0.22	0.17	0.11	0.12	0.15
0.3	0.40	0.34	0.22	0.18	0.29
0.4	0.58	0.69	0.34	0.27	0.41
0.5	N.A.	N.A.	0.47	0.35	0.54

Lastly, our method does not appear to be very sensitive to the estimated LNG
fuel consumption level in the case experiments. In the "Realistic" price scenario,
LNG consumption levels can be 33% above those of HFO and MGO before the
overall exploitation costs of the LNG dual-fuel configuration become higher than the
conventional configuration, when considering HFO and MGO consumption levels
very similar to the case experiments ($U_2 = U_3 = 0.3$)

ECA presence

The results from the experiments with different percentages of ECA presence
(ranging between 0 and 100% in steps of 20 percentage point), enable identifying
the ECA presence at which the LNG dual-fuel configuration is more economically
feasible than a conventional configuration.

The results indicate that LNG-fueled vessels are already economically beneficial,
compared to conventional configurations, for very low ECA presence (0-30%) when
LNG price trends remain much below the MGO price trend (i.e., the "Realistic",
"What if 1" and "What if 4" scenarios). Furthermore, the exploitation costs
of LNG-fueled vessels react less strongly to differences in ECA presence than
conventional vessels for all experiments conducted (e.g. scenario "Realistic", see
Fig. 3.5). This indicates that higher ECA presence favors LNG-fueled vessels, which
confirms the findings of Wang and Notteboom (2014) and Burel et al. (2013). It also

suggests that LNG-fueled vessels offer more stable exploitation cost under variable route profiles. Less strong reactions of LNG-fueled vessels to ECA presence can be explained by a lower dependence on MGO prices when sailing in ECA zones.
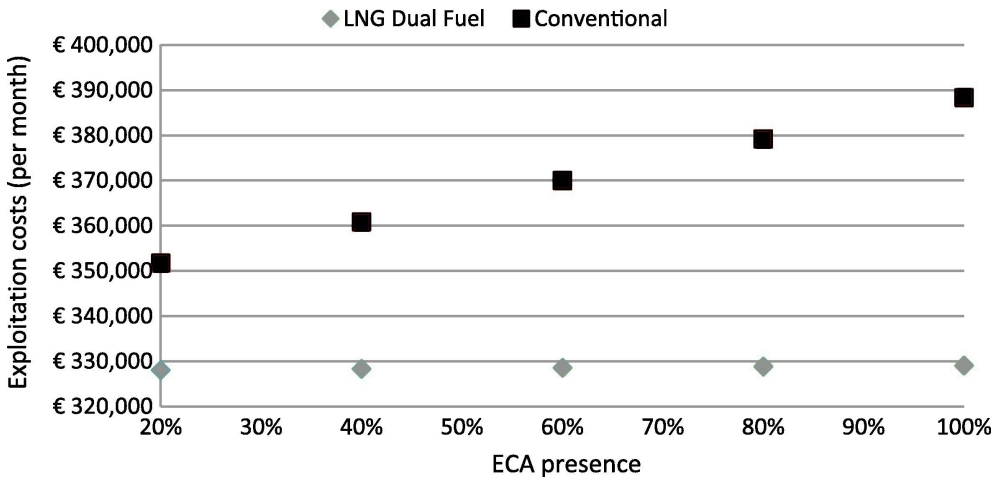

Figure 3.5: ECA presence and exploitation costs for scenario "Realistic" ($T_{k,i}^{total} = 250$).

A relatively high minimum ECA presence of 68% is required for price scenario "What if 2". This implies that a relatively large ECA presence is needed for price spreads which reflect the fuel prices at the time of writing. When the LNG price increases (much) beyond the price for MGO and HFO (i.e., scenario "What if 3"), even 100% ECA presence would not be sufficient for LNG-fueled vessels to have lower exploitation costs than conventional vessels.

3.5 Conclusion

More stringent emission regulations stimulate vessel owners to consider the adoption of cleaner, alternative fuels, such as LNG. In this paper, we presented a new investment appraisal method to support vessel owners in their decision to invest in LNG-fueled vessels. We use this method to analyze the fuel costs and overall exploitation costs of LNG-fueled and conventional vessels by simulating bunker planning practices under stochastic fuel prices, ECA presence and route lengths. Moreover, we consider a broad range of future price developments for different

marine fuels.

The results presented in this paper delineate the conditions under which
LNG-fueled vessels have lower overall exploitation costs than their conventional
counterparts.   Firstly, the fuel costs of LNG-fueled vessels are lower than
conventional vessels for all price scenarios considered in this study—even for the
scenario where the fuel price for LNG grows considerably above the price of
conventional fuels.   To be economically viable, however, these lower fuel costs
need to outweigh the additional initial investment associated with LNG-fueled
vessels.   Our analyses show that this is the case as long as the price for MGO
stays considerably above that of LNG, regardless of the price for HFO. Secondly, the
exploitation costs of LNG-fueled vessels are lower for larger fuel consumption levels
of all fuel types. Finally, LNG-fueled vessels are more competitive at higher levels
of ECA presence relative to conventional vessels, but in a realistic price scenario
also a low ECA presence would already result in lower overall exploitation costs.
The exploitation costs of conventional vessels react more strongly to changes in ECA
presence than LNG-fueled vessels, which results in more stable costs for LNG-fueled
vessels under variable route profiles.

We have also shown the broader applicability of our method and its outcomes
by conducting a series of numerical analyses. These indicate that the results of
our method remain unaffected by different route lengths and apply to a large
range of route profiles. Our numerical study also suggests that price volatility
does not notably affect the outcomes of our method. Marginal exploitation costs
of LNG-fueled vessels decline for higher levels of LNG consumption when MGO
and HFO consumption is low due to bunker choices that favor HFO or MGO.
Lastly, it was found that our method is not very sensitive to fuel consumption levels,
indicating that a mistake in the LNG fuel consumption estimation provided by the
engine producer would not directly affect the outcomes.

Investment appraisal methods are prone to limitations, and ours forms no
exception.   Firstly, the results in this paper only apply when vessel operators
seek to optimize their bunker planning decisions for every single trip.   Indeed,
bunker planning policies become particularly important when sailing with an LNG
dual-fuel configuration as the economic benefits of this configuration mainly stem
from having an additional, potentially cheaper, fuel to choose from. Secondly, our
method determines the average expected monthly exploitation costs as a measure

to compare LNG-fueled with conventional vessels. Yet, the economic benefits of LNG-fueled vessels are not evenly distributed over the exploitation period. Depending on future price developments, fuel cost reductions may emerge only later and it is likely that some of the required extra initial investment must be born at the start of the exploitation period. Future work could expand our method to include cash flow differences during the exploitation period of the vessel. Thirdly, our study does not include lost revenue that stems from a reduced cargo space due to extra fuel tanks. Therefore, future research could investigate the extent to which reduced cargo space influences the economic viability of LNG-fueled vessels. Future work may also incorporate the effect of a limited LNG bunkering infrastructure on the economic feasibility of LNG-fueled vessels to further examine the nuances associated with the decision to adopt LNG as a marine fuel.
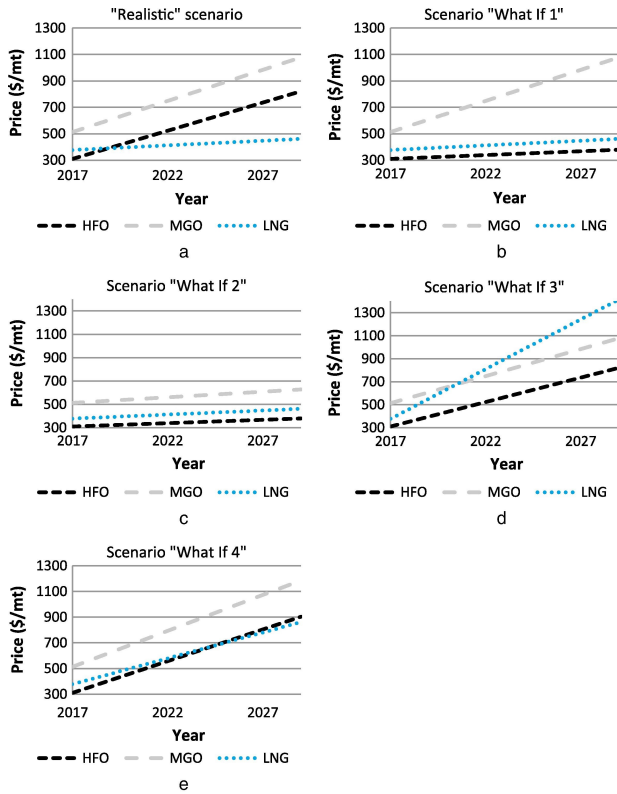
3.6 Acknowledgements

3.7 Appendix

Figure 3.6: Price scenarios.

Chapter 4

Combining biogas, wind and solar energy to match local demand: The production–storage trade-off

Abstract. *The transition from fossil fuels to cleaner alternatives presents challenges such as the need to match increasing fluctuations in supply and demand. For rural communities of houses and farms, electricity needs can be supplied locally using a combination of biogas, wind and solar energy. The mismatch between energy demand and renewable energy supply creates a trade-off in the need for storage and installed production capacities. In this study, we examine which mix of renewable energy sources is needed when minimizing a specific combination of storage and production capacity. By matching supply and demand using empirical time series data, we take into account the effect of seasonality and determine the hourly storage, consumption and curtailment decisions. Our model avoids the inclusion of costs, because investment costs are uncertain and this enables determining a suitable mix of sources purely based on profiles before making any investments. We find that biogas, which has a constant supply profile, takes the largest share of the supply. Wind energy becomes increasingly important in reducing storage needs when total production levels range between 116% and 122% of total demand. We also show how and why the optimal shares change*

when a certain overcapacity is installed. This has important implications for planning future investments regarding the mix of renewable energy sources. It important to note that these conclusions are specific to the Dutch situation and might be different in other countries due to differences in weather and the resulting renewable energy production levels.

4.1   Introduction

It is generally agreed that improving energy efficiency and increasing the share of renewables is necessary to accommodate the rising trend in energy demand worldwide and the transition from fossil fuels to cleaner alternatives Alanne and Cao (2017a); Li et al. (2013a). However, the intermittent nature of both demand and renewable energy supply poses challenges in matching supply and demand. This generally leads to high storage requirements Reuß et al. (2017). Higher penetration levels of renewable energy increasingly necessitate hydrogen storage Won et al. (2017), because hydrogen can be stored in large amounts at the terawatt-hour scale Reuß et al. (2017) and, in contrast to batteries, it does not lose its energy content over time when stored properly.

At a regional scale, rural communities of farms and households can produce and consume renewable energy generated by wind, solar energy and biogas. Communities of farms can be suitable renewable energy providers owing to the availability of land for solar energy and wind, as well as to the availability of biomass such as manure for producing biogas. Households are also increasingly adopting solar energy to supply their electricity needs. However, matching the differences in supply and demand profiles at a regional scale can be challenging. Biogas has a relatively constant production profile, while wind and solar energy are more variable Bett and Thornton (2016), but none of them can be flexibly adjusted Hahn et al. (2014).

Combining the various production profiles of multiple renewable energy sources can be an effective way to reduce the required storage or production capacities. These can be minimized for given supply-and-demand profiles by determining the capacity and relative share of wind, solar energy and biogas production Lee et al. (2018).

In determining the size of a storage facility, decision-makers need to decide on the level of installed production capacity, and vice versa. If the total yearly supply

of renewables were at its lowest level to meet demand, extreme amounts of storage
would be needed. Investing in excess production capacity reduces storage needs.
For rural communities of households and farms, the question arises as to what mix of
renewable sources is required for certain levels of excess production capacity and/or
storage.

In this paper, we examine which energy mix is needed in the respective cases
when storage is either existent or non-existent and how the energy mix changes
with different levels of production and storage capacity for a regional community
of households and farms. In contrast to the existing literature, we simultaneously
determine the capacities of each renewable source and the operational decisions
that specify the times at which energy from each source is either consumed or
stored. We address this problem from the perspective of production and storage
capacities by focusing purely on production and demand profiles rather than on
costs. Since future investment costs are uncertain, this perspective allows us to
obtain insight into the behavior of inventory levels and the optimal capacities of
each source resulting from the installation of a certain combination of production
capacity or storage capacity. As Fig. 4.1 shows, we assume that the energy from
all renewable sources is generated as electricity, stored as hydrogen and again
consumed as electricity using fuel cells.

4.2   Literature review

In this section, we position our problem and approach in the context of the
existing literature. Studies in the literature have mostly determined the capacities
of renewable sources and storage of a single proposed system by evaluating the
performance with regards to indicators such as cost conditions. Most papers have
included only wind and solar energy, and only limited work has been done on the
inclusion of stable sources such as biogas in the context of farms surrounding a
community of households. Most work has focused on batteries as a storage medium,
which disregards the problem of seasonality. To the best of our knowledge, there
have been no studies specifically addressing the relationship between storage and
production capacity, and the related shares of each source, by matching variable
supply and demand profiles.

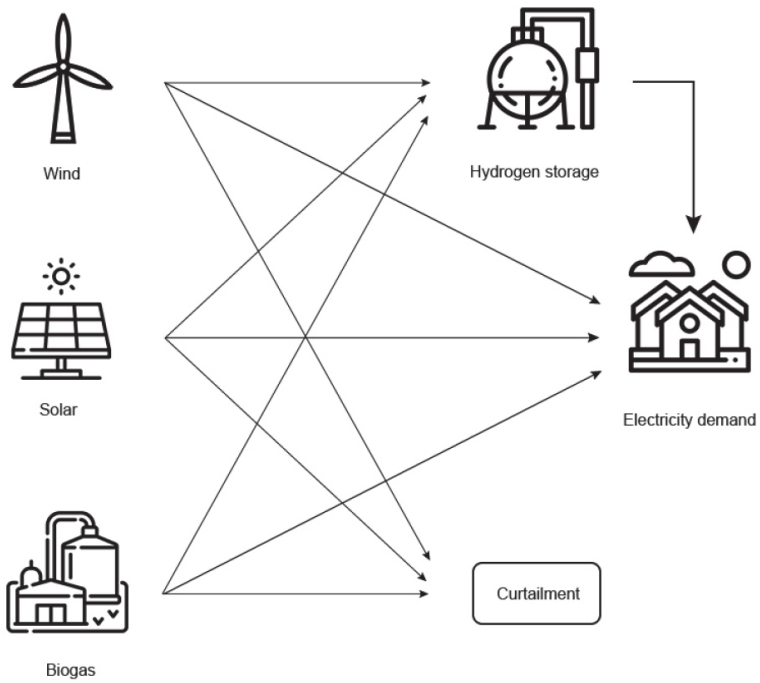Papers that specifically address the shares of multiple renewable sources in

Figure 4.1: Shares of wind, solar energy and biogas, storage capacity, local demand, and curtailment

the total energy mix include Kaabeche et al. (2011); Kaabeche and Ibtiouen (2014);
Mazzeo et al. (2018); Weitemeyer et al. (2015).   For example, Kaabeche et al.
(2011) and Kaabeche and Ibtiouen (2014) show how costs and emissions behave for
specific combinations of solar and wind capacities. Mazzeo et al. (2018) shows how
operational decisions such as the energy sent and drawn from the grid are affected
by different capacity combinations of solar energy and wind. Papers that focus on
the relationship between storage and production capacity include Rodrigues et al.
(2015); Weitemeyer et al. (2015). Weitemeyer et al. (2015) show how combinations of
wind and solar energy shares and storage affect the share of a renewable in meeting
demand after curtailment. Rodrigues et al. (2015) show how a battery can be used
and sized to reduce curtailment during off-peak times. This allows the associated
shares between solar and wind energy to be obtained. However, none of these
papers provide insights in the relationship between storage and production capacity
and how this affects the shares and operational decisions for each renewable source
in the energy mix.

Even though the stable supply pattern of biogas presents opportunities to reduce
storage requirements, most papers have focused on configurations in which the
sizing of photovoltaic (PV) panels and wind energy is addressed. For example,
Ángel A. Bayod-Rújula et al. (2013) analyze the influence of sizing hybrid wind
and PV systems on the interactions with the electricity grid. Bartolucci et al. (2018)
evaluate how the sizing of PV installations affects the resilience of the system and
the environmental impact. Bianchi et al. (2014) investigate the feasibility of PV
panels combined with batteries and obtain optimal battery sizes. Castaneda et al.
(2013) address the control strategies and sizing of standalone hydrogen storage in
combination with PV solar panels. Eltamaly et al. (2016) address optimizing the
design of systems comprising of solar panels, wind energy, diesel and batteries to
minimize cost and maximize reliability. Moreover, Iverson et al. (2013) minimize
the levelized cost of energy for power demand in a residential network. Malheiro
et al. (2015) similarly focus on minimizing the levelised cost of energy by obtaining
optimal combinations of wind, PV, diesel and batteries. Ren et al. (2016) minimize
the running cost of a system consisting of solar panels, batteries and hydrogen for
a residential setting. Jorgenson et al. (2018a) address how transmission and storage
capacity can help in reducing curtailment of wind and solar energy. Kim and Kim
(2017) only consider wind in determining wind farm layouts for hydrogen-based

storage. Samsatli et al. (2016) also focus on determining locations and sizes of storage and transport facilities of wind-based hydrogen and electricity networks. Finally, Kaviani et al. (2009) address the design of wind and solar-based hydrogen systems to minimize annual costs.

Relatively few studies have included biogas in the combination of renewables. For example, Lee et al. (2018) provide a framework for sizing solar energy, wind and biogas for multiple storage facilities and demands. However, their approach focuses on minimizing costs and grid-imported electricity and they do not examine the relationship between storage and production. Chauhan and Saini (2016) conduct a feasibility study on the development of a renewable energy system with multiple sources with battery storage. Upadhyay and Sharma (2015) consider biogas, hydroenergy, PV panels, diesel and batteries and optimize the capacities of each renewable energy source. Hurtado et al. (2015) also consider biomass in combination with solar energy and batteries. Heydari and Askarzadeh (2016) determine both the size of PV panels and installed capacity of biogas digesters without considering storage, in which excess energy is discarded. Ho et al. (2014) address the sizing of the combination of biogas with solar energy. They assume that excess generated energy is stored. While these papers focus on the inclusion solar and wind energy, it is still unclear how including stable supply profiles such as biogas would affect the shares of multiple renewable energy sources for different production and storage capacities.

While seasonal storage is regarded as an important requirement of renewable energy supply Reuß et al. (2017), most studies have focused on battery-only systems, which are not directly suitable for seasonal storage owing to their high cost and limited capacity. Batteries have been the most prevalent storage method in previous and recent research. In addition to the above-mentioned articles that include batteries, the following studies also incorporate batteries in their configurations. For example, Ogunjuyigbe et al. (2016) study the cost of energy for different configurations that include PV, wind and diesel generators. Zhao et al. (2014) consider the sizing of the same combination of energy sources and optimize this for multiple objectives which include costs, emissions and renewable energy penetration. Ahadi et al. (2016) also optimize combinations of wind, PV and batteries, but do so for a standalone community without diesel. We refer to Yang et al. (2018); Khare et al. (2016) for literature reviews on renewable energy configurations that include batteries. However, although batteries are suitable for

daily variability, this is not the case for seasonal storage owing to capacity limitations
arising from extremely high costs and limited lifespan Malheiro et al. (2015). We
focus in this paper on hydrogen storage to bridge the seasonality gap between
supply and demand.

   We aim to fill this gap by determining the optimal shares of wind, solar energy
and biogas and the operational decisions required for different combinations of
production and storage capacities. In doing so, we develop a model that avoids
the inclusion of costs due to the uncertainty related to future prices. We determine
the optimal sizes and shares of each source in producing electricity, such that the
variable profiles of supply and demand are most effectively matched for a certain
level of (excess) production and storage capacity.

4.3   Problem description

The main problem addressed in this paper is concerned with deciding on the size of
each renewable source and the level of storage capacity. This decision requires that
the variable supply and demand profiles be matched such that excess production is
either stored or curtailed. Oversizing the production capacity of an energy source
requires less storage and leads to higher excess production at specific times than
reduced production capacity.

   It should be emphasized that we aim to examine which variable supply profiles
connect well with the demand profile without addressing investment costs. While
costs are an important component in investment decisions, these can be uncertain
for long planning horizons in which future prices and technological developments
cannot be easily predicted. Incorporating costs provides insights only about
configurations under certain cost conditions. Not including costs enables allows an
examination to be made as to how the variability profiles of each supply source and
demand can be matched effectively using a combination of production and storage
capacity. Accordingly, we use a weight parameter C that indicates the relative
importance of each of these in the objective function. The objective function consists
of two components. The first component consists of the peak inventory levels for a
hydrogen tank supplied by wind, solar energy and biogas during a given planning
horizon. The peak inventory level represents the required storage capacity during
the planning horizon. The second component represents the total weight of the total

energy generated. Since increased production capacity leads to increased amounts of supply, we express the production capacity as the total amount of energy generated. This approach allows us to quantify the relationship between production capacity and storage capacity. The objective is minimized by determining the relative size of each renewable source and the operational decisions that specify the movement and direction of energy flows for a given supply-and-demand profile for each period in time.

We define the following sets, parameters and variables (see Table 4.1). Let $\mathcal{T}$ be the set of periods within the planning horizon N. These represent 1-hour time intervals in our model. We also define a set of renewable sources $\mathcal{R} = \{0, 1, 2\}$, representing solar energy, wind energy and biogas.

We define the following parameters. S_{rt} denotes the supply in kilowatt-hours of renewable source $r \in \mathcal{R}$ at time $t \in \mathcal{T}$. The efficiency of energy transferred to storage by renewable source $r \in \mathcal{R}$ is denoted by E_r, whereas the energy transferred from source $r \in \mathcal{R}$ directly to demand is denoted by E_r^d. The energy transferred from storage to demand is denoted by E^f. The demand in period $t \in \mathcal{T}$ is denoted by D_t. C denotes a steering parameter that defines the weight of the total energy generated during the planning horizon relative to the storage capacity. Instead of determining costs of each explicitly, we only vary this ratio to generate different feasible combinations of production capacity and storage capacity and the related sizes of each renewable energy source.

We define i_t as the inventory level in the storage tank at time $t \in \mathcal{T}$. Moreover, k_r represents the sizing factor of renewable source $r \in \mathcal{R}$. It is used to multiply the energy supply S_{rt} by the sizing factor k_r to derive the actual supply s_{rt} of renewable source $r \in \mathcal{R}$ that is needed at time $t \in \mathcal{T}$ to supply the total demand. a_{rt} is defined as the amount of energy transferred from $r \in \mathcal{R}$ to storage at time $t \in \mathcal{T}$. We also define f_t as the amount of energy obtained from storage at time $t \in \mathcal{T}$. We define d_{rt} as the amount of energy directly consumed from renewable source $r \in \mathcal{R}$ at time $t \in \mathcal{T}$. We define p as the peak inventory level inside the storage during the planning horizon. The peak inventory level represents the amount of storage required in the planning horizon. y represents the inventory level at both the beginning and end of the planning horizon. We define y as a decision variable to deal with potential inventory initialization bias. In particular, setting the initial inventory equal to the inventory level in the last period allows us to obtain stable inventory conditions and

makes the levels cyclic in a repetitive pattern of deterministic supply and demand. Finally, c_{rt} represents the excess produced energy or curtailment from renewable source $r \in \mathcal{R}$ at $t \in \mathcal{T}$ that will not be stored. This excess-produced energy can be injected into a grid or deliberately discarded, but will be referred to as curtailment.

Table 4.1: Sets, parameters and variables.

Sets	
$\mathcal{T}$	Set of periods (1-hour intervals) $\mathcal{T} = \{1, \ldots, N\}$
$\mathcal{R}$	Set of renewable sources (wind, solar energy and biogas) $\mathcal{R} = \{0, \ldots, E\}$
Parameters	
S_{rt}	Energy supplied by renewable source $r \in \mathcal{R}$ at time $t \in \mathcal{T}$ in kWh
E_r	Efficiency in % of the energy transferred *to* storage from renewable source $r \in \mathcal{R}$
E_r^d	Efficiency in % of the energy transferred *directly* to demand from renewable source $r \in \mathcal{R}$
E^f	Efficiency in % of the energy transferred *from* storage
D_t	Electricity demand in kWh at time $t \in \mathcal{T}$
C	The relative weight of 1 kWh of total energy generated compared with 1 kWh of storage capacity required
Variables	
i_t	Inventory level in kWh at time $t \in \mathcal{T}$
k_r	Sizing factor of renewable source $r \in \mathcal{R}$
a_{rt}	Amount of kWh transferred from $r \in \mathcal{R}$ to storage at time $t \in \mathcal{T}$
f_t	Amount of kWh obtained from storage at time $t \in \mathcal{T}$
d_{rt}	Amount of kWh directly consumed from renewable source $r \in \mathcal{R}$ at time $t \in \mathcal{T}$
s_{rt}	Actual supply in kWh of renewable source $r \in \mathcal{R}$ at time $t \in \mathcal{T}$
p	Storage capacity (highest inventory level) in kWh
y	Starting inventory level in kWh
c_{rt}	Amount of curtailment in kWh from renewable source $r \in \mathcal{R}$ at time $t \in \mathcal{T}$

A certain combination of storage and production capacity can result in many optimal solutions in which various operational decisions of each source lead to the same objective value. For example, the decision to store or curtail a certain amount of energy can be made by any of the supply sources in the case of production overcapacity. Therefore, we introduce ϵ and γ_t, which have very small values in order to favor a consistent choice of operational decisions without affecting the overall solution in terms of storage and production capacities. Whereas ϵ is a constant, γ_t is time-dependent and ensures that when curtailment takes place, it is scheduled in successive periods and as late as possible in the planning horizon without loss of generality. This choice is made because, in a stochastic situation, it would be sensible to store energy at an early time and defer curtailment in order to avoid situations in which energy is unavailable. γ_t is given by

$$\gamma_t = \frac{\epsilon \, (2N - t)}{N} \qquad\qquad \forall \, t \in \mathcal{T}. \qquad (4.1)$$

Having explained this, we define the objective function of our LP problem. The objective function minimizes the weighted combination of storage needs and the total amount of energy generated. Storage needs are expressed as the highest inventory level that occurs in kilowatt-hours. The total amount of energy generated is the sum of the actual supply s_{rt} for all periods and renewables. However, we subtract a small fraction of total curtailment.

Curtailment was included in the objective function using γ_t for two reasons. First, it is included in order to slightly reward curtailment in favor of storage. Since energy flows that move through storage create conversion losses, multiple optimal solutions may exist in which energy is either curtailed through the normal curtailment route or moved to and from storage in the same period, creating "hidden curtailment". Slightly favoring curtailment over storage alleviates the issue of curtailment through storage and makes sure that all curtailment is measured by c_{rt}. Second, we schedule any curtailment late in the planning horizon in order to reduce the number of optimal solutions without loss of generality and to avoid the issue of performing both curtailment and storage decisions at random times. Unnecessary interchanges between curtailment and storage due to multiple optimal solutions would impede our analysis and are undesirable in practice, because the electrolyzer would operate at a highly variable load. This leads to the following objective function:

$$\min \quad p + C \left(\sum_{t \in \mathcal{T}} \sum_{r \in \mathcal{R}} s_{rt} - \sum_{t \in \mathcal{T}} \sum_{r \in \mathcal{R}} \gamma_t c_{rt} \right). \tag{4.2}$$

Constraints (4.3) calculate the actual supply used in the model by multiplying the sizing factor k_r with the supply parameter S_{rt} for each renewable source r and period t:

$$s_{rt} = k_r S_{rt} \qquad \qquad \forall \, r \in \mathcal{R}, t \in \mathcal{T}. \tag{4.3}$$

Constraints (4.4) calculate the inventory levels in storage at the end of period t by taking into account the efficiencies of energy moving to and from a storage facility:

$$i_t = i_{t-1} + \sum_{r \in \mathcal{R}} (\theta_r + E_r) a_{rt} - f_t \qquad \qquad \forall \, t \in \mathcal{T}. \tag{4.4}$$

To reduce the number of optimal solutions without loss of generality, storage by

wind is given slightly higher to-storage efficiencies using $\theta_r = \{0, 1 + \epsilon, 1 + 2\epsilon\}$. Thus, if a choice is made about which source to send to storage and which source to use directly to fulfill demand, wind will be stored. This makes sure that storage decisions can be distinguished between sources and are meaningful for analyses.

Constraints (4.5) calculate the inventory levels in storage at the end of the first period in the planning horizon ($t = 0$):

$$i_0 = y + \sum_{r \in \mathcal{R}} (\theta_r + E_r)\, a_{r0} - f_0. \tag{4.5}$$

Constraints (4.6) ensure that the peak inventory level p is below or equal to the inventory level i_t for each period t:

$$i_t \leq p \qquad\qquad\qquad \forall\, t \in \mathcal{T}. \tag{4.6}$$

Constraints (4.7) ensure that the starting inventory level in storage is equal to the ending inventory level in order to obtain a solution that can be repeated each year and to alleviate a possible confounding effect of initial inventory levels:

$$y = i_N. \tag{4.7}$$

Constraints (4.8) ensure that the starting inventory y is also lower or equal to the peak inventory level p:

$$y \leq p. \tag{4.8}$$

Constraints (4.9) ensure that the energy transferred to storage and the direct consumed energy are equal to the actual supply at period t:

$$a_{rt} + d_{rt} + \beta_r c_{rt} = s_{rt} \qquad\qquad \forall\, r \in \mathcal{R}, t \in \mathcal{T}. \tag{4.9}$$

To reduce the number of optimal solutions that lead to the same objective value, curtailment of wind is slightly favored using $\beta_r = \{1, 1 - \epsilon, 1 - 2\epsilon\}$. This enables the distinction of curtailment decisions between the different sources of supply.

Constraints (4.10) ensure that the energy obtained from storage and the directly

obtained energy are equal to demand in period t:

$$E^f f_t + \sum_{r \in \mathcal{R}} E^d_r d_{rt} = D_t \qquad\qquad\qquad \forall\, t \in \mathcal{T}. \qquad\qquad (4.10)$$

4.4   Experiment definitions

This section provides an overview of the experiments we conducted in our study. We apply our model to real-life data and perform sensitivity analyses. We assume that the wind, biogas and solar energy supplies are known in advance.

4.4.1   Data and parameter settings

For all experiments, we obtained aggregated consumption data of multiple households in the Netherlands for the year 2009. The aggregated household hourly electricity consumption has a mean of 1.85 MW and a standard deviation of 0.72 MW. The total amount of energy consumed in 2009 was 16.2 GWh. The data consisted of 1-hour measurements, and no data were missing. We also obtained solar generation data from Eelde in the Netherlands for 2009 from the Photovoltaic Geographical Information System (European Commission). The data on solar energy generation levels reflect an installed capacity of 2.5 kWp with a mean generated energy of 0.286 kWh and a standard deviation of 0.49 kWh. Hourly wind data were also obtained from Eelde in 2009 via the Dutch National Meteorological Institute (KNMI). The data were measured in meters per second. These values were converted to power levels using a power curve with a cut-in speed of 3 m/s, a rated speed of 14 m/s at 3 MW and a cut-out speed of 25 m/s. The hourly generated energy has a mean of 0.39 MWh per hour and a standard deviation of 0.48 MWh per hour. Since biogas production is a very stable process, we assume a constant biogas production rate of 1 MWh per hour. It should be noted that the installed capacity of an energy source in the original data is not relevant for our model. This is because the sizing factor in our model is determined during the optimization process and is used to derive the actual sizes of the installed capacity for each source.

Table 4.2 shows the conversion efficiencies for each source. Since we consider the production of hydrogen to enable storage of electricity from solar energy, wind and biogas, we assume conversion losses for each conversion step. To avoid unequal

weights for the generation of each source in the objective function, each source
is represented by the amount of electricity generated from it. Therefore, biogas
is represented in terms of the energy contents available after having generated
electricity using a combined power and heat (CHP) engine. Accordingly, the
efficiencies of supplying directly to demand and to storage were set equal for each
source. Conversion efficiencies for direct consumption were set at 1 for all sources,
since the possible small losses would be equal for all sources and also occur after
electricity generation from hydrogen. The conversion efficiencies of all sources to
hydrogen using an electrolyzer were set at 70%, since efficiencies between 65%
and 75% are common for proton exchange membrane (PEM) electrolyzers Koponen
et al. (2017). Furthermore, the fuel cell efficiency in which hydrogen is converted to
electricity was set at 50% Iverson et al. (2013).

Table 4.2: Overview of conversion efficiencies.

Description	Efficiency
Solar energy to demand (E_0)	1
Wind to demand (E_1)	1
Biogas to demand (E_2)	1
Solar energy to storage (E_0^d)	0.7
Wind to storage (E_1^d)	0.7
Biogas to storage (E_2^d)	0.7
Storage to demand with fuel cell (E^f)	0.5

4.4.2 Experiments

The experimental setup is summarized in Table 4.3. For the main experiments, we
executed experiments (set 1) with 100 levels of C on a scale between 0 and 1 to derive
insights into the behavior of storage requirements and sizes of each of the renewables
for different levels of storage capacity and production capacity. To understand how
these levels interact in a real-life context, the experiments were conducted using
the real-life data introduced in Section 4.4.1. One hundred levels appeared to be a
sufficient resolution to create a clear picture of the trade-off between excess capacity
and storage needs. To enhance the accuracy for very low and high storage and
production capacities, we performed additional experiments for very low and high
values of C, resulting in a total of 133 experiments.

Table 4.3: Overview of experimental setup.

Description	Experiment set	Number of experiments	Years (solar and wind)
Main experiments	1	133	2009
Exclude wind	2	133	2009
Exclude biogas	3	133	2009
Limited biogas availability (≤371 kW, 20% of demand)	4	133	2009
Smooth wind size curve	5	133	2009
Sensitivity to different years	6	1064 (133 × 8)	2009–2016

Because constant sources such as biogas may not always be available in every environment and to evaluate the storage requirements of configurations with a more limited set of sources, we performed experiments in which either wind or biogas was excluded (sets 2 and 3). Since biogas availability is limited by a limited supply of manure, we performed an additional set of experiments (set 4) in which the size of biogas was set to a maximum of 20% (371 kW) of the total energy demand. This percentage was derived from the average maximum electricity potential that could be produced using biogas in the Dutch province of Friesland (27%) if all available manure were digested. Since 27% is the maximum potential of converting biogas to electricity, we chose 20% in order to be conservative. Furthermore, we tested the sensitivity of wind shares based on the findings of the original experiments.

We performed a further sensitivity analysis to evaluate the extent to which the relationship between production and storage capacity, and the sizes and shares of each energy source, change for different years of wind and solar supply (set 5). This gave us insight into the level of safety production or storage capacity that may be needed to account for differences between years of wind and solar supply. The experiments of set 1 with the real-life data were repeated with supply data for the same location of wind and solar energy for the years ranging between 2009 and 2016. The electricity demand was fixed for the year 2009, in order to investigate the influence of different wind and solar patterns in supplying demand.

The experiments for each of these factors were conducted with a Gurobi 7.0.2 solver using four cores.

4.5   Results and discussion

In this section, we present and discuss the results of the experiments. These indicate how the storage capacity and the optimal sizes of the renewable sources are affected

by different levels of total energy generated as a result of excess production capacity.

We consider the demand and supply profiles of the real-life data introduced in Section 4.4.1. First, we illustrate the relationship between storage capacity and production capacity for the real-life data. We show how the production levels expressed in percentages of annual demand of each renewable source are affected by different levels of energy generated as a percentage of demand. Second, we zoom into the flows of each source that are used to directly satisfy demand, are moved into storage or will be curtailed, which, for example, may imply grid injection or deliberate discarding. Third, we optimize the shares of each source and then exclude or limit the shares of the energy sources to compare the differences in storage and production capacity requirements. Finally, we show the influence of different years of wind and solar energy supply.

4.5.1   Relationship between production and storage capacity

The results in Fig. 4.2 show the storage requirements on the y-axis and the total energy generated on the x-axis for the experiments in set 1 in which C was varied. Note that a high value of C is associated with low production capacity and vice versa (see the left and right sides of Fig. 4.2, $C = 1000$ and $C = 0.005$). In Fig. 4.2, the C-values of specific points that will be analyzed more deeply have been highlighted.

The results in Fig. 4.2 show that the trade-off curve between storage and production capacity is convex and smooth. Owing to efficiency losses when electricity has to be stored, the minimum amount of energy that had to be generated was 116% of demand. An increase in production from 116% to 117% leads to a relatively high marginal reduction in storage capacity of 1% point, whereas a production increase from 140% to 141% yields a relatively lower storage reduction of 0.1% points. For production levels above 140%, storage requirements approach zero. This shows the importance for decision makers of deciding the levels of storage capacity and production capacity at which to reside. A small amount of excess production capacity greatly reduces storage capacity (see the left side of Fig. 4.2), whereas production capacity that is sized too large does not yield significant reductions in storage capacity (see Fig. 4.2 on the right).
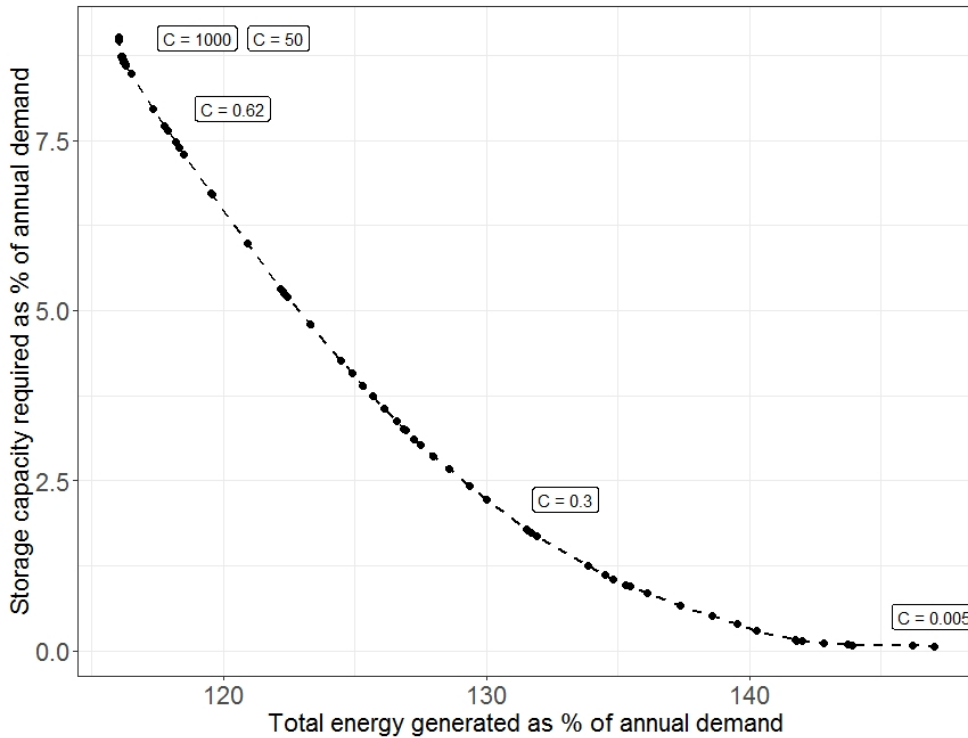
Figure 4.2: Storage capacity required for different levels of total energy generated (% of demand) for experiment set 1.

4.5.2   Renewable shares and production and storage requirements

The results in Table 4.4 illustrate the relative shares of each renewable source as percentages of the total amount of energy produced, the storage capacities and the total production levels for different levels of C. Moreover, Fig. 4.2 sets the storage capacity requirements against the levels of energy generated in percentages of annual demand for the experiments in set 1. The combinations result from optimizing for different levels of C. High levels of C apply to the left side of the x-axis, whereas low levels of C apply to the right side.

The results in Table 4.4 indicate that the shares of biogas range between 91.3% and 98.9%. In particular, they are high for low levels of C, while the lowest shares occur for $C = 0.48$. This indicates that the constant production profile of biogas is highly suitable in supplying demand, especially in situations of overcapacity with high

curtailment and relatively low storage. Overall, the high shares of biogas suggest
that constant sources are important in supplying the demand profiles in combination
with more variable sources such as wind for all levels of production capacity. While
the high levels of biogas shares may not be feasible or desirable in practice owing
to a limited supply of biomass and high cost, this does indicate that constant energy
sources are important in designing renewable energy systems and help in supplying
base-load levels of demand. If sufficient biomass is available, this implies that biogas
can play an important role in the renewable electricity supply of a local community.

The share of wind energy exhibits the opposite relationship to storage capacity.
Wind becomes more important in the energy mix for levels of storage capacity
between 0.2% and 5.2% of the total demand. Wind shares are highest in the
optimized model at $C = 0.48$ for the C-values in the experimental design with a
share of 9.2% of the total energy generated and a storage capacity of 5.2% of demand.
This shows that adding small shares of wind in the energy mix can contribute to
minimizing combinations of production and storage capacities, especially for storage
capacities up to 5% of the total annual demand. In Section 4.5.5, we analyze how
much additional storage capacity is required when wind is excluded.

The shares of 0% for solar energy indicate that the supply profile of solar energy
is less favorable than those of biogas and wind based on the Dutch data. This can
be attributed to the variability in solar supply within days and between days, the
absence of energy generation at night, and the seasonal mismatch between supply
and demand. Therefore, including solar energy creates higher storage or production
requirements than the profiles of wind and biogas in the specific instances studied.
These results also indicate that the profile of wind energy is more favorable than that
of solar energy in capturing peak levels in demand when a constant source such as
biogas is included in the energy mix.

4.5.3   Explaining optimal shares from the operational decisions

Fig. 4.3 extends Table 4.4 by showing more precisely how the production levels
for wind (Fig. 4.3a) and biogas (Fig. 4.3b) change for different levels of total
production. Solar production levels were zero for all experiments. We will explain
the remarkable pattern of wind production by analyzing the underlying optimal
operational decisions. Fig. 4.4 shows the operational decisions regarding wind
supply in week 14 (Fig. 4.4a), the hydrogen inventory levels over time for $C = 1000$

Table 4.4: Renewable shares, storage capacities and production capacity for different levels of C.

C	Share of solar (%)	Share of wind (%)	Share of biogas (%)	Storage capacity (% of demand)	Energy generated (% of demand)
0.1	0.0	1.1	98.9	0.2	141.7
0.2	0.0	1.1	98.9	1.1	134.8
0.3	0.0	1.5	98.5	2.2	130.0
0.4	0.0	4.2	95.8	3.3	126.9
0.5	0.0	8.7	91.3	5.2	122.3
0.6	0.0	6.8	93.2	7.6	117.9
0.7	0.0	5.8	94.2	8.6	116.2
0.8	0.0	5.5	94.5	8.7	116.2
0.9	0.0	5.0	95.0	8.7	116.2
1.0	0.0	4.7	95.3	8.7	116.1
1000	0.0	1.6	98.4	9.0	116.0

and $C = 0.62$ (Fig. 4.4b) and the curtailment levels for wind as a percentage of actual wind supply (Fig. 4.4c, $C = 0.62$). These values of C represent the highlighted points on the left-side of Fig. 4.3a. In Fig. 4.4(a), the red dashed curves indicate wind curtailment levels, the green curves portray wind energy that is directly consumed by demand and the black curves indicate the amount of wind energy that is stored as hydrogen for both levels of C. In Fig. 4.4(b), the dark red curve shows the optimal annual inventory levels for $C = 1000$ over time, whereas the blue curve indicates optimal inventory associated with $C = 0.62$. The gray curve in Fig. 4.4(c) shows the annual wind curtailment levels associated with $C = 0.62$.

Fig. 4.3(a) illustrates how wind production increases more than 5 percentage points for the first 1 percentage-point increase in total production. Wind production becomes more important in minimizing combinations of storage and production capacity when total production capacity increases just above the minimal feasible total production level of 116%. In contrast, Fig. 4.3(b) shows that biogas production levels increase when total production levels exceed 118.5%.

To explain the high marginal increase in wind supply associated with the first percentage-point increase in total production capacity, we compare the optimal inventory levels in Fig. 4.4 for $C = 1000$ and $C = 0.62$, i.e. the highlighted points on the left side of Fig. 4.3(a).

For the lowest level of total production due to setting C high ($C = 1000$), we show the following. The dark red curve in Fig. 4.4(b) shows that inventory levels decrease

during winter and increase immediately after having reached zero. At this point,
the inventory levels accumulate to bridge the seasonal gap in supply and demand
during winter at the end of the year. Since the total production capacity is minimal,
any curtailment is prevented. Therefore, inventory levels increase as soon as these
have reached zero. This is confirmed by the black curve on the right in Fig. 4.4(a),
which shows that unfortunately timed wind peaks need to be stored rather than
curtailed at the time in which inventory has reached zero in week 14. However, the
much lower wind production for $C = 1000$ avoids the need for storage of the large
amounts that were curtailed at $C = 0.62$.

As can be seen from the blue curve in Fig. 4.4(b), wind curtailment at this time of
the year for $C = 0.62$ allows postponement of inventory accumulation for the winter,
which reduces the overall storage requirements. This is confirmed by Fig. 4.4(c), in
which the gray curve illustrates 100% wind curtailment levels, which only occur at
the time at which the inventory is zero. The difference in storage requirements for
$C = 0.62$ and $C = 1000$ can be fully attributed to the difference in curtailment levels
that occur when the inventory is zero.

For relatively high total production levels above 130%, wind production levels
approach zero. The constant biogas production levels can now cover most of
the demand, in which case all excess production is curtailed rather than stored.
Accordingly, the variable wind profile becomes less attractive in supplying demand
peaks.

This shows that when curtailment is allowed, the variable profile of wind can be
an important component in the energy mix when combined with constant sources
in order to minimize combinations of storage and production. Curtailing wind
before accumulating seasonal storage reduces storage requirements. However, when
curtailment has to be avoided, unfortunate wind peaks can cause high storage
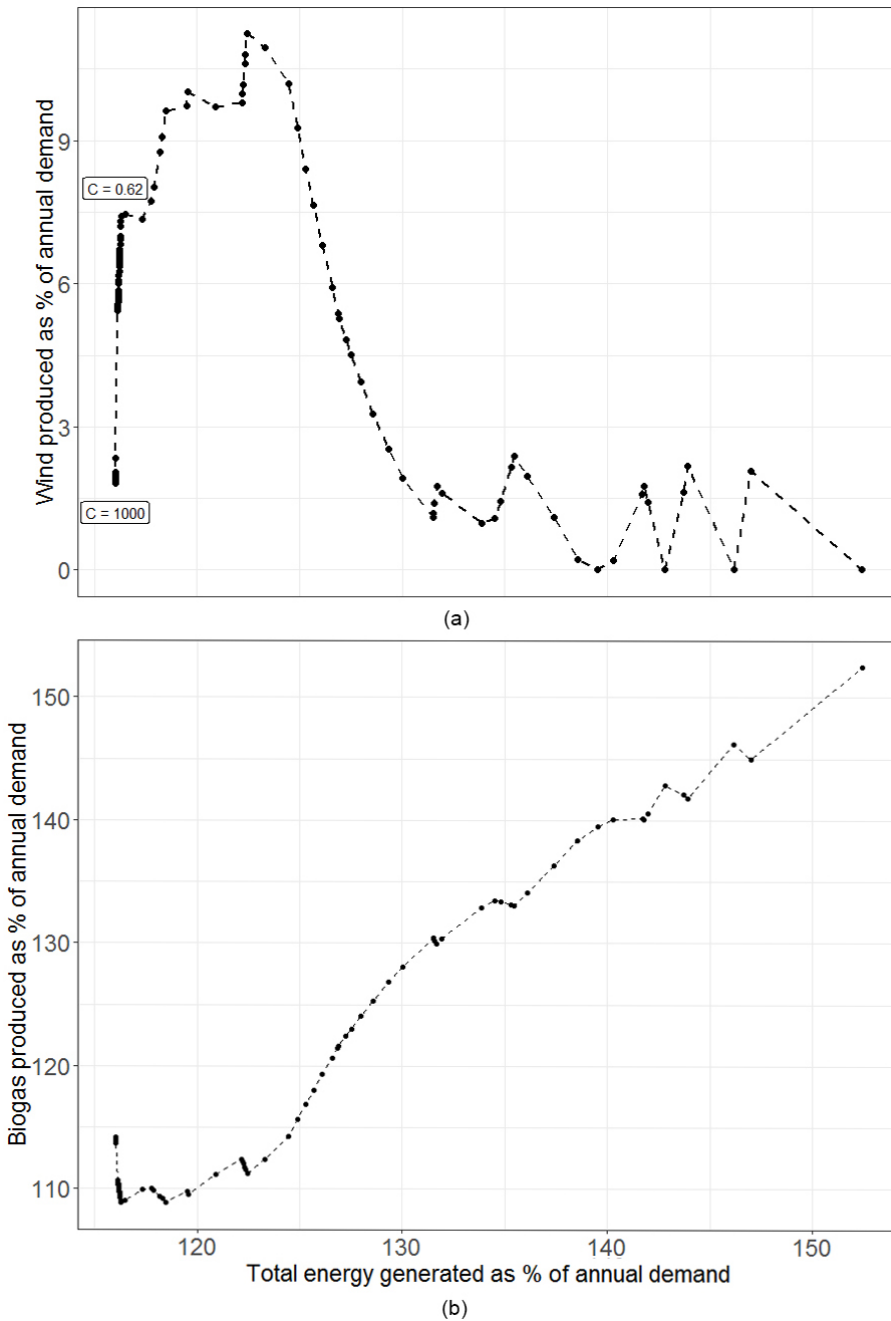requirements.

Figure 4.3: Optimal wind and biogas sizes (as % production levels of demand) for different total production levels
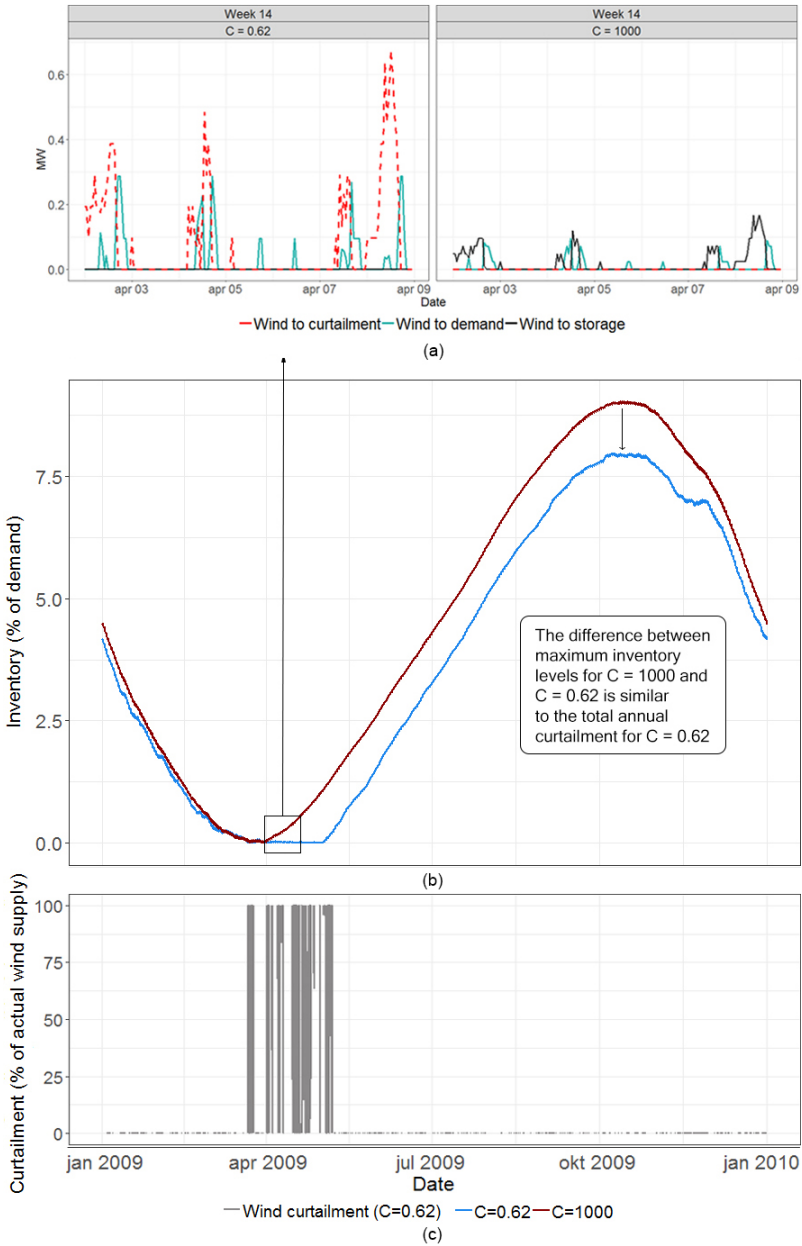
Figure 4.4: (a) Operational decisions in week 14. (b) Inventory over time for $C = 1000$ and $C = 0.62$. (c) Curtailment levels for wind as percentage of actual wind supply for $C = 0.62$.

4.5.4   Operational decisions in general

In Section 4.5.3, we looked briefly into the operational decisions to better understand the optimal strategic choices between renewables. However, the optimal operational decisions are a relevant outcome of our model in themselves. We will focus our discussion of results on two levels of production capacity and storage (resulting from $C = 0.3$ and $C = 50$; see Fig. 4.3) and zoom into a week in winter and a week in summer.

The graphs in Figures. 4.5 and 4.6 show the operational decisions after application of the optimization model for both high and low production capacities in the second week of February (winter) and the last week of July (summer). In Figures. 4.5 and 4.6, the blue curves indicate the amounts of biogas and wind energy, respectively, sent directly to demand on an hourly basis, the black curves indicate the amounts stored as hydrogen, and the dashed red curves indicate the curtailment levels for in each hour.

Biogas

When we install low production capacity owing to a high value of C, the following aspects occur in the winter (Fig. 4.5b). First, the blue curve shows that the demand that is satisfied directly during the day does not include any peaks in demand. Second, the black curve shows that the constant supply of biogas enables the use of storage to supply differences in demand between night and day. The dashed red curve shows that curtailment levels are zero, because the low total production capacity prevents any curtailment. In the summer (Fig. 4.5d), the reduced demand falls below the production capacity of biogas. This enables the peaks in demand to also be provided by biogas. The black curve shows that the excess supply is stored during both day and night. Again, curtailment is non-existent in the summer.

When we install high production capacity due to a low value of C, the following changes occur in winter (Fig. 4.5a). First, the blue curve shows that the direct flows to demand are higher than when total production is low. It can be seen that these flows during the day are not always flat, which indicates that portions of the demand peaks are covered by biogas. In the summer (Fig. 4.5c), the blue curve shows that demand is fully covered by biogas. The dashed red curve shows that all excess-produced biogas is curtailed. This is due to the fact that a high total production capacity is

associated with larger biogas sizes compared with the case when total production
capacity is low.

Wind

When a low total production capacity is installed owing to a high value of C,
the following aspects occur for wind (Fig. 4.6b). In the winter, the blue curve
illustrates direct flows to demand, which occur throughout the day. Whereas
the biogas-to-demand curves are flat at these times, wind peaks are used to
accommodate daily demand fluctuations. The black curve shows that wind is mostly
stored at night when demand is lower. The low level of total production capacity
again prevents curtailment. In the summer, all wind is stored, because demand is
lower than in winter and curtailment is avoided. Biogas already covers all demand
at this time of the year, since biogas production exceeds demand in the summer.

When a high production capacity is installed owing to a low value of C, the
following changes occur in winter (Fig. 4.6a). Wind supplies slightly less to demand
directly than for a low total production capacity. This is because biogas covers larger
portions of demand directly at this time of the year. This results in larger wind
storage levels than for a low level of total production capacity, which is illustrated
by the black curve. In contrast to a low total production capacity, all wind is curtailed
rather than stored in the summer.

These results indicate that, in the optimized model, the roles of wind and biogas
change depending on the levels of production capacity and total production capacity.
For low levels of total production, biogas acts as a provider of base-load in which
the demand peaks are shaved by wind energy. Wind is mostly stored in winter and
curtailed in summer, even though the storage capacity is low. For high levels of
excess production capacity, biogas supplies both peaks and base-load at most times
in the year. Moreover, peaks in wind supply are supplied to demand directly in the
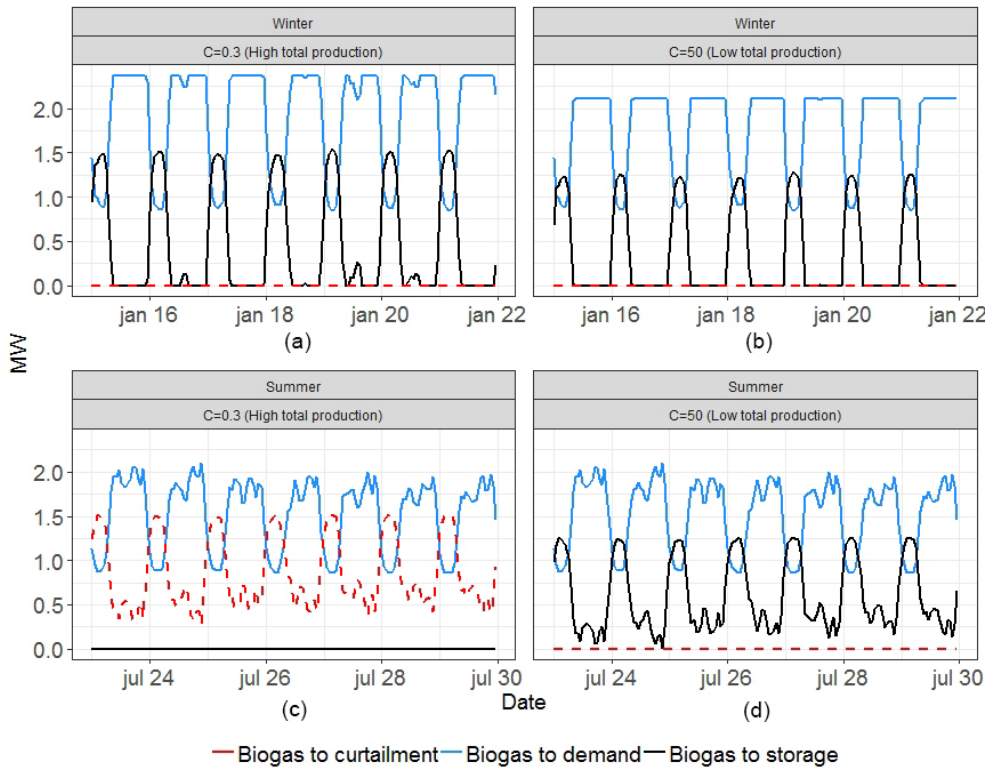winter and are stored in the summer.

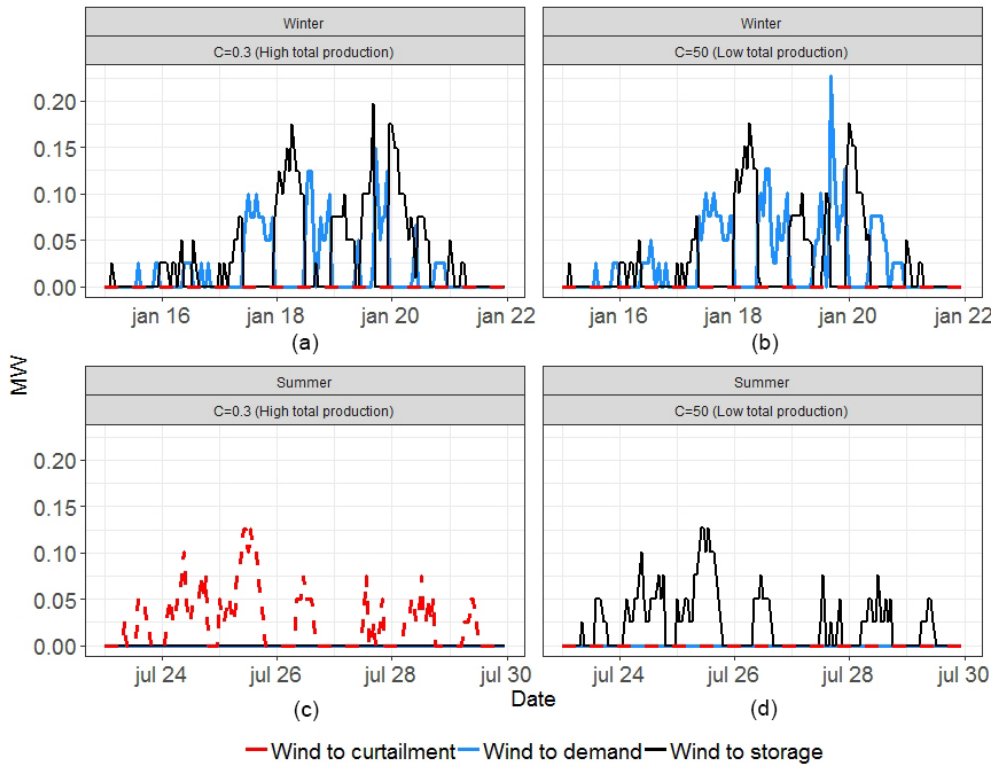Figure 4.5: Biogas allocation decisions in summer and winter.

Combining biogas, wind and solar energy to match local demand: The
production–storage trade-off
105

Figure 4.6: Wind allocation decisions in summer and winter.

4.5.5   Sensitivity analysis

Since the optimal shares calculated for each renewable may not reflect real-life opportunities, we tested the sensitivity of our findings for several alternatives. First we ran experiments in which biogas was limited and excluded. Second, we examined whether a smooth relationship between the wind share and total production affects storage requirements compared with the optimal solutions, which appear to be non-smooth (see Fig. 4.8). In doing so, we ran experiments in which we controlled wind production so that it followed a smooth function. Finally, we ran experiments in which wind was excluded.

Excluding or limiting electricity from biogas

In this analysis, we first exclude biogas and examine the sizes and storage requirements of solar and wind energy. Second, we limit the size of biogas to 371 kW, which corresponds to 20% of the total annual energy demand. The supply of biomass is limited in practice.

The red and blue curves in Fig. 4.7 show the relationships between storage and production capacity when biogas is excluded and when it is limited to 20% of demand, respectively. The green curve portrays the storage and production for the original experiments where all sources are included.

The red curve in Fig. 4.7 shows that when biogas is excluded, both a relatively high total production capacity and a relatively high storage capacity are needed compared with the case when all sources are included (the green curve). The lowest possible total production capacity with biogas included is 116% of demand and requires a storage capacity of 9%, whereas the lowest possible total production level without biogas is 169% and requires 16% storage capacity. This shows that relying solely on wind and solar energy requires much higher total production and storage and emphasizes the importance of constant profiles in the energy mix in matching supply and demand.

The blue curve in Fig. 4.7 shows that including a limited supply of biogas (20% of demand) reduces storage requirements compared with the case when biogas is completely excluded. When the biogas supply is limited, the lowest possible total production capacity is 155% and requires a storage capacity of 14%. This shows that adding a limited supply of biogas to the energy mix effectively reduces storage and
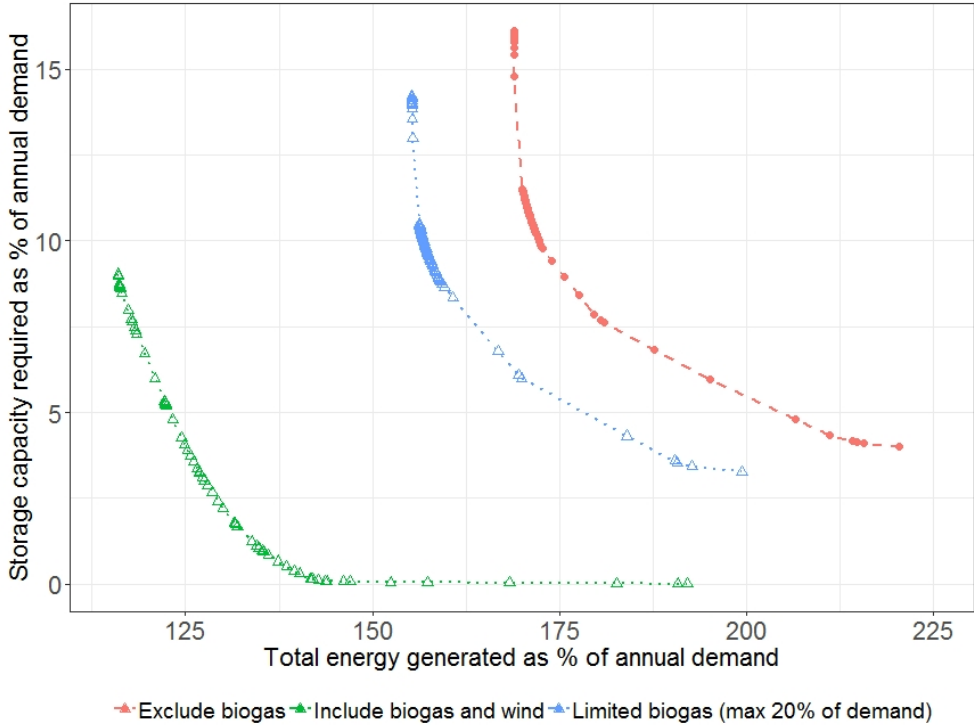
production requirements.

Figure 4.7: Storage capacity requirements and total energy generated (percentage of demand) when biogas is either limited or excluded.

Smooth wind sizes and excluding wind

As the non-smooth optimal pattern of wind shares reflected in Fig. 4.3 is difficult to translate into a simple rule, we checked the relevance of small increases or decreases of the optimal wind share in avoiding storage. We conducted additional experiments in which the wind sizes (k_1) were fixed for every value of C, such that the relationship with wind sizes and total production was smooth, up to a total production level of 129% by using a truncated sine function (see Fig. 4.8). Moreover, we also ran experiments in which wind was excluded from the energy mix, in order to examine the extent to which the variable wind profile provides an advantage in reducing storage requirements.

In Fig. 4.8, the red curve indicates the wind production levels of the optimal solutions, and the green curve indicates the wind production levels that were fixed for the different values of C. In Fig. 4.9, the blue curve shows the storage and total production levels for optimal wind sizes, and the green curve illustrates the storage and production relationship in which wind production was smoothed according to Fig. 4.8. The red curve in Fig. 4.9 shows the production–storage curve when wind is excluded.

Fig. 4.9 shows that the curves for the optimal and smooth wind sizes are very similar. The non-smooth behavior of the wind production levels in Fig. 4.3 could be attributed to the presence of multiple near-optimal solutions. This also suggests that a smooth wind size curve can be used when specifying rules to determine appropriate wind sizes for different total production levels. In a practical setting, this enables the percentage of wind production needed for a certain total production level to be determined more easily, since a deviation from the optimal wind size may still lead to a very good solution. The red curve in Fig. 4.9, in which wind is excluded, shows that overall storage and production requirements are slightly higher than when wind is included. This confirms that including wind according to the wind size curves in Fig. 4.8 enables reduced storage and production requirements compared with relying solely on solar energy and biogas. However, excluding wind gives less of a burden than even partly excluding biogas as analyzed in Section 4.5.5.

Different years of wind and solar energy

We examined the sensitivity of storage requirements for different years of solar and wind supply ranging from 2009 to 2016. In the original experiments, the optimal sizes of each renewable were determined for 2009 for each value of C. These sizes were fixed for the remaining years. This allowed insight to be obtained into the ways in which storage requirements differ for each year when the production capacity decisions for each source are based on the wind and solar energy profiles of a single year.

Fig. 4.10 illustrates the storage requirements on the y-axis plotted against the total production levels for 2009 on the x-axis. Each curve represents the storage requirements for a different year.

Using Fig. 4.10, we derive the following. First, storage requirements for all years are similar when total production levels are at the lowest feasible production
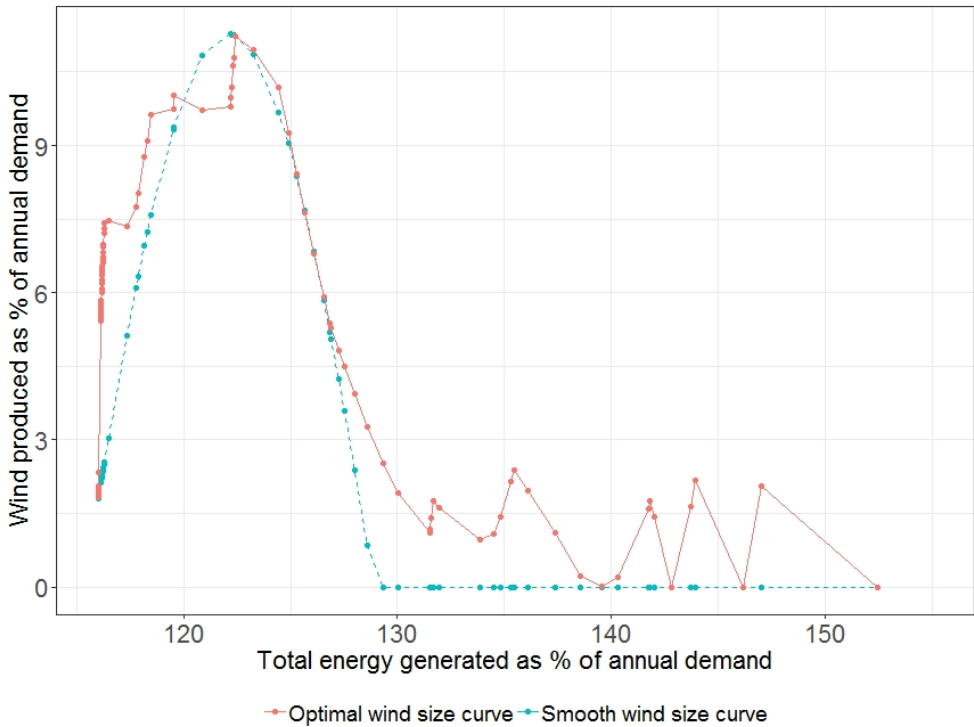
Figure 4.8: Optimal and fixed smooth wind sizes (as percentage of production levels
of demand) for different total production levels.

level. For total production levels between 116% and 130%, differences in storage
requirements are substantial. At a total production level of 121%, the greatest
difference in storage requirements is 3 percentage points of demand. This implies
that 2010 would have 1.85 times the storage needs of 2015. For total production levels
exceeding 130%, differences in storage requirements appear to converge. This is due
to an abundance of energy availability. Accordingly, storage capacity differences
between each year are negligible for the lowest total production levels and for
relatively high total production levels above 140%. In between, the substantial
differences in storage needs require a sufficient safety margin when the decision is
made to install a certain storage capacity.

Even though the production capacities for each source and year were fixed at
the optimal sizes for 2009, it was still assumed that the operational decisions in
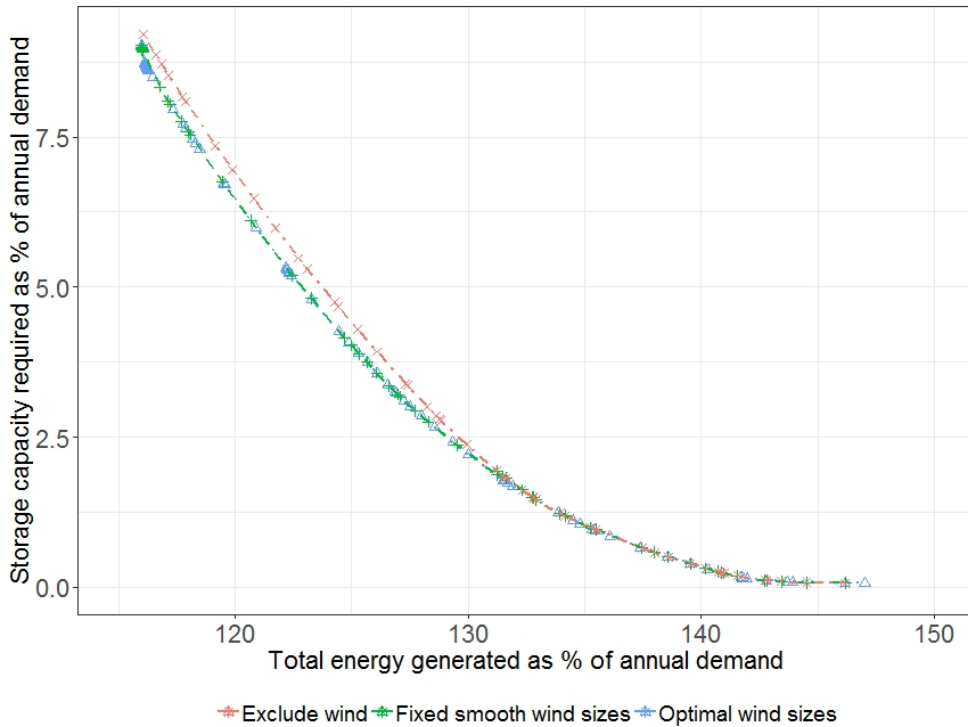the remaining years could be be optimally determined in advance. However, in

Figure 4.9: Relationship between storage and production levels for optimal wind
sizes, fixed smooth wind sizes (see Fig. 4.8) and excluding wind

practice, the uncertainties associated with wind and solar energy supplies preclude
such optimal decisions. Therefore, the differences in storage requirements between
different years may be even larger in practice when the optimal operational decisions
cannot be determined in advance.

4.6   Conclusion

The transition from fossil fuels to cleaner forms of energy presents challenges related
to matching fluctuations in supply and demand, and determining in which form
energy should transported from producers to suppliers. In transitioning to an
energy supply characterized by a high share of renewables, the mismatch between
supply and demand at a community level creates storage and production needs.
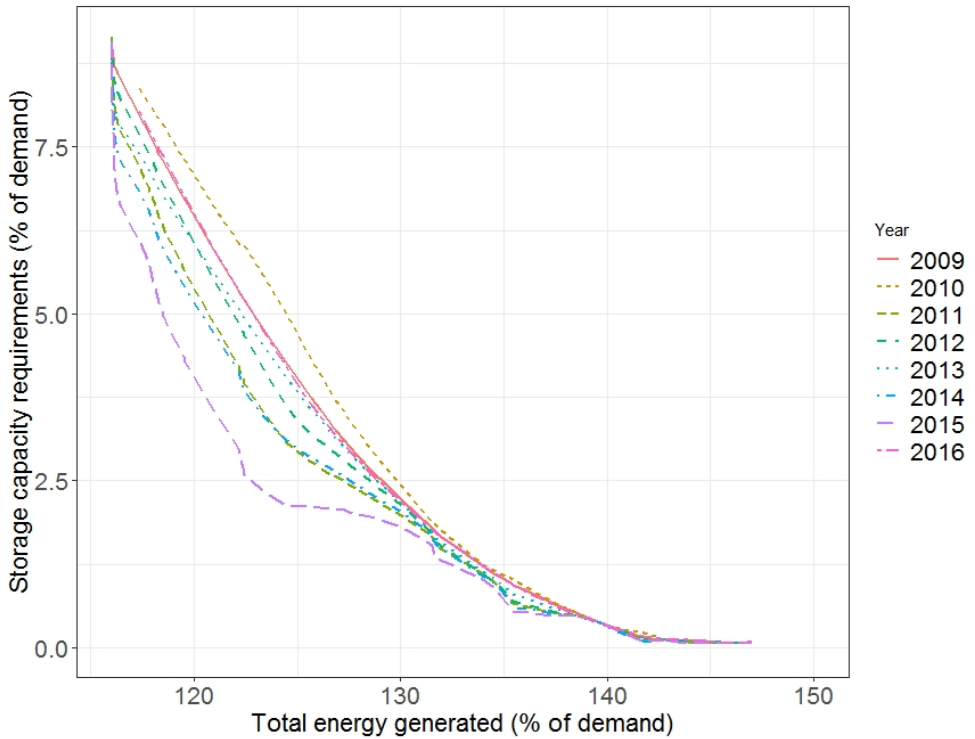This study investigated the relationship between storage and production capacity

Figure 4.10: Storage capacity requirements and total energy generated (percentage
of demand) for wind and solar energy in different years of (experiment set 6).

by examining how different renewables with their specific supply profiles can be mixed in order to minimize storage and production requirements. Considering which mix of renewables to install is important in avoiding unnecessary storage and production.

It was found that the capacity size, the share and the operational decisions of each renewable that should be installed are dependent on the combination of storage and production capacity. The results indicate that, based on Dutch data, the variable production profile of solar energy is least suited to supply demand compared with wind or biogas, resulting in zero shares for the experiments conducted. This is due to the unavailability of solar energy at night and the seasonal mismatch between solar supply and demand. The optimal sizes and the roles of wind and a constant source such as biogas change for different total production levels. For small production levels, biogas can supply both peaks and base-load, leading to relatively high storage requirements in which mostly biogas is stored. For higher levels of total production, the optimal share of wind production increases, because some excess production allows for curtailment of unfortunately timed wind peaks, which allows substantial reductions to be made in storage requirements. Curtailing wind peaks after inventory has reached zero levels allows postponement of inventory accumulation that is needed to bridge the seasonality gap in supply and demand before the summer. Wind then supplies peaks in demand, whereas biogas provides base-load levels of demand. For very high total production levels, exceeding 130% of demand, the high energy availability favors biogas for supplying all levels of demand.

These amounts of biogas might not be available in practice. The results show that excluding or limiting a constant source such as biogas in the energy mix leads to 1.8 or 1.6 times as much storage capacity, respectively, at the lowest total production levels. This indicates the importance of constant supply profiles in the energy mix. Furthermore, the inclusion of wind is beneficial in minimizing storage and production combinations. Excluding wind from the energy mix slightly increases storage requirements.

Experiments with multiple years of wind and solar energy suggest that, in the range of total production between 116% and 130% of demand, differences in storage requirements are substantial and amount to 3 percentage points of annual demand. Storage needs are likely to be even larger when operational decisions

are not optimal owing to uncertainty of wind and solar energy supply in practice. Therefore, significant additional storage capacity is necessary when deciding on a combination of production and storage capacity to accommodate changes in wind and solar energy supply for different years.

It important to note that these conclusions are specific to the Dutch situation and might be different in other countries due to differences in weather and the resulting renewable energy production levels.

Acknowledgements

Chapter 5

Strategic seasonal hydrogen storage for renewable energy producers

Abstract. *We consider a profit-maximizing renewable energy producer operating in a rural area with limited electricity distribution capacity to the grid. While maximizing profits, the energy producer is responsible for the electricity supply of a local community that aims to be self-sufficient. Energy storage is required to deal with the energy productions' uncertain and intermittent character. A promising, new solution is to use strategic hydrogen reserves. This provides a long-term storage option to deal with seasonal mismatches in energy production and the local community's demand. Using a Markov decision process, we provide a model that determines optimal daily decisions on how much energy to store as hydrogen and buy or sell from the power grid. We explicitly consider the seasonality and uncertainty of production, demand, and electricity prices. We show that ignoring seasonal demand and production patterns is suboptimal and that introducing hydrogen storage transforms loss-making operations into profitable ones. Extensive numerical experiments show that the distribution capacity should not be too small to prevent local grid congestion. A higher storage capacity increases the number of buying actions from the grid, thereby causing more congestion, which is problematic for the grid operator. We conclude that a profit-maximizing hydrogen storage operation alone is not an alternative to grid expansion to solve congestion, which is essential knowledge for policy-makers and grid operators.*

5.1   Introduction

Renewable energy sources have become increasingly popular. For example, renewable energy production in the EU has increased from 9.6% in 2004 to 18.9% in 2018 (Eurostat, 2020). However, seasonality mismatches between supply and demand are among the main challenges that should be dealt with to facilitate growth in renewable energy production. Large solar parks tend to be located in rural areas where land is relatively cheap, even though the electricity grid infrastructure is often limited. This typically causes cable congestion at the location where the solar park is connected to the grid, which causes outages, grid balance problems, and affects operational costs of the electricity grid (Vargas et al., 2014; Kumar et al., 2005). The high peaks of solar energy production in summer often cause cable congestion, which may inhibit the installation of new solar parks. For the grid operator, designing electricity grids that can accommodate location-specific energy generation and do consider physical constraints is a challenging task Märkle-Huß et al. (2020).

Connecting hydrogen storage to solar parks is a promising method to spread the feed-in to the electricity grid throughout the year, thereby mitigating cable congestion in the summer (Alanne and Cao, 2017b). It is also suitable as a long-term and strategic buffer to alleviate seasonal mismatches in production and local electricity demand.

Owners of solar parks with hydrogen storage (SPH) facilities connected to an external electricity grid face variable electricity prices as a result of market mechanisms to balance the grid, match supply and demand, and reduce congestion. For example, location-specific (nodal) electricity prices are a solution to reduce grid congestion caused by renewable energy sources (Papaefthymiou and Dragoon, 2016). Furthermore, time-of-use tariffs are expected to become more common since these provide advantages to grid operators in alleviating expected congestion Soares et al. (2020). The resulting market mechanisms facilitate the re-dispatching of energy production by stimulating additional production in areas without congestion and reducing production in areas of congestion by using nodal or zonal prices (Wang et al., 2017). Electricity prices are also determined by other factors such as congestion in other areas of the grid, the balancing market, and supply and demand at the national level. As a result, facility owners' electricity prices are stochastic and

uncertain. This requires SPH facility owners to take into account these stochastic prices to maximize their profits.

Electricity generated by solar parks directly supplies a local electricity demand of connected households in a rural area. Excess-produced electricity can also be fed to the electricity grid or stored in a nearby hydrogen storage location. The local consumption of the generated electricity avoids energy-transportation over long distances. It enables fulfilling a local electricity demand of households who require a stable supply of green electricity and desire to be self-sufficient. The electricity demand of consumers and solar energy production is characterized by differences in seasonality (Arora and Taylor, 2016; Boland, 2020). The confinement of the produced energy in the area of generation, seasonality differences in supply and local demand, and variable electricity prices have significant consequences for the facility owner's decision to store energy and the resulting congestion levels at the cable connection observed by the grid operator. Efficient long-term strategies that determine when energy is stored as hydrogen and sold to or bought from the electricity grid are vital in achieving successful renewable energy penetration. Since hydrogen storage is characterized by relatively high investment costs and limited conversion efficiencies, these strategies become even more critical in enhancing the economic viability of hydrogen storage.

This paper focuses on a profit-maximizing SPH facility that faces daily decisions on how much hydrogen to store, how much electricity to buy from and sell to the grid while providing a local electricity demand of connected households with a stable supply of green electricity. While our primary focus is on the SPH facility owner, we also investigate the congestion levels at the cable connection from the grid operator's perspective due to the SPH owner's profit-maximizing decisions. The decision to store energy by the SPH facility owner is affected by the presence of seasonality in supply and demand. It is also dependent on the level of solar energy production, the amount of local electricity demand, the amount of hydrogen in storage, and the current electricity price. Additionally, solar energy production levels, electricity demand, and prices in the future are uncertain. For example, even though solar energy production can be predicted rather accurately for several days in advance, specific days' solar energy production levels are uncertain when predicted for more extended periods, such as months. As a result of seasonal patterns, solar energy production and electricity demand's stochastic behavior is time-dependent.

These aspects affect storage decisions throughout the year. A Markov decision process formulation is proposed to obtain optimal policies for the above problem. Although we take daily aggregated decisions that ignore intra-day fluctuations, it does not affect our long-term strategic focus for which hydrogen storage is most suitable. Namely, inspired by practice, we assume that a battery handles the intra-day fluctuations so that, from a technical perspective, the electrolyzer is provided with stable loads to maximize its conversion efficiency.

We make the following contributions. Firstly, we identify the characteristics of optimal storage policies for solar field operators with hydrogen storage. These policies differ from short-term battery storage policies due to seasonality effects, annual timescales, and hydrogen storage for long-term and strategic energy storage. The policy characteristics include price thresholds for each period which depend on the inventory level, price, and net production after demand. Secondly, we show how the facility owner's profit-maximizing decisions either solves or creates congestion problems for the grid operator, which occur at the cable to which the solar park is connected. This results from selling or buying-related decisions depending on the cable distribution capacity and includes the actions taken during overages and shortages throughout the year. Thirdly, we indicate how different combinations of storage and distribution capacity affect these decisions. Next, we analyze profits, congestion levels, and electrolyzer utilization by highlighting the trade-off between profits for the facility owner and congestion levels for the grid operator. Finally, we show how conversion losses and differences between selling and buying prices affect these results.

Results show that the optimal policies are characterized by price thresholds that separate different types of actions. These include buying the maximum possible quantity, selling exact overages or buying exact shortages, storing overages or obtaining shortages from storage, or selling the maximum amount possible. For the grid operator, congestion at the cable connection is mostly caused by buying-related actions in winter. These buying-related actions cover potential future shortages when distribution capacity is constrained. For higher distribution capacity levels, congestion is mostly caused by selling-related actions of the overages in the summer. While it may be expected that storage enables reducing congestion at cable connection, increased levels of storage capacity negatively affect congestion. This is because storage enables increasing buying-related actions to prevent future

shortages and exploit price differences. We found that the grid operator's price markups on the selling price effectively reduce local congestion. Results also indicate that a lower electrolyzer utilization (resulting from a large capacity) is associated with higher profits than a low electrolyzer capacity (with a higher utilization rate). Hence, a high utilization level of the electrolyzer is not necessarily an indication of improved feasibility. These results highlight that, while high levels of storage and electrolyzer capacity lead to higher revenues for the SPH facility owner, they do not solve congestion or peak utilization at the cable connection for the grid operator when the facility owner aims to maximize profit. Therefore, the facility owner should refrain from profit-maximizing trading with the grid. The grid operator needs to expand distribution capacity and impose price markups on the selling price to mitigate local congestion.

The remainder of this paper is organized as follows. A literature review is presented in Section 6.2. Section 6.3 describes the problem and Section 5.4 formulates a model. Section 5.5 provides an overview of the calibration of the parameter settings and the base case system that we consider. Section 5.6 provides a sensitivity analysis of key performance indicators based on the parameter settings of each of the system elements' capacities. Section 6.6 provides concluding

5.2   Literature review

The existing literature has mostly addressed energy management strategies in which the owner of an energy storage device decides when to buy or sell energy from or to the grid. For a detailed review of energy management decisions for electric storage systems, we refer to Weitzel and Glock (2018) and Zakaria et al. (2020). While seasonality differences between supply and demand are important characteristics of renewable energy systems, most papers focus on intraday and day-ahead buying and selling decisions using battery storage for short planning horizons and small discretization levels. In contrast, our approach focuses on hydrogen storage decisions for longer planning horizons covering seasonality during a year. We take into account limited electricity grid distribution capacity that supports the need for local storage. Seasonal patterns in supply and demand, limited grid infrastructure, and electrolyzer and fuel-cell constraints all affect storage decisions.

The literature on energy management decisions optimizes grid interactions using

storage by treating supply levels as deterministic (Dufo-López, 2015; Zhang et al., 2017; Pelzer et al., 2016) or by optimizing the buying, selling, or storage decisions in which the uncertainty of the generated renewable energy is taken into account (Jiang and Powell, 2015b,a; Shin et al., 2017; Grillo et al., 2015; Hannah and Dunson, 2011; Hassler, 2017; Gönsch and Hassler, 2016; Keerthisinghe et al., 2019). Literature on energy procurement decisions without storage include Wang and Deng (2019) and Woo et al. (2006). For example, Wang and Deng (2019) analyze an energy procurement problem for a centralized energy aggregator that can control both procurement and consumption within a 24-hour planning horizon in which wind energy is generated. From the perspective of a grid distribution operator, Woo et al. (2006) address the energy procurement decisions of a grid distributor that need to balance procurement risks and expected costs. Regarding prices, Densing (2013); Zhou et al. (2019); Jiang and Powell (2015b,a); Hassler (2017) specifically take into account stochastic electricity prices, whereas Keerthisinghe et al. (2019); Steffen and Weber (2016); Grillo et al. (2015); Shin et al. (2017) treat these as deterministic. These studies are explained in more detail below.

Studies that jointly optimize the use of storage and the decision to buy from or sell to the grid mostly focus on detailed intra-day decisions (Jiang and Powell, 2015b,a; Shin et al., 2017; Grillo et al., 2015; Hannah and Dunson, 2011; Hassler, 2017; Gönsch and Hassler, 2016; Keerthisinghe et al., 2019). For example, Jiang and Powell (2015b) address the arbitrage problem with energy storage to place bids in an hour-ahead spot market. Grillo et al. (2015) optimally schedule batteries with renewable energy. Hassler (2017); Gönsch and Hassler (2016) optimize energy arbitrage decisions for short time horizons within one day and time intervals of 15 minutes. Keerthisinghe et al. (2019) develop energy-storing policies for a battery in a residential home within single days. In contrast, Shin et al. (2017) have addressed the problem for both intraday and yearly planning horizons. Zhou et al. (2019) address the energy storage arbitrage problem within a week for 5-minute periods. They address seasonality by using specific parameter settings for each week that is solved. While these papers all address detailed arbitrage and storing decisions for batteries and short time horizons using batteries, none of them consider hydrogen, which is seen as a more viable option for long-term storage. Most papers also do not provide an integrated approach to address the issue of seasonality over one year.

The related literature on energy storage and arbitrage that has included

transmission or distribution capacity constraints is relatively scarce. Fertig and Apt (2011) investigate the economics of pairing a wind farm with compressed air energy storage and limited transmission capacity. They use heuristic control policies to decide on buying and selling to the grid. Most work that incorporates transmission constraints focuses on energy storage planning from a strategic perspective rather than an operational perspective. For example, Babrowski et al. (2016) optimize storage planning for the German electricity sector while including transmission constraints. Wang et al. (2017) examine to what extent transmission congestion affects the profitability of arbitrage by energy storage, including transmission constraints. Jorgenson et al. (2018b) analyze to what extent transmission or storage can assist in reducing curtailment.

To the best of our knowledge, Zhou et al. (2019) and Gönsch and Hassler (2016) are the only papers that have included transmission constraints in focusing on the operational decision of when to buy, sell or store. They have addressed wind-based electricity with co-located storage. However, their numerical study encompasses only one week and does not consider hydrogen storage, which would become relevant for longer terms. To the best of our knowledge, the seasonal effects related to production, demand, and nodal prices of large-scale renewable energy generation and storage have not yet been considered.

5.3   Problem description

We consider a profit-maximizing renewable energy producer using a photovoltaic (PV) system (i.e., solar panels) who is also the owner of a hydrogen storage facility and is responsible for satisfying local electricity demand. For instance, it may form a self-sufficient community together with a small village. The energy producer can also sell or buy electricity from the electricity grid, and the co-located hydrogen storage is used to store electricity in the form of hydrogen temporarily. We consider a time horizon $\mathcal{T}$ that resembles a complete year, and each period $t \in \mathcal{T}$ resembles a single day. Figure 5.1 provides a graphical overview of the considered system Flaticon (2020). The left side of Figure 5.1 shows the solar energy producer and the hydrogen storage facility, and the right side shows the local electricity demand and electricity grid connection. Our goal is to decide upon when and how much to 1) sell and buy electricity from the grid, 2) store or consume hydrogen from our local

storage to satisfy local demand and maximize profits. We assume the owner of the storage and PV facilities and the households are connected to the grid through an external connection and are the single users of this connection.
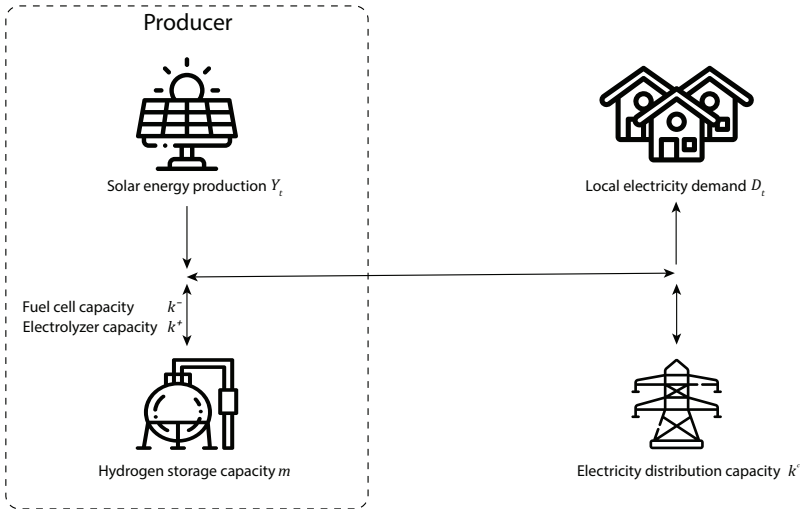

Figure 5.1: Visual representation of the studied system

In the following, we describe our system in detail. Table 5.1 provides an overview of all the parameters and variables.

The installed capacity of solar energy production in MWp is assumed constant throughout the year and denoted by w. Solar energy production per day is a random variable Y_t, where the dependency on the period follows from seasonal differences in energy production throughout the year. Local electricity demand is denoted by the random variable D_t and is normally distributed with mean μ_t and a period-independent standard deviation σ. As it is optimal to satisfy local demand with local supply of solar energy (this comes at no cost), we assume that the produced electricity Y_t is first used to supply the local demand D_t. We then convert our production and demand process in a net solar energy production level $\bar{Y}_t = Y_t - D_t$. The net solar energy production per day $\bar{Y}_t$ can then be modeled via a truncated probability distribution $f^{\bar{y}}(t)$ with a maximum of l_t^+ in period t due to a restricted installed capacity of solar energy.

Hydrogen inventory x_t is held inside a hydrogen storage tank with energy capacity m. The tank is filled using an electrolyzer with a maximum rate k^+ at

which energy can be stored per period and a conversion efficiency of α where $\alpha \leq 1$. Moreover, the producer can obtain at most k^- energy units per period from storage due to a limited fuel cell capacity. The grid distribution capacity k^c determines the maximum electricity amount sold to or bought from the grid in each period. Throughout this paper, capacities (except the installed solar energy capacity) are defined as the maximum amount of energy per period that our system's related component can handle.

Electricity prices are stochastic and are modeled as an autoregressive AR(1) process via $C_t = \theta C_{t-1} + \xi_t$, where $\xi_t \sim N(0, \sigma^c)$. Similar to Densing (2013) and Zhou et al. (2019), we assume that the energy producer is sufficiently small so that it is a price taker that cannot influence electricity prices. Since we explicitly consider long-term strategic decisions, we assume that prices are exogenous, stochastic, and therefore independent of the facility owner's decisions. Consequently, solar energy can be sold to the grid for C_t. The producer can also buy from the grid at a price $C_t + c^+$, where $c^+ \geq 0$ is a fixed price markup which the grid operator imposes to discourage excessive selling to the grid. Similar mechanisms occur in the Netherlands for example, in which annual net production differences sold to the grid are priced at a lower level. As is commonly assumed, it is not possible to simultaneously buy and sell from the grid (see, e.g., Zhou et al., 2019).

The solar energy producer makes the buying, selling, and storing decisions at the end of each period $t \in \mathcal{T}$. Since hydrogen conversion is associated with relatively high conversion losses and electrolyzers perform better at stable loads, we assume that a battery handles intra-day load fluctuations of net production levels.

The storage owner's objective is to maximize the expected future profits related to interacting with the electricity grid during the planning horizon. The decisions made in each period affect the total profit. These decisions have to satisfy several detailed constraints and depend on the system's state at the end of a period. We discuss these aspects in the next section.

5.4 Markov Decision Process Formulation

We formulate our problem as a Markov decision process (MDP). We first describe our state and action spaces, and the constraints upon them. We also specify our reward function. We then discuss how we discretized our state and action spaces,

Table 5.1: Sets, parameters and state variables

Sets	
$\mathcal{T}$	Set on the number of periods $\mathcal{T} = \{0, \ldots, T\}$
Parameters	
w	Installed peak capacity of the solar park (MWp)
l_t^+	Maximum amount of solar energy that can be generated (MWh) in period t
m	Maximum hydrogen inventory level (storage capacity, MWh)
k^c	Maximum load sent to the grid per period (distribution capacity, MW)
k^+	Maximum load at which energy can be stored per period (electrolyzer capacity, MWh)
k^-	Maximum load from storage to electricity per period (fuel-cell capacity, MWh)
c^+	Price markup added to the selling price for buying energy from the grid
α	Conversion efficiency to storage
s	Penalty per unit of unmet demand
State variables	
$\bar{y}_t$	Net production realization after demand (MWh) in period t
c_t	Prevailing selling price of electricity in period t
x_t	Inventory level (MWh) in period t
Stochastic variables	
Y_t	Solar energy production in period t
$\bar{Y}_t$	Net production level after demand in period t
C_t	Electricity prices in the local spot market in period t
D_t	Local electricity demand in period t

and formally define our MDP which we solve via backward dynamic programming.

5.4.1   State and action space

At the end of period t, we observe an inventory level x_t, the current and previous price level c_t and c_{t-1} and net production level after demand $\bar{y}_t$. The price c_{t-1} is included in the state because we consider prices to be an autoregressive process. The transition probability between states also depends on the price level in the previous period. Let $S_t(\bar{y}_t, x_t, c_t, c_{t-1}) \in \mathcal{S}$ be the state of our system in period t. We write $\mathcal{S}$ for the state space. For each state $S_t \in \mathcal{S}$, we define the action $u(S_t) \in \mathbb{R}$ as the number of energy units to buy from or sell to the grid at the end of period t. Negative values represent the number of energy units to buy from the grid.

The action u is bounded by the characteristics of the state S_t. It is most easily described if we consider the range of actions $[-u^{\min}(S_t), u^{\max}(S_t)]$. Here, $u^{\min}(S_t) \geq 0$ denotes the maximum amount of energy bought from the grid at the end of a period, and $u^{\max}(S_t) \geq 0$ denotes the maximum amount of energy that can be sold to the grid at the end of a period. In the following, we describe for each state $S_t \in \mathcal{S}$

how to obtain $u^{\min}(S_t)$ and $u^{\max}(S_t)$.

The maximum amount of energy that can be bought $u^{\min}(S_t)$, for all $S_t \in \mathcal{S}$ is the largest value which must satisfy three constraints such that

$$u^{\min}(S_t) \leq k^c \tag{5.1}$$

$$u^{\min}(S_t) \leq (m - x_t)/\alpha - \alpha \max\{0, \bar{y}_t\} - \min\{0, \bar{y}_t\} \tag{5.2}$$

$$u^{\min}(S_t) \leq k^+ - \max\{0, \bar{y}_t\}. \tag{5.3}$$

These constraints ensure that the distribution capacity is respected, that we do not store more energy than fits in the storage tank, and that the electrolyzer capacity is respected. The minima and maxima within these constraints ensure correctness in case of net overages and shortages. The maximum amount of energy that can be sold $u^{\max}(S_t)$, for all $S_t \in \mathcal{S}$ is the largest value such that

$$u^{\max}(S_t) \leq k^c, \quad u^{\max}(S_t) \leq x_t + \bar{y}_t, \quad u^{\max}(S_t) \leq k^-, \tag{5.4}$$

which indicates that the cable distribution capacity should be respected, that we can sell at most the inventory we have plus the net overage, and that the fuel cell capacity should be respected. Note that these actions allow for unmet demand, in case $\bar{y}_t < 0$. We, therefore, introduce a penalty s per unit of unmet demand that represents a very large negative number to avoid this could happen under any optimal policy. The action space U can then be defined as

$$U = \left\{ \left[-u^{\min}(S_t), u^{\max}(S_t) \right] \mid S_t \in S, \text{s.t. (1) and (2)}, t \in \mathcal{T} \right\}. \tag{5.5}$$

The reward $r(u(S_t))$ of taking action $u(S_t)$ is the sum of the revenues and costs during period t as a result of interacting with the grid. It is defined as

$$r(u(S_t)) = u(c_t + \mathbb{I}_{\{u \leq 0\}} c^+) + \mathbb{I}_{\{x_{t+1} | u < 0\}} s, \tag{5.6}$$

where $\mathbb{I}_{(\cdot)}$ equals 1 if $(\cdot)$ evaluates to true, and is 0 otherwise. Here, by slight abuse of notation, we denote by $x_{t+1} \mid u$ the hypothetical inventory level at time $t+1$ given action $u(S_t)$. If that is negative, demand is unmet and penalty costs s are incurred.

Note that if energy is sent to storage, that is for any state S_t, $-u + \bar{y}_t \geq 0$, the amount of energy that is stored depends on the conversion efficiency α. To avoid

numerical issues in the MDP implementation associated with conversion losses for both charging and discharging and resulting fractional numbers, we directly calculate the round-trip conversion losses when sending energy to storage, which is exact.

5.4.2 Discretization

For the numerical analysis, we need to discretize the state space. We discretize the amount of hydrogen inventory, the net production throughout the year, and the observed prices. We define $\mathcal{X}$ as the set of possible net inventory levels, where Δx_t represents the interval size of the inventory levels. The intervals to which an action u belongs are split into equally-sized intervals which correspond to the discretization of the inventory levels Δx_t. We denote the discretized set of actions by $\mathcal{U}$. The stochastic net solar energy production $\bar{Y}_t$ is discretized according to Δj_t, and electricity prices are discretized with Δc_t. Accordingly,

$$\mathcal{X} = \{0, \Delta x_t, 2\Delta x_t, \dots, m\}, \tag{5.7}$$

$$\bar{\mathcal{Y}}_t = \{l_t^-, \Delta j_t, 2\Delta j_t, \dots, l_t^+\}, \tag{5.8}$$

$$\mathcal{C} = \{0, \Delta, 2\Delta c_t, \dots, C\}. \tag{5.9}$$

5.4.3 MDP for storing, buying from or selling to the grid

The selling and buying policies result in an inventory process over time in which an immediate reward of $r(u(S_t)))$ is earned after choosing an action at the end of period t. The action is chosen after the solar production and electricity prices have been fully observed at the end of a period. Therefore, the decision-maker knows with certainty to which new inventory level the action will lead in the next period. The future inventory x_{n-1} in period $n-1$ with $n = T - t$ can be defined as[1]

$$x_{n-1}(u, \bar{y}_n) = x_n + \begin{cases} \alpha(u + \bar{y}_n) & \text{if } u + \bar{y}_n \geq 0 \\ u + \bar{y}_n & \text{if } u + \bar{y}_n < 0. \end{cases} \tag{5.10}$$

---

[1]For readability, we ignore the case that inventory becomes negative, but this is trivially excluded by taking the maximum of x_{n-1} and 0

The transition probability $p_{n-1}(\bar{y}_{n-1}, c_{n-1}, c_n)$ is defined as the probability of net production realization of $\bar{y}_{n-1}$ and a price realization of c_{n-1} in period $n-1$ given price c_n in period n. Similar to Zhou et al. (2019), we assume that the underlying stochastic processes are independent. We define $V_0(S_0)$ as the total expected profit at the end of the horizon with $n = 0$ periods to go. We assume that

$$V_0(S_0) = 0. \tag{5.11}$$

For all other time periods in which $n > 0$, action $u(S_n) \in \mathcal{U}$ can be executed. Accordingly, we define

$$V_n(S_n) = \max_{u(S_n) \in \mathcal{U}} \left\{ r(u(S_n)) + \sum_{\bar{y}_n \in \bar{\mathcal{Y}}_n} \sum_{c_n \in \mathcal{C}} p_{n-1}(\bar{y}_{n-1}, c_{n-1}, c_n) V_{n-1}(S_{n-1}) \right\}. \tag{5.12}$$

Via backwards dynamic programming, $V_n(S_n)$ can be obtained for all periods-to-go $n \in \mathcal{T}$. The associated optimal periodic policy $(u_1^*(S_1), u_2^*(S_2), \ldots, u_T^*(S_T))$ that minimizes long-term average rewards is then obtained by iteratively applying backwards dynamic programming upon this system, where $V_0(S_0)$ is calculated according to equation (5.12) with $V_{n-1}(S_{n-1})$ equal to $V_T(S_T)$ of the previous iteration (equaling zero for the first iteration). Convergence to optimality is proven if all values $V_n(S_n)$ change with the same value (i.e., the long-run average reward) between iterations (Puterman, 2014).

5.5 Numerical Analysis

We start our numerical section by introducing a base-case system for which we provide a detailed numerical analysis (see Section 5.5.1) and then describe how the price and production processes are fitted (see Section 5.5.2). We end the section by examining the optimal policy for the base-case system while focusing on the differences between summer and winter. To provide a comparison for the viability of the base-case system, we compare the optimal policy to a system without any hydrogen storage options. A more extensive sensitivity analysis in which all system parameters deviate one-by-one is postponed to Section 5.6.

5.5.1 Base-case system

The experiments are based on a planned project of a rural village in the Netherlands in which electricity needs are supplied by a solar park. It comprises a hypothetical solar park with a peak capacity w of 5 MWp that is connected to a local electricity grid in which the connection has a maximum load (k^c) of 30 MWh per day (which corresponds to 1.25 MW). Distribution capacities of 2.5 MW are common in practice for lines that operate at the distribution (local) level rather than the (national) transmission level. In our experiments, we set a more constrained distribution capacity of 1.25 MW, to represent the situation in which the distribution capacity is more constrained. We assume the solar park is connected to a 2.1 MW electrolyzer and a 2.1 MW stack of fuel cells. For both the electrolyzer and fuel cell, this translates to a maximum inflow (k^+) and outflow (k^-) to and from storage of 50 MWh per day. Since only relatively small amounts (up to 16 MWh Bünger et al. (2016)) can be stored inside pressurized vessels, we assume that hydrogen is stored in a co-located large-scale storage location with a capacity of 1000 MWh. Moreover, we assume a round-trip efficiency α of 0.5.

5.5.2 Fitting the price, production, and demand process

Day-ahead hourly wholesale electricity prices in euro/MWh in the Netherlands between 2015 and 2019 are obtained from ENTSOE Transparency Platform (ENTSOE, 2019). These prices are aggregated to daily prices using the intra-day mean. We assume that the electricity prices which apply to the storage owner exhibit similar behavior to wholesale day-ahead electricity prices.

The average daily day-ahead prices exhibited strong autocorrelation (0.872 for a time lag of 1). Moreover, weekly autocorrelation is observed in which autocorrelation is stronger for weekly time intervals than for intra-week intervals. For example, the autocorrelation decreases to 0.773 for lags up to 6 and jumps to 0.815 for lag 7, suggesting that weekday effects are existent. Seasonal effects are not directly apparent from the data.

Inspired by existing approaches in literature (e.g., Zhou et al. (2019)), we test three different AR(1) models of the form $C_t = \phi + \theta C_{t-1} + \xi_t$, where $\xi_t \sim N(0, \sigma^c)$, C_t is the predicted value, C_{t-1} is the observation at $t-1$, ϕ is a constant, and θ is the AR term with a time lag of 1. First, we fit an AR(1) process to the daily electricity

prices in which both monthly and weekday effects are removed from the original observations. Secondly, we fit an AR(1) process to prices in which only weekday effects are removed. Thirdly, we fit an AR(1) process to the original observations. We compare the models by evaluating the standard error of the estimate in relation to the actual observations. The month day and weekday effects are removed similarly as in Zhou et al. (2019). To evaluate the fit of the AR(1) models, the standard error is calculated as $\sqrt{\sum_{t=2}^{T}(C_t - \hat{C}_t)^2/T}$, where T is the number of periods and $\hat{C}_t = \phi + \theta C_{t-1} + f'(t) + \xi_t$ is the predicted price in period t. The seasonality effects of the electricity prices are described by $f'(t)$ which is defined similarly as in Zhou et al. (2019). For the models in which monthly and weekday effects are removed from the observations, the seasonality function incorporates monthly and weekday effects $f'(t) = \gamma^1 + \gamma^2 \sum_{i=1}^{11} D_t^{2i} + \gamma^3 \sum_{j=1}^{7} D_t^{3j}$, where γ^1 is a constant, and γ^2 and γ^3 are coefficients of dummy variables D_t^{2i} and D_t^{3j} related to monthly and weekly effects respectively. These equal one if day t is in month i or in week j. The coefficients are estimated using linear regression on the actual daily electricity prices. For models 1 and 2, the AR(1) process is fitted to the observations after the seasonality function is subtracted. Because the standard error of the model which is fitted to the original data is the lowest (7.7), as is given in Table 5.2, it is found to be unnecessary to include the seasonality function. Since the aggregated data also shows no consistency in seasonality effects throughout the 4 years, we do not include month and weekday effects in our AR(1) process.

Table 5.2: AR(1) parameters and standard error

Model	θ	ϕ	Std. error
1. Remove both month and weekday effects	-0.004	0.89	37.7
2. Remove weekday effects	-0.006	0.91	38.3
3. Fit to original data	5.23	0.87	7.7

To model the electricity demand in our base-case system, we assume that the solar park and hydrogen fuel cells connect directly to a set of 1500 houses that are responsible for the local electricity demand. We have obtained data on electricity consumption from the society of the Dutch Energy Data Exchange (NEDU). The data represents average electricity consumption levels per 15 minutes as a fraction of the total yearly consumption level for 3001 measurements during the years 2016, 2017, and 2018. Since the data is highly aggregated, the data can be scaled to 1500

households to represent our base-case system. We assume that one household on average consumes 2990 kWh in electricity per year (Nibud, 2019). The scaled daily consumption levels, as used in our base-case system, have a minimum of 9.9 MWh, a mean of 12.3 MWh, and a maximum of 16.1 MWh per day.

The data exhibits a strong linear relationship with time in which the average consumption levels follow a V-shape throughout the year. Accordingly, we split the data into two subsets of observations and fit a linear regression to each subset. The splitting procedure is based on minimizing the sum of the standard errors for both models. According to this procedure, model 1 is based on day 1 to 199, whereas model 2 is based on day 200 to 365. It is important to note that the splitting procedure is not based on seasonality differences in demand, but on the day that yields the lowest sum of the standard errors for both models. The fitted models are displayed in Table 5.3. Since the original data is highly aggregated, we assume the data is normally distributed (i.i.d.) with a daily average μ_t and a constant standard deviation σ. Since the standard errors are relatively similar, we chose the highest standard error of both models ($\sigma = 0.62$) as the standard deviation of electricity demand in the experiments. The demand process can be written as $D_t \sim N(\mu_t, \sigma)$.

Table 5.3: Linear models on electricity consumption

Model	Intercept	Slope	σ
Day 1 to 199	15.3	-0.0302	0.62
Day 200 to 365	1.79	0.0372	0.55

We assume that the daily solar energy production levels are stochastic. For each day, hourly solar energy production levels between 2005 and 2016 have been obtained from PVGIS (PVGIS, 2016) and were aggregated to daily amounts. The production levels correspond to an installed capacity of 5 MWp. The original data is aggregated to daily production levels. For each week, the daily observations within the week of 11 years were normalized to a range between 0 and 1 and fitted to a beta distribution to increase the number of observations. Accordingly, daily solar energy production levels are represented by shape parameters for each timer period α_t and β_t. Hence, $Y_t \sim B(\alpha_t, \beta_t)$. Beta distributions are commonly used in modeling daily solar energy production levels Ettoumi et al. (2002); Koudouris et al. (2017). Similar to Boland (2020) and Soubdhan et al. (2009), we assume that Y_t is independent and identically distributed for each period.
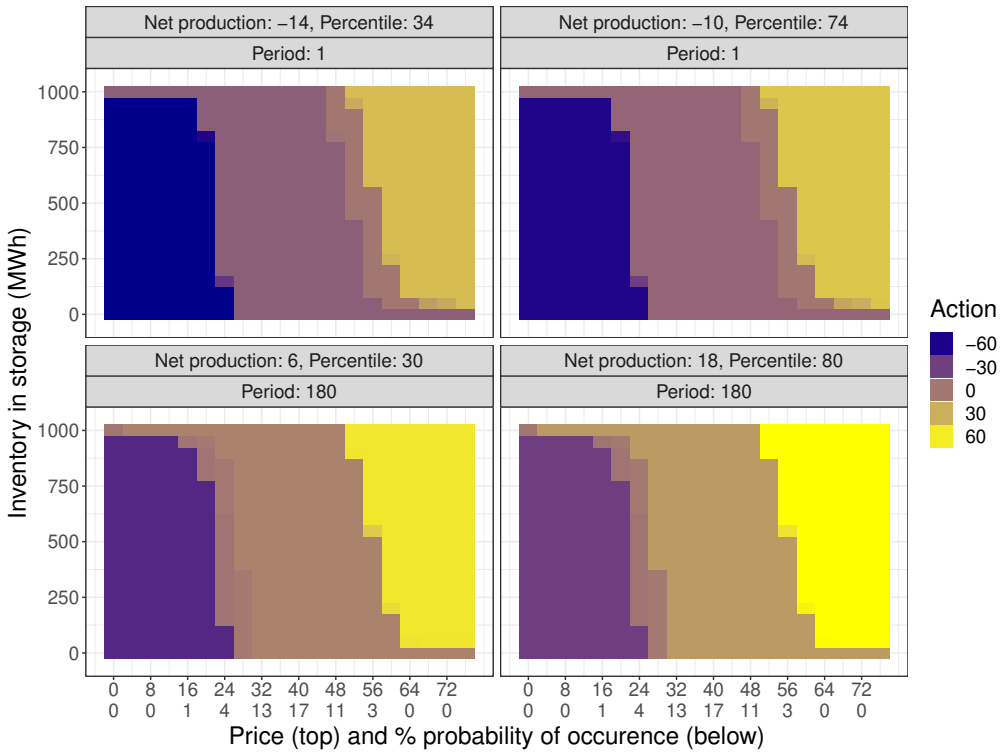
Figure 5.2: Optimal policies for winter (top) and summer (below) and for the first (left) and third (right) quantiles of net production

5.5.3 Optimal Policy Structure

We solve the MDP associated with the base-case system employing backward dynamic programming. As our states are dependent on the day of the year, we consider 50 years. This is done for numerical certainty, in which this provides the long-term average reward. The results presented correspond to the optimal policy of year 0, and can be interpreted as the policy that maximizes long-term average rewards (see, for a similar approach, Byon and Ding (2010)). Implementation is done in C++17 and the MDP is solved on an Intel Xeon 2.5Ghz processor using 4 threads. In the following, we discuss the structure of the optimal policy of the base-case system. The performance of this policy is discussed separately in Section 5.5.4.

Figure 5.2 shows the optimal policies (i.e., the amount of electricity to sell to the grid) for a period in the winter (Period 1) and in the summer (Period 2). For both

periods, we present the optimal policies for the first and third quantile of the net production distribution. On the x-axis, we show the observed electricity price and the probability of occurrence. On the y-axis, we portray the inventory level of the hydrogen storage facility. In this way, the four graphs represent a cloudy winter day (top left), a sunny winter day (top right), a cloudy summer day (bottom left), and a sunny summer day (bottom right).

From Figure 5.2, one can observe four different types of actions that are taken in the optimal policy, in any of the depicted situations. First, if prices are relatively low, the optimal policy prescribes buying as much electricity from the grid as possible. Second, if prices start to increase, it is best to buy or sell the observed net production. Third, dependent on the actual day of the year, it might be optimal to not buy or sell electricity from the grid, as long as enough inventory is on hand. Fourth, if prices are high enough, it is best to sell as much electricity as possible. We observe that the action to not interact with the grid ($u = 0$) takes place for relatively low prices in the summer and high prices in the winter. In the summer, "no interaction" is optimal for relatively low price levels and the net production is then converted to hydrogen. In the winter, net shortages are fulfilled by converting hydrogen to electricity, which also avoids interaction with the grid.

To better understand how the optimal policy differs throughout the year, Figure 5.3 presents the optimal action as a function of time and the inventory level for the 25% net production percentile and the two price levels ($c_t = 20$ and 60). Figure 5.4 does the same for the 75% net production percentile. The action is represented as the resulting change in inventory level.

We observe that the change in inventory has a period-dependent threshold. In the summer (the middle part of both pictures), the inventory at which optimal actions lead to an inventory increase is lower than in the winter, due to oversupply of electricity in the summer and shortages in winter. The inventory levels at which these thresholds occur are similar for both low and high net production levels. Figure 5.4 shows that inventory-increasing actions are also prevalent in summer when prices are low (i.e., $c_t = 20$). This indicates the prevalence of seasonal effects in the optimal policies.

This behavior can be attributed to the following dynamics. Early in the year, a higher probability exists of encountering future electricity shortages than later in the year. Therefore, energy is stored at times of low prices early in the year
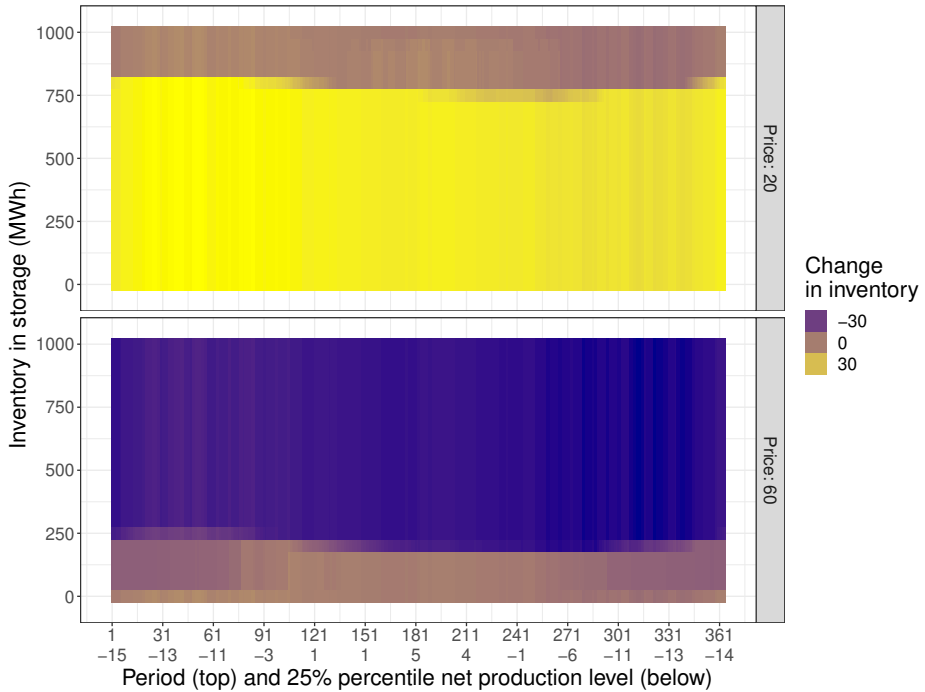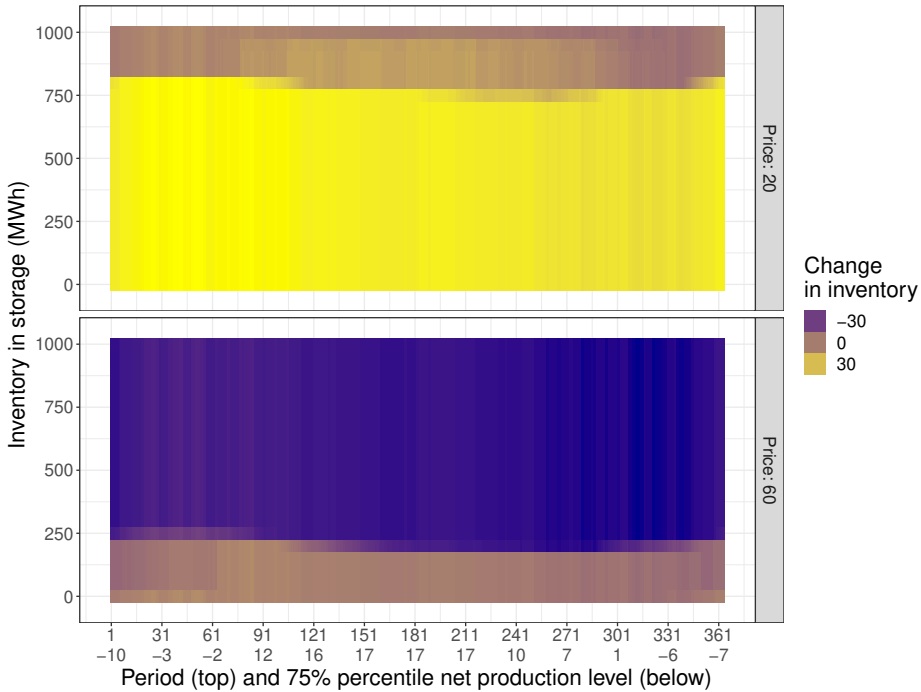
Figure 5.3: Optimal policies as the change in inventory (Δx_t) for a low price ($c_t = 20$, top) and high price ($c_t = 60$, below), and a net production percentile of 25%

to enable accumulating sufficient inventory for moments of shortages later in the year. Furthermore, buying decisions made early in the year facilitate the potential to benefit from price differences later in the year. These dynamics will be explained in more detail in Section 5.5.4.

5.5.4   Optimal Policy Performance

We simulate the optimal policy of the base-case system for a total of 1,100,000 years, using the first 100,000 years as a warm-up for the simulation. Key performance indicators are given in Table 5.4. As a benchmark, we also provide the statistics of our base-case system if no hydrogen storage is available (BM1), and in case the optimal policy for a yearly average, constant net production (i.e., ignoring seasonal effects) is applied to our base-case system (BM2). Our key performance indicators are mean profits, electrolyzer utilization, and the mean percentage of the time

Figure 5.4: Optimal policies as the change in inventory (Δx_t) for a low price ($c_t = 20$, top) and high price ($c_t = 60$, below), and a net production percentile of 75%

in which congestion occurs at the cable connected to the solar park. Similar to Cretì and Fontini (2019), we define congestion as the event in which the amount of electricity sent to or obtained from the distribution grid equals the distribution capacity to which the supplier or consumer, in this case, the solar park with storage, is connected. Accordingly, the mean percentage of time congestion is measured as the mean percentage of time in which selling or buying energy equals the grid distribution capacity. The electrolyzer utilization is given as the percentage use of its full capacity.

Table 5.4: Summary statistics reference case

KPI	Base-case system	BM1 (no storage)	BM2 (ignoring seasonality)
Mean profit per year	6579.4	-4060.5	6387.0
Mean electrolyzer utilization (%)	22	-	22.4
Mean % time congestion (%)	8.6	-	8.8

From Table 5.4, we observe that adding storage increases mean profit per year from -4060.5 to 6579.4. It is also clear that ignoring seasonality is suboptimal, as the mean profit per year decreases by 2.9% comparing BM2 to the base-case system. The mean electrolyzer utilization denotes the amount of electricity converted to hydrogen given that the electrolyzer is used. It increases 1.6% when we ignore seasonality. The mean percentage of time the cable is used to its full capacity, reflecting situations in which congestion occurs at the cable to which the solar park is connected, equals 8.6% and 8.8% for the base case and when ignoring seasonality (BM2), respectively.

We further detail the expected fraction of times over all observations in which particular actions are taken throughout the year. In Figure 5.5, we detail these actions for a net overage (a) and a net shortage (b). Note, all the actions (i.e., curves) together in (a) and (b) sum up to 1.

Given a net shortage, the red points indicate the fraction of times less than the shortage is bought while the remainder is obtained from storage. The green points indicate that more is bought than the shortage while the remainder is stored. The blue points indicate the fraction of times the exact amount of the shortage is bought. The purple points indicate that more inventory is sold than the shortage. Given a net overage, the red points indicate the fraction of times exactly the net overage is sold. The green points indicate the fraction of times the overage is sold plus additional inventory. The blue points indicate the part of the overage that is sold while the remainder is stored. The purple points indicate the fraction of times the overage is stored and additional inventory is bought.

In the case of a net overage for the base-case system, the red points in Figure 5.5 (a) show that policies in which exactly the overages are sold to the grid are most prevalent. These follow the seasonality pattern associated with solar electricity production and occur most frequently at 69% of the time in the summer. Policies in which additional electricity is sold out of storage are associated with exploiting price difference possibilities. These are the least common during overages and are highest in summer occurring 5% of the time. Selling less than the overage is also not a common strategy and occurs maximally at 7.7% of the time. This indicates that storage is not used frequently in cases of overages. This also suggests that excess net production can at best be sold directly to the grid to avoid conversion losses when using storage, even at low prices.

For cases of net shortage in Figure 5.5 (b), occurrences in which the exact shortage is bought from the grid are most prevalent. The blue points show that the fraction of times the exact amount of the shortage is bought follows an inverse pattern compared to policies in which exactly overages are sold during net overages. These are highest in winter up to 79% and lowest in summer down to 5%. Other policies are very uncommon for the conducted experiments.

Even though these policies are relatively uncommon, the less frequent action types that include not simply selling or buying net production differences, are important for the feasibility of a solar park in rural, possibly congested, areas. For instance, in The Netherlands, it is not allowed to install a solar park with a maximum capacity higher than the distribution capacity, even peaks only occur on clear summer days. The results presented in Figure 5.5 indicate that using a storage facility will not interact structurally different from a classic solar park without storage, only its distribution capacity is limited. These are exactly the moments when the less-frequent actions depicted in Figure 5.5 play an important role to keep the base-case system feasible. This includes the ability to exploit price differences and to fulfill shortages at times when prices are high. As can be seen in Table 5.4, a solar park without a storage facility (connected to local electricity demand) yields negative mean profits when demand needs to be solely fulfilled from the electricity grid.

5.6 Sensitivity Analysis

We further investigate the performance of our system, using the key performance indicators already presented in Section 5.4. We first investigate the impact of changing the distribution capacity (Section 5.6.1) and afterward discuss the impact of the storage capacity on the performance of the system (Section 5.6.2). For the distribution and storage capacity, we also provide insights into the interaction with the grid, as this is relevant for future solar park owners and legislators due to its relation to grid congestion issues. We end this section by concisely showing the impact of changing the electrolyzer capacity, conversion efficiency, price mark-up, and production capacity in Sections 5.6.3-5.6.6. In each section, we only vary the parameter that is being discussed and set the other parameter values equal to the base-case system.
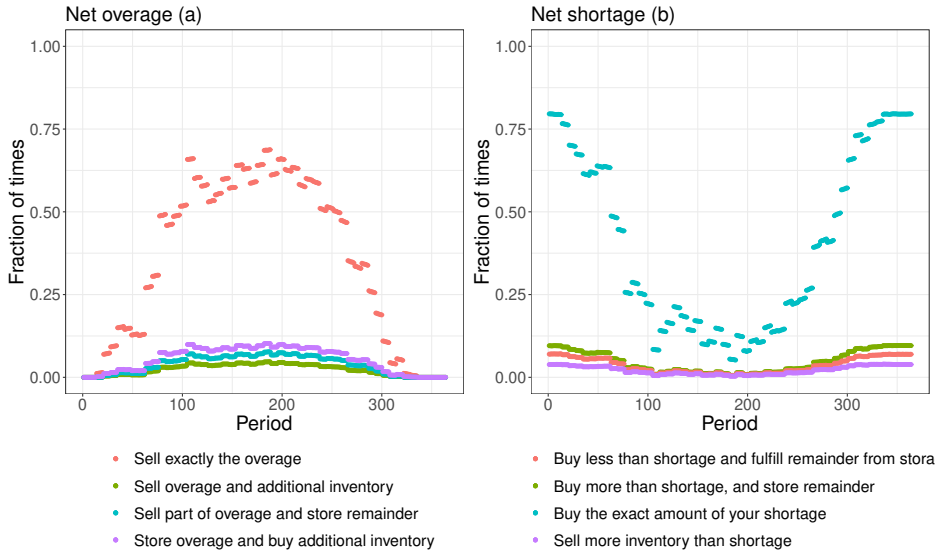
Figure 5.5: Fraction of time a certain action occurs over time during a net overage (left) or shortage (right)
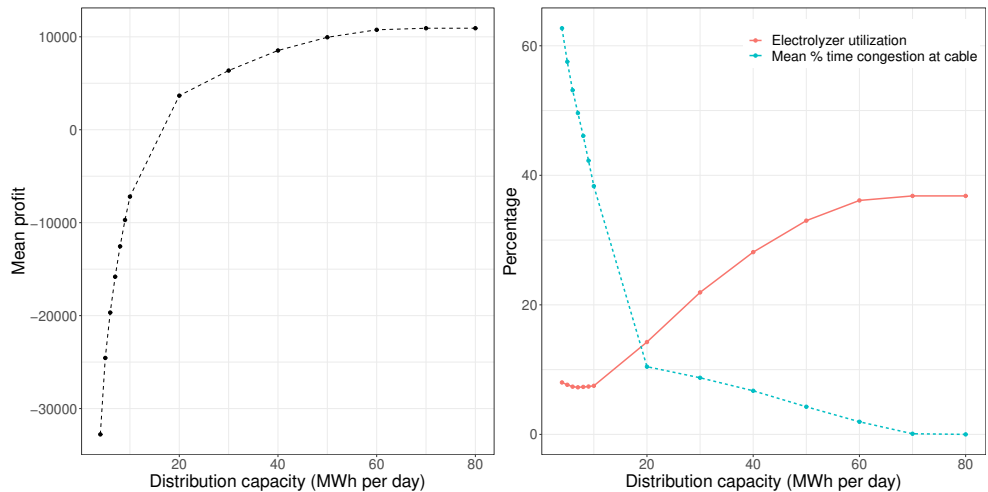
5.6.1   Distribution capacity

Figure 5.6: Summary statistics and distribution capacity (k^c)

We vary the distribution capacity between 1 MWh to 80 MWh per day, which

corresponds to 0.04 to 3.3 MW. In Figure 5.6, we see that the mean profit increases for larger distribution capacities, between 4 MWh and 80 MWh per day, because our system becomes less constrained. Distribution capacities below 4 MWh per day are infeasible for our parameter settings, due to unmet demand.

Low distribution capacities up to 10 MWh per day lead to negative profits, which is due to the limited possibility to exploit price differences as local demand should always be satisfied first. For increasing distribution capacities, the electrolyzer utilization increases up to 36.8%. This due to the exploitation of price differences. If prices are low, electricity is bought from the grid to sell it again when prices are high. Finally, the percentage of the time the distribution capacity is fully utilized with congestion at the connected cable approaches 0%, which is expected since the distribution capacity is then only constraining the system for high net production overages.

Figure 5.7 (b) (bottom) shows the fraction of times in which the amount of energy bought equals the distribution capacity for different levels of distribution capacity. We label this event as buying-induced congestion that takes place at the connection with the electricity grid. Figure 5.7 (a) (top) shows the fraction of times in which sold energy equals the distribution capacity, causing selling-induced congestion.

Figure 5.7 shows that relatively low levels of distribution capacity (e.g., $k^c = 5$) cause a combination of buying-induced and selling-induced congestion. This is the result of preventing future shortages and exploiting price difference opportunities. Both types of congestion follow a seasonal pattern. Whereas buying-induced congestion is highest in the winter months, selling-induced congestion is highest in the summer. This can be attributed to net production shortages that occur in the winter and net production overages that occur in the summer. In line with the results in Figure 5.5, this indicates that selling net overages and buying net shortages from the grid is a preferred action in general.

When the distribution capacity becomes larger (i.e., $k^c = 10$), more selling-induced congestion occurs since the optimal policy is less impacted by possible shortages in winter. Consequently, less energy is stored and more energy is sold to exploit price differences. Buying-induced congestion simply decreases for higher distribution capacities as the distribution capacity becomes less-often the limiting factor when net-shortages occur. When capacity increases even more (i.e., $k^c = 20, 60$), the occurrence of both types of congestion decreases, as the

net-production realizations can be sold or bought completely from the grid without being restricted by the distribution capacity. Price differences are exploited in higher quantities, while fewer congestion events are observed.
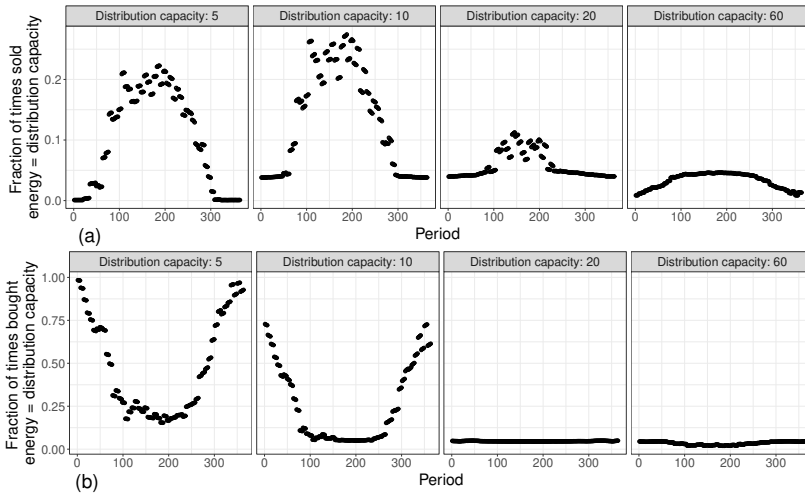

Figure 5.7: Fraction of time that sold (a) and bought (b) energy equals the distribution capacity (selling and buying-induced congestion)

5.6.2   Storage capacity

While the base case used a storage capacity of 1000 MWh and a distribution capacity of 1.25 MW (30 MWh per day), we vary the storage capacity between 100 and 1000 MWh with increments of 100, for three different levels of distribution capacity (10, 40, and 80 MWh per day), see Figure 5.8. In this way, we investigate how storage can facilitate congestion reduction when distribution capacity is constrained. Additionally, it allows us to study how profits are affected when distribution capacity is sufficient.

Figure 5.8 shows negative mean profits which increase at a marginally decreasing rate with storage capacity for each distribution capacity. For distribution capacity $k^c = 10$ (a), the mean profits are negative due to the highly constrained distribution capacity. Note that storage capacities smaller than 300 MWh are not displayed in Figure 5.8 (a). This is because these capacities result in systems where it is not possible to always satisfy local demand. Here, the percentage of unmet demand
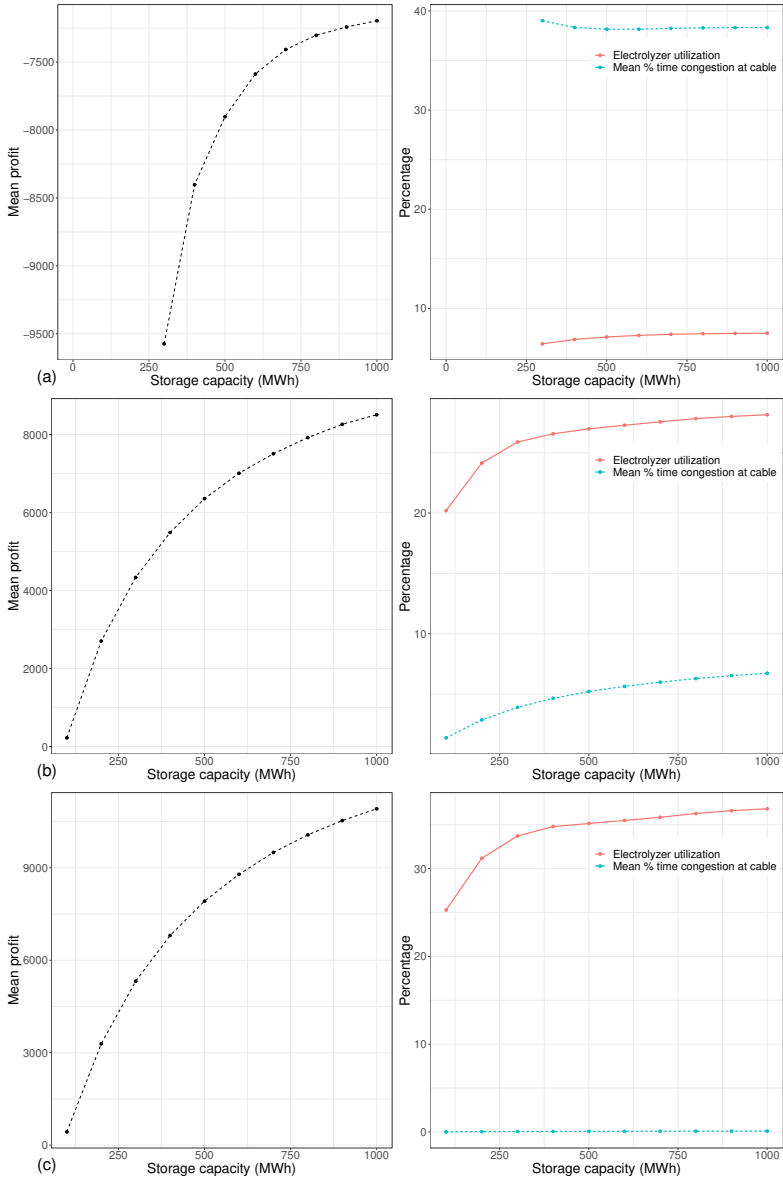
Figure 5.8: Summary statistics for varying the storage capacity, for distribution capacities equal to $k^c = 10$ (a), $k^c = 40$ (b) and $k^c = 80$ (c)

ranges between 0.005% and 8%, and a penalty for unmet demand is incurred. Electrolyzer utilization levels remain relatively constant (between 6.9% and 7.5%),

and congestion levels are not affected by the storage capacity of 300 MWh or higher (the mean percentage time congestion remains between 38.2% and 38.3%). These results indicate that the distribution capacity is too limited across all levels of storage capacities to enable positive profit levels, more effective use of the electrolyzer, and to reduce congestion issues.

Results for $k^c = 40$ and $k^c = 80$ in Figure 5.8 (b) and (c) show that congestion issues are not relevant anymore for our distribution capacity. Furthermore, increasing storage capacity to $k^c = 40$ leads to more congestion at the cable connection, due to increasing interactions with the electricity grid. This is in line with the observed electrolyzer utilization for higher storage capacities.

Concluding, hydrogen storage used to supply electricity does not lead to profits when distribution capacity is too constrained and the storage owner aims to maximize profits. While increased levels of distribution capacity reduce peak utilization and the resulting local congestion, seasonal storage does not solve local congestion problems of the grid operator at the connected cable, regardless of the level of installed distribution capacity. To address this, we advise that (1) the grid operator increases distribution capacity and (2) the storage operator should be encouraged to refrain from short-term trading.

5.6.3   Electrolyzer capacity

We vary electrolyzer capacities k^+ between 2 and 50 MWh per day. Figure 5.9 shows that mean profits increase, at a marginally decreasing rate, for increasing electrolyzer capacity. Utilization levels decrease and range between 50% and 29.9% for $k^+ = 2$ to $k^+ = 50$. Profits are positive when the electrolyzer capacity is at least 6 MWh per day (250 kW). Without considering capital expenditures, this suggests that over dimensioning the electrolyzer capacity leads to increased profits, even though utilization levels are reduced. These results suggest that electrolyzer utilization is not a good proxy for profitability as large electrolyzer capacities with a relatively low electrolyzer utilization may lead to more profits than smaller electrolyzer capacities with a relatively high electrolyzer utilization. This only applies to operational profits as capital expenditures are not taken into account.

The mean time in which congestion occurs due to the full utilization of the connected cable increases with higher electrolyzer capacities (up to 50 Mwh per day) and ranges between 0.7 and 8.7%. This can be attributed to the increased trading

with the grid. While this enables increased profits for the facility owner, it leads
to local congestion for the grid operator. From the perspective of a grid operator,
it is, therefore, more beneficial to install a lower-capacity electrolyzer that limits
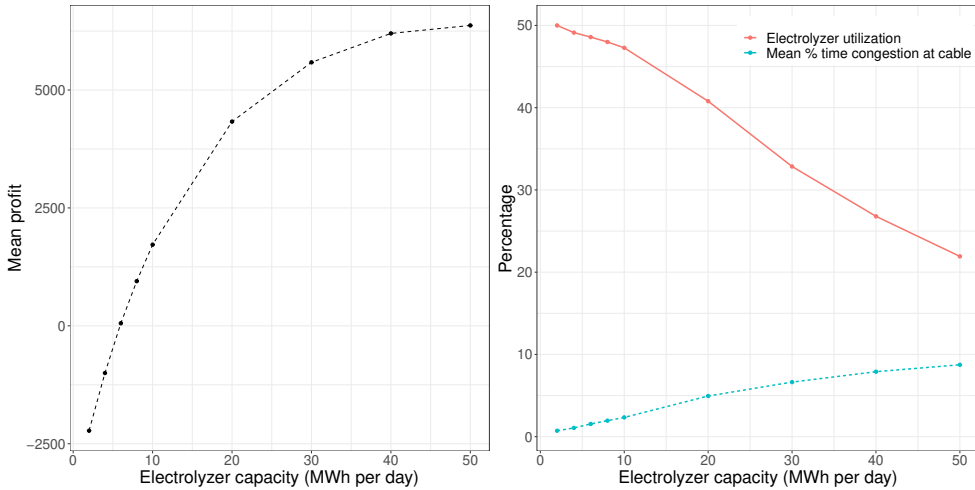congestion problems when the SPH facility owner aims to maximize profits.

Figure 5.9: Summary statistics and electrolyzer capacity (k^+)

We illustrate the (optimal) actions taken by the facility owner as a result of
different electrolyzer capacities. We portray the two combinations of electrolyzer
capacities in Figure 5.10 ($k^+ = 2, k^+ = 10$). It shows the mean fraction of times
an action occurs for a net shortage (a) and a net overage (b). The x-axis indicates the
period (day) and the y-axis indicates the fraction of time a particular action occurred.
The same actions as in Figure 5.5 are given.

Given a net shortage and a low electrolyzer capacity (i.e., $k^+ = 2$), the green
points in Figure 5.10 (a) show that buying the exact amount of the shortage is
most prevalent in winter and least prevalent in summer. Other actions are almost
non-existent. For a high electrolyzer capacity (i.e., $k^+ = 10$), buying more electricity
than the shortage occurs 8 percent points less frequently on average than for a low
electrolyzer capacity (i.e., $k^+ = 2$).

Given a net overage and a low electrolyzer capacity (i.e., $k^+ = 2$), the blue points
in Figure 5.10 (b) show that actions in which part of the overage is sold and the
remainder stored are more prevalent than for high capacity (i.e., $k^+ = 2$), indicating
that storing part of an overage is mostly needed for low electrolyzer capacities to

cover potential future shortages.

These results indicate that the higher electrolyzer utilization at low capacity (i.e., $k^+ = 2$) is caused by buying and storing additional electricity from the grid in times of shortages or storing in times of overages. The stored energy can be used to cover potential future shortages during times of high prices. When the capacity is higher (i.e., $k^+ = 10$), the risk of supplying future potential shortages from the grid at high prices is reduced, and storing energy is not beneficial.
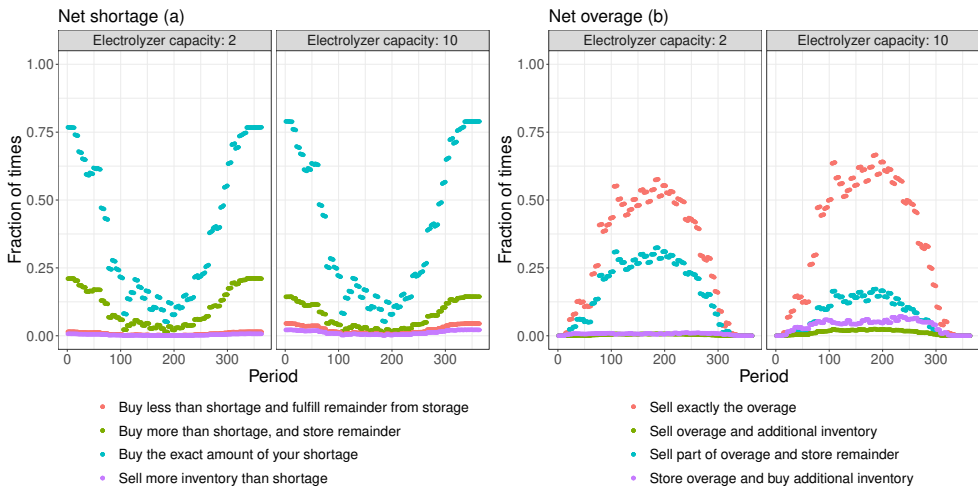
Figure 5.10: Fraction of time a certain action occurs over time during a net overage (left) or shortage (right)

5.6.4   Conversion efficiency

Figure 5.11 shows that mean profits are positively related to conversion efficiency since storage becomes increasingly beneficial in both exploiting price differences and covering shortages that do not need to be bought from the grid. For this reason, electrolyzer utilization is also positively related to conversion efficiency. Moreover, congestion at the connected cable increases for higher conversion efficiencies due to a higher frequency of peak loads at the cable connections. This indicates that technological improvements related to hydrogen storage which lead to higher efficiencies also cause increased levels of local congestion at the cable connection.
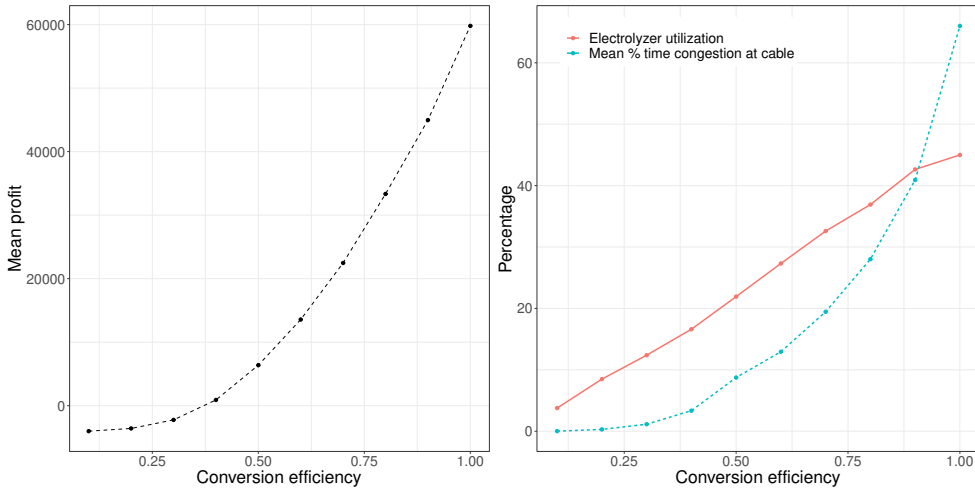
Figure 5.11: Summary statistics and conversion efficiency (α)

5.6.5 Price markup

We vary the price markup that is imposed by the grid operator and is related to buying electricity from the grid (i.e., c^+) between 0 and 5. Figure 5.12 illustrates that mean profits are negatively related to the price markup on the buying price. This is expected because price markups on buying electricity discourage the use of storage to benefit from price differences over time. The electrolyzer utilization is reduced from 29% to 22% between price markups of 0 and 5. Reduced grid interaction as a result of higher price markups reduces congestion levels as well. This indicates that the electrolyzer is used less often to buy energy from the grid to benefit from price differentials. This facilitates the use of storage to prevent congestion. This also indicates that price markups are effective as an instrument to the grid operator to reduce congestion levels in which markups can be raised until using storage is not profitable anymore.

5.6.6 Production capacity

We vary the production capacities of the solar park (i.e., w) between 1 and 10 MWp. Figure 5.13 indicates that mean profits appear to increase linearly with increased production capacities. Up to 4 MWp of the conducted experiments, profits are negative, due to a high reliance on the grid to cover shortages and the inability
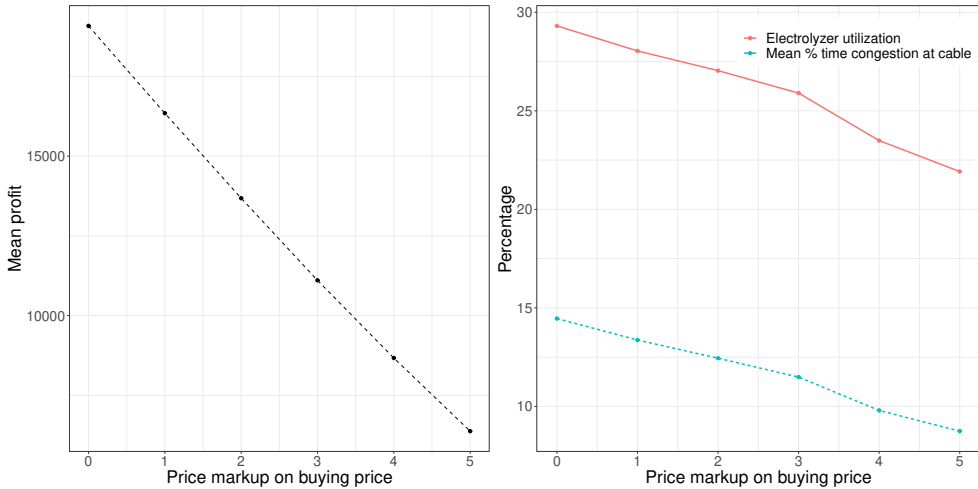
Figure 5.12: Summary statistics and price markup on buying price (c^+)

to store energy when prices are low to cover future shortages. Increased reliance on the grid at low production capacities is reflected in the electrolyzer utilization rates, which increase for solar energy production capacities between 3 and 6 MWp and decrease for higher capacities. At low production capacities (e.g., $w = 1$), the electrolyzer is deployed to store energy that is bought from the grid to cover future shortages. Congestion at the connected cable increases nearly linearly for production capacities above 6 MWp. This is attributed to increased overages which are sold to the grid during summer. This highlights the importance of avoiding the installation of excess solar park capacity.

5.7   Conclusion

Increased decentralization of renewable energy sources such as solar parks leads to grid congestion in rural areas where grid distribution capacity is limited. At the same time, supplying local villages in the vicinity of solar parks reduces the need for long-distance energy transportation through the electricity grid. To reduce congestion and supply electricity to a local demand of households, hydrogen storage can be an important flexibility option to bridge the seasonality gap associated with supply and a local electricity demand when external distribution capacity is limited.
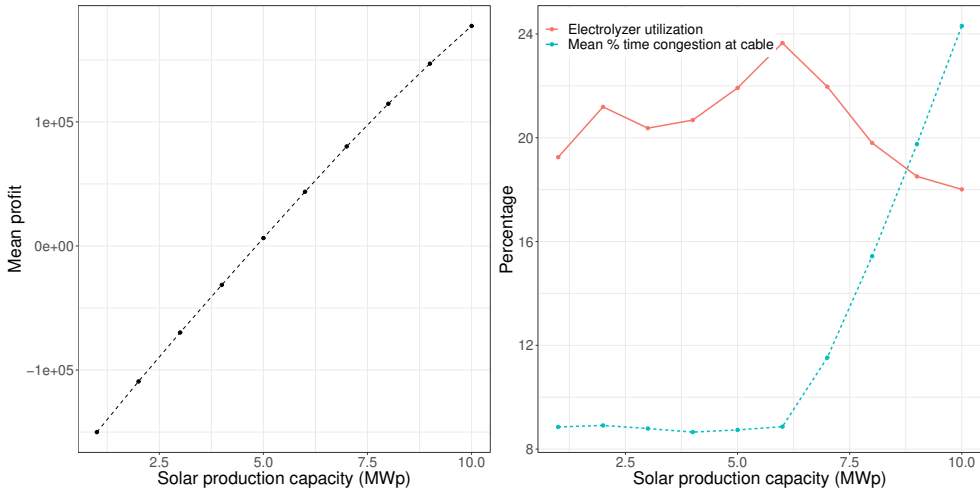
Figure 5.13: Summary statistics and solar production capacity (w)

In this paper, we examine the problem of the owner of a solar park with local hydrogen storage who needs to decide how much to store, sell to or buy from an external electricity grid throughout the year and can supply energy to local electricity demand by households. Furthermore, the solar energy production and local electricity demand are seasonal and there is uncertainty associated with solar electricity supply, electricity demand, and variable electricity prices in the external electricity market. We propose a Markov decision process formulation to the above problem to optimize the expected profits per year from the perspective of the facility owner. We detail the optimal policies with regard to the period in which the actions take place (e.g., summer or winter). Moreover, we illustrate which actions are taken during overages and shortages throughout the year. We show how congestion levels for the grid operator and electrolyzer utilization are affected by conversion efficiency and strategic decisions such as the distribution capacity, storage capacity, and production capacity.

It is found that optimal policies are characterized by price thresholds that separate different types of actions. These include buying the maximum possible quantity, selling exactly overages or buying exact shortages, storing overages or obtaining shortages from storage, or selling the maximum amount possible. When distribution capacity is unconstrained, storage is not used for large periods of time. When distribution capacity is constrained, local congestion at the cable to which

the solar park is connected is mostly caused by buying-related actions in winter, which are needed to cover potential future shortages. Under these conditions, increasing the level of storage capacity does not reduce congestion levels, because buying actions in winter remain necessary to cover shortages. For higher levels of distribution capacity, local congestion is mostly caused by selling-related actions of the overages in the summer. Counter-intuitively, local congestion increases for increased levels of storage capacity, because this enables increasing buying-related actions to prevent future shortages and exploiting price differences.

Mean profits are highly sensitive to the level of electrolyzer capacity and appear to increase linearly with capacity. Moreover, a lower electrolyzer utilization as a result of a large capacity is associated with higher profits than a low electrolyzer capacity with a higher utilization rate as a result of interacting with the electricity grid. This indicates that a high utilization rate of the electrolyzer is not necessarily an indication of increased profits. Hydrogen storage used to supply electricity does not lead to profits when distribution capacity is too small. Moreover, storage also does not aid in reducing local congestion at the connected cable when the associated distribution capacity is too small. This is because buying actions to prevent future shortages and benefit from price differences cause buying-related congestion at the cable connection. These actions are not aimed at reducing congestion, but at maximizing profits. Higher production capacities are associated with higher profits, even though this also causes higher congestion levels due to increased selling to the grid at times of abundant supply or high prices.

While a limited level of storage capacity is needed to cover shortages and overages when the distribution capacity is insufficient to handle peak loads of the solar park, a high level of storage capacity leads to increased local congestion problems for the grid operator when the SPH facility owner maximizes profits. Accordingly, the role of profit-oriented storage for solar parks as a source of flexibility to mitigate local congestion is limited, and a grid operator may need to expand distribution capacity to deal with this. Hence, we advise the grid operator to 1) establish price markups on sold electricity, 2) setting limits on the capacity of the solar park, 3) increase distribution capacity to alleviate local congestion problems.

The opportunities for future research are numerous and can be divided into two areas. The first area is centered around extending the model that we present in this work. For instance, new concepts arise in which local demand not only

consists of electricity but also of hydrogen and, for example, demand for heat. Additionally, one could investigate the potential correlation between production and demand, or physical properties of using hydrogen as an energy carrier. Other future approaches may be focused on minimizing congestion instead of maximizing the storage owner's profits.

The other avenue for further research is the transition towards more strategic models. For instance, one may investigate the impact of multiple renewable energy systems with co-located storage facilities in grid-congestion issues. It would be interesting to research how the location of renewable energy systems in a grid can be optimized, with the aim of minimizing grid congestion.

Acknowledgements

Chapter 6

The operation of solar parks with seasonal hydrogen storage to avoid potential congestion

Abstract. *The occurrence of seasonal peaks in the electricity grid due to increased electricity production by solar parks leads to potential congestion problems. This requires expanding the capacity of the cable connection or the use of flexibility options such as hydrogen storage connected to solar parks. While seasonal hydrogen storage connected to solar parks may help to stabilize the feed-in to the grid, the profit-maximization behavior of solar parks with storage may not facilitate this as a result of opportunistic buying and selling. Operating the facility to bridge seasonal differences in supply and demand rather than to maximize profit may help to stabilize the interaction with the grid. This also provides local electricity consumers with a stable supply of green electricity, that comes directly from the solar park with storage. We study the impact of commercially versus non-commercially operating solar parks with seasonal hydrogen storage (SPH) connected to a local electricity demand of households to facilitate an evenly distributed feed-in to the electricity grid. We compare two different heuristic policies that are oriented towards either profit-maximization or by prioritizing storage to bridge the seasonality gap between solar electricity production and local electricity demand. We show that operating the SPH facility independently from prices by always prioritizing the use of storage reduces curtailment and is far more effective in evenly distributing the sold electricity to the grid. Profit-oriented operation leads to peak utilization of the grid connection and curtailment when storage is full. The decision to expand the grid connection capacity should be done with care and leads to unevenly distributed feed-in to the grid for both profit and non-profit oriented operation strategies. This has important consequences for*

grid operators in managing congestion and stability problems and deciding on capacity expansion.

6.1   Introduction

The transition towards increased electricity supply by solar parks leads to an increased occurrence of peaks in the electricity supply, due to the intermittent nature of solar energy and the effects of seasonality. In the Netherlands for example, solar parks have been built in rural areas where land is relatively cheap, but the electricity grid capacity is limited. Connecting solar parks to the electricity grid may lead to grid congestion due to unevenly distributed feed-in to the grid and at moments of high peak loads. At these times, the generated power becomes confined to the direct environment in which it is produced. The occurrence of high peak loads differs throughout the year as a result of seasonality. Grid congestion is a result of network constraints that threaten grid balance and cause outages (Vargas et al., 2014; Kumar et al., 2005). In the Netherlands for example, this prevents the installation of new renewable energy production capacity in the form of solar parks and hinders the progression of the energy transition.

There are different potential solutions to alleviate this problem. First, a Distribution System Operator (DSO), that operates regional grid infrastructure, can increase the grid connection capacity. Secondly, the solar electricity producers can use storage in the form of batteries or hydrogen to flatten the supply to the grid (Schill and Zerrahn, 2018). Hydrogen storage enables the bridging of seasonal differences in solar energy production and electricity demand (Korpås and Greiner, 2008). Finally, geographically-specific zonal or nodal prices can also prevent congestion problems by matching supply and demand and stimulate interactions with the grid when required (Papaefthymiou and Dragoon, 2016).

The expansion of the grid connection capacity enables the handling of increased loads en thereby reduces potential congestion. This can be effective as a long-term structural solution. However, network expansions are costly and may have long development times due to government licenses and limited resources. This is further complicated by the expected growth of renewables in the future that may render current grid expansion plans already insufficient for the future.

The combination of a solar park with a hydrogen storage facility can provide a connected nearby neighborhood of households with a stable supply of green

electricity. We assume that the households are unable to buy and sell from the
electricity grid and that these decisions are managed by operator and owner of
the solar park with the hydrogen storage facility (SPH). However, the operational
buying and selling decisions of the SPH facility owner affect the volatility of the
feed-in to electricity grid over time. This has consequences for grid congestion
elsewhere in the electricity grid.

The buying and selling decisions of the SPH facility with the aim to maximize
profits do not always facilitate an evenly distributed feed-in to the electricity
grid over time. This is because the profit maximization behavior of the SPH
leads to opportunistic buying and selling to benefit from zonal price differences
Fokkema et al. (2020a). In contrast, operational decisions of SPH facilities that
operate independently of prices and that aim to bridge seasonal differences in solar
electricity production and local electricity demand can be more suitable to enable a
more stable feed-in to the grid. With a stable feed-in, we refer to a low volatility of
the amounts of electricity that the SPH facility sells to the grid over time. Therefore, it
is important to (1) identify whether or not the SPH facility should be operated either
with a profit orientation or by bridging seasonal differences in supply and demand,
(2) investigate under which price conditions a profit-oriented storage operator may
act in the interest of evenly spreading the selling decisions throughout the year, (3)
examine how expanding the grid connection capacity affects the above-mentioned
dynamics.

The main problem considered in this paper is to determine under which price and
grid connection capacity conditions the solar park with hydrogen storage should be
operated with a profit or a non-profit orientation to facilitate a stable feed-in with the
electricity grid. We compare two different heuristic policies which are either oriented
towards profit or towards prioritizing the use of storage to bridge the seasonal
differences between solar electricity production and local electricity demand. Hence,
the policies of the second heuristic are price-independent. We show that operating
the SPH facility by prioritizing storage independent of prices is more effective in
evenly distributing the feed-in to the grid than operating it from a profit-oriented
perspective. While grid operators address capacity problems in many cases by
expanding the grid capacity, we argue that it is important to consider how the SPH
facility is operated. Our results indicate that grid connection capacity expansion of
the connection to the grid should be done with care, since it leads to more overall

variability of the grid feed-in for both profit and price-independent policies, and higher storage requirements and reduced revenues for the price-independent SPH facility operator.

This paper is organized as follows. A literature review is presented in Section 6.2. Section 6.3 describes the problem and formulates a simulation model. Section 6.4 provides an overview of the experimental design. Section 6.5 provides results and a discussion. Section 6.6 provides concluding remarks.

6.2   Literature review

The literature which addresses storage planning in combination with renewable energy production focuses on planning energy storage facilities and electricity pricing. Energy storage-related papers mostly deal with planning investments for energy storage and determining storage capacities, as well as using storage to address grid congestion. Papers that address electricity pricing specifically focus on computing prices in order to maximize social welfare. However, existing literature has not yet compared the conditions under which a solar park with hydrogen storage should be operated commercially and non-commercially to facilitate a stable feed-in to the grid. Existing research has also not yet considered how electricity prices and grid connection capacity expansion affect these dynamics.

Papers on storage planning mostly deal with the optimization of the size and control of storage systems in distribution networks. We refer to Haas et al. (2017); Saboori et al. (2017) for reviews on energy storage planning. According to Saboori et al. (2017), many storage applications aim to minimize a combination of investment and operational costs, in which operational costs are often measured in terms of energy purchase costs, network losses, emission costs, or curtailment costs. For example, Alnaser and Ochoa (2016) propose a planning framework to size battery storage in wind power-rich distribution networks are were able to reduce curtailment with optimal charging and discharging strategies. Denholm and Hand (2011) examined storage requirements for different renewable energy penetration and curtailment levels. Schill and Zerrahn (2018) examine storage requirements for various shares of renewable energy and find that these depend on costs and availability of other flexibility options. They found that storage requirements increase significantly when renewable energy shares exceed 80%. Soini

et al. (2020) have found and discussed how storage can assist wind and solar to replace dispatchable power production. They found that large storage volumes strongly affect the operation and replacement of conventional dispatchable power production facilities. Dufo-López (2015) consider prices in the optimization and control of grid-connected battery storage, even though they mostly focused on the optimization of a single configuration under specific prices. Brouwer et al. (2016) are more concerned with evaluating the role of storage under various scenarios of renewable energy penetration and concluded that power storage is too expensive when renewable energy shares exceed 60%. The above-mentioned papers have addressed the role of storage in transitioning to systems with increased penetration of renewable energy sources. While these papers investigate how storage should be planned in the future, they have not considered how the operation of storage with solar energy production facilitates affects the interaction with the grid and potential congestion problems at the grid connection.

Other papers include storage and the occurrence of congestion in their analyses (Wang et al., 2017; Babrowski et al., 2016; Jorgenson et al., 2018b; Hemmati et al., 2017b,a). For example, (Del Rosso and Eckroad, 2014) found that placing a battery near a congestion point can successfully mitigate congestion problems in transmission networks. Babrowski et al. (2016) optimize storage planning decisions both geographically and in terms of capacity for the German electricity sector and show that storage systems should be mainly located near congested grid lines. Their approach mostly encompasses storage and energy plants as expansion options to deal with growing demand and congestion but does not take into account transmission expansion. Wang et al. (2017) examine the extent to which transmission congestion affects the profitability of arbitrage by energy storage devices. They consider a merchant storage device that maximizes profits and a market-clearing mechanism that calculates the resulting prices. In their book, Cretì and Fontini (2019) provide supply curves and economic models for prices as a result of congestion. They define congestion as taking place when the generated energy supplied to the grid equals the capacity of the connection. However, they do not incorporate the use of storage to smooth the feed-in to the grid over time. In contrast to other papers that address storage and congestion, Bussar et al. (2016) combine the planning of both storage and network capacity expansion in Europe in size and allocation. However, these do not explicitly take into account the extent to which amounts sold to the grid

are evenly distributed. While these papers address either storage and congestion or both storage and transmission capacities, none of these papers have considered the effectiveness of seasonal hydrogen storage for solar parks to facilitate stable feed-in to the grid as a result of the operation of solar parks with storage, grid connection capacity expansion, and price conditions.

Papers on electricity pricing have mostly addressed the computation of nodal or zonal prices to maximize social welfare. In the literature, nodal prices are also referred to as locational marginal pricing (LMP) (Weibelzahl, 2017). Weibelzahl (2017) provides a survey and framework on uniform, zonal, and nodal pricing strategies in the context of transmission constraints. Jafarian et al. (2020) propose a combined nodal and uniform pricing mechanism for including renewable generation to maximize social welfare. They found that storage and price signals to network users are effective in mitigating congestion, in which revenues from congestion prices to the network operator should be reinvested into grid bottlenecks. Li et al. (2021) propose a nodal pricing scheme which is decomposed into 5 components that include, congestion, energy prices, reactive and passive power losses, and voltage levels. Yuan et al. (2018) propose a hierarchical nodal pricing scheme that enables the computation of prices based on the transmission, distribution, and embedded networks. Papavasiliou (2018) presents various approaches to understanding locational marginal prices and they highlight the importance of clarifying the communication between TSOs, DSOs and aggregators. Feng Ding and Fuller (2005) show that zonal and uniform prices give perverse incentives for generation expansion. In the case of nodal prices, they found that it can be profitable for suppliers to add production capacity to frequent and consistent changes in nodal feed-in constraints. While these papers have addressed the consequences and computations of zonal and/or nodal prices, these have not investigated how the price conditions affect the effectiveness of a solar park with hydrogen storage to mitigate potential local congestion problems.

6.3   Problem description

To avoid peak utilization of the grid connection and congestion as a result of a volatile grid feed-in, electricity prices, the implementation of storage and expansion of the grid connection capacity are solution options. However, the operation

strategies of the storage facility are important in reaching this objective. The problem addressed in this paper is concerned with how storage should be operated to mitigate peak utilization of the grid connection and volatile grid feed-in. Moreover, the extent to which electricity prices respond to solar energy availability affect these dynamics. We compare two types of storage operation policies which are aimed at either maximizing revenues from interacting with the grid, or prioritizing the use of storage to cover shortages and overages. We shall refer to these heuristics as the 1) profit-oriented and 2) storage-priority heuristic in Section 6.3.2 and 6.3.2. We determine the conditions of price elasticity and grid connection capacity under which a solar park with hydrogen storage should be operated with a profit orientation or by prioritizing storage to facilitate evenly distributed buying and selling policies from and to the grid.

We consider a solar park which is connected to an external electricity grid and uses a total peak capacity of solar panels w (MWp) and a hydrogen storage facility with a capacity of m MWh (see Figure 6.1), which leads to the generated supply level s_t. Hydrogen is produced with an electrolyzer with a capacity that enables a storage inflow of k^+ (MWh per day). Hydrogen obtained from the storage facility for consumption or sales to the grid is converted to electricity by a fuel cell with a storage outflow level of k^- (MWh per day). We assume that a battery is connected to the electrolyzer and covers daily fluctuations in solar electricity production while providing a constant load to the electrolyzer. Since we focus on seasonal differences in solar electricity production and local demand, the daily battery operation is considered out of the scope of this paper. Hence, we discretize time in days in which each period $t \in \mathcal{T}$ represents one day in a year. The amount of solar electricity generated (MWh) during period t is given by s_t. Moreover, we assume the solar park is directly connected to a group of households which constitute the local electricity demand d_t and is assumed to be obtained from a normal distribution with a period-dependent mean and a constant standard deviation. The distribution parameters are based existing aggregated electricity demand data. The solar energy production level during each period t is represented by s_t and is obtained from Beta distributions based on historical production levels related to the installed capacity w. The level of net production in period t after local demand is given by $y_t = s_t - d_t$, which can be both positive and negative. This becomes directly available and can be either fed to the grid or stored in the hydrogen storage facility. The solar park always

prioritizes the direct provision of the local electricity demand when possible in order to minimize storage-related conversion losses and costs due to obtaining electricity from the external electricity grid. The amounts that can be stored or obtained from storage during during period t depend on the electrolyzer and fuel-cell capacities. We define the maximum inflow before conversion and outflow after conversion to and from storage in MWh per period as k^+ and k^- respectively. Electricity sent to or obtained from storage is subject to conversion losses α^+ and α^- respectively. We assume that electricity costs related to compression of hydrogen are reflected in the conversion losses. The inventory level in the storage tank at the end of period t is denoted by I_t. We assume that the electricity producer with storage is subject to a zonal electricity price in a region in which solar energy production is most prevalent and which depends on the net production availability after demand. Accordingly, the prevailing electricity price p_t at the end of period t is partly dependent on the level of net production. Even though we assume that there is always sufficient demand externally for the electricity that is sent to the electricity grid, any external demand is also reflected in the electricity price. During each time period $t \in \mathcal{T}$, the electricity producer can interact with the grid by selling Q_t units of electricity. Selling or buying electricity from the grid results in revenue or cost R_t. It is determined by the amount bought or sold and the prevailing price. Hence, $R_t(Q_t, p_t) = Q_t p_t$. During period t, the electricity feed-in by the producer can not exceed k^c, due to grid connection capacity constraints.

6.3.1 Electricity prices

Our approach to the determination of prices is based on the notion that zonal prices in a rural region are determined by the level of net solar energy production after local demand which becomes available to feed to the grid. Therefore, we assume that prices are affected by the net production level in the region.

We split the price into two components consisting of an external process determined by external market conditions and a component that depends on the net production level that becomes available. For the first component, we define β_t as the base price which applies during the day, which is the price under normal conditions and determined by external processes. We define the base price in period t as an auto regressive AR(1) process $\beta_t = c + \varphi \beta_{t-1} + \epsilon_t$, in which $\epsilon_t \sim \mathcal{N}(0, \sigma^2)$. We assume that the producer is sufficiently small, such that there will always be demand

Table 6.1: Parameters and variables in the simulation model

Sets	
$\mathcal{T}$	Set on the number of periods $\mathcal{T} = \{0, \ldots, T\}$
Parameters	
w	Installed capacity of solar panels (MWp)
m	Storage tank size (in MWh)
k^c	Grid connection capacity (in MWh per day)
k^+	Maximum storage inflow per period (in MWh per day)
k^-	Maximum storage outflow per period (in MWh per day)
l	Sensitivity of price to solar electricity production
α^+	Conversion efficiency to storage
α^-	Conversion efficiency from storage
c	Intercept price related to the AR(1) process of the base price β_t
p_i^-	Price threshold i that is approached during a shortage ($y_t < 0$)
p_i^+	Price threshold i that is approached during an overage ($y_t \geq 0$)
Stochastic inputs	
s_t	The amount of solar electricity (MWh) produced during period t
d_t	Local electricity demand during period t
y_t	Net production after fulfilling demand $s_t - d_t$ in period t
p_t	Prevailing price of electricity in period t
β_t	Base price in period t which follows an (external) AR(1) process
Decision and performance variables	
Q_t	Amount sold to (positive) or bought from (negative) the grid during period t
I_t	Inventory level at the end of period t
R_t	Profit or cost in period t

for the produced electricity when it is fed into the grid. Hence, the base price is not influenced by the presence of the producer. We define l as a sensitivity parameter which specifies how sensitive the price reacts to the amount of net production that becomes available to the grid at the end of each period. Since oversupply in any market generally leads to lower prices, we assume that prices and net production are inversely related.

We assume that the prevailing price that applies to the electricity producer p_t is positive and is given by

$$p_t(y_t, l, \beta_t) = \beta_t - ly_t + \mu^\beta - l\mu^y \tag{6.1}$$

where μ^β is the average of the base price and μ^y represents the average annual net production. This ensures that the prices are dependent on the elasticity l to net production, while the average price remains equal to the average of the AR(1) process. This enables to fully capture the price behavior which depends on a level of elasticity without the requirement to adjust the the buying and selling policies which
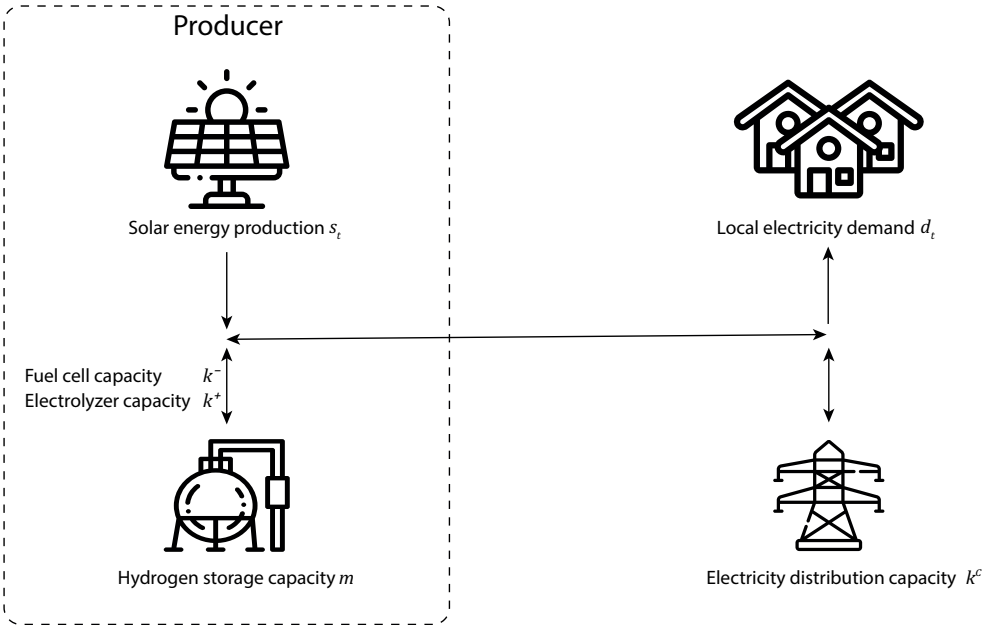
Figure 6.1: The studied configuration (see Fokkema et al. (2020a))

will be explained in detail in Section 6.3.2.

6.3.2   Buying, selling and storage policies

Since the operational decisions of the producer with storage strongly affect both operational costs and and the volatility of the feed-in to the electricity grid, our model considers the underlying operational problem associated with buying, selling and storing energy. This decision entails choosing how much to store, buy from and sell to the grid at time t.

The heuristic policies aim to determine Q_t which represents the quantity of electricity sold to or bought from the grid. In each time period, the amount sold to or bought from the grid depends on the current inventory level and the prevailing price at the end of a period. A negative value of Q_t represents electricity bought, whereas a positive value represents electricity sold.

Similar to Fokkema et al. (2020a), the quantity sold or bought is bounded by several conditions and can best be described as a range $[-Q^{\min}(I_t, y_t), Q^{\max}(I_t, y_t)]$, where $Q^{\min}(I_t, y_t) \geq 0$ represents the maximum amount that can be bought in a

period and $Q^{\max}(I_t, y_t)$ represents the maximum that can be sold in a period.

The maximum quantity bought $Q^{\min}(I_t, y_t)$ is bounded by the constraints

$$Q^{\min}(I_t, y_t) \leq k^c \tag{6.2}$$

$$Q^{\min}(I_t, y_t) \leq k^+ - y_t \tag{6.3}$$

$$Q^{\min}(I_t, y_t) \leq \begin{cases} (m - I_{t-1} - \alpha^+ y_t)/\alpha^+ & \text{if } y_t \geq 0 \\ y_t + (m - I_{t-1})/\alpha^+ & \text{if } y_t < 0. \end{cases} \tag{6.4}$$

Constraints 6.2, 6.4 and 6.3 represent the maximum grid connection capacity, the maximum storage inflow and the remaining inventory after net production and respectively by taking into account the conversion efficiency of the electrolyzer.

The maximum quantity sold is bounded by the constraints

$$Q^{\max}(I_t, y_t) \leq k^c \tag{6.5}$$

$$Q^{\max}(I_t, y_t) \leq \alpha^- I_{t-1} + y_t \tag{6.6}$$

$$Q^{\max}(I_t, y_t) \leq \alpha^- k^- + y_t. \tag{6.7}$$

Constraints 6.5, 6.7 and 6.6 represent the maximum grid connection capacity, the available inventory and the maximum storage outflow respectively by taking into account the conversion efficiency of the fuel cell.

Below, we detail two heuristic policies which take into account the above-mentioned constraints. The profit-oriented heuristic is based on the maximization of profits, whereas the storage-priority heuristic is only geared towards the bridging of the seasonality gap between solar electricity production and local demand.

Profit-oriented heuristic

We assume that the profit-oriented storage operator aims to maximize the total operational rewards with this decision and defines a (heuristic) policy which determines how much to buy or sell at time t, in order to maximize rewards. In the paper by Fokkema et al. (2020a), an optimal policy was determined to

maximize profits for a storage owner by using stochastic dynamic programming for a simplified case of the problem. To reflect the profit-maximizing behavior of the storage owner, our profit-oriented policy is based on the behavior of their policy and depends on the available inventory left in storage, the net production level and the prevailing price.

Figure 6.2 shows the heuristic policy which describes the decisions taken by the SPH operator. The left side of Figure 6.2 shows the policies which apply during a shortage, whereas the right side shows policies related to an overage.

We define three price thresholds $p_i^{'}(I_t), i \in \{0, 1, 2\}$ which separate four different types of decisions that depend on the available inventory in storage. The decisions indicated in Figure 6.2 include (a) buying as much as possible, (b) conducting no storage transactions and use the grid to handle shortages and overages, (c) using storage to replenish shortages or store overages, and (d) sell as much as possible. Note that the regions for (b) and (c) switch in case of an overage compared to a shortage situation. For an overage $y_t \geq 0$, the price thresholds are given by

$$p_0^{'}(I_t) = \frac{\phi}{I_t - m} + p_0^{-} \tag{6.8}$$

$$p_i^{'}(I_t) = \frac{\phi}{I_t} + p_i^{-} \qquad\qquad \forall i \in \{1, 2\}. \tag{6.9}$$

For a shortage ($y_t < 0$),

$$p_i^{'}(I_t) = \frac{\phi}{I_t} + p_i^{+} \qquad\qquad \forall i \in \{0, 1\} \tag{6.10}$$

$$p_2^{'}(I_t) = \frac{\phi}{I_t - m} + p_2^{+}. \tag{6.11}$$

where ϕ is a constant tuning parameter based on the shape of the price thresholds in (Fokkema et al., 2020a). In addition, p_i^{+} and p_i^{-} are obtained from (Fokkema et al., 2020a) and represent the price thresholds when inventory levels are extremely small or large for overages and shortages respectively (see Figure 6.2).

We define Q_t as the policy that the SPH facility adopts during each time period. It is represented by the amount sold to (positive) or bought from (negative) the grid. It depends on whether a shortage or overage net production level has occurred during
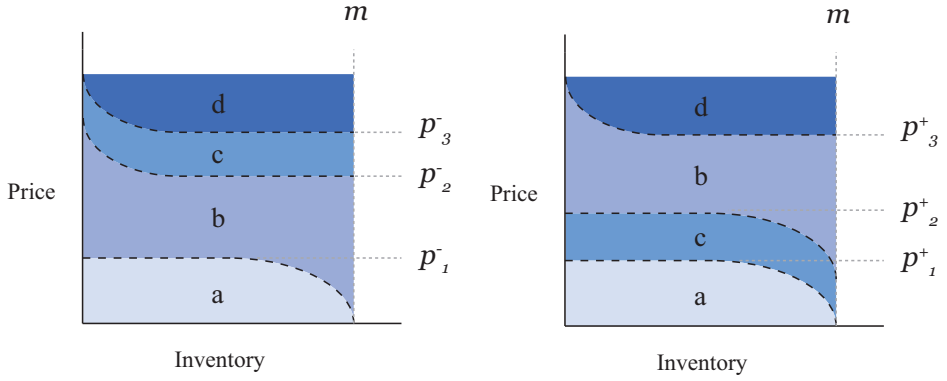
Figure 6.2: Profit-oriented policy for a shortage ($y_t < 0$, left) and overage ($y_t \geq 0$, right)

each time period.

If $y_t < 0$ (see the left side of Figure 6.2),

$$
Q_t(I_t, p_t, y_t) = \begin{cases} Q_t^{\min} & \text{if } p_t < p_1'(I_t) \\ Q_t' & \text{if } p_1'(I_t) \leq p_t < p_2'(I_t) \\ Q_t''' & \text{if } p_2'(I_t) \leq p_t < p_3'(I_t) \\ Q^{\max} & \text{if } p_3'(I_t) \leq p_t. \end{cases} \tag{6.12}
$$

If $y_t \geq 0$, (see the right side of Figure 6.2),

$$
Q_t(I_t, p_t, y_t) = \begin{cases} Q_t^{\min} & \text{if } p_t < p_1'(I_t) \\ Q_t''' & \text{if } p_1'(I_t) \leq p_t < p_2'(I_t) \\ Q_t' & \text{if } p_2'(I_t) \leq p_t < p_3'(I_t) \\ Q^{\max} & \text{if } p_3'(I_t) \leq p_t. \end{cases} \tag{6.13}
$$

The maximum amount that can be bought, $-Q_t^{min}$ applies to region (a) in Figure 6.2. We define Q_t', which applies to region (b) as the amount bought from or sold to the grid by prioritizing to use the grid and not use storage to fulfill a shortage or overage. This takes into account the above-mentioned restrictions. It is given by

$$Q_t' = \begin{cases} y_t & \text{if } -Q^{\min} \leq y_t \leq Q^{\max} \\ -Q^{\min} & \text{if } y_t < -Q^{\min} \\ Q^{\max} & \text{if } y_t > Q^{\max}. \end{cases} \tag{6.14}$$

We define Q_t'' as the amount sold to or bought from the grid by prioritizing the use of storage, provided that $y_t \in [-Q^{\min}, Q^{\max}]$. There are cases in which an overage is so large that only selling actions can be performed and $Q^{\min} \geq 0$. In contrast, shortages may also cause only buying actions to be feasible when $Q^{\max} < 0$. In those cases, storage is prioritized by choosing the policy which minimizes interaction with the grid. Hence,

$$Q_t'' = \begin{cases} -Q^{\min} & \text{if } -Q^{\min} \geq 0 \\ Q^{\max} & \text{if } Q^{\max} < 0 \\ 0 & \text{else}. \end{cases} \tag{6.15}$$

We define Q_t''', which applies to region (c) as the amount sold to or bought from the grid by prioritizing the use of storage. This also includes cases in which the net production is outside of the boundary of policies. When this is not the case, the policy of Q_t'' is maintained which indicates that storage transactions with the grid are prioritized and grid transactions are minimized. For all other cases, the policy is limited by the boundary of policies. Accordingly,

$$Q_t''' = \begin{cases} Q_t'' & \text{if } -Q^{\min} \leq y_t \leq Q^{\max} \\ -Q^{\min} & \text{if } y_t < -Q^{\min} \\ Q^{\max} & \text{if } Q^{\max} < y_t. \end{cases} \tag{6.16}$$

To summarize, the adopted policy $Q_t(I_t, p_t, y_t)$ depends on the inventory level, price and the net production level. In region (a) of Figure 6.2, the maximum possible quantity $Q^{\min}$ is bought from the grid due to a relatively low price. In region (b), the policy which prioritizes using the grid to cover overages or shortages Q_t' is bought

from or sold to the grid. In this case, storage transactions are avoided when possible, since the price is not sufficiently favorable to use storage for buying or selling more than the shortage or overage respectively. Storage transactions only occur when $y_t < -Q^{\min}$ or $y_t > Q^{\max}$. In price region (c), storage transactions are prioritized with policy Q_t''' in which no interaction with the grid is conducted if possible. In region (d), the maximum amount possible $Q^{\max}$ is sold to the grid due to the relatively high price.

As can be seen in Figure 6.2, we define the policy for both a shortage and an overage, in which the main difference is the shape and location of region (c) and the corresponding policy Q_t'''.

Storage-priority heuristic

Our second heuristic does not respond to prices and prioritizes the use of storage. We assume this reflects the behavior of a non-private party that operates the solar park with hydrogen storage primarily to cover seasonal differences in solar electricity production and local demand. Hence, it naturally follows the seasonality differences associated with the net production levels that become available during each period. Therefore, it is reflected by $Q_t := Q_t'''$ which is independent of the price and equal to the storage priority element of the profit-oriented heuristic described above.

Inventory, curtailment and unmet demand

For both heuristics, the change in inventory is defined as

$$\Delta I_t(Q_t, y_t) = \begin{cases} \alpha^+(-Q_t + y_t) & \text{if } y_t - Q_t \geq 0 \\ \frac{-Q_t + y_t}{\alpha^-} & \text{if } y_t - Q_t < 0. \end{cases} \tag{6.17}$$

The inventory in storage at the end of period t is then

$$I_t(Q_t, y_t) = \begin{cases} I_{t-1} + \Delta I_t & \text{if } 0 \leq I_{t-1} + \Delta I_t \leq m \\ m & \text{if } I_{t-1} + \Delta I_t > m \\ 0 & \text{if } I_{t-1} + \Delta I_t < 0. \end{cases} \tag{6.18}$$

Situations may occur in which the net production overage is too large to store, sell or consume by the local electricity demand. In contrast, the net production shortage may be too low to fulfill the local electricity demand. Hence, these situations create curtailment or unmet demand, respectively. Excess production or curtailment is given by $I_{t-1} + \Delta I_t - m$ if $I_{t-1} + \Delta I_t > m$, whereas unmet demand is given by $I_{t-1} + \Delta I_t$ if $I_{t-1} + \Delta I_t < 0$.

6.3.3 Simulation model

Our simulation model calculates the decision and performance variables mentioned in Table 6.1 using hydrogen storage near a solar park for a specific time horizon. The model is implemented in Python according to the logic flow diagram in Fig. 6.3. We perform each simulation for 100,000 consecutive years in which a warm-up time of 1000 years was proven sufficient.

In each period t, the solar electricity generated and local demand is obtained. These values are then used to calculate the prevailing price p_t as described in Section 6.3.1. Based on the price, the buying and selling policy of the producer with storage is determined (see Section 6.3.2).

For each day in the simulation, the revenue or cost is calculated based on the buying or selling policy with the grid. When the time horizon of one year is not yet reached, the inventory levels are updated and a new day is created. The total revenue consists of 1) revenue from buying from and selling to the grid, and 2) revenue from selling electricity to the connected households. In our analyses, the revenue from selling to the local demand is

6.4 Experiments

This section provides an overview of the experiments that are conducted in our study. The experiments have been conducted for both heuristics. We present the main experiments in which we apply our simulation method to a practical context. We compare both heuristics based on the average inventory levels per time period, the standard deviation of selling decisions, the mean fraction of runs the grid connection was fully utilized, curtailment, unmet demand. We also derive insights on the relationship between the elasticity of prices to net production levels for the
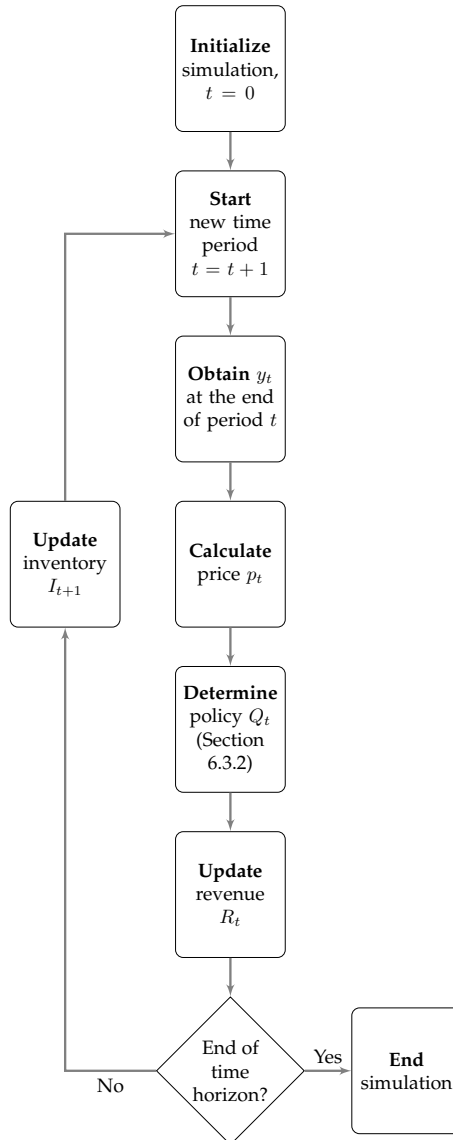
Figure 6.3: Simulation model of the studied system

profit-oriented operator, as well as how grid connection capacity expansion affects these dynamics. The experimental design is summarized in Table 6.3.

6.4.1 Parameter settings

Reference case

The experimental factors in the experiments are the price elasticity to net production levels l and the grid connection capacity k^c. To determine the ranges of our experimental factors, we first consider a hypothetical solar park of 5 MWp in the Netherlands which is located next to a surrounding village of 1500 households that can directly consume the generated electricity. The solar park connects to a hydrogen storage facility for which an alkaline electrolyzer and a stack of fuel cells which both enable a total storage inflow and outflow rate of 50 MWh per day respectively, which corresponds to 2.1 MW. We assume that the hydrogen storage facility has a capacity of 400 MWh. This level is such, that it is mostly sufficient for seasonal storage in our parameter settings, but will just not enable complete self-sufficiency. Therefore, it requires using the grid as well. The electrolyzer efficiency α^- was set at 0.6 (Đukić and Firak, 2011) and the alkaline fuel cell efficiency α^+ was also set at 0.6 (Lamy, 2016). These constant parameter settings are shown in Table 6.2. On sunny summer days the net production regularly peaks at levels of around 10.5 MWh.

Table 6.2: Constant parameters

System dimensions						Policy					
Installed solar capacity (w)	Storage (m)	Storage inflow (k^+)	Storage outflow (k^-)	α^+	α^-	p_1^-	p_2^-	p_3^-	p_1^+	p_2^+	p_3^+
5	400	50	50	0.6	0.6	26	46	50	26	30	50

Demand, prices and solar energy production

We use the same demand, price and solar energy production data and model calibration settings as in Fokkema et al. (2020a). Several fixed parameter settings have been summarized in Table 6.2. These include the values of the price thresholds p_i^- and p_i^+ correspond to the those in the optimal policy which was determined in Fokkema et al. (2020a) (see Table 6.3).

For the local electricity demand, aggregated data of 2015 to 2019 was obtained from NEDU (the Dutch Society of Energy Data Exchange) (NEDU, 2020). The data

represents average electricity consumption levels per 15 minutes as a fraction of
the total yearly consumption level for 3001 measurements during the years 2016,
2017, and 2018. The data was normalized to 1500 households, by assuming that
one household consumes on average 2990 KWh per year Nibud (2019). The scaled
daily average electricity consumption levels, as used in our base-case system, have
a minimum of 9.9 MWh, a mean of 12.3 MWh, and a maximum of 16.1 MWh per
day. We assume electricity consumption per day is normally distributed (i.i.d.) with
a day-specific mean and a constant standard deviation. To represent the stochastic
behavior of electricity consumption, we determine normal distribution parameters
by applying two linear regression models to the scaled data. The first model was
applied to the first 199 days and the second to the remaining days in a year, since
the average electricity demand follows a V-shape throughout the year. The splitting
procedure to determine which day separates the two models is based on minimizing
the sum of the standard errors for both models. Accordingly, we use the same data
and linear models as in Fokkema et al. (2020a).

The base price β_t which represents the external wholesale electricity prices, was
modeled in the same way as in Fokkema et al. (2020a). The AR(1) process of the
base price was fitted to daily wholesale electricity prices of the Netherlands which
occurred between 2015 and 2019.

Similar to Fokkema et al. (2020a), solar energy production levels between 2005
and 2016 were obtained from PVGIS PVGIS (2016) and correspond to an installed
capacity of 5 MWp. The production levels per week were fitted to beta distributions.
Similar to Fokkema et al. (2020a), Boland (2020) and Soubdhan et al. (2009), we
assume that production levels S_t are independent and identically distributed for
each period.

6.4.2 Experimental factors

To gain more insights on how prices and grid capacity expansion affects potential
congestion (i.e. peak utilization of the grid connection and the volatility of the grid
feed-in) for both storage operation policies, experiments are performed by varying
the price elasticity to net production levels and the installed grid connection capacity.
Grid capacity expansion is common in addressing congestion, and increasing solar
energy production capacity causes electricity prices to be more responsive to solar
energy availability. Therefore, choosing these experimental factors enables both

the grid operator and the facility owner to assess the consequences of the different storage operation policies in mitigating potential congestion when performing grid capacity expansion, and the implications of stronger price responses to solar energy availability.

Table 6.3: Experiment settings

Experiment	Grid connection (k^c)	Price elasticity l
Low grid connection capacity	10	0
	10	1
	10	2
Expanded grid connection capacity	30	0
	30	1
	30	2

Price elasticity to net production

In order to determine the effectiveness of storage in evenly spreading buying or selling decisions under different price conditions, three levels of the price elasticity l have been included in the experimental design, being 0, 1 and 2 (see Table 6.3). This enables the investigation of how the profit-oriented policies are affected by different levels of price elasticity, and to what extent storage enables a stable interaction with the electricity grid when prices respond more strongly to overages and shortages.

Grid connection capacity

In order to examine how the grid connection capacity affects the effectiveness of both heuristics to enable a stable interaction with the grid, we vary the grid connection capacity between 10 MWh and 30 MWh per day (see Table 6.3). These represent the cases in which the grid connection capacity is close to the average net production level and the case in which the grid connection capacity is highly sufficient.

6.5   Results and discussion

This section presents and discusses the results of the experiments. We compare the two heuristics for different levels of price elasticity and grid connection capacity,

and analyze each of the following decision variables and performance indicators.
Firstly, we illustrate the inventory levels over time. Secondly, the next subsection
indicates the average amounts sold and bought by the facility owner over time for
the different price elasticity levels. Thirdly, we analyze the standard deviation of
the sold electricity. This denotes the level of volatility of the grid feed-in. Fourthly,
we examine the fraction of runs in which sold electricity equals the grid connection
capacity to indicate peak utilization levels of the grid connection. Curtailment and
unmet demand are also analyzed, whereas the last subsection shows the revenue as
a result of buying and selling electricity by the facility owner.

The results indicate the effectiveness of the profit-oriented and the
storage-priority policies to spread the selling decisions from and to the grid
throughout the year. This is reflected in the average standard deviation of electricity
sold per run. Moreover, the results show how the standard deviation of selling
decisions is affected by the elasticity of the price to net production levels for
the profit-oriented heuristic. The results show the effectiveness of supply-based
pricing mechanisms to stabilize feed-in to the grid. We analyze how both profit
and non-profit operation strategies lead to curtailment, unmet demand or peak
utilization of the cable connection and inventory buildup that follows seasonal
patterns. Finally, the results provide insights on how expanding the grid connection
capacity affects the selling decisions for the above-mentioned dimensions.

6.5.1   Inventory levels

Figure 6.4 and 6.5 show the inventory levels for distribution capacity levels (k_c) of 10
and 30 respectively. Each point on the curves reflects the average across all runs. The
blue curves apply to the profit-oriented heuristic while the red curves apply to the
storage-priority heuristic. The x-axis represents the days in the year. The different
graphs from left to right apply to the three levels of price elasticity.

Figure 6.4 shows that the inventory levels for both heuristic policies follow the
seasonal shape of the net production levels and the maximum storage capacity of 400
MWh is not reached. Since the grid connection capacity is limited to the maximum
average net production level per day during the year (10 MWh per day), there is
not much room for opportunistic buying and selling. The limited grid capacity
also causes shortages and limits the level of inventory that can be stored as will
be explained in Section 6.5.5. For increased levels of price elasticity, it can be seen

that the profit oriented policy stores more since more energy can be bought at lower prices during the summer. While the storage priority heuristic does not respond to prices, we include it in all figures for comparison purposes.

For a higher grid connection capacity ($k_c = 30$), the blue curve in Figure 6.5 indicates that the profit-oriented heuristic is less responsive to seasonal differences than the storage-prioritizing heuristic, as a result of being more dependent on prices. This is because the higher grid connection capacity enables additional trading with the grid in addition to the coverage of shortages or overages. For prices that do not respond to net production levels ($l = 0$), the profit-oriented heuristic thus uses storage primarily for short-term opportunistic trading with the grid if price spreads are sufficient to cover the conversion losses. For a price elasticity of 2, storage levels follow more closely the seasonal patterns in net production levels, since prices reflect these patterns. In contrast, the red curve shows that the storage-priority heuristic fully uses the storage capacity in the summer and strongly follows seasonal patterns. Since the grid connection capacity is also sufficient to prevent shortages when the storage facility is empty in the winter, storage can be fully used to cover the seasonal differences between supply and the local demand.
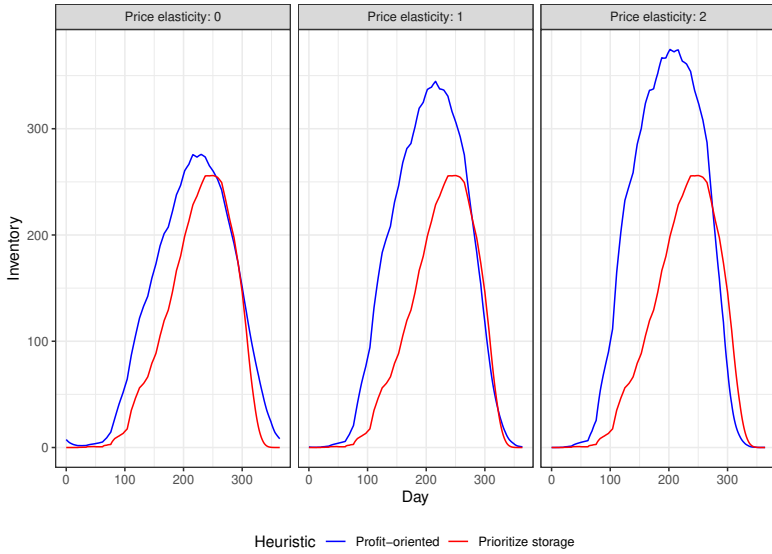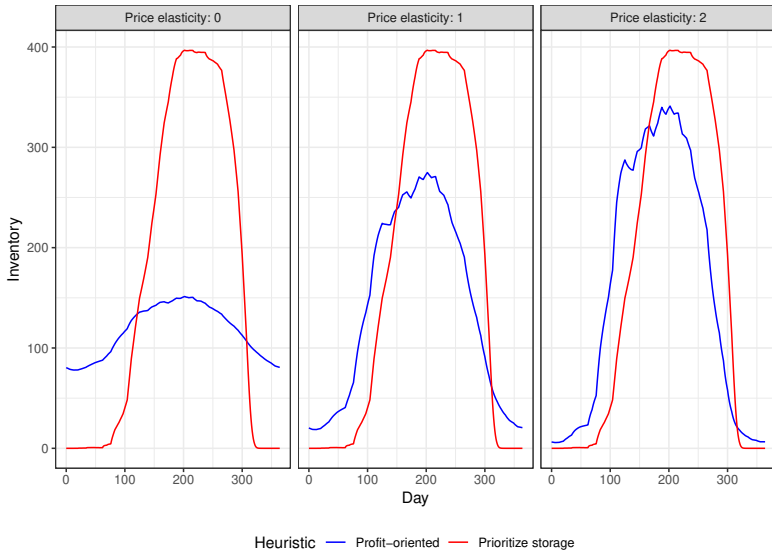
Figure 6.4: Average inventory per day ($k_c = 10$)

Figure 6.5: Average inventory per day ($k_c = 30$)

6.5.2   Average amounts bought and sold

Figure 6.6 and 6.7 indicates the average amounts bought and sold for each heuristic and for a grid connection capacity of 10 MWh and 30 MWh per day respectively. For a limited cable capacity ($k_c = 10$, see Figure 6.6), it can be seen that the policies for both heuristics follow a similar seasonal pattern in which energy is sold in the summer and bought in the winter. Since the grid connection capacity limits the amount that can be bought and sold, storage is mostly used for covering additional shortages and overages to prevent unmet demand. Hence, the average amount sold and bought for the profit-oriented heuristic is not affected by different price-elasticity levels.

For a higher grid connection capacity at low price elasticity ($k_c = 30$ and $l = 0$, see Figure 6.7), the average amounts bought and sold increases with 25.3% and 56.6% for both heuristics. This indicates that more energy is sold on average to the grid than for the lower grid connection capacity. The grid connection capacity enables the selling of more electricity per day. The red line shows that the average amount sold related to the storage priority heuristic increases in the winter between day 0 and 100, and flattens after that during spring. This plateau in the curve can be explained as follows. The heuristic chooses to use storage primarily for storing the overages. These become more common in spring as the summer is approached. When inventory levels reach the maximum storage capacity more often in the simulations, the average amount sold rises again, because the electricity which cannot be stored is sold during summer.

6.5.3   Evenness of grid feed-in across a year

Figure 6.8 shows the standard deviation across days of the amounts sold for a relatively low (a, $k_c = 10$) and high grid connection capacity (b, $k_c = 30$) respectively. For a low grid connection capacity and ($l = 0$), the red curve shows that the standard deviation of selling decisions by the storage-priority policies is 0.01 relative to the standard deviation of 3.1 of the profit-oriented policies. Furthermore, the profit-oriented selling policies become slightly less stable for increased levels of price elasticity. This indicates that, for a limited grid connection capacity, storage-priority policies are far more effective to evenly distribute the sold electricity to the grid. However, it also shows that profit-oriented storage does not become more effective
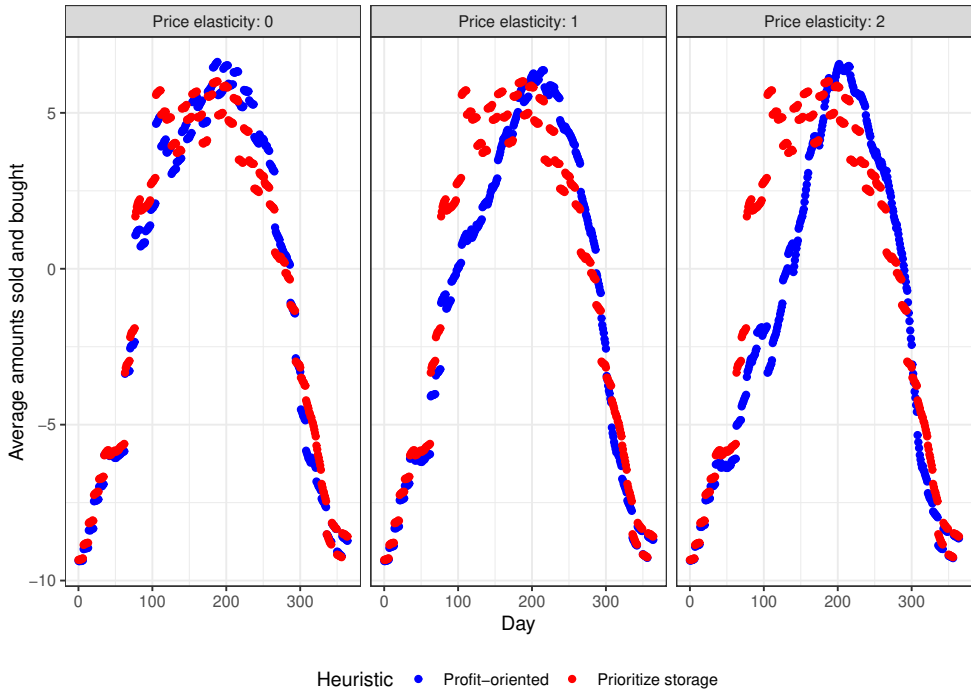
Figure 6.6: Average amounts bought and sold ($k_c = 10$)

to evenly distribute the sold energy to the grid when prices react more strongly to
differences in net production levels.

For a high grid connection capacity ($k_c = 30$) and $l = 0$, Figure 6.8 the red and
blue curve indicate that the standard deviation of sold electricity increases up to 5.9
and 7.9 for the storage-priority and profit-oriented heuristic respectively compared
to a low grid connection capacity ($k_c = 10$). Again, the prioritization of storage
yields the most stable feed-in to the grid compared to the profit-oriented decisions.
A high price elasticity to net production levels leads to only a small increase in the
standard deviation of sold electricity for the profit-oriented policies. This indicates
that seasonal-dependent prices which react more strongly to net production levels
do not facilitate more stable grid feed-in for profit-oriented operators.

These results show that expansion of the connected grid capacity leads to more
unstable feed-in to the grid for both heuristics. For both levels of grid connection
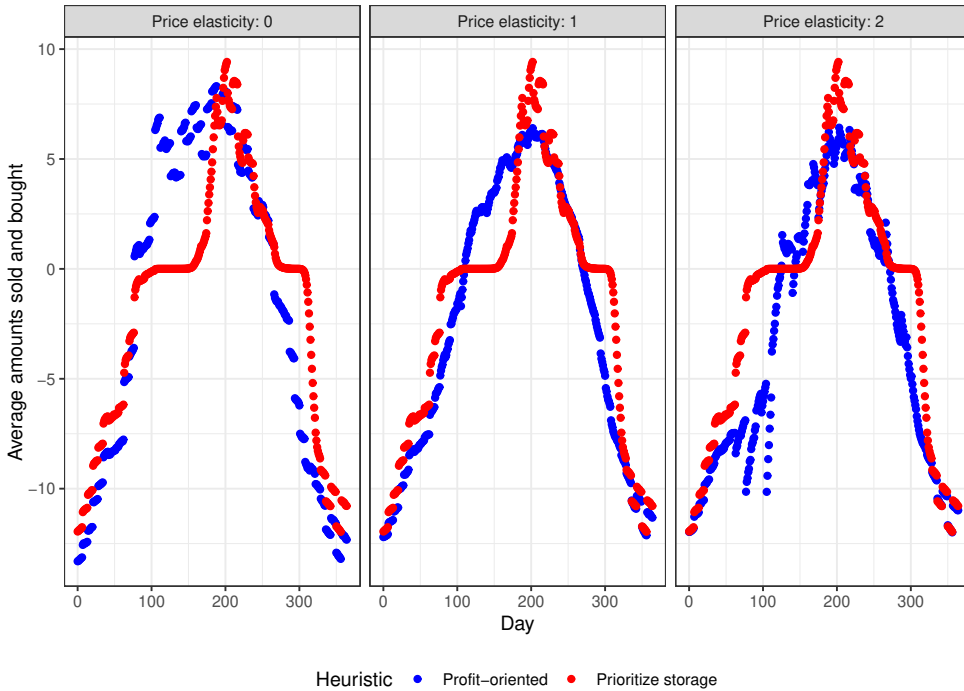capacity, the storage priority heuristic leads to much more stable grid feed-in than

Figure 6.7: Average amounts bought and sold ($k_c = 30$)

the profit-oriented heuristic. The profit-oriented operator is likely to engage in more opportunistic trading when the grid connection capacity is expanded, which causes a more unstable feed-in to the grid. The storage-priority heuristic also causes more unstable feed-in at a higher grid connection capacity, but these are the result of a full storage facility in the summer and variations in solar energy production which cannot always be stored. Seasonal-dependency of prices stimulate slightly more unstable behavior of a profit-oriented operator for both levels of grid connection capacity, due to additional trading to benefit from price differences.

6.5.4 Peak utilization of the grid connection capacity

Figure 6.9 and 6.10 show the fraction of runs in which the sold electricity equals the grid connection capacity for both a limited ($k_c = 10$) and high ($k_c = 30$) grid connection capacity. For $k_c = 10$, Figure 6.9 illustrates that the profit-oriented and storage-priority policies behave similarly in the sense that both reach the grid
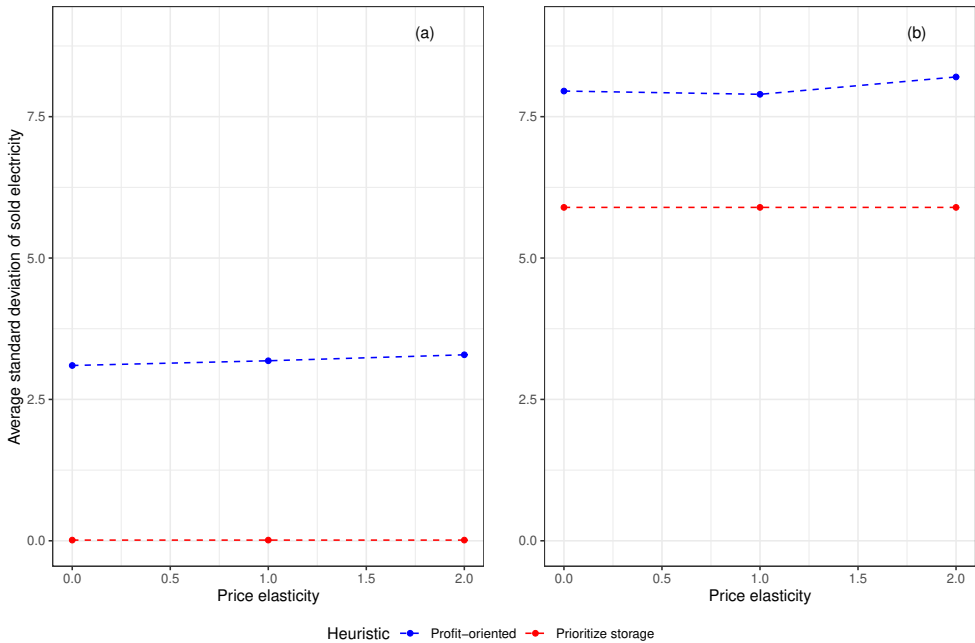
Figure 6.8: Standard deviation per run of sold electricity for a low grid connection capacity (a, $k_c = 10$) and high grid connection capacity (b, $k_c = 30$)

connection capacity limit in the summer peak for 62% and 60% of the runs in the simulation respectively. Price elasticity levels do not influence the behavior of the profit-oriented SPH operator, because the limited grid connection capacity does not allow additional trading on the grid.

For a high grid connection capacity ($k_c = 30$), the heuristic which prioritizes storage does not reach the grid connection capacity limit, since it only sells to the grid when storage capacity is reached, whereas the profit-oriented heuristic also sells from storage to the grid. The profit-oriented heuristic reaches the grid connection capacity limit less often, that is, 6.7% of the runs during the summer. It can also be observed that increased levels of price elasticity lead to a reduced fraction of runs in which the capacity limit is reached due to reduced selling as a result of low prices in summer.

These outcomes indicate that the storage-priority heuristic avoids using all grid connection capacity. This is because the heuristic stores the overages whenever possible and only sells to the grid when the storage capacity is reached.
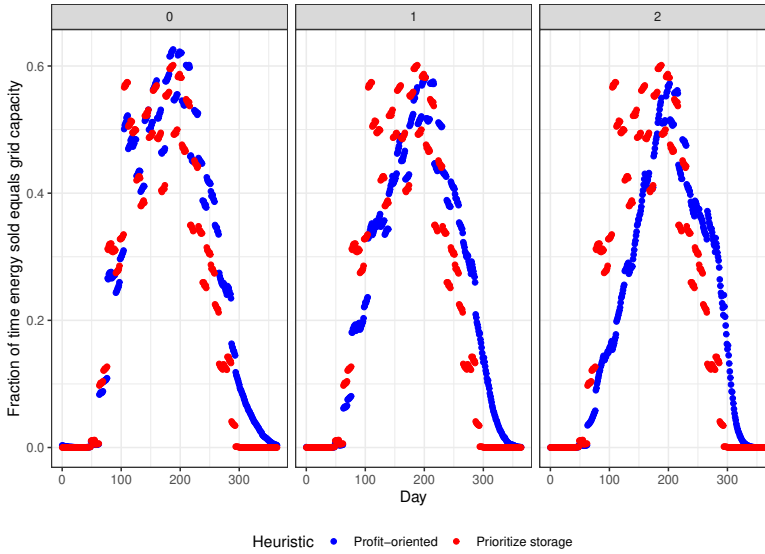
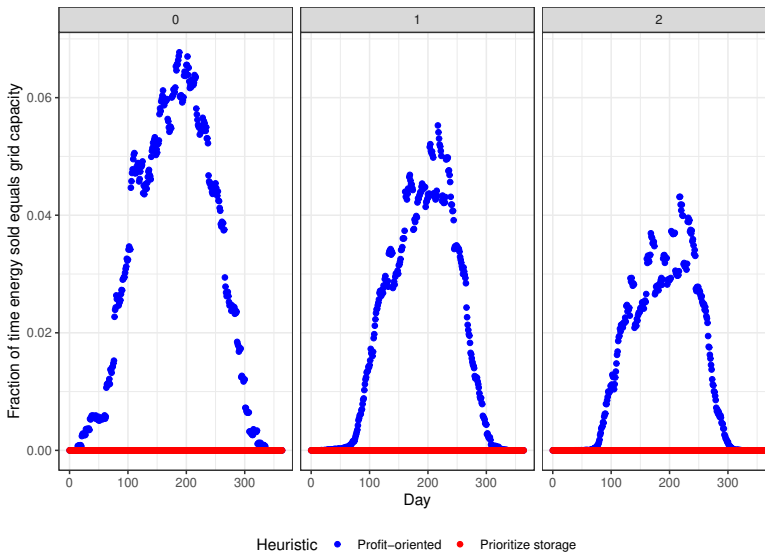Figure 6.9: Fraction of runs sold electricity is equal to grid connection capacity ($k_c = 10$)

Figure 6.10: Fraction of runs sold electricity is equal to grid connection capacity ($k_c = 30$)

6.5.5 Curtailment and unmet demand

Figure 6.11 illustrates the fraction of runs in which curtailment occurs for a limited grid connection capacity ($k_c = 10$) and different price-elasticity levels. It can be seen that the storage-priority policies do not cause any curtailment, whereas the profit-oriented policies lead to curtailment. This is because the storage-priority policies do not lead to reaching the maximum storage capacity, and sufficient storage capacity remains available. The fraction of runs in which curtailment occurs increases from peak levels of 3.2% to peak levels of 20.9% for price elasticity levels up to 2 for the profit-oriented policies. This indicates that the operation of storage with profit-oriented policies leads to curtailment-related losses which increase when prices react more strongly to differences in net production levels.

Figure 6.12 shows that, for a limited grid connection capacity of 10 MWh per day, both policies lead to similar levels of unmet demand. In the winter, these occur most frequently for the storage-priority heuristic with up to 74% of the runs. Price elasticity levels do not drastically affect the frequency of these shortages.

For a grid connection capacity of 30 MWh per day, both curtailment and unmet demand are not present for both types of policies. These results highlight that profit-oriented storage in combination with limited grid connection capacity and zonal prices may lead to curtailment losses, whereas the use of storage primarily to bridge seasonality differences in solar electricity production and local demand can help to avoid curtailment.
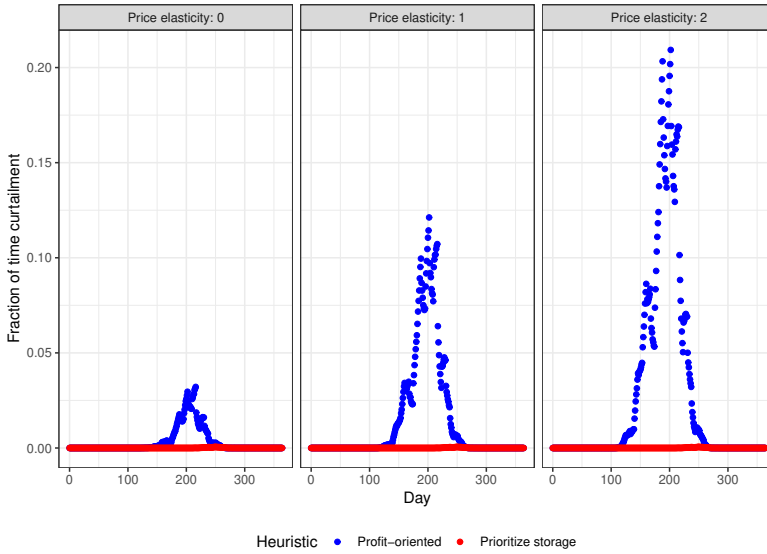
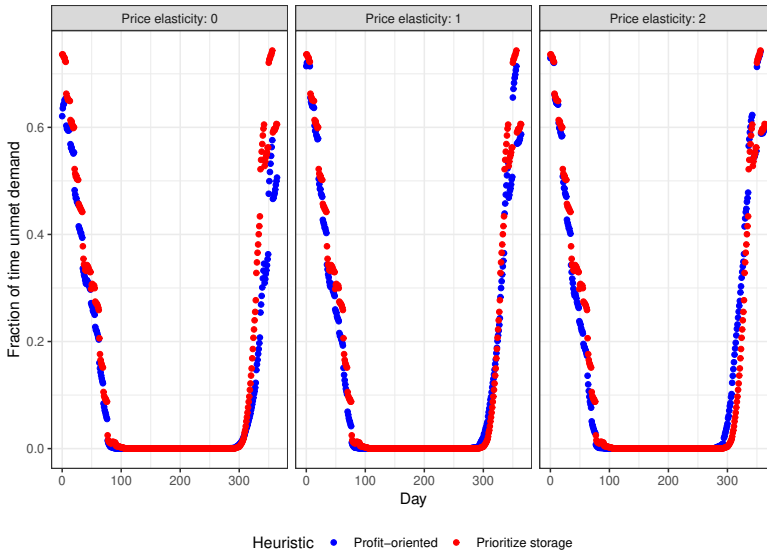Figure 6.11: Fraction of runs curtailment occurs ($k_c = 10$)

Figure 6.12: Fraction of runs curtailment occurs ($k_c = 10$)

6.5.6   Revenue as a result of buying and selling

Figure 6.13 shows the average total annual revenue for the profit-oriented (blue) and
storage-priority heuristic (red) as a result of buying from and selling to the grid for
different levels of price elasticity. The total revenue displayed in Figure 6.13 contains
revenues from both 1) interacting with the grid, and 2) the revenue from selling to
the local demand. We include revenues from selling to the local demand to avoid
negative revenues as a result of interacting with the grid. The revenue from the
local demand is constant and known and amounts to 180,477. It is calculated as the
average price times the average yearly consumption. The left and right graphs show
the total revenues for a low ($k_c = 10$) and high ($k_c = 30$) grid connection capacity
respectively.

Figure 6.13 indicates that revenues are negatively related to the price elasticity
to net production levels for both heuristics. The lower prices in summer outweigh
the higher prices in winter, even though the storage facility enables selling energy in
winter.

Grid connection capacity expansion leads to higher revenues for the
profit-oriented operator since this enables more trading with the grid. In contrast,
this reduces revenues for the non-profit-oriented operator that prioritizes the use of
storage to cover shortages and overages. While capacity expansion enables reducing
unmet demand and curtailment, the lower profits are caused by selling decisions at
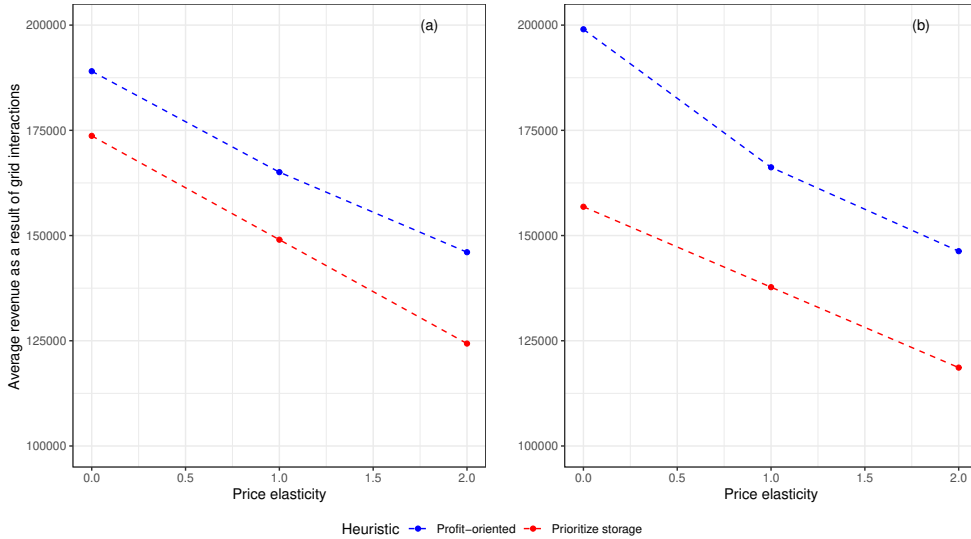times of unfavorable prices when storage is prioritized.

Figure 6.13: Average revenue per year as a result of buying and selling for a low grid connection capacity (a, $k_c = 10$) and high grid connection capacity (b, $k_c = 30$)

6.6   Conclusion

Development of solar parks starts to cause congestion problems at electricity grids, which increasingly leads to the need for curtailment. To avoid curtailment and congestion, seasonal hydrogen storage, supply-based pricing, and grid capacity expansion are possible solutions problems by stabilizing the supply to the grid. Particularly hydrogen storage may help to solve seasonality differences in supply and demand while mitigate peak supply to the grid connection. Moreover, supply-based pricing motivates the storage of energy during high availability and discharge during low availability. However, the profit-maximization behavior of a privately-owned SPH facility with hydrogen storage may disturb this mechanism due to opportunistic buying and selling.

In this study, we have examined whether solar parks with hydrogen storage should be operated with a profit-orientation or a non-profit-orientation with the aim to stabilize feed-in to the grid. We develop heuristics for both cases and compare their effect in terms of selling decisions to the grid. We also studied how the volatility

of electricity sold to the electricity grid is affected by different price elasticity levels
and grid connection capacities.

Our results show that while profit-oriented storage operations facilitate seasonal
storage buildup most of the time, the price-based opportunistic sales to the
grid cause unnecessary maximum utilization of the grid connection capacity,
while curtailment is needed at other times when storage is full. Moreover, the
profit-maximizing objective of the SPH facility creates unstable selling decisions
which lead to peaks in the utilization of the cable connection in case storage solutions
are also in place. In contrast, non-profit-oriented decisions which are independent of
prices and prioritize the use of storage also create similar seasonal storage patterns,
but enable much more stable selling decisions to the grid and result in lower storage
requirements. This is because prices do not affect the related storage decisions.

The results also reveal that grid connection capacity expansion should be done
with care. While it reduces the levels of curtailment and unmet demand for
both types of policies, it leads to selling decisions that introduce a much higher
variability of feed-in to the electricity grid. This is the case for both profit and
non-profit oriented storage, even though the selling decisions of the latter remain
more stable. Grid connection capacity expansion creates higher revenues for the
profit-oriented facility owner, but reduces revenues in case the facility is operated
when prioritizing the use of storage. This is unfavorable from the perspective of
the grid operator, because the considered non-profit oriented storage yields the most
stable selling decisions. While capacity expansion of the grid connection also reduces
the peaks in which the facility utilizes the maximum capacity, the higher levels
of supply-induced variability into the electricity network are not desirable from a
congestion management perspective and potential resulting congestion problems
elsewhere in the grid.

The elasticity of prices to net production levels do not affect the stability of the
amounts sold, while, as expected, they do have a negative impact on revenues and
lead to curtailment in the case of profit-oriented policies. Therefore, this suggests
that prices which react more strongly to the net energy availability are not beneficial
for both SPH facility operators and the grid, since these lead to reduced revenues,
curtailment and do not contribute to a stable grid feed-in.

In conclusion, the non-profit-oriented operation of the SPH facility that
prioritizes storage to cover shortages and overages is most beneficial in terms of

stable feed-in to the grid. Expensive grid connection capacity expansion should be done with care when storage is already installed, since it leads to more overall variability of the grid feed-in for profit and non-profit oriented policies, and higher storage requirements and reduced revenues for the non-profit-oriented SPH facility operator. Therefore, a balance must be found in which a combination of non-profit-oriented storage with capacity expansion reduces peak utilization of the cable, curtailment and unmet demand, but prevents a high variability of feed-in to the grid.

Chapter 7

Conclusions

In this thesis, we executed five studies that all contributed to the main research question of this thesis: *How should the decentralized storage and distribution of biogas, solar, and wind energy be organized and adapted to enable effective embedding in existing grid infrastructure?* Together the studies addressed three different domains, being "Transportation logistics", "Seasonal matching of supply and demand", and "Operation of storage".

In this chapter, we first draw conclusions starting with the detailed conclusions from each of the studies. Next, we reflect on the theoretical and societal implications for each of the distinguished domains and present opportunities for further research. Since the conclusions have already been thoroughly discussed in each chapter, we will limit this section to a summary of specific findings that are relevant to the considered domains.

7.1 Conclusions

In this section, we start by summarizing the insights from each of the studies for the related research domain and end with conclusions regarding our main research question.

7.1.1 Transportation logistics

Within the domain of transportation logistics, we answer two specific research questions that contribute to gaining more understanding of transportation logistics problems in the energy transition.

In Chapter 2, we have addressed the research question: *How should biogas be distributed using trucks with tube trailers from digesters to centralized upgrading facilities?* We studied a biogas inventory-constrained routing problem in continuous-time in which trucks exchange empty cylinders for full ones at each farm to transport these to an upgrading and injection facility. We provided a mathematical formulation and introduced valid inequalities which were effective in reducing the computation times on average with 93%. The solutions indicate that transportation time is minimized when the number of available cylinders at each farm is larger than or equal to the truck capacity. This enables the vehicle to visit fewer farms per tour. Both the average transportation time and the average number of suppliers visited per tour generally decrease for larger supplier storage capacities until the storage capacity is larger than or equal to the vehicle capacity. In 95% of the studied instances, the average content levels of the cylinders exceed 99.6% in the optimized solutions. This indicates that there are limited benefits related to collecting cylinders while partly filled to reduce the transportation time of the schedules.

In Chapter 3, we have addressed the research question: *Under which conditions is the application of LNG economically viable for LNG-fueled ships compared to conventional ships?* We have developed an investment appraisal model to compare the total exploitation costs of LNG-fueled ships with conventional ships. We found that fuel costs of LNG-fueled ships are often lower than conventional ships, even for unfavorable LNG prices. The cost-effectiveness of LNG-fueled ships is strengthened for larger ships that have higher overall fuel consumption levels and ships that have a high presence in ECA zones. This also indicates that using biogas as bio-LNG can be economically viable as a fuel in shipping.

7.1.2 Seasonal matching of supply and demand

In Chapter 4, we have addressed the research question: *How should biogas, wind, and solar energy be combined across seasons and how is this affected by the level of total production capacity and storage capacity?* We studied this question to realize the lowest

production and storage capacity requirements when supplying a self-sufficient community of households with locally produced electricity. We examined the shares of each source for different combinations of production and storage capacity and found that constant sources such as biogas in combination with wind energy are most effective in reducing combined storage and production requirements. For small total production levels, biogas can supply both peaks and base-load, leading to relatively high storage requirements in which mostly biogas is stored. For higher levels of total production, the optimal share of wind production increases, because some excess production allows for curtailment of unfortunately-timed wind peaks, which allows substantial reductions to be made in storage requirements. When the total production capacity exceeds 130% of the total demand, the optimal share of wind approaches zero, in which curtailment of electricity from biogas enables very low storage requirements.

7.1.3   Operation of storage

In Chapter 5, we have addressed the research question: *Under which conditions should the owner of solar fields with hydrogen buy and sell from and to the grid to maximize profits?* We studied the problem of a solar park owner with hydrogen storage that supplies electricity to a connected set of households and is also connected to the electricity grid. Using a Markov Decision Process, we determine the optimal daily buying and selling decision of the facility owner to maximize the expected profits. We explicitly take into account seasonality differences in supply and demand and the uncertainty associated with electricity prices, electricity consumption, and solar energy production. We found that optimal policies are characterized by price thresholds that separate different types of actions. These include buying the maximum possible quantity, selling exactly overages or buying exact shortages, storing overages or obtaining shortages from storage, or selling the maximum amount possible. We also show that ignoring seasonal demand and production patterns is suboptimal and that introducing hydrogen storage transforms loss-making interactions with the grid into profitable ones. We found that the distribution capacity should not be too small to prevent local grid congestion. In contrast to what may be expected, a higher storage capacity increases the number of buying actions from the grid, thereby causing more congestion, which is problematic for the grid operator. Accordingly, profit-maximizing hydrogen storage operation

alone is not an alternative to grid expansion to solve congestion, which is essential knowledge for policy-makers and grid operators.

In Chapter 6, we have addressed the research question: *How should solar fields with hydrogen storage be operated to alleviate congestion?* We compare profit-oriented storage operation strategies with the strategy that always prioritizes storage to cover net overages or shortages. Profit-maximization by the storage owner creates an unstable feed-in to the grid, which may lead to potential congestion problems elsewhere in the grid. In contrast, the operation of storage by prioritizing the use of storage to cover net production differences leads to a lower level of volatility of the feed-in to the grid. It also reduces storage requirements by creating a similar seasonal storage pattern. Expanding the distribution capacity for both profit-oriented and storage-prioritizing operation strategies increases the volatility of grid feed-in. This reduces revenues for storage-prioritizing strategies, which is unfavorable for the grid operator because this negatively affects the economic viability of these price-independent strategies.

7.1.4   General conclusions

The findings of each study provided a small contribution to answering the main research question *How should the decentralized storage and distribution of biogas, solar, and wind energy be organized and adapted to enable effective embedding in existing grid infrastructure?* It can be concluded that biogas production has a useful role in decentralized energy systems both as a gas, in the form of LNG, and after conversion to electricity. To enable effective embedding in existing infrastructure, the biogas can serve to complement fossil methane in existing gas grids and provide a constant electricity source by complementing other renewable sources. Biogas can be stored in cylinders located close to biomass sources. Being further away from gas injection points, it can be transported with vehicles with tube trailers. To minimize the transportation time, biogas-producing farms should have sufficient storage capacity to allow for full truckloads and single tours. Clean fuels such as (bio-) LNG also have an important role in the transportation sector, in which LNG was found to be an economically viable alternative to conventional oil-based fuels in shipping. When biogas is converted to electricity, it can complement other renewable sources by providing a base-load level of electricity for the local demand of households. Wind and solar energy can then provide energy during peaks in electricity demand. This helps to reduce the overall storage and production capacity requirements. In

general, wind shows a better matching supply profile than solar as an addition to base-load supply. While solar energy is a relatively cheap form of electricity, it can also cause peak loads at the electricity grid connection and potentially lead to congestion problems. Hydrogen storage is a solution to reduce peak loads but also to bridge seasonality differences between supply and demand. Optimizing the buying and selling decisions for a storage owner/operator can increase revenues and help to increase the economic viability of hydrogen. However, operating storage to benefit from price differences increases the volatility of the grid feed-in, which is problematic from a broader perspective. Operating storage independent of prices helps to stabilize the feed-in to the grid. However, this leads to lower revenues for the facility owner, and thus requires further consideration.

The combined conclusions from the executed studies bring us some steps forward in our thinking on how decentralized storage and distribution of biogas, solar, and wind energy should be organized in the energy transition. Still, the implications should be carefully considered before making any recommendations on transition policies.

7.2   Implications and further research

In this section, we present a discussion in which we reflect on both the societal and scientific implications of the research projects developed in this thesis and we provide directions for further research. We present the discussion separately for each of the three domains and the studies executed within these domains.

7.2.1   Transportation logistics related to biogas and LNG

In the research developed in Chapters 2 and 3, we study the distribution problem of biogas to centralized upgrading and injection facilities and study the viability of one application of biogas as LNG in the shipping sector.

Biogas distribution to upgrading facilities

Biogas can play an important role as an energy source in the energy mix of areas, due to its constant output profile and due to its applicability in providing a stable and constant electricity source with a Combined-Heat and Power (CHP) engine. It

can also complement natural gas in existing gas grids after having been upgraded to green gas. However, it is important in the supply chain of biogas, to keep production close to biomass sources to avoid long-distance transportation of low-energy-density feedstock (Pierie et al., 2015). Based on the findings by (Hoang et al., 2019), in which the authors found that co-digestion causes higher nitrogen emissions than mono-digestion, the production of biogas by mainly utilizing mono-digestion is recommended. This limits environmental problems associated with excess nitrogen flows in using digestate as fertilizer and limits the interference with existing agricultural practices. However, mono-digestion is considered less economically viable due to its lower biogas output.

In enhancing the economic viability of green gas supply chains, it is imperative to minimize the required transportation related to biogas. In Chapter 2, we developed a model to construct efficient transportation schedules and routes of trucks with tube trailers in which transportation time is minimized. Based on the findings in Chapter 2, we recommend that, in the studied transportation system, the number of exchangeable cylinders at each farm should be at least equal to the vehicle capacity to minimize the transportation time. This enables trucks to collect full cylinders and make full use of the vehicle's capacity. We advise transportation planners to construct schedules and routes such that trucks visit single farms in which the operator exchanges and collects as many cylinders as possible. We advise against combining tours with multiple farms since this increases the transportation time and thus leads to less efficient routes. From the perspective of the farm, it is advisable to implement mono-digestion facilities, since mono-digestion in which local manure is utilized limits the transportation of other low-energy-density feedstock compared to co-digestion while the biogas with a high energy density is collected by trucks that transport the biogas to upgrading and injection facilities.

It is important to note that, in the solutions found in Chapter 2, the trucks remain idle for relatively long periods between tours. Therefore, it is important that the trucks are used for other transportation purposes and that schedules are combined with trucks performing other tours in schedule gaps. Based on the solutions in Chapter 2, feasible and efficient schedules can be made when introducing time windows that enable truck drivers to work during working hours. It is also important to note that our model may create unevenly distributed arrival times of cylinders at the upgrading and injection facility. This should be taken into account

when implementing such transportation systems in practice. Within our study, the utilization levels of upgrading facilities would directly result from the studied supply quantities. In future studies, utilization may be an important performance metric as low utilization levels are undesirable for the economic viability of the facility. A similar consideration relates to the handling times of the cylinders which need to be connected, disconnected, and loaded onto a truck. These were not explicitly modeled in our studies since these times could be reflected in the transportation time for each connection to the upgrading facility. But in future practices, they may need explicit attention.

Further research

We recommend further research to focus on the above-mentioned aspects, which include the examination of obtaining evenly distributed arrivals of cylinders at the upgrading facility. Other research avenues include solving problem instances with multiple vehicles, and the minimization of the needed cylinders. This could even be made part of the objective function of the used model. Finally, future research may focus on optimal fleet sizes of vehicles and the development of models that can solve larger instances.

The application and viability of LNG in shipping

LNG is recognized as a promising transition fuel in making the shipping sector cleaner and replacing oil-based fuels. It is also an important fuel in complying with IMO 2020 regulations which limit the use of those fuels with sulfur contents that cannot exceed 0.1% m/m. However, the economic viability of LNG depends on the combination of LNG prices, investment costs of the engines, and the execution of optimal bunker strategies that make use of the time spent in Emission Controlled Areas (ECA) during a tour in switching between different fuels.

Our findings suggest that LNG in the shipping industry can be economically viable for ship-owners. It is important to examine the conditions under which the total exploitation costs of LNG-fueled vessels are lower than conventional vessels to facilitate the adoption of LNG dual-fuel engines. Based on the findings in Chapter 3, this is the case if conventional Marine Gasoil (MGO) prices are considerably higher than LNG and for ships that spent a high percentage of time

in ECA zones. Moreover, LNG-fueled vessels were even more competitive than conventional vessels at relatively unfavorable LNG prices. This indicates that LNG is a promising fuel to comply with ECA regulations. However, there are still issues associated with LNG, that hinder adoption. This includes the limited bunkering infrastructure in ports worldwide. Moreover, the use of LNG in shipping is also associated with possible small levels of methane slip, in which methane enters the atmosphere. This is problematic since methane is a potent greenhouse gas. Moreover, recent developments related to hydrogen as a fuel for ships may lead to the adoption of hydrogen as one of the main future fuels in shipping. This may compete with LNG as a future fuel, in which green hydrogen is a cleaner alternative to LNG.

Further research

We recommend further research to focus on developing more comprehensive frameworks to evaluate the use of LNG as a fuel that includes other aspects such as the limited bunkering infrastructure and competing fuels, besides research into the opportunities for hydrogen in the shipping industry.

7.2.2   The combination of biogas with wind and solar energy

In Chapter 4, we study the trade-off between installed production capacity and storage capacity requirements when combining biogas with wind and solar energy in supplying electricity to a self-sufficient community of households. This is useful, because a high level of production capacity reduces the need for storage, but leads to high curtailment due to excess availability of electricity. However, a lower level of production capacity increases the amount of required storage to prevent shortages. In matching the production profiles of biogas, wind, and solar energy to the electricity demand profile, it is important to think carefully about the share of each source of the installed capacity. Whereas biogas production is relatively constant, solar and wind supply are dependent on the weather.

This study highlights the usefulness of having constant energy sources in the electricity mix, even if these sources are supply-driven and inflexible. In particular, this holds when matching constant energy sources to the electricity demand of households. Constant energy sources can provide a baseload level of supply, and

in combination with wind energy, can be better matched with demand as a result of peaks in wind production. However, it is important to note that our study suggests that the shares of wind and biogas to minimize combinations of storage and production capacity are such, that this cannot be realized on a large scale in practice. For example, large-scale biogas production does not provide sufficient electricity and might require a lot of low-energy-density feedstock to be transported over large distances. This also raises the question of whether biogas should be used to such an extent for generating electricity. It is also important to consider biogas as a source to contribute to heat demand. At the same time, this underlines the applicability and usefulness of biogas in supplying energy to local communities and villages from a logistics perspective. Local villages with an abundance of manure can effectively use the manure for energy production, provided that the manure is not transported over large distances. It is important to note that we have not considered the viability aspect and avoided the inclusion of costs in our study to focus specifically on the production and demand profiles.

Further research

Further research avenues include investigating how different shares of renewable sources in the energy mix and storage capacity levels affect the electricity load sent to the grid and lead to potential grid congestion problems. Since our study only included electricity demand by households, future research may incorporate the 1) changing electricity demand profiles as a result of increased adoption of heat pumps in transitioning from natural gas-based to electricity-based fulfillment of heat demand, and the 2) energy demand in different forms such as hydrogen or (upgraded) green gas.

7.2.3   The operation of solar parks with hydrogen storage and local grid congestion

In Chapter 5-6, we study the operation of solar parks connected to local communities which aim to be self-sufficient and the electricity grid. Since complete self-sufficiency requires extremely high storage requirements, a connection with the grid is sensible. However, the peak utilization of the grid connection and associated congestion due to solar energy production in the summer is problematic, and hydrogen storage is

a possible solution. The solar parks convert the generated electricity into hydrogen and store it in a nearby facility. This raises the question of what kind of buying, selling, and storing decisions are sensible for the facility owner who faces uncertain electricity prices, demand, and solar energy production levels. These decisions have important consequences for the utilization of the cable connection and the associated congestion. Chapter 5 determines the profit-maximizing buying, selling, and storing decisions and shows how these affect the peak utilization of the cable connection, whereas Chapter 6 examines alternative strategies.

The results in Chapter 5 indicate that profit-maximizing hydrogen storage transforms loss-making grid interactions into profitable ones. This is beneficial from the standpoint of the economic viability of hydrogen and the development of hydrogen markets. However, the results indicate that storage flexibility is not necessarily effective in reducing congestion problems, since profit-oriented owners of solar fields with hydrogen will also create congestion problems at the distribution connection as a result of opportunistic trading with the grid. Based on the results of Chapter 6, it is more effective to reduce local congestion when owners operate their storage independently from prices by prioritizing the use of storage to cover shortages or overages in the net production after the local electricity demand of connected households has been fulfilled. While this is associated with lower revenues, it reduces both the volatility of feed-in to the grid and the number of times in which peak utilization of the distribution connection occurs. Therefore, additional solutions must be studied which enable more stable grid interactions. One such solution could be the operation of storage by non-commercial parties.

The results in Chapter 6 also indicate that grid operators should be careful in expanding the distribution capacity of the grid connection, both when profit-oriented and price-independent storage systems are applied. For both types of storage operation strategies, the volatility of feed-in to the grid increases, potentially increasing congestion elsewhere in the grid. While the storage owner of the price-independent operation feeds electricity to the grid with the lowest volatility, its profits decline when distribution capacity is expanded, which reduces the incentive to utilize storage facilities connected to solar fields. It is important to note that markets for flexibility aimed at mitigating congestion should incentivize the profit-oriented facility operator to only feed in electricity when no congestion is expected. In electricity markets for congestion flexibility, prices are reduced when

the grid operator forecasts congestion in the network. However, the accuracy of price responses to local congestion depends on the geographic resolution of prices in the market. In the case of zonal prices, which are most common, a relatively low geographic resolution applies and prices are uniform for a certain zone. In this case, prices do not fully respond to congestion caused by the individual facility operator within a zone. This creates opportunities for the facility owner to engage in opportunistic trading. In contrast, higher-resolution nodal prices can alleviate this, in which prices can be determined for single grid connections. However, nodal markets are characterized by a low level of liquidity, because very few market participants are active (Ehrenmann and Smeers, 2005). Moreover, the facility owner can then possibly influence prices due to a low number of local market participants. To the best of our knowledge, the interactions between electricity prices and the offerings of storage facility owners, and the relationship with congestion in nodal markets are not yet fully known. This is also the case for multiple market participants that operate storage facilities, in which their interactions and implications to congestion problems are not directly evident.

Further research

Further research avenues include the investigation of the interaction between electricity prices and the offerings of storage facility owners and the relationship with grid congestion in nodal price-based electricity markets. Multi-objective optimization models might provide further insights into the possibilities to combine the objectives of maximizing storage profits with minimizing congestion problems. Moreover, the interaction between multiple market participants with storage facilities on congestion throughout electricity networks is another relevant research direction. Finally, future research may address the role and activities of distribution system operators (DSO) in combination with storage facilities in mitigating congestion and ensuring sufficient revenues and the economic viability of hydrogen storage facilities.

7.2.4   Implications for the energy transition

This thesis was initiated from the ADAPNER project to successfully organize the energy transition from both an environmental and logistics perspective. In doing so,

we address solutions for five logistics problems, which contribute to this goal. We first addressed a biogas transportation problem and an economic viability problem related to a cleaner fuel such as LNG in shipping. This was followed by combining multiple energy sources and settings that include hydrogen storage. When looking at the thesis as a whole, it becomes clear that all the challenges and insights are interrelated. Below, we present our view on the organization and application of decentralized renewable energy systems.

Useful role of biogas

Firstly, we argue that biogas does have a useful role in electricity systems and the application of transition fuels in the transportation sector. This is because 1) its constant supply profile enables reduced storage and production capacity requirements in the electricity supply chain, 2) manure which is abundantly available in rural areas the energy potential, and 3) (bio-) LNG can be a suitable transition fuel in other sectors such as in the shipping industry. While mono-digestion limits excess nitrogen flows when using the digestate as fertilizer (Hoang et al., 2019), it is important to mention that the use of digestate instead of manure to fertilize soils is interfering with the present agricultural practices (Hoang et al., 2019). These issues should be addressed before biogas production on dairy farms can take place at large scales. Furthermore, combining the production of electricity with a CHP engine with biogas upgrading and injection into pipeline grids creates opportunities for short-term flexibility, since CHP engines can be turned on or off and create heat that can be captured when operated.

Multi-commodity energy systems

Secondly, our view on energy systems is that they should be multi-commodity energy systems that consist of multiple sources and which are stored in multiple forms. This enables increased opportunities for flexibility and is in line with other literature (D'Souza et al., 2018; Mancarella, 2014; van der Burg et al., 2015). Since we recommended avoiding unnecessary conversion steps, multi-commodity systems are needed, because energy is demanded by consumers in multiple forms, and the different profiles of different sources and consumer demand create opportunities for reducing the needed storage and production capacity. Storage and production

capacity have an important relationship, in which high production capacity leads to low storage requirements, but high curtailment and vice versa. This relationship and the role of different renewable sources are important to consider when designing multi-commodity energy systems.

Grid connection capacity balanced with storage

Thirdly, we argue that energy systems should have electricity grid infrastructure in which the grid connection capacity is balanced with storage systems to avoid the expensive investment in overcapacity of either electricity grids or storage facilities. To remain adaptive for future changes in production and consumption levels, this balance is especially important, since future increases in production and consumption levels would require sufficient storage and electricity grid connection capacity levels. The successful functioning of these systems depends on the development of markets for flexibility in which prices are established with a sufficient geographical resolution, and that respond such that they provide the proper incentives to profit-maximizing facility owners with storage facilities to avoid congestion. Future research must address the organization of these markets that include storage facilities. Other options include the operation of storage facilities by a Distribution Service Operator (DSO) to exercise control over the in- and out-feed of storage. This also alleviates issues related to illiquidity in nodal price markets and the high market power of storage owners when storage is owned by a private market participant. Storage can then be seen as an alternative to grid extension available to the DSO.

The above-mentioned aspects underline the importance of considering the energy transition from multiple domains to effectively organize the decentralized storage and distribution of biogas, solar, and wind energy and enable effective embedding in existing grid infrastructure.

Bibliography

Acciaro. 2014a. Alternative fuels for shipping, prices and availability. URL http://www.zerovisiontool.com/sites/www.zerovisiontool.com/files/attachments/si_michele_acciaro.pdf.

Acciaro, Michele. 2014b. Real option analysis for environmental compliance: Lng and emission control areas. *Transportation Research Part D: Transport and Environment* **28** 41–50.

Adachi, Masaki, Hiroyuki Kosaka, Tetsugo Fukuda, Shota Ohashi, Kazuyoshi Harumi. 2014. Economic analysis of trans-ocean lng-fueled container ship. *Journal of Marine Science and Technology* **19**(4) 470–478.

Aghezzaf, El-Houssaine, Birger Raa, Hendrik Van Landeghem. 2006. Modeling inventory routing problems in supply chains of high consumption products. *European Journal of Operational Research* **169**(3) 1048–1063.

Aghezzaf, El-Houssaine, Yiqing Zhong, Birger Raa, Manel Mateo. 2012. Analysis of the single-vehicle cyclic inventory routing problem. *International Journal of Systems Science* **43**(11) 2040–2049.

Agra, Agostinho, Marielle Christiansen, Alexandrino Delgado. 2017. Discrete time and continuous time formulations for a short sea inventory routing problem. *Optimization and Engineering* **18**(1) 269–297.

Ahadi, Amir, Sang-Kyun Kang, Jang-Ho Lee. 2016. A novel approach for optimal combinations of wind, PV, and energy storage system in diesel-free isolated communities. *Applied Energy* **170** 101–115.

Al-Khayyal, Faiz, Seung-June Hwang. 2007. Inventory constrained maritime routing and scheduling for multi-commodity liquid bulk, part 1: Applications and model. *European Journal of Operational Research* **176**(1) 106 – 130.

Alanne, Kari, Sunliang Cao. 2017a. Zero-energy hydrogen economy (ZEH2E) for buildings and communities including personal mobility. *Renewable and Sustainable Energy Reviews* **71** 697–711.

Alanne, Kari, Sunliang Cao. 2017b. Zero-energy hydrogen economy (ZEH2E) for buildings and communities including personal mobility. *Renewable and Sustainable Energy Reviews* **71** 697–711.

Alnaser, Sahban W., Luis F. Ochoa. 2016. Optimal sizing and control of energy storage in wind power-rich distribution networks. *IEEE Transactions on Power Systems* **31**(3) 2004–2013.

Alvarez, Aldair, Pedro Munari, Reinaldo Morabito. 2018. Iterated local search and simulated annealing algorithms for the inventory routing problem. *International Transactions in Operational Research* **25**(6) 1785–1809.

Amponsah, Samuel Kwame, Said Salhi. 2004. The investigation of a class of capacitated arc routing problems: the collection of garbage in developing countries. *Waste Management* **24**(7) 711–721.

Andersson, Joakim, Stefan Grönkvist. 2019. Large-scale storage of hydrogen. *International Journal of Hydrogen Energy* **44**(23) 11901–11919.

Anily, S., A. Federgruen. 1990. One warehouse multiple retailer systems with vehicle routing costs. *Management Science* **36**(1) 92–114.

Archetti, Claudia, Luca Bertazzi, Gilbert Laporte, Maria Grazia Speranza. 2007. A branch-and-cut algorithm for a vendor-managed inventory-routing problem. *Transportation Science* **41**(3) 382–391.

Archetti, Claudia, Leandro C. Coelho, M. Grazia Speranza. 2019. An exact algorithm for the inventory routing problem with logistic ratio. *Transportation Research Part E: Logistics and Transportation Review* **131** 96 – 107.

Archetti, Claudia, Guy Desaulniers, M. Grazia Speranza. 2017. Minimizing the logistic ratio in the inventory routing problem. *EURO Journal on Transportation and Logistics* **6**(4) 289–306.

Arora, Siddharth, James W. Taylor. 2016. Forecasting electricity smart meter data using conditional kernel density estimation. *Omega* **59** 47 – 59.

Avella, Pasquale, Maurizio Boccia, Antonio Sforza. 2004. Solving a fuel delivery problem by heuristic and exact approaches. *European Journal of Operational Research* **152**(1) 170–179.

Babrowski, Sonja, Patrick Jochem, Wolf Fichtner. 2016. Electricity storage systems in the future german energy sector: An optimization of the german electricity generation system until 2040 considering grid restrictions. *Computers & Operations Research* **66** 228 – 240.

Bard, Jonathan F., Liu Huang, Patrick Jaillet, Moshe Dror. 1998. A decomposition approach to the inventory routing problem with satellite facilities. *Transportation Science* **32**(2) 189–203.

Bartolucci, Lorenzo, Stefano Cordiner, Vincenzo Mulone, Vittorio Rocco, Joao Luis Rossi. 2018. Hybrid renewable energy systems for renewable integration in microgrids: Influence of sizing on performance. *Energy* **152** 744–758.

Bell, Walter J., Louis M. Dalberto, Marshall L. Fisher, Arnold J. Greenfield, R. Jaikumar, Pradeep Kedia, Robert G. Mack, Paul J. Prutzman. 1983. Improving the distribution of industrial gases with an on-line computerized routing and scheduling optimizer. *Interfaces* **13**(6) 4–23.

Bertazzi, Luca, Giuseppe Paletta, M. Grazia Speranza. 2002. Deterministic order-up-to level policies in an inventory routing problem. *Transportation Science* **36**(1) 119–132.

Bett, Philip E., Hazel E. Thornton. 2016. The climatological relationships between wind and solar energy supply in Britain. *Renew Energy* **87** 96–110.

Bianchi, M., L. Branchini, C. Ferrari, F. Melino. 2014. Optimal sizing of grid-independent hybrid photovoltaic–battery power systems for household sector. *Applied Energy* **136** 805–816.

Boland, John. 2020. Characterising seasonality of solar radiation and solar farm output. *Energies* **13**(2) 471.

Boland, Natashia, Mike Hewitt, Luke Marshall, Martin Savelsbergh. 2019. The price of discretizing time: a study in service network design. *EURO Journal on Transportation and Logistics* **8**.

Boudia, Mourad, Christian Prins. 2009. A memetic algorithm with dynamic population management for an integrated production–distribution problem. *European Journal of Operational Research* **195**(3) 703–715.

Brailsford, Timothy J, Robert W Faff. 1996. An evaluation of volatility forecasting techniques. *Journal of Banking & Finance* **20**(3) 419–438.

Brockwell, Peter J, Richard A Davis, Stephen E Fienberg. 1991. *Time series: theory and methods: theory and methods*. Springer Science & Business Media.

Brouwer, Anne Sjoerd, Machteld van den Broek, William Zappa, Wim C. Turkenburg, André Faaij. 2016. Least-cost options for integrating intermittent renewables in low-carbon power systems. *Applied Energy* **161** 48 – 74.

Bunker Index. 2015. Bunker prices worldwide. URL `http://www.bunkerindex.com/`.

Burel, Fabio, Rodolfo Taccani, Nicola Zuliani. 2013. Improving sustainability of maritime transport through utilization of liquefied natural gas (lng) for propulsion. *Energy* **57** 412–420.

Bussar, Christian, Philipp Stöcker, Zhuang Cai, Luiz Moraes Jr., Dirk Magnor, Pablo Wiernes, Niklas van Bracht, Albert Moser, Dirk Uwe Sauer. 2016. Large-scale integration of renewable energies and impact on storage demand in a european renewable power system of 2050—sensitivity study. *Journal of Energy Storage* **6** 1 – 10.

Byon, Eunshin, Yu Ding. 2010. Season-dependent condition-based maintenance for a wind turbine using a partially observed markov decision process. *IEEE Transactions on Power Systems* **25**(4) 1823–1834.

Bünger, U., J. Michalski, F. Crotogino, O. Kruck. 2016. 7 - large-scale underground storage of hydrogen for the grid integration of renewable energy and other

applications. Michael Ball, Angelo Basile, T. Nejat Veziroğlu, eds., *Compendium of Hydrogen Energy*. Woodhead Publishing Series in Energy, Woodhead Publishing, Oxford, 133–163.

Campbell, Ann Melissa, Martin W. P. Savelsbergh. 2004. A decomposition approach for the inventory-routing problem. *Transportation Science* **38**(4) 488–502.

Castaneda, Manuel, Antonio Cano, Francisco Jurado, Higinio Sánchez, Luis M Fernandez. 2013. Sizing optimization, dynamic modeling and energy management strategies of a stand-alone PV/hydrogen/battery-based hybrid system. *International Journal of Hydrogen Energy* **38**(10) 3830–3845.

Chauhan, Anurag, R.P. Saini. 2016. Techno-economic feasibility study on integrated renew energy system for an isolated community of india. *Renewable and Sustainable Energy Reviews* **59** 388–405.

Chien, T. William, Anantaram Balakrishnan, Richard T. Wong. 1989. An integrated inventory allocation and vehicle routing problem. *Transportation Science* **23**(2) 67–76.

Chitsaz, Masoud, Jean-François Cordeau, Raf Jans. 2019. A unified decomposition matheuristic for assembly, production, and inventory routing. *INFORMS Journal on Computing* **31**(1) 134–152.

Chitsaz, Masoud, Ali Divsalar, Pieter Vansteenwegen. 2016. A two-phase algorithm for the cyclic inventory routing problem. *European Journal of Operational Research* **254**(2) 410 – 426.

Christiansen, Marielle. 1999. Decomposition of a combined inventory and time constrained ship routing problem. *Transportation Science* **33**(1) 3–16.

Coelho, Leandro C., Jean-François Cordeau, Gilbert Laporte. 2014. Thirty years of inventory routing. *Transportation Science* **48**(1) 1–19.

Cretì, Anna, Fulvio Fontini. 2019. *Economics of Electricity: Markets, Competition and Rules*. Cambridge University Press.

Cretì, Anna, Fulvio Fontini. 2019. *Economics of Electricity: Markets, Competition and Rules*. Cambridge University Press.

Cullinane, Kevin, Rickard Bergqvist. 2014. Emission control areas and their impact on maritime transport.

Del Rosso, A. D., S. W. Eckroad. 2014. Energy storage for relief of transmission congestion. *IEEE Transactions on Smart Grid* **5**(2) 1138–1146.

Deloitte. 2015. Canadian domestic forecast, base case forecast effective september 30 2015. URL https://www2.deloitte.com/content/dam/Deloitte/ca/Documents/REA/ca-en-rea-data-summary-price-forecast-september-2015.pdf.

Denholm, Paul, Maureen Hand. 2011. Grid flexibility and storage required to achieve very high penetration of variable renewable electricity. *Energy Policy* **39**(3) 1817 – 1830.

Densing, M. 2013. Dispatch planning using newsvendor dual problems and occupation times: Application to hydropower. *European Journal of Operational Research* **228**(2) 321 – 330.

Diz, Gustavo Souto Dos Santos, Fabrício Oliveira, Silvio Hamacher. 2017. Improving maritime inventory routing: application to a brazilian petroleum case. *Maritime Policy & Management* **44**(1) 42–61.

D'Souza, A., K. Bouw, H. Velthuijsen, G.B. Huitema, J.C. Wortmann. 2018. Designing viable multi-commodity energy business ecosystems: Corroborating the business model design framework for viability. *Journal of Cleaner Production* **182** 124–138.

Dufo-López, Rodolfo. 2015. Optimisation of size and control of grid-connected storage under real time electricity pricing conditions. *Applied Energy* **140** 395–408.

Easwaran, Gopalakrishnan, Halit Üster. 2009. Tabu search and benders decomposition approaches for a capacitated closed-loop supply chain network design problem. *Transportation Science* **43**(3) 301–320.

Eckner, Andreas. 2012. A framework for the analysis of unevenly spaced time series data. *Preprint* .

Ehrenmann, Andreas, Yves Smeers. 2005. Inefficiencies in european congestion management proposals. *Utilities policy* **13**(2) 135–152.

Ekici, Ali, Okan Örsan Özener, Gültekin Kuyzu. 2015. Cyclic delivery schedules for an inventory routing problem. *Transportation Science* **49**(4) 817–829.

Eltamaly, Ali M., Mohamed A. Mohamed, Abdulrahman I. Alolah. 2016. A novel smart grid theory for optimal sizing of hybrid renewable energy systems. *Solar Energy* **124** 26–38.

ENTSO-E. 2021. Sector-coupled open optimisation model of the european energy system. URL https://pypsa-eur-sec.readthedocs.io/en/latest/.

ENTSOE. 2019. Transparency platform. URL https://transparency.entsoe.eu/transmission-domain/r2/dayAheadPrices/show.

Ettoumi, F. Youcef, A. Mefti, A. Adane, M.Y. Bouroubi. 2002. Statistical analysis of solar measurements in Algeria using beta distributions. *Renewable Energy* **26**(1) 47 – 67.

Eurostat. 2020. Renewable energy statistics. URL https://ec.europa.eu/eurostat/statistics-explained/index.php/Renewable_energy_statistics.

Federgruen, Awi, Paul Zipkin. 1984. A combined vehicle routing and inventory allocation problem. *Operations Research* **32**(5) 1019–1037.

Feng Ding, J. D. Fuller. 2005. Nodal, uniform, or zonal pricing: distribution of economic surplus. *IEEE Transactions on Power Systems* **20**(2) 875–882.

Fertig, Emily, Jay Apt. 2011. Economics of compressed air energy storage to integrate wind power: A case study in ERCOT. *Energy Policy* **39**(5) 2330 – 2342.

Flaticon. 2020. Icons made by Freepik and itim2101 from www.flaticon.com. URL www.flaticon.com.

Fokkema, Jan Eise, Michiel AJ Broek, Albert H Schrotenboer, Martin J Land, Nicky D Van Foreest. 2020a. Seasonal hydrogen storage decisions under constrained electricity distribution capacity. *arXiv preprint arXiv:2007.08230* .

Fokkema, Jan Eise, Paul Buijs, Iris F.A. Vis. 2017. An investment appraisal method to compare lng-fueled and conventional vessels. *Transportation Research Part D: Transport and Environment* **56** 229–240.

Fokkema, Jan Eise, Martin J. Land, Leandro C. Coelho, Hans Wortmann, George B. Huitema. 2020b. A continuous-time supply-driven inventory-constrained routing problem. *Omega* **92** 102151.

Gallego, Guillermo, David Simchi-Levi. 1990. On the effectiveness of direct shipping strategy for the one-warehouse multi-retailer r-systems. *Management Science* **36**(2) 240–243.

Ghosh, Sugoutam, Loo Hay Lee, Szu Hui Ng. 2015. Bunkering decisions for a shipping liner in an uncertain environment with service contract. *European Journal of Operational Research* **244**(3) 792–802.

Golden, C., A. Assad, R. Dahl. 1984. Analysis of a large scale vehicle routing problem with an inventory component. *Large Scale Systems in Information and Decision Technologies* **7**(2-3) 181–190.

Gönsch, Jochen, Michael Hassler. 2016. Sell or store? An ADP approach to marketing renewable energy. *OR spectrum* **38**(3) 633–660.

Grillo, Samuele, Antonio Pievatolo, Enrico Tironi. 2015. Optimal storage scheduling using Markov decision processes. *IEEE Transactions on Sustainable Energy* **7**(2) 755–764.

Guimarães, Thiago A., Leandro C. Coelho, Cleder M. Schenekemberg, Cassius T. Scarpin. 2019. The two-echelon multi-depot inventory-routing problem. *Computers & Operations Research* **101** 220 – 233.

Haas, J., F. Cebulla, K. Cao, W. Nowak, R. Palma-Behnke, C. Rahmann, P. Mancarella. 2017. Challenges and trends of energy storage expansion planning for flexibility provision in low-carbon power systems – a review. *Renewable and Sustainable Energy Reviews* **80** 603 – 619.

Hahn, Henning, Bernd Krautkremer, Kilian Hartmann, Michael Wachendorf. 2014. Review of concepts for a demand-driven biogas supply for flexible power generation. *Renewable and Sustainable Energy Reviews* **29** 383–393.

Hannah, Lauren, David B. Dunson. 2011. Approximate dynamic programming for storage problems. *ICML*. 337–344.

Hassler, Michael. 2017. Heuristic decision rules for short-term trading of renewable energy with co-located energy storage. *Computers & Operations Research* **83** 199 – 213.

Hein, Fanny, Christian Almeder. 2016. Quantitative insights into the integrated supply vehicle routing and production planning problem. *International Journal of Production Economics* **177** 66 – 76.

Hemmati, Reza, Hedayat Saboori, Mehdi Ahmadi Jirdehi. 2017a. Stochastic planning and scheduling of energy storage systems for congestion management in electric power systems including renewable energy resources. *Energy* **133** 380 – 387.

Hemmati, Reza, Hedayat Saboori, Pierluigi Siano. 2017b. Coordinated short-term scheduling and long-term expansion planning in microgrids incorporating renewable energy resources and energy storage systems. *Energy* **134** 699 – 708.

Heydari, Ali, Alireza Askarzadeh. 2016. Optimization of a biomass-based photovoltaic power plant for an off-grid application subject to loss of power supply probability concept. *Applied Energy* **165** 601–611.

Ho, W.S., H. Hashim, J.S. Lim. 2014. Integrated biomass and solar town concept for a smart eco-village in Iskandar Malaysia (IM). *Renew Energy* **69** 190–201.

Hoang, Dieu Linh, Chris Davis, Henri C. Moll, Sanderine Nonhebel. 2019. Impacts of biogas production on nitrogen flows on dutch dairy system: Multiple level assessment of nitrogen indicators within the biogas production chain. *Journal of Industrial Ecology* **24**(3) 665–680.

Holmgren, Johan, Zoi Nikopoulou, Linda Ramstedt, Johan Woxenius. 2014. Modelling modal choice effects of regulation on low-sulphur marine fuels in northern europe. *Transportation Research Part D: Transport and Environment* **28** 62–73.

Hurtado, Elías, Elisa Peñalvo-López, Ángel Pérez-Navarro, Carlos Vargas, David Alfonso. 2015. Optimization of a hybrid renewable system for high feasibility application in non-connected zones. *Applied Energy* **155** 308–314.

HyUnder. 2014. Hydrogen storage sizes. URL `https://www.sciencedirect.com/topics/engineering/large-scale-hydrogen-storage`.

Iassinovskaia, Galina, Sabine Limbourg, Fouad Riane. 2017. The inventory-routing problem of returnable transport items with time windows and simultaneous pickup and delivery in closed-loop supply chains. *International Journal of Production Economics* **183** 570 – 582.

IMO. 2019. Cutting sulphur oxide emissions. URL `https://www.imo.org/en/MediaCentre/HotTopics/Pages/Sulphur-2020.aspx`.

IRENA. 2019. Hydrogen: A rrenewable energy perspective. URL `https://www.irena.org/-/media/Files/IRENA/Agency/Publication/2019/Sep/IRENA_Hydrogen_2019.pdf`.

Iverson, Zachariah, Ajit Achuthan, Pier Marzocca, Daryush Aidun. 2013. Optimal design of hybrid renewable energy systems (HRES) using hydrogen storage technology for data center applications. *Renew Energy* **52** 79–87.

Jafarian, Matin, Jacquelien M.A. Scherpen, Kees Loeff, Machiel Mulder, Marco Aiello. 2020. A combined nodal and uniform pricing mechanism for congestion management in distribution power networks. *Electric Power Systems Research* **180** 106088.

Jiang, Daniel R, Warren B Powell. 2015a. An approximate dynamic programming algorithm for monotone value functions. *Operations Research* **63**(6) 1489–1511.

Jiang, Daniel R., Warren B. Powell. 2015b. Optimal hour-ahead bidding in the real-time electricity market with battery storage using approximate dynamic programming. *INFORMS Journal on Computing* **27**(3) 525–543.

Jiang, Liping, Jacob Kronbak, Leise Pil Christensen. 2014. The costs and benefits of sulphur reduction measures: Sulphur scrubbers versus marine gas oil. *Transportation Research Part D: Transport and Environment* **28** 19–27.

Johansson, Ola M. 2006. The effect of dynamic scheduling and routing in a solid waste management system. *Waste Management* **26**(8) 875–885.

Jorgenson, Jennie, Paul Denholm, Trieu Mai. 2018a. Analyzing storage for wind integration in a transmission-constrained power system. *Applied Energy* **228** 122 – 129.

Jorgenson, Jennie, Paul Denholm, Trieu Mai. 2018b. Analyzing storage for wind integration in a transmission-constrained power system. *Applied Energy* **228** 122–129.

Kaabeche, A., M. Belhamel, R. Ibtiouen. 2011. Sizing optimization of grid-independent hybrid photovoltaic/wind power generation system. *Energy* **36**(2) 1214–1222.

Kaabeche, Abdelhamid, Rachid Ibtiouen. 2014. Techno-economic optimization of hybrid photovoltaic/wind/diesel/battery generation in a stand-alone power system. *Solar Energy* **103** 171–182.

Kaviani, A. Kashefi, G.H. Riahy, SH.M. Kouhsari. 2009. Optimal design of a reliable hydrogen-based stand-alone wind/PV generating system, considering component outages. *Renew Energy* **34**(11) 2380–2390.

Keerthisinghe, C., A. C. Chapman, G. Verbič. 2019. PV and demand models for a Markov Decision Process formulation of the home energy management problem. *IEEE Transactions on Industrial Electronics* **66**(2) 1424–1433.

Khare, Vikas, Savita Nema, Prashant Baredar. 2016. Solar–wind hybrid renewable energy system: A review. *Renewable and Sustainable Energy Reviews* **58** 23–33.

Kim, Minsoo, Jiyong Kim. 2017. An integrated decision support model for design and operation of a wind-based hydrogen supply system. *International Journal of Hydrogen Energy* **42**(7) 3899–3915.

Koponen, Joonas, Antti Kosonen, Vesa Ruuskanen, Kimmo Huoman, Markku Niemelä, Jero Ahola. 2017. Control and energy efficiency of PEM water electrolyzers in renewable energy systems. *International Journal of Hydrogen Energy* **42**(50) 29648–29660.

Korpås, Magnus, Christopher J. Greiner. 2008. Opportunities for hydrogen production in connection with wind power in weak grids. *Renewable Energy* **33**(6) 1199 – 1208.

Koudouris, Giannis, Panayiotis Dimitriadis, Theano Iliopoulou, Nikos Mamassis, Demetris Koutsoyiannis. 2017. Investigation on the stochastic nature of the solar radiation process. *Energy Procedia* **125** 398 – 404.

Kumar, Ashwani, S.C. Srivastava, S.N. Singh. 2005. Congestion management in competitive power market: A bibliographical survey. *Electric Power Systems Research* **76**(1) 153 – 164.

Lahyani, Rahma, Leandro C Coelho, Mahdi Khemakhem, Gilbert Laporte, Frédéric Semet. 2015. A multi-compartment vehicle routing problem arising in the collection of olive oil in Tunisia. *Omega* **51** 1–10.

Lamy, Claude. 2016. From hydrogen production by water electrolysis to its utilization in a pem fuel cell or in a so fuel cell: Some considerations on the energy efficiencies. *International Journal of Hydrogen Energy* **41**(34) 15415 – 15425.

Larrain, Homero, Leandro C Coelho, Alejandro Cataldo. 2017. A variable mip neighborhood descent algorithm for managing inventory and distribution of cash in automated teller machines. *Computers & Operations Research* **85** 22–31.

Lauer, Markus, Jason K. Hansen, Patrick Lamers, Daniela Thrän. 2018. Making money from waste: The economic viability of producing biogas and biomethane in the idaho dairy industry. *Applied Energy* **222** 621–636.

Law, Averill M, W David Kelton, W David Kelton. 2000. *Simulation modeling and analysis*, vol. 3. McGraw-Hill New York.

Lee, Jui-Yuan, Kathleen B. Aviso, Raymond R. Tan. 2018. Optimal sizing and design of hybrid power systems. *ACS Sustainable Chem Eng* **6**(2) 2482–2490.

Li, Danny H.W., Liu Yang, Joseph C Lam. 2013a. Zero energy buildings and sustainable development implications – a review. *Energy* **54** 1–10.

Li, Kunpeng, Bin Chen, Appa Iyer Sivakumar, Yong Wu. 2014. An inventory–routing problem with the objective of travel time minimization. *European Journal of Operational Research* **236**(3) 936 – 945.

Li, Yanhui, Hao Guo, Lin Wang, Jing Fu. 2013b. A hybrid genetic-simulated annealing algorithm for the location-inventory-routing problem considering returns under e-supply chain environment. *The Scientific World Journal* **2013**(125893) 1–10.

Li, Zhenhao, Chun Sing Lai, Xu Xu, Zhuoli Zhao, Loi Lei Lai. 2021. Electricity trading based on distribution locational marginal price. *International Journal of Electrical Power & Energy Systems* **124** 106322.

Liu, Bailing, Hui Chen, Yanhui Li, Xiang Liu. 2015. A pseudo-parallel genetic algorithm integrating simulated annealing for stochastic location-inventory-routing problem with consideration of returns in e-commerce. *Discrete Dynamics in Nature and Society* **2015**(586581) 1–15.

Liu, Shu-Chu, Chich-Hung Chung. 2009. A heuristic method for the vehicle routing problem with backhauls and inventory. *Journal of Intelligent Manufacturing* **20**(1) 29–42.

Lund, Peter D, Juuso Lindgren, Jani Mikkola, Jyri Salpakari. 2015. Review of energy system flexibility measures to enable high levels of variable renewable electricity. *Renewable and sustainable energy reviews* **45** 785–807.

Malheiro, André, Pedro M. Castro, Ricardo M. Lima, Ana Estanqueiro. 2015. Integrated sizing and scheduling of wind/PV/diesel/battery isolated systems. *Renewable Energy* **83** 646–657.

Mancarella, Pierluigi. 2014. Mes (multi-energy systems): An overview of concepts and evaluation models. *Energy* **65** 1–17.

Mazzeo, Domenico, Giuseppe Oliveti, Cristina Baglivo, Paolo M. Congedo. 2018. Energy reliability-constrained method for the multi-objective optimization of a photovoltaic-wind hybrid system with battery storage. *Energy* **156** 688–708.

Mes, Rivera, Schutten. 2014. Inventory routing for dynamic waste collection. *Waste Management* **34**(9) 1564 – 1576.

Märkle-Huß, Joscha, Stefan Feuerriegel, Dirk Neumann. 2020. Cost minimization of large-scale infrastructure for electricity generation and transmission. *Omega* **96** 102071.

NEDU. 2020. User profiles - NEDU. URL `https://www.nedu.nl/documenten/verbruiksprofielen/`.

Nibud. 2019. Energy and water, national institute for budget education. URL `https://www.nibud.nl/consumenten/energie-en-water/`.

Ogunjuyigbe, A.S.O., T.R. Ayodele, O.A. Akinola. 2016. Optimal allocation and sizing of PV/wind/split-diesel/battery hybrid energy system for minimizing life cycle cost, carbon emission and dump energy of remote residential building. *Applied Energy* **171** 153–171.

Papaefthymiou, G., Ken Dragoon. 2016. Towards 100% renewable energy systems: Uncapping power system flexibility. *Energy Policy* **92** 69 – 82.

Papavasiliou, A. 2018. Analysis of distribution locational marginal prices. *IEEE Transactions on Smart Grid* **9**(5) 4872–4882.

Pelzer, D., D. Ciechanowicz, A. Knoll. 2016. Energy arbitrage through smart scheduling of battery energy storage considering battery degradation and electricity price forecasts. *2016 IEEE Innovative Smart Grid Technologies - Asia (ISGT-Asia)*. 472–477.

Persson, Jan A., Maud Göthe-Lundgren. 2005. Shipment planning at oil refineries using column generation and valid inequalities. *European Journal of Operational Research* **163**(3) 631 – 652.

Pierie, F., C.E.J. van Someren, R.M.J. Benders, J. Bekkering, W.J.Th. van Gemert, H.C. Moll. 2015. Environmental and energy system analysis of bio-methane production pathways: A comparison between feedstocks and process optimizations. *Applied Energy* **160** 456–466.

Plum, Christian Edinger Munk, Peter Neergaard Jensen, David Pisinger. 2014. Bunker purchasing with contracts. *Maritime Economics & Logistics* **16**(4) 418–435.

Post, Roel M, Paul Buijs, Michiel AJ uit het Broek, Jose A Lopez Alvarez, Nick B Szirbik, Iris FA Vis. 2018. A solution approach for deriving alternative fuel station infrastructure requirements. *Flexible Services and Manufacturing Journal* **30**(3) 592–607.

Puterman, Martin L. 2014. *Markov decision processes: discrete stochastic dynamic programming*. John Wiley & Sons.

PVGIS. 2016. JRC photovoltaic geographical information system (PVGIS) - European Commission. URL `https://re.jrc.ec.europa.eu/pvg_tools/en/tools.html#MR`.

Raa, Birger. 2015. Fleet optimization for cyclic inventory routing problems. *International Journal of Production Economics* **160** 172–181.

Raa, Birger, El-Houssaine Aghezzaf. 2008. Designing distribution patterns for long-term inventory routing with constant demand rates. *International Journal of Production Economics* **112**(1) 255–263.

Raa, Birger, El-Houssaine Aghezzaf. 2009. A practical solution approach for the cyclic inventory routing problem. *European Journal of Operational Research* **192**(2) 429–441.

Raa, Birger, Wout Dullaert. 2017. Route and fleet design for cyclic inventory routing. *European Journal of Operational Research* **256**(2) 404–411.

Rahimi, Mohammad, Armand Baboli, Yacine Rekik. 2017. Multi-objective inventory routing problem: A stochastic model to consider profit, service level and green criteria. *Transportation Research Part E: Logistics and Transportation Review* **101** 59 – 83.

Ren, Hongbo, Qiong Wu, Weijun Gao, Weisheng Zhou. 2016. Optimal operation of a grid-connected hybrid PV/fuel cell/battery energy system for residential applications. *Energy* **113** 702–712.

Reuß, M., T. Grube, M. Robinius, P. Preuster, P. Wasserscheid, D. Stolten. 2017. Seasonal storage and alternative carriers: A flexible hydrogen supply chain model. *Applied Energy* **200** 290–302.

Robinson, Stewart. 2014. *Simulation: the practice of model development and use*. Palgrave Macmillan.

Rodrigues, E.M.G., G.J. Osório, R. Godina, A.W. Bizuayehu, J.M. Lujano-Rojas, J.C.O. Matias, J.P.S. Catalão. 2015. Modelling and sizing of NaS (sodium sulfur) battery energy storage system for extending wind power performance in Crete Island. *Energy* **90** 1606–1617.

Saboori, Hedayat, Reza Hemmati, Seyyed Mohammad Sadegh Ghiasi, Shahab Dehghan. 2017. Energy storage planning in electric power distribution networks – a state-of-the-art review. *Renewable and Sustainable Energy Reviews* **79** 1108 – 1121.

Samsatli, Sheila, Iain Staffell, Nouri J. Samsatli. 2016. Optimal design and operation of integrated wind–hydrogen–electricity networks for decarbonising the domestic transport sector in Great Britain. *International Journal of Hydrogen Energy* **41**(1) 447–475.

Savelsbergh, Martin, Jin-Hwa Song. 2008. An optimization algorithm for the inventory routing problem with continuous moves. *Computers & Operations Research* **35**(7) 2266–2282.

Schill, Wolf-Peter, Alexander Zerrahn. 2018. Long-run power storage requirements for high shares of renewables: Results and sensitivities. *Renewable and Sustainable Energy Reviews* **83** 156 – 171.

Shin, Joohyun, Jay H Lee, Matthew J Realff. 2017. Operational planning and optimal sizing of microgrid considering multi-scale wind uncertainty. *Applied Energy* **195** 616–633.

Shyshou, Aliaksandr, Irina Gribkovskaia, Gilbert Laporte, Kjetil Fagerholt. 2012. A large neighbourhood search heuristic for a periodic supply vessel planning problem arising in offshore oil and gas operations. *INFOR: Information Systems and Operational Research* **50**(4) 195–204.

Sindhuchao, Sombat, H Edwin Romeijn, Elif Akçali, Rein Boondiskulchok. 2005. An integrated inventory-routing system for multi-item joint replenishment with limited vehicle capacity. *Journal of Global Optimization* **32**(1) 93–118.

Soares, Inês, Maria João Alves, Carlos Henggeler Antunes. 2020. Designing time-of-use tariffs in electricity retail markets using a bi-level model – estimating bounds when the lower level problem cannot be exactly solved. *Omega* **93**.

Soini, Martin Christoph, David Parra, Martin Kumar Patel. 2020. Does bulk electricity storage assist wind and solar in replacing dispatchable power production? *Energy Economics* **85** 104495.

Solyalı, Oğuz, Haldun Süral. 2011. A branch-and-cut algorithm using a strong formulation and an a priori tour-based heuristic for an inventory-routing problem. *Transportation Science* **45**(3) 335–345.

Solyalı, Oğuz, Haldun Süral. 2008. A single supplier–single retailer system with an order-up-to level inventory policy. *Operations Research Letters* **36**(5) 543 – 546.

Soubdhan, Ted, Richard Emilion, Rudy Calif. 2009. Classification of daily solar radiation distributions using a mixture of dirichlet distributions. *Solar Energy* **83**(7) 1056–1063.

Soysal, Mehmet. 2016. Closed-loop inventory routing problem for returnable transport items. *Transportation Research Part D: Transport and Environment* **48** 31 – 45.

Speranza, Maria Grazia, Walter Ukovich. 1994. Minimizing transportation and inventory costs for several products on a single link. *Operations Research* **42**(5) 879–894.

Srivastava, Samir K. 2008. Network design for reverse logistics. *Omega* **36**(4) 535 – 548.

Stanzani, Amélia de Lorena, Vitória Pureza, Reinaldo Morabito, Bruno Jensen Virginio da Silva, Denise Yamashita, Paulo César Ribas. 2018. Optimizing multiship routing and scheduling with constraints on inventory levels in a brazilian oil company. *International Transactions in Operational Research* **25**(4) 1163–1198.

Steffen, Bjarne, Christoph Weber. 2016. Optimal operation of pumped-hydro storage plants with continuous time-varying power prices. *European Journal of Operational Research* **252**(1) 308 – 321.

SUSCON. 2005. Sustainable energy conservation. URL `http://www.suscon.org/pdfs/news/biomethane_report/Full_Report.pdf`.

Telaretti, Enrico, Mariano Ippolito, Luigi Dusonchet. 2016. A simple operating strategy of small-scale battery energy storages for energy arbitrage under dynamic pricing tariffs. *Energies* **9**(1).

Upadhyay, Subho, MP Sharma. 2015. Development of hybrid energy system with cycle charging strategy using particle swarm optimization for a remote area in India. *Renewable Energy* **77** 586–598.

U.S. Department of Energy. 2005. Liquefied natural gas, understanding the basic facts. URL `https://energy.gov/sites/prod/files/2013/04/f0/LNG_primerupd.pdf`.

van der Burg, Robbert-Jan H, George B Huitema, Hans Wortmann. 2015. Developing flexibility services in hybrid energy systems. *Proceedings of the 22nd EurOMA conference*. 1–8.

Vansteenwegen, Pieter, Manuel Mateo. 2014. An iterated local search algorithm for the single-vehicle cyclic inventory routing problem. *European Journal of Operational Research* **237**(3) 802 – 813.

Vargas, Luis S, Gonzalo Bustos-Turu, Felipe Larraín. 2014. Wind power curtailment and energy storage in transmission congestion management considering power plants ramp rates. *IEEE Transactions on Power Systems* **30**(5) 2498–2506.

Vidović, Milorad, Dražen Popović, Branislava Ratković. 2014. Mixed integer and heuristics model for the inventory routing problem in fuel delivery. *International Journal of Production Economics* **147** 593 – 604.

Viswanathan, S., Kamlesh Mathur. 1997. Integrating routing and inventory decisions in one-warehouse multiretailer multiproduct distribution systems. *Management Science* **43**(3) 294–312.

Wang, Siyuan, Theo Notteboom. 2014. The adoption of liquefied natural gas as a ship fuel: A systematic review of perspectives and challenges. *Transport Reviews* **34**(6) 749–774.

Wang, Tian, Shiming Deng. 2019. Multi-period energy procurement policies for smart-grid communities with deferrable demand and supplementary uncertain power supplies. *Omega* **89** 212 – 226.

Wang, Yishen, Yury Dvorkin, Ricardo Fernández-Blanco, Bolun Xu, Daniel S Kirschen. 2017. Impact of local transmission congestion on energy storage arbitrage opportunities. *2017 IEEE Power & Energy Society General Meeting*. IEEE, 1–5.

Weibelzahl, Martin. 2017. Nodal, zonal, or uniform electricity pricing: how to deal with network congestion. *Frontiers in Energy* **11**(2) 210–232.

Weitemeyer, Stefan, David Kleinhans, Thomas Vogt, Carsten Agert. 2015. Integration of renew energy sources in future power systems: The role of storage. *Renew Energy* **75** 14–20.

Weitzel, Timm, Christoph H. Glock. 2018. Energy management for stationary electric energy storage systems: A systematic literature review. *European Journal of Operational Research* **264**(2) 582 – 606.

Wild Ingenieurbüro. 2005. Determination of energy cost of electrical energy on board sea-going vessels. URL `http://www.effship.com/PartnerArea/MiscPresentations/Dr_Wild_Report.pdf`.

Won, Wangyun, Hweeung Kwon, Jee-Hoon Han, Jiyong Kim. 2017. Design and operation of renewable energy sources based hydrogen supply system: Technology integration and optimization. *Renew Energy* **103** 226–238.

Woo, Chi-Keung, Ira Horowitz, Arne Olson, Brian Horii, Carmen Baskette. 2006. Efficient frontiers for electricity procurement by an LDC with multiple purchase options. *Omega* **34**(1) 70 – 80.

Yamashita, Denise, Bruno Jensen Virginio da Silva, Reinaldo Morabito, Paulo César Ribas. 2019. A multi-start heuristic for the ship routing and scheduling of an oil company. *Computers & Industrial Engineering* **136** 464 – 476.

Yang, Yuqing, Stephen Bremner, Chris Menictas, Merlinde Kay. 2018. Battery energy storage system size determination in renewable energy systems: A review. *Renewable and Sustainable Energy Reviews* **91** 109–125.

Yuan, Z., M. R. Hesamzadeh, D. R. Biggar. 2018. Distribution locational marginal pricing by convexified acopf and hierarchical dispatch. *IEEE Transactions on Smart Grid* **9**(4) 3133–3142.

Zakaria, A., Firas B. Ismail, M.S. Hossain Lipu, M.A. Hannan. 2020. Uncertainty models for stochastic optimization in renewable energy applications. *Renewable Energy* **145** 1543 – 1571.

Zhang, Yang, Pietro Elia Campana, Anders Lundblad, Jinyue Yan. 2017. Comparative study of hydrogen storage and battery storage in grid connected photovoltaic system: Storage sizing and rule-based operation. *Applied Energy* **201** 397–411.

Zhao, Bo, Xuesong Zhang, Peng Li, Ke Wang, Meidong Xue, Caisheng Wang. 2014. Optimal sizing, operating strategy and operational experience of a stand-alone microgrid on Dongfushan Island. *Applied Energy* **113** 1656–1666.

Zhao, Qiu-Hong, Shuang Chen, Cun-Xun Zang. 2008. Model and algorithm for inventory/routing decision in a three-echelon logistics system. *European Journal of Operational Research* **191**(3) 623–635.

Zhou, Yangfang (Helen), Alan Scheller-Wolf, Nicola Secomandi, Stephen Smith. 2019. Managing wind-based electricity generation in the presence of storage and transmission capacity. *Production and Operations Management* **28**(4) 970–989.

Ángel A. Bayod-Rújula, Marta E. Haro-Larrodé, Amaya Martínez-Gracia. 2013. Sizing criteria of hybrid photovoltaic–wind systems with battery storage and self-consumption considering interaction with the grid. *Solar Energy* **98** 582–591.

Đukić, Ankica, Mihajlo Firak. 2011. Hydrogen production using alkaline electrolyzer and photovoltaic (pv) module. *International Journal of Hydrogen Energy* **36**(13) 7799 – 7806.

Summary

Supply chain and operations management decisions are important in the transition from fossil-based energy sources to renewable energy. This thesis addresses decision-making problems related to balancing and organizing the storage and distribution of biogas, hydrogen, and electricity from solar energy, and wind energy for energy producers. The decisions aim at balancing and operating storage, production, and transportation in rural areas to avoid excess production or storage capacity, electricity grid congestion, and curtailment. They also aim to provide a stable supply of renewable energy to rural communities. Moreover, this thesis addresses the use of LNG in the transportation sector, by showing under which conditions LNG-fueled ships are more economically viable than conventional ships. The need for a more sustainable energy system and the shift to renewable energy and less polluting fuels causes logistics problems related to the renewable energy supply. In particular, the transition towards more renewables creates problems related to supply-driven energy generation, location differences between energy production and energy demand, and the mismatch in production and demand profiles over time. This leads to curtailment of energy, irregular feed-in to the electricity grid, and transportation challenges related to the distribution of biogas.

From both a logistics and societal standpoint, it is sensible that the production-related logistics problems should be addressed based on a decentralized approach, in which energy that is produced locally is consumed locally as much as possible. This enables avoiding transmission losses, excessive feed-in to the electricity grid, curtailment, and transportation. From a societal perspective, a decentralized approach also addresses the desires of local communities that reside close to renewable energy production facilities who do not want to live near energy facilities when the produced energy is consumed elsewhere.

While production and consumption can both occur locally, a decentralized approach still requires efficient transportation systems to connect the supply to the demand elsewhere. This is needed, because (partly) self-sufficient systems with fewer actors create fewer possibilities for flexibility. Additionally, (peak) energy production of wind, solar, and biogas needs sufficient distribution infrastructure in the form of an electricity or pipeline grid. This makes the organization of logistics imperative.

In the transition period, transportation of gasses by trucks and ships may be expected. This requires the transportation industry to also adapt to the transition towards cleaner fuels, by making more use of less polluting fuels such as hydrogen, LNG, and biogas. In particular, ships are increasingly adopting alternative fuels to reduce emissions. However, the adoption of new fuels creates decision problems for ship-owners related to the investment in ships and infrastructure.

In the transition to cleaner fuels, storage plays an important role in which it can act as a temporary buffer for the transportation of hydrogen, LNG, or biogas. Storage is also important for the bridging of seasonal and short-term differences between supply and demand in electricity, and to avoid curtailment and electricity grid congestion. Short-term storage can be realized in the form of batteries that can mitigate intra-day fluctuations in production and consumption. Seasonal storage of electricity requires storage in a converted form such as hydrogen or methane.

This thesis is based on the project entitled "ADAPNER" (Adaptive logistics in a circular economy) which aims to "Determine optimized adaptable and sustainable configurations for different distribution alternatives regarding biomass and biogas in a circular economy". The objective of this thesis is to determine these configurations for different decentralized renewable energy production, storage, and distribution alternatives. These include wind, photovoltaic (PV), biogas, LNG, and hydrogen. Our main research question is: *How should the decentralized storage and distribution of biogas, solar energy, and wind energy be organized and adapted to enable effective embedding in existing grid infrastructure?*

In five different chapters, we have contributed with the above research question to three domains that include 1) Transportation logistics, 2) Seasonal matching of supply and demand, and 3) Operation of storage facilities. Each chapter contributes to different aspects of these domains.

Chapter 2 and 3 focus on the domain "Transportation logistics". In Chapter

2, we have addressed the research question: *How should biogas be distributed using trucks with tube trailers from digesters to centralized upgrading facilities?* Accordingly, we have addressed the routing and inventory decisions of vehicles that transport biogas in cylinders from decentralized farms to centralized upgrading facilities that inject the gas into the pipeline grid. We have provided a mathematical formulation and introduced valid inequalities that have been effective in reducing computation times with 93% on average. We found that the transportation time is minimized when vehicles make single uncombined tours in visiting the farms and when the storage capacity in the number of cylinders at each farm exceeds the vehicle capacity. We also found that there are no benefits related to collecting cylinders that are partially filled.

In Chapter 3, we addressed the research question: *Under which conditions are the application of LNG economically viable for LNG-fueled ships compared to conventional ships?* We developed an investment appraisal model and compared the total exploitation costs of LNG-fueled ships with conventional ships. We found that fuel costs of LNG-fueled ships are often lower than conventional ships, even for unfavorable LNG prices relative to other marine fuels. The cost-effectiveness of LNG-fueled ships is strengthened for larger ships that have higher overall fuel consumption levels and ships that have a high presence in ECA (Emission Controlled Areas). This also indicates that using biogas as bio-LNG can potentially be economically viable as a fuel in shipping.

In Chapter 4, we focus on balancing local supply and local demand of electricity in a rural environment across seasons. We addressed the research question: *How should biogas, wind, and solar energy be combined and how is this affected by the level of total production capacity and storage capacity?* The main goal is to realize the lowest production and storage requirements when supplying self-sufficient households with electricity produced locally. We investigated the shares of electricity production from wind, solar, and biogas for different combinations of storage and production capacity. We found that for relatively low production levels, biogas can supply both peaks and base-load, leading to relatively high storage requirements in which mostly electricity based on biogas is stored. For higher levels of total production, the optimal share of wind production increases, because some excess production allows for curtailment of unfortunately-timed wind peaks, which allows substantial reductions to be made in storage requirements. When the total production capacity exceeds

130% of the total demand, however, the optimal share of wind approaches zero, in which curtailment of electricity from biogas enables very low storage requirements.

In Chapter 5, we addressed the research question: *Under which conditions should the owner of solar fields with hydrogen buy and sell from and to the grid to maximize profits?* We considered the problem of a solar park owner with facilities for hydrogen production and storage that supplies electricity to a set of connected households and the electricity grid. Using a Markov Decision Process, we determined the optimal daily buying and selling decision of the facility owner to maximize the expected profits. We explicitly take into account seasonality differences in supply and demand and the uncertainty associated with electricity prices, electricity consumption, and solar energy production. We found that optimal policies are characterized by price thresholds that separate different types of actions. These include buying the maximum possible quantity from the grid, selling exact overages or buying exact shortages, storing overages or obtaining shortages from storage, or selling the maximum amount possible to the grid. We also show that ignoring seasonal demand and production patterns is suboptimal and that introducing hydrogen storage transforms loss-making interactions with the grid into profitable ones. We found that the distribution capacity should not be too small to prevent local grid congestion. In contrast to what may be expected, a higher storage capacity increases the number of buying actions from the grid, thereby causing more local congestion at the grid connection, which is problematic for the grid operator. Accordingly, profit-maximizing hydrogen storage operation alone is not an alternative to grid expansion to solve congestion, which is essential knowledge for policy-makers and grid operators.

In Chapter 6, we have addressed the research question: *How should solar fields with hydrogen storage be operated to alleviate congestion?* We compare profit-oriented storage operation strategies with the strategy that always prioritizes storage to cover net overages or shortages. Profit-maximization by the storage owner creates an unstable feed-in to the grid, which may lead to potential congestion problems elsewhere in the grid. In contrast, the operation of storage by prioritizing the use of storage to cover net production differences leads to a lower level of volatility of the feed-in to the grid. It also reduces storage requirements by creating a similar seasonal storage pattern. Expanding the distribution capacity increases the volatility of grid feed-in for both profit-oriented and storage-prioritizing operation strategies. This reduces revenues

for storage-prioritizing strategies, which is unfavorable for the grid operator because this negatively affects the economic viability of these price-independent strategies.

It can be concluded that biogas production has a useful role in decentralized energy systems both as a gas, in the form of bio-LNG, and after conversion to electricity. To enable effective embedding in existing infrastructure, the biogas can serve to complement fossil methane in existing gas grids and provide a constant electricity source by complementing other renewable sources. It can be transported in tubes and upgraded and injected into the pipeline grid. This requires sufficient storage capacity at each farm so that vehicles can make single uncombined tours. When biogas is converted to electricity, it can complement other renewable sources by providing a base-load level of electricity for the local demand of households. Wind and solar energy can then provide energy during peaks in electricity demand. This helps to reduce the overall storage and production capacity requirements. In general, wind shows a better matching supply profile than solar as an addition to base-load supply. While solar energy is a relatively cheap form of electricity, it can also cause peak loads at the electricity grid connection and potentially lead to congestion problems. Hydrogen storage is a solution to reduce peak loads but also to bridge seasonality differences between supply and demand. Optimizing the buying and selling decisions for a storage owner/operator can increase revenues and help to increase the economic viability of hydrogen. However, operating storage to benefit from price differences increases the volatility of the grid feed-in, which is problematic from a broader perspective. Operating storage independent of prices helps to stabilize the feed-in to the grid. However, this leads to lower revenues for the facility owner, and thus requires further consideration.

Overall, we conclude that the combined results from the executed studies bring us some steps forward in our thinking on how decentralized storage and distribution of biogas, solar, and wind energy should be organized in the energy transition. Still, the implications should be carefully considered before making any recommendations on transition policies.

Samenvatting

Beslissingen op het gebied van logistiek zijn belangrijk bij de overgang van fossiele energiebronnen naar hernieuwbare energie. Dit proefschrift behandelt besluitvormingsproblemen met betrekking tot het balanceren en organiseren van de opslag en distributie van biogas, waterstof en elektriciteit uit zonne-energie en windenergie voor energieproducenten. De beslissingen zijn gericht op het balanceren en beheren van opslag, productie en transport in landelijke gebieden om overproductie of teveel opslagcapaciteit, congestie op het elektriciteitsnet en teveel-geproduceerde energie te voorkomen. Deze beslissingen streven ook naar een stabiele levering van hernieuwbare energie aan plattelandsgemeenschappen. Bovendien behandelt dit proefschrift het gebruik van LNG in de transportsector, door te laten zien onder welke omstandigheden LNG-aangedreven schepen economisch rendabeler zijn dan conventionele schepen.

De behoefte aan een duurzamer energiesysteem en de verschuiving naar hernieuwbare energie en minder vervuilende brandstoffen zorgt voor logistieke problemen met betrekking tot een duurzame energievoorziening. Met name de overgang naar meer hernieuwbare energiebronnen zorgt voor problemen met betrekking tot aanbod-gestuurde energieopwekking, locatieverschillen tussen energieproductie en energievraag, en de verschillen in productie- en vraagprofielen over tijd. Dit leidt tot teveel geproduceerde energie, onregelmatige teruglevering aan het elektriciteitsnet en transportuitdagingen in verband met de distributie van biogas.

Zowel vanuit logistiek als maatschappelijk oogpunt is het verstandig om de productiegerelateerde logistieke problemen decentraal aan te pakken, waarbij lokaal geproduceerde energie zoveel mogelijk lokaal wordt verbruikt. Hierdoor kunnen transportverliezen, overmatige teruglevering aan het elektriciteitsnet, overproductie

en onnodig transport worden vermeden. Vanuit een maatschappelijk perspectief komt een gedecentraliseerde aanpak ook tegemoet aan de wensen van lokale gemeenschappen die dicht bij productiefaciliteiten voor hernieuwbare energie wonen. Deze willen vaak niet wonen naast hernieuwbare energie productie faciliteiten terwijl de geproduceerde energie elders wordt geconsumeerd.

Hoewel productie en consumptie van hernieuwbare energie lokaal kan plaatsvinden, vereist een decentrale aanpak nog steeds efficiënte transportsystemen om het aanbod en de vraag elders te verbinden. Dat is nodig, omdat (deels) zelfvoorzienende systemen met minder participanten minder mogelijkheden voor flexibiliteit bieden. Daarnaast heeft de (piek) energieproductie van wind, zon en biogas voldoende distributie-infrastructuur nodig in de vorm van een elektriciteits- of pijpleidingnet. Dit maakt de organisatie van de logistiek noodzakelijk.

In de overgangsperiode is transport van gassen per vrachtwagens en schepen te verwachten. Dit vereist dat ook de transportsector zich aanpast door meer gebruik te maken van minder vervuilende brandstoffen zoals waterstof, LNG en biogas. Vooral schepen gebruiken steeds vaker alternatieve brandstoffen om de uitstoot te verminderen. De invoering van nieuwe brandstoffen zorgt echter voor beslissingsproblemen voor reders met betrekking tot investeringen in schepen en infrastructuur.

Bij de transitie naar schonere brandstoffen speelt opslag een belangrijke rol waarbij opslag kan fungeren als tijdelijke buffer voor het transport van waterstof, LNG en biogas. Ook bij elektriciteit is opslag van energie belangrijk voor het overbruggen van seizoens- en korte termijnverschillen tussen vraag en aanbod en om overproductie en congestie van het elektriciteitsnet te voorkomen. Opslag van elektriciteit voor de korte termijn kan worden gerealiseerd met batterijen die fluctuaties in het verbruik gedurende de dag kunnen opvangen; energie opslag voor fluctuaties in seizoenen moet in de vorm van methaan of waterstof worden gerealiseerd.

Dit proefschrift is gebaseerd op het project getiteld "ADAPNER" (Adaptieve logistiek in een circulaire economie) dat tot doel heeft "Geoptimaliseerde aanpasbare en duurzame configuraties te bepalen voor verschillende distributie-alternatieven met betrekking tot biomassa en biogas in een circulaire economie". Het doel van dit proefschrift is om configuraties te bepalen voor verschillende decentrale alternatieven voor de productie, opslag en distributie van hernieuwbare energie.

Deze omvatten wind, zonne-energie (PV), biogas, LNG (Liquefied Natural Gas) en waterstof. Onze hoofdonderzoeksvraag is: *Hoe moet de decentrale opslag en distributie van biogas, zonne-energie en windenergie worden georganiseerd en aangepast om een effectieve inbedding in bestaande netinfrastructuur mogelijk te maken?*

In vijf verschillende hoofdstukken hebben we met bovenstaande onderzoeksvraag een bijdrage geleverd aan drie domeinen waaronder 1) Transportlogistiek, 2) Seizoen afstemming van vraag en aanbod, en 3) Beheer van opslagfaciliteiten. Elk hoofdstuk draagt bij aan verschillende aspecten van deze domeinen.

Hoofdstuk 2 en 3 richten zich op het domein "Transportlogistiek". In hoofdstuk 2 hebben we de onderzoeksvraag beantwoord: *Hoe moet biogas worden gedistribueerd met behulp van vrachtwagens met opleggers die gas cilinders vervoeren van biogas vergisters naar gecentraliseerde gas opwaardeerfabrieken?* We hebben de route- en voorraadbeslissingen behandeld van voertuigen die biogas vervoeren in cilinders van gedecentraliseerde boerderijen tot centrale opwaarderingsfaciliteiten die het gas in het pijpleidingnet injecteren. Het doel is hier om transportschema's te maken die herhaaldelijk kunnen worden uitgevoerd, waarbij de totale reistijd geminimaliseerd is. Om deze beslissingen te optimaliseren, hebben we hebben een wiskundige formulering ontwikkeld die effectief is gebleken in het verminderen van rekentijden met gemiddeld 93%. We ontdekten dat de transporttijd is geminimaliseerd wanneer voertuigen enkele ritten maken bij het bezoeken van de boerderijen (waarbij boerderijen dus niet worden gecombineerd in een enkele rit) en wanneer de opslagcapaciteit in aantal cilinders op elke boerderij de voertuigcapaciteit overschrijdt. We ontdekten ook dat er geen voordelen zijn verbonden aan het vervoeren van cilinders die maar gedeeltelijk gevuld zijn.

In Hoofdstuk 3 hebben we de onderzoeksvraag beantwoord: *Onder welke voorwaarden is de toepassing van LNG economisch haalbaar voor LNG-aangedreven schepen in vergelijking met conventionele schepen?* We hebben een investeringsbeoordelingsmodel ontwikkeld en vergeleken de totale exploitatiekosten van LNG-aangedreven schepen met conventionele schepen. We ontdekten dat de brandstofkosten van LNG-aangedreven schepen vaak lager zijn dan die van conventionele schepen, zelfs bij ongunstige LNG-prijzen in vergelijking met andere scheepsbrandstoffen. De kosteneffectiviteit van LNG-aangedreven schepen wordt versterkt voor grotere schepen met een

hoger algemeen brandstofverbruik en schepen die veel aanwezig zijn in ECA (emissie-gecontroleerde) zones. Dit geeft ook aan dat het gebruik van biogas als bio-LNG mogelijk economisch levensvatbaar kan zijn als brandstof in de scheepvaart.

Hoofdstuk 4 richt zich op het domein "Seizoen afstemming van vraag en aanbod". Hier hebben we de onderzoeksvraag beantwoord: *Hoe moeten biogas, wind- en zonne-energie over de seizoenen heen worden gecombineerd en hoe wordt dit beïnvloed door het niveau van de totale productiecapaciteit en opslagcapaciteit van elektriciteit?* Het hoofddoel is het realiseren van de laagste productie- en opslagbehoefte bij het voorzien van zelfvoorzienende huishoudens van lokaal geproduceerde elektriciteit. We hebben de aandelen van elektriciteitsproductie uit wind, zon en biogas onderzocht voor verschillende combinaties van opslag- en productiecapaciteit. We ontdekten dat biogas bij relatief lage productieniveaus zowel pieken als basislast van de elektriciteitsvraag kan leveren, wat leidt tot relatief hoge opslagniveaus van elektriciteit waarin vooral energie uit biogas wordt opgeslagen. Voor hogere totale productieniveaus neemt het optimale aandeel van de windproductie toe, omdat een deel van de totale overproductie het mogelijk maakt om windpieken op ongunstige momenten verloren te laten gaan en niet op te slaan. Hierdoor kunnen de opslagvereisten aanzienlijk worden verminderd. Wanneer echter de jaarlijkse totale productiehoeveelheid groter is dan 130% van de totale vraag, vermindert het optimale aandeel van windenergie aanzienlijk, waarbij overproductie van elektriciteit uit biogas een zeer lage opslagbehoefte mogelijk maakt.

In Hoofdstuk 5 en 6 hebben we een bijdrage geleverd aan het domein "Beheer van opslagfaciliteiten". In Hoofdstuk 5 hebben we de onderzoeksvraag beantwoord: *Onder welke voorwaarden moet de eigenaar van zonnevelden met faciliteiten voor waterstof-productie en -opslag op het elektriciteitsnet kopen en verkopen om de winst te maximaliseren?* We onderzoeken het probleem van een eigenaar van een zonnepark met waterstofopslag en brandstofcellen die elektriciteit levert aan een aantal aangesloten huishoudens en het elektriciteitsnet. Met behulp van een Markov-beslissingsproces bepalen we de optimale dagelijkse koop- en verkoopbeslissing van de opslag eigenaar om de verwachte winst te maximaliseren. We houden expliciet rekening met seizoensverschillen in vraag en aanbod en de onzekerheid die gepaard gaat met elektriciteitsprijzen, elektriciteitsverbruik en zonne-energieproductie. We ontdekten dat optimaal beleid wordt gekenmerkt door

prijsdrempels die verschillende soorten acties scheiden. Deze omvatten het kopen van de maximaal mogelijke hoeveelheid elektriciteit, het verkopen van overschotten of het kopen van tekorten aan elektriciteit, het opslaan van overschotten of het verkrijgen van tekorten uit opslag aan elektriciteit, of het verkopen van de maximaal mogelijke geproduceerde en opgeslagen hoeveelheid elektriciteit. We laten ook zien dat het negeren van seizoensgebonden vraag- en productiepatronen suboptimaal is en dat het gebruik van waterstofopslag verliesgevende interacties met het elektriciteitsnet kan omzetten in winstgevende beslissingen. We vonden dat de distributiecapaciteit van de verbinding met het net niet te klein mag zijn om lokale netcongestie te voorkomen. In tegenstelling tot wat mag worden verwacht, verhoogt een hogere opslagcapaciteit het aantal inkoopacties van het net, waardoor er meer lokale congestie ontstaat, wat problematisch is voor de netbeheerder. Daarom is alleen winst-gedreven waterstofopslag geen alternatief voor netuitbreiding om congestie op te lossen, wat essentiële informatie is voor beleidsmakers en netbeheerders.

In Hoofdstuk 6 hebben we de onderzoeksvraag beantwoord: *Hoe moeten zonnevelden met waterstofopslag worden beheerd om congestie te verminderen?* We vergelijken winst gedreven strategieën voor opslagbeheer met een opslagstrategie die altijd prioriteit geeft aan opslag om die te gebruiken voor overschotten of tekorten gedurende het jaar. Winstmaximalisatie door de opslageigenaar zorgt voor een instabiele teruglevering aan het net, wat kan leiden tot mogelijke congestieproblemen elders in het net. Daarentegen leidt het gebruik van opslag, waarbij prioriteit wordt gegeven aan het afdekken van netto productieverschillen tussen vraag een aanbod, tot een lagere volatiliteit in de teruglevering aan het net. Het vermindert ook de opslagvereisten door een opslagpatroon te creëren die alleen seizoensverschillen in vraag en aanbod opslaat. Bij beide opslag strategieën, zowel die winstgericht zijn als degene die opslag prioriteit geven, neemt de volatiliteit van de teruglevering van het net toe wanneer men de distributiecapaciteit uitbreidt. Uitbreiding van de distributiecapaciteit kan dus de inkomsten verminderen voor opslageigenaars die niet winst gedreven zijn. Dit is ongunstig is voor de netbeheerder en de opslageigenaar.

Geconcludeerd kan worden dat biogasproductie een nuttige rol speelt in decentrale energiesystemen, zowel als gas, in de vorm van bio-LNG, en na conversie naar elektriciteit. Om een effectieve inbedding in bestaande infrastructuur

mogelijk te maken, kan biogas dienen als een aanvulling op fossiel methaan in bestaande gasnetwerken en door als constante elektriciteitsbron energie te leveren en hierbij andere hernieuwbare bronnen aan te vullen. Het kan in cilinders worden vervoerd naar faciliteiten waar de kwaliteit van biogas kan worden opgewaardeerd, waarna het in het pijpleidingnet kan worden geïnjecteerd. Dit vereist voldoende opslagcapaciteit bij elk vertrekpunt, zodat voertuigen enkele ritten kunnen maken die niet met elkaar gecombineerd worden. Wanneer biogas wordt omgezet in elektriciteit, kan het andere hernieuwbare bronnen aanvullen door een basisniveau van elektriciteit te leveren voor de lokale vraag van huishoudens. De meer grillige patronen van wind- en zonne-energie zorgen ervoor dat deze dan energie kunnen leveren tijdens pieken in de elektriciteitsvraag. Dit helpt om de totale vereisten voor opslag- en productiecapaciteit te verminderen. Wind laat over het algemeen een beter passend aanbodprofiel zien dan zon als aanvulling op het basisaanbod. Zonne-energie is weliswaar een relatief goedkope vorm van elektriciteit, maar kan ook voor piekbelastingen op de elektriciteitsnetaansluiting zorgen en mogelijk tot congestieproblemen leiden. Waterstofopslag is een oplossing om piekbelastingen te verminderen, maar ook om seizoensverschillen tussen vraag en aanbod te overbruggen. Het optimaliseren van de aan- en verkoopbeslissingen voor een opslageigenaar of exploitant kan de inkomsten verhogen en de economische levensvatbaarheid van waterstof helpen vergroten. Het exploiteren van opslag om te profiteren van prijsverschillen verhoogt echter de volatiliteit van de teruglevering aan het net, wat vanuit een breder perspectief problematisch is. Door opslag onafhankelijk van de prijs te exploiteren, wordt de teruglevering aan het net gestabiliseerd. Dit leidt echter tot lagere inkomsten voor de opslag eigenaar en exploitant en vraagt dus om nadere afwegingen.

Uiteindelijk kunnen we concluderen dat de gecombineerde resultaten van de uitgevoerde studies ons een stap dichter brengen in het denken over hoe gedecentraliseerde opslag en distributie van energie uit biogas, zon en wind moet worden georganiseerd in de energietransitie. Daarentegen is het belangrijk dat de implicaties voorzichtig worden overwogen voordat er aanbevelingen worden gedaan over het transitiebeleid.

Acknowledgements

times we had, which included lots of laughter during conferences and having coffee breaks with our sometimes homebrewed coffee.

I would also like to thank Bartjan Pennink and Togar Simatupang for supervising my Bachelor's thesis in Indonesia and making me enthusiastic about doing research.

I especially appreciate my parents (and the rest of my family) for always supporting me throughout this process. I could not have done this without your help.

About the author

Jan Eise Fokkema was born in Colombo, Sri Lanka and grew up on a farm in Friesland before moving to Groningen for studies. He obtained a Bachelor's degree in International Business at the University of Groningen in 2014 and as part of the program, he studied in Bandung in Indonesia for 1.5 years at the Institute of Technology. He combined his studies with a Bachelor's degree in Jazz Piano at the Prince Claus Conservatory in Groningen. Subsequently, he obtained the Master's degree Technology and Operations Management in 2015. During his studies, he became interested in quantitative modeling and decided to learn more about simulation, programming and optimization. When being offered a PhD position that gave him the chance to develop these interests in the field of Renewable Energy Logistics, he quickly accepted. He currently works as a researcher and teacher at the University of Groningen. In his time off, he likes to play jazz piano and to go sailing. In the future, he aims to contribute to the energy transition as both a practitioner and researcher.